

Assignment of functional impact  
on genetic data in two mouse models  
of affective disorders

Dissertation

Faculty of Biology  
Ludwig Maximilian University, Munich

Regina Widner-Andrä

December 14<sup>th</sup> 2011

Erstgutachter                      Prof. Dr. Rainer Landgraf

Zweitgutachter                    Prof. Dr. Gisela Gruppe

Tag der Abgabe: 14. Dezember 2011

Tag der mündlichen Prüfung: 8. Mai 2012

*“Nothing in life is to be feared. It is only to be understood.”*

Marie Curie

This dissertation is dedicated to my father, Gottfried Widner († February 2001).

---

## Table of contents

Table of contents.....	1
1 Abstract.....	7
2 Introduction .....	9
2.1 The current concept of depression scale disorders .....	9
2.2 Comorbidity of depression .....	10
2.3 Generalized anxiety disorder .....	11
2.4 Stress and reactivity of the hypothalamic-pituitary-adrenal axis .....	11
2.5 Genetics of depression and associated diseases .....	13
2.6 Genome-wide association studies .....	14
2.7 Pharmacological therapy options for depression and associated diseases .....	15
2.8 Psychopharmacotherapy of the future – a step towards personalized medicine? .....	16
2.9 The use of animal models to unravel neurobiological underpinnings of depression and associated diseases .....	17
2.9.1 The HAB/LAB mouse model reflecting extremes in trait anxiety .....	18
2.9.2 The stress reactivity mouse model .....	20
2.10 Technical progress in methods applied for the generation of transcriptome- and sequence-based genomic data .....	22
2.11 Aim and scope of this study .....	22
3 Animals, materials, and methods.....	25
3.1 Experimental animals .....	25
3.1.1 Inbred mouse models.....	25
3.1.2 Heterozygous Cofilin-1 knockout mice .....	25
3.1.3 C57BL/6 wild-type mice.....	26
3.1.4 CD-1 mice.....	26
3.2 Behavioral experiments .....	26
3.2.1 Assessment of anxiety-related behavior.....	26
3.2.1.1 Open field test.....	26
3.2.1.2 Elevated plus-maze test.....	27
3.2.1.3 Dark-light box test.....	28
3.2.2 Assessment of depression-like behavior .....	29
3.2.2.1 Tail suspension test .....	29
3.2.2.2 Forced swim test.....	30
3.2.3 Assessment of stress reactivity .....	31
3.2.4 Behavioral test batteries performed in this study .....	32

3.2.4.1	Behavioral test battery conducted for phenotypic characterization of <i>Cfl-1<sup>+/-</sup></i> vs. WT mice.....	32
3.2.4.2	Behavioral test battery conducted for phenotypic characterization of an outbred population of CD-1 mice.....	33
3.3	Sacrifice of animals .....	33
3.4	Dissection of embryos .....	34
3.5	Collection of brain and hippocampal tissue from embryonic and adult mice ....	34
3.6	Nucleic acid based methods.....	34
3.6.1	RNA based methods.....	34
3.6.1.1	Extraction of total RNA from hippocampal tissue .....	34
3.6.1.2	Control measures of RNA quality and determination of RNA concentration.....	35
3.6.1.3	Reverse transcription of RNA into cDNA.....	35
3.6.1.4	RNA amplification for array analysis .....	36
3.6.1.5	Serial analysis of gene expression.....	36
3.6.2	DNA based methods.....	37
3.6.2.1	DNA extraction from mouse tissue.....	37
3.6.2.2	Polymerase-chain reactions and gel electrophoresis .....	38
3.6.2.3	Gel electrophoresis.....	39
3.6.2.4	Precipitation of cDNA.....	39
3.6.2.5	Quantitative real-time PCR .....	40
3.6.2.6	Table of oligonucleotides .....	41
3.7	Protein based methods.....	43
3.7.1	Mitochondrial proteomics .....	43
3.7.1.1	Preparation of mitochondrial protein lysates .....	43
3.7.1.2	Bradford assay .....	44
3.7.1.3	Two-dimensional gel electrophoresis .....	44
3.7.2	Cytochrome c immunoassay.....	46
3.7.3	Cytochrome c oxidase staining .....	47
3.7.4	Quantification of plasma corticosterone via radioimmunoassays.....	48
3.8	Statistical and bioinformatical methods.....	49
3.8.1	Statistical analyses of microarray experiment .....	49
3.8.1.1	Univariate analysis.....	49
3.8.1.2	Multivariate analysis .....	49
3.8.2	Statistical analyses of the SAGE experiment .....	50
3.8.3	Cluster analyses of differentially regulated genes .....	51
3.8.3.1	Database for annotation, visualization, and integrated discovery .....	51

---

3.8.3.2	Gene ontology analyses.....	51
3.8.4	High-density screening for single-nucleotide polymorphisms and detection of segmental copy number variants by means of the Jax Mouse Diversity Genotyping array.....	51
3.8.4.1	Detection of segmental copy number variation based on data from Jax Mouse Diversity Genotyping array.....	52
3.8.5	Principle component analyses of phenotypic features.....	52
3.8.6	Calculation of association via WG-Permer.....	53
3.8.7	Generation of CD-1 strain-specific haplotype map.....	53
3.8.8	Statistical data analyses, graphical illustration, and common bioinformatical processes.....	53
4	Results.....	55
4.1	Gene expressional profiling of the SR mouse model.....	55
4.1.1	Differentially expressed genes according to univariate analysis of the microarray experiment.....	55
4.1.2	Genes detected as differentially expressed in the SAGE experiment.....	55
4.1.3	Overlapping pool of genes detected as differentially expressed in both gene expression profiling approaches.....	55
4.1.4	Univariate vs. multivariate analysis of microarray data.....	56
4.1.5	Cluster analyses of differentially expressed genes.....	57
4.1.5.1	Identification of significant gene clusters in microarray candidates using the DAVID Bioinformatics Database.....	57
4.1.5.2	Identification of significant gene clusters in SAGE candidates using DAVID Bioinformatics Database.....	58
4.1.6	GO analyses of differentially expressed genes detected in the microarray study.....	62
4.1.7	Insufficient yield of mitochondrial protein lysate for 2D gel analysis.....	63
4.1.8	No differences in cytochrome c release from mitochondrial bilayer into cytoplasm in HR vs. LR mice.....	63
4.1.9	Cytochrome c oxidase activity in the hippocampus of HR vs. LR female mice.....	63
4.1.10	Confirmation of microarray candidates via qPCR analyses.....	64
4.1.11	Neurodevelopmental study.....	66
4.1.11.1	Expressional profiling of neurodevelopmentally expressed genes in hippocampal tissue of adult animals.....	66
4.1.11.2	Expressional profiling of neurodevelopmental genes in hippocampal tissue of ED 18 mice.....	67

4.1.11.3	Expressional profiling of neurodevelopmental genes in hippocampal tissue of PND 7 mice .....	68
4.1.11.4	Expressional profiling of neurodevelopmental genes in hippocampal tissue of PND 28 mice .....	70
4.2	From gene expressional profiling to behavior – tracking one candidate gene to a behavioral phenotype .....	71
4.2.1	Non-detection of differential expression of <i>Cfl-1</i> in hippocampal tissue of HR vs. LR mice in microarray study .....	71
4.2.2	Behavioral phenotype in heterozygous <i>Cfl-1<sup>+/-</sup></i> mice.....	71
4.2.2.1	No distinct behavior of <i>Cfl-1<sup>+/-</sup></i> vs. WT mice in the OF .....	71
4.2.2.2	Anxiety-related behavior in <i>Cfl-1<sup>+/-</sup></i> vs. WT mice on the EPM.....	72
4.2.2.3	Detection of increased anxiety-related behavior in female <i>Cfl-1<sup>+/-</sup></i> vs. WT mice in the DL box.....	75
4.2.2.4	FST data indicate more active stress-coping style of female <i>Cfl-1<sup>+/-</sup></i> vs. WT mice.....	78
4.2.2.5	Increased stress reactivity in <i>Cfl-1<sup>+/-</sup></i> vs. WT mice.....	79
4.3	Segmental copy number variation and SNP profiling of HAB vs. LAB and HR vs. LR mice .....	84
4.3.1	Regions of segmental copy number variation in DNA copy numbers differing in HAB vs. LAB and in HR vs. LR mice.....	84
4.3.2	Influence of segmental variation in DNA copy numbers on gene expression in the hippocampus of HR and LR mice .....	86
4.3.3	SNP profiling of HAB vs. LAB and HR vs. LR animals using the JAX Mouse Diversity Genotyping array .....	87
4.4	Phenotypic characterization of an outbred population of CD-1 male mice .....	89
4.4.1	Results of behavioral testing of 384 CD-1 male mice .....	89
4.4.1.1	Results of EPM testing.....	89
4.4.1.2	Results of OF testing .....	93
4.4.1.3	Results of FST .....	96
4.4.1.4	Results of SRT .....	100
4.4.1.5	Results of TST .....	103
4.4.1.6	No correlation between phenotypes collected in behavioral experiments of the ‘CD-1 panel’ .....	105
4.5	Association study – attribution of functional relevance to SNPs.....	106
4.5.1	Selection of 32 phenotypically characterized CD-1 mice based on behavioral data .....	106

---

4.5.1.1	PCA of quantitative behavioral traits confirmed correlation of phenotypes which served as selection criterion .....	106
4.5.1.2	Polymorphic SNPs detected in 32 selected CD-1 mice .....	107
4.5.1.3	Generation of the first CD-1 specific haplotype map .....	107
4.5.1.4	Primary associations identified between genotypes and phenotypes of selected CD-1 mice.....	107
4.5.1.5	Identified associations between genotypes and phenotype of selected CD-1 mice.....	109
4.5.1.6	Confirmation of the predictive validity of an association study in 32 animals .....	113
4.5.1.7	Potential expansions of the association study in 32 CD-1 mice to the total population of the 'CD-1 panel' .....	115
4.6	Overview supplementary data .....	116
5	Discussion.....	117
6	Perspectives.....	145
7	Abbreviations.....	147
8	Bibliography .....	149
9	Acknowledgements .....	169
10	Curriculum vitae .....	171
11	Declaration/Erklärung.....	173



## 1 Abstract

The remarkable technical development over the last decade allowed the generation of genetic data in a high-throughput manner, challenging scientists with enormous amounts of data to be stored and analyzed. The functional attribution of genetic data remains the key task and turned out to be particularly provoking in the field of affective disorders. Being aware that the behavior of an individual is determined by a variety of factors – genes, epigenetic modifications, environment, experiences, and interactions of all these components – the attribution of the functional impact of genetic data depicts a challenging, but inevitable task, as the molecular underpinning of depression and associated diseases are still largely unknown, although the incidences of these psychiatric diseases are alarming.

Animal models based on selective breeding approaches, such as the HAB/LAB mice representing extremes in anxiety-related behavior and HR/LR mice representing extremes in stress reactivity, serve as model organisms, which are providing both distinct quantitative traits at the behavioral level and an accumulated and conserved pool of genomic features determining quantitative traits at a genetic level.

Therefore, as a first attempt towards the genetic characterization of the stress reactivity mouse model, the transcriptome of HR vs. LR mice was investigated combining microarray-based and serial analysis of gene expression (SAGE) experiments. The detected pool of differentially expressed genes in the hippocampus of HR vs. LR mice was further characterized via bioinformatical analyses, the phenotypic characterization of heterozygous Cofilin-1 knockout mice, and a neurodevelopmental follow-up study. All these attempts clearly indicated the mitochondria as the origin of the differences in stress reactivity and HPA axis dysfunction in HR vs. LR mice. More precisely, evidence for a disturbed energy metabolism was collected, potentially generating different levels of reactive oxygen species and determining different apoptosis rates between the lines. To that effect, extremes in stress reactivity seem to show similarities to the growing list of neurodegenerative disorders with a known mitochondrial impact. Furthermore, an anxiety-related, depression-like, and stress reactivity phenotype was attributed to heterozygous Cofilin-1 knockout mice giving rise to the hypothesis that Cofilin-1 dose-dependently influences the respective quantitative traits in a U-shaped manner.

In addition, in analogy to the founder populations of the inbred mouse models, an outbred population of CD-1 mice was phenotypically characterized in respect to anxiety-related and depression-like behaviors as well as stress reactivity. From these CD-1 mice,

32 animals were selected to represent the continuum of quantitative traits of the inbred mouse models, and were subsequently genotyped for more than 620,000 SNP loci genome-wide. Based on these genotypes, the first CD-1 specific haplotype map was calculated and, furthermore, preliminary associations were calculated resulting in the identification of several loci, which were already reported in a broader neurobiological context, but not directly in relation to affective disorders so far. The haplotype map allows the genome-wide selection of tag-SNPs in accordance to the linkage disequilibrium clustering of CD-1 mice and might serve as the basis for a future development of a customized tag-SNP assay to test for associations in the entire CD-1 population. As the overall coverage and reliability of this tag-SNP approach seems questionable, a high throughput-SNP-screening will alternatively be considered.

In either case, the availability of the inbred mouse models provides the unique opportunity to test associations detected in the extended approach. A possible first attempt to assess the functional impact of an associated locus on the quantitative traits of the inbred mouse models could be the pharmacological manipulation of the protein product encoded by the detected locus.

## 2 Introduction

*One of the oldest medical recordings is an approximately 3,600 years old Egyptian papyrus which Georg Ebers, a German Egyptologist and author, bought in 1872 in Thebes, Egypt. Ebers translated the 108 papyrus columns into German and found among several chapters the probably first description of what today is called 'depression'. The nameless editor of the papyrus described a 'weakness in the head' which was translated as pathological exhaustion and debility (Joachim, 1890).*

*Roughly 3,600 years after this presumably first description of symptoms shown by depressed patients, this phenomenon is on the way to becoming a major health and socioeconomic issue of our time.*

### 2.1 The current concept of depression scale disorders

Depression according to today's concept is a disease of the central nervous system (CNS) (Insel and Charney, 2003) comprising distinct disease patterns with similar symptoms. The World Health Organization (WHO) defined depression as a mental state characterized by depressed mood, a general loss of interest, feelings of guilt, low self-esteem, the inability to feel pleasure, disturbed sleep and appetite, poor energy, and concentration levels. Depression is a recurrent and chronic state and is therefore followed by impairment in accomplishing the everyday life. The personal burden for the patient coming along with the symptomatology culminates in roughly 850,000 cases of suicide world-wide every year (<http://www.who.int/mentalhealth/management/depression/definition/en/index.html>).

Depressive disorders are highly prevalent diseases. The lifetime prevalence for women was estimated with 25%, for men with 12%, though these estimations differ depending on the source. Depressions are therefore becoming an increasingly large problem to the public health systems. The recurrent and chronic course of the disease made it a frequent cause for permanent impairment, hence making it a worldwide source for disability (Cassano and Fava, 2002; Cryan and Holmes, 2005; Gelenberg, 2010; Hamet and Tremblay, 2005; Lohoff, 2010). The WHO estimates that by the year 2020 depression will be the second most prominent cause for disability in the world (Williams *et al.*, 2009a). Furthermore, according to a calculation of the German Federal Office of Statistics, the costs in Germany caused by depression in the year 2008 were 5.2 billion

Euros, which made a 32% cost increase from 2002 to 2008 for dementia and depression (press release Statistisches Bundesamt, no. 280, 11.08.2010). The increasing number of patients entailing raising costs sensitized politics and society for this topic.

The term depression encompasses a group of related, but still distinct forms of the disease. Major depressive disorder (MDD; also called melancholic, typical or endogenous depression) is characterized by melancholic episodes of anxiety, insomnia, loss of appetite, fear of the future, and seems to be associated with increased activity of the hypothalamic-pituitary-adrenal (HPA) axis (Gold and Chrousos, 2002; Gold *et al.*, 1988). MDD can be sub-classified into two prominent forms of the disease which are unipolar and bipolar courses. In unipolar depression the patient's constitution remains in the melancholic phase, whereas a bipolar course of the disease is characterized by bimodality with alternating manic and hypomanic phases (Parker *et al.*, 2011). The second most prominent form next to MDD is atypical depression. Patients suffering from atypical depressions show to a certain extent reverse symptoms of MDD, like for example lethargy, fatigue, hypersomnia, and hyperphagia (Gold and Chrousos, 1999; Gold and Chrousos, 2002).

Depressive disorders are multifactorial and heterogeneous diseases (Gold and Chrousos, 2002) and precise understanding of the etiology remains elusive (Colman and Atallahjan, 2010; Jacobson and Cryan, 2007). Comprehension of the multidimensional interplay between genetic, epigenetic, environmental and psychosocial components (Freeborough and Kimpton, 2011; Tarantino *et al.*, 2011) finally determining the individual susceptibility for depressive disorders is a complex but unavoidable challenge necessary to counter the current advance of depressive disorders.

## **2.2 Comorbidity of depression**

Depressive disorders are strongly associated with anxiety disorders, such as panic disorders or generalized anxiety disorder (GAD), with substance abuse, and impulse-control disorders, like for example bulimia or antisocial personality disorder (Kessler *et al.*, 2003). As mentioned above, depressions are further known to be accompanied by alternations of physiological stress hormone systems. The sympathetic nervous system and the HPA axis are dysregulated during the course of depressive disorders linking disturbed stress reactivity and depression. Both, HPA axis hypo- and hyperactivity and increased sympathetic vs. parasympathetic tone were reported in this context (Muller and Holsboer, 2006; Nosjean *et al.*, 1995; Touma *et al.*, 2008). In addition, cardiovascular diseases, stress reactivity, and depression share numerous neurobiological features strongly implying an association of cardiovascular and affective

disorders (Grippe and Johnson, 2009). Neither surprising, co-occurrence of depression and neurodegenerative disorders, such as Parkinson's or Alzheimer's disease, is a widely known phenomenon. On the one hand, this comorbidity could be explained by the personal burden coming along with neurodegenerative diseases, but on the other hand, crucial neurotransmitter and neuropeptide systems, for example, the dopaminergic system and the arginine vasopressin (AVP) system, are impaired in either illness. This common ground of impaired neurobiological mechanisms between affective disorders and neurodegenerative disease seems an obvious basis of comorbidity between them (Anisman *et al.*, 2008).

### **2.3 Generalized anxiety disorder**

GAD is defined as “an uncontrollable disposition to worry about one's welfare and that of one's immediate kin” (Akiskal, 1998). It is the most prevalent anxiety disorder and is very often associated with psychiatric diseases, in particular with MDD (Simon, 2009). Even more, it seems like GAD could be a prodrome for MDD, as in a study by Kessler and colleagues it was shown that the probability of MDD onset is increased within the first year of an initial period of GAD (Kessler *et al.*, 1996). Others reported about simultaneous onset of GAD and MDD being as frequent as GAD onset prior to MDD or *vice versa* (Moffitt *et al.*, 2007). However, there is consensus regarding the highly comorbid nature of GAD and MDD and GAD can be considered both, a risk factor as well as a biological marker for the development of other affective disorders later in lifetime. It was hypothesized that GAD might act as biological stressor and, hence, trigger a subliminal predisposition for MDD via dys-regulation of affected neurotransmitter systems, such as the serotonergic system or of the HPA axis. Furthermore, accumulated evidence points towards shared genetic risk factors for GAD and depression, in particular for GAD and MDD (Cerdeira *et al.*, 2010; Simon, 2009). For example, Hettema and colleagues demonstrated a pronounced genetic correlation ( $R^2 = 0.98$ ) between GAD and MDD after examination of more than 9,000 twins from the Virginia Adult Twin Study of Psychiatric and Substance Abuse Disorders (Hettema *et al.*, 2006).

### **2.4 Stress and reactivity of the hypothalamic-pituitary-adrenal axis**

The hypothalamic-pituitary-adrenal (HPA) axis is a major part of the body's neuroendocrine system and involves the paraventricular nucleus (PVN) of the hypothalamus, the anterior lobe of the pituitary gland, and the adrenal cortices of the adrenal glands (Figure 1). It contributes on a regulatory level to a variety of physiological

functions, such as developmental, immunological, metabolic and cardiovascular processes and, in particular, to stress response. It is liable to a pulsatile rhythmicity with in humans highest activity shortly before awakening under baseline conditions.

Briefly, the signaling cascade of the HPA axis includes the release of corticotropin-releasing hormone (CRH) and AVP from a sub-fraction of parvocellular neurons of the PVN as a primary reaction to stress. CRH stimulates, among others, the anterior pituitary which, in turn, secretes the adrenocorticotropin hormone (ACTH). This release of ACTH is synergistically supported by AVP. ACTH is transported by the systemic blood stream to the *zona fasciculata* of the adrenal cortex prompting glucocorticoid release. Glucocorticoids, which are the target effectors in the signaling cascade of the HPA axis, in turn are involved in a multiplicity of physiological and pathophysiological processes. The most prominent glucocorticoid is cortisol in humans and corticosterone in mice, respectively (Melmed *et al.*, 2011). They execute their pleiotropic functions via the ubiquitously expressed glucocorticoid receptor. Upon activation, this cytoplasmic receptor diffuses from binding proteins, homodimerizes and translocates into the nucleus acting as transcription factor via binding to glucocorticoid responsive elements on genomic DNA. In addition, transrepressive effects of glucocorticoid receptor signaling which does not necessarily involve binding to DNA and fast mediated glucocorticoid signaling via membrane-associated effector molecules were reported. Glucocorticoids also initiate the negative feedback mechanism of the HPA axis limiting CRH and ACTH secretion (Charmandari *et al.*, 2005; Groeneweg *et al.*, 2011a; Groeneweg *et al.*, 2011b; Heitzer *et al.*, 2007; Lightman and Conway-Campbell, 2010; Mormede *et al.*, 2011; Silberstein *et al.*, 2009).

Dysregulation of the HPA axis in depressed patients is often associated with constantly increased levels of cortisol. The reversibility of this hypercortisolemia by application of antidepressant agents was known (Holsboer, 2001; Sterner and Kalynchuk, 2010; Vreeburg *et al.*, 2009). Furthermore, an increase in anxiety-related behavior upon exogenous corticosterone application has also repeatedly been reported (Murray *et al.*, 2008; Pego *et al.*, 2008).

Importantly, a high degree of heritability was shown for components along the HPA axis, which strongly suggests a genetic determination of stress response and therefore, stress pathology. The genetic influence ranges from HPA axis functionality itself to the mode of stress physiological adaptation to environmental stimuli (Franz *et al.*, 2010; Mormede *et al.*, 2011; Wust *et al.*, 2004).

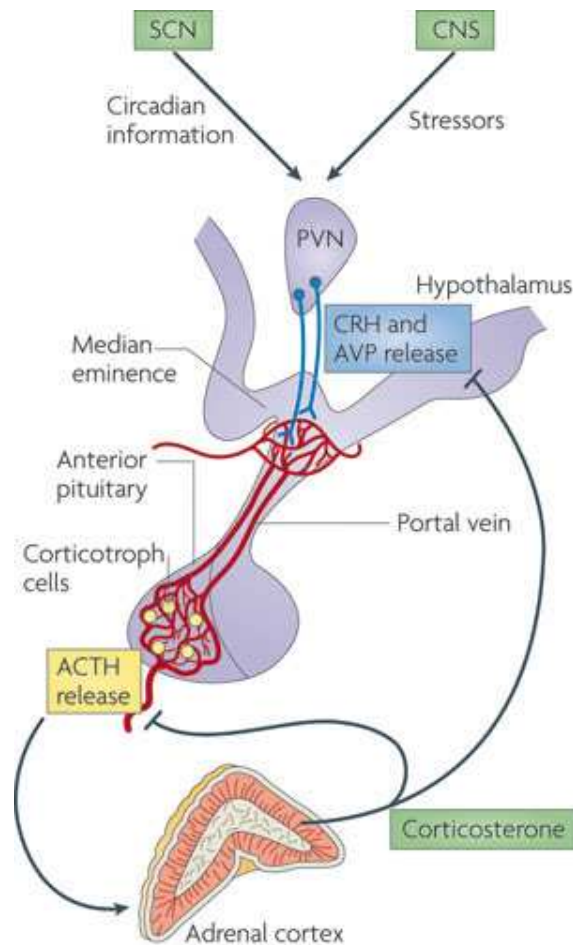


Figure 1: Schematic illustration of HPA axis components. Stimulation of the PVN, either by stressors conciliated from the central nervous system or circadian information from the suprachiasmatic nucleus (SCN) induces CRH and AVP secretion. Thus, the anterior pituitary secretes ACTH which triggers the release of glucocorticoids from the adrenal cortices. In addition to manifold physiological and pathophysiological processes, glucocorticoids limit HPA axis activation via initiation of the negative feedback mechanism. (Figure adopted from Lightman and Conway-Campbell, 2010.)

## 2.5 Genetics of depression and associated diseases

Besides various circuits in the CNS, the genetic underpinning of depression is one component among a variety of determinants entailing the development of depression and associated diseases.

Although twin-studies suggest a heritability of up to 50% for MDD and family studies showed a clearly increased risk for first-degree relatives to also develop MDD (Lohoff, 2010), the identification of genetic risk factors for depression was – like for other complex diseases, too – accompanied by obstacles. The reasons therefore are multifold. First, depression is a multigenic disease determined by the interplay of several genetic factors. Second, the contribution of each single gene can presumably be disregarded (Lohoff, 2010). The assumption of a multitude of genetic risk factors determines the susceptibility

for depression. And third, this multitude of genetic risk factors is heterogeneous (Lohoff, 2010). To a certain degree, there might be an overlap of risk factors between one individual and the other, but the other fraction of this factor allocation differs from one individual to the other. Based on the individual assembly of genetic risk factors, epigenetic and environmental influences differ, too (Lohoff, 2010). Along these lines, the term of “multigenic composite inheritance theory” was formed to “define inheritance of a finite group of seemingly unrelated genes”. The idea behind is that depression and associated diseases are determined by a genetic interplay comprising differential gene expression, polymorphic differences in contributing clusters of genes which are not obviously related, as well as environmental adaptations which could appear in the epistatic modification of genes, post-transcriptional and post-translational modulation, and also spontaneous mutations (Raymer *et al.*, 2005).

A further and only very recently developing idea in the field of molecular genomics is the potential influence of structural changes in the DNA, namely segmental copy number variants. It was shown that CNVs might influence expressional activity of genes encoded by the respective multiplied sequence. This contributes to both, physiological genomic variability as well as disease susceptibility. For schizophrenia, for example, it was shown that structural changes can enhance the risk for the disease by about 25-fold (Murphy *et al.*, 1999).

The presumable interaction of all those genetic parameters highlights the complexity of depression and associated diseases on a genetic level and clarifies the hurdles genetic research of the field encountered so far. In this context, to some extent the disappointing balance of genome-wide association studies (GWAS) (Bondy, 2011) appears self-evident. The successful identification of susceptibility loci making use of GWAS can though not be contradicted (Schulze, 2010). Further approaches typically conducted in order to reveal genetic underpinnings of complex disorders, such as linkage studies and candidate gene analyses (Lohoff, 2010), appear appropriate to an even lesser extent. In fact, integrative approaches embracing the multi-faceted components of genetic participation to susceptibility for depression and associated diseases are required. The embedding of GWAS into integrative approaches provides a promising tool to further progress in the identification of susceptibility loci for these diseases (Schulze, 2010).

### **2.6 Genome-wide association studies**

GWAS involve the significant co-occurrence of genotypic characteristics with phenotypic traits in case vs. control groups. Unlike linkage studies, GWAS are usually performed based on unrelated populations (Craddock *et al.*, 2008).

As depression and associated diseases are complex diseases and a variety of genetic loci with individual markers contributing to a small effect size only, GWAS can provide an adequate tool for the detection of genetic determinants of affective disorders. A reasonable high marker density throughout the genome, which means 500,000 to one million markers, makes prior gene selection dispensable (Craddock *et al.*, 2008; Lohoff, 2010) and enables the detection of novel candidates beyond “usual suspect” components (Schulze, 2010), such as the serotonin or the dopaminergic system.

In commercial single nucleotide polymorphism (SNP) assays, these polymorphic markers are typically positioned in genomic regions with minor allele frequencies above 5%, which results in unequal marker distribution throughout the genome and in disrespect of low-frequency alleles (Craddock *et al.*, 2008). Tagging designs, which comprise the selection of informative SNPs representative for the respective linkage disequilibrium (LD) mapping, are an option to systematically cover the genome with SNP markers, though the detection of minor allele frequencies based on tag-SNP approaches was recently shown to not be improved (Siu *et al.*, 2011).

GWAS, on the one hand, harbor considerable pitfalls, such as a locus detected to not be significantly associated cannot *per se* be considered as uninvolved in respect to the respective trait (Craddock *et al.*, 2008). In fact, positive results might require confirmation in form of repeated detection in independent cohorts, meta-analysis, or biological relevance of a locus detected as significantly associated (Cichon *et al.*, 2009; Levinson, 2005; Lydall *et al.*, 2011; Shyn *et al.*, 2011). This also means, that massive amounts of data need to be produced entailing expenses and statistical issues (Lohoff, 2010). On the other hand, GWAS constitute an unbiased approach, which allows the identification of causative factors (Cichon *et al.*, 2009). Considering the multi-faceted etiology of depression and associated diseases, alternative methods can hardly be considered.

Along this line, a Psychiatric GWAS Consortium (PGC) was recently initiated aimed to consolidate GWAS meta-analyses for major psychiatric disorders (attention deficit hyperactivity disorder, autism, bipolar disorder, MDD, and schizophrenia). PGC comprises GWAS conducted in the field and conveys these data sets to meta-analyses with the expectation to maximize the performance of separate association studies in this collaborative intent (Sullivan, 2010).

## **2.7 Pharmacological therapy options for depression and associated diseases**

Antidepressant drugs are, in general, supposed to alleviate mood and depressive symptoms and are therefore applied against depressions and anxiety disorders. The most established groups are selective serotonin reuptake inhibitors (SSRIs), serotonin-

norepinephrine reuptake inhibitors (SNRIs), monoamine oxidase inhibitors (MAOIs), and tricyclic antidepressants (TCAs).

Current first-line treatment for psychiatric disorders is the application of SSRIs. These drugs execute their psychotropic effect via the inhibition of neuronal uptake pumps for serotonin (5-hydroxytryptamine, 5-HT). This property they share with TCAs and SNRIs, but with the distinction to specifically inhibit serotonin reuptake pumps and no further neuronal receptors or central potassium and fast sodium channels. This specificity explains the increased compliance of SSRIs in contrast to neuropsychopharmacological treatment options developed earlier.

The mechanism via SSRIs exert their therapeutic effect is the increase of 5-HT levels in the synaptic cleft of serotonergic neurons by blocking its uptake into the post-synapse and, therefore, rendering 5-HT in its active state and side. They are influencing the 5-HT system, which does not remain free of unfavorable side effects. The antagonism of the 5-HT reuptake pump goes along with negative allosteric modulation of the 5-HT receptor which is probably the cause of side effects, such as for example gastrointestinal and neurological side effects. A further flaw is the delayed onset of the entire efficacy spectrum. In the initial 14 days of treatment, the increased 5-HT level in the synaptic cleft induces desensitization of the respective receptors. Only after this initial period, the serotonergic excretion is stimulated resulting in an increased serotonergic neurotransmission, finally relieving the patient from symptoms (Pacher and Kecskemeti, 2004; Vaswani *et al.*, 2003). Data regarding the remission rate after SSRI treatment depend on study set-up, but however, remission rates are clearly below 50% (Maoz, 2007; Trivedi *et al.*, 2006). In the case of therapy failure, dosage augmentation or switching to other pharmacological agents is an option (Connolly and Thase, 2011). On the long run, the development of novel antidepressant agents is the attempt of basic research and pharmaceutical industry, and the perspective for the rising number of patients suffering from depression and anxiety-disorders. Furthermore, the question, why established psychopharmacological agents achieve remission in one patient but not in the other, the issue of genomic variability in depression and associated diseases needs to be addressed anew.

### **2.8 Psychopharmacotherapy of the future – a step towards personalized medicine?**

Treatment success after application of well established psychopharmacological agents was shown to be influenced by SNPs in genes contributing to biological circuitries which are known to be involved in depression and anxiety disorders. Binder and colleagues

reported that a SNP within the gene encoding for the human corticotropin releasing hormone binding protein (CRHBP) is significantly influencing both, remission as well as improvement of depressive symptoms in response to citalopram application, though in an ethnicity-dependent manner (Binder *et al.*, 2010). Based on findings like this, allelic genotypes can be attributed to poorer or advantageous treatment response. SNP genotyping prior to treatment initiation might support the selection of the psychopharmacological agent best suiting the patient and, hence, serve as prognostic tool to therapy success.

## **2.9 The use of animal models to unravel neurobiological underpinnings of depression and associated diseases**

With the objective to unravel neurobiological underpinnings of depression and associated diseases, animal models have long been used. Complex human diseases and, in particular, affective disorders are though not to be captured in their entirety of aspects, but the modeling of precise neurobiological and pathophysiological features was done successfully in the past (Matthews *et al.*, 2005). Independent of the pathobiological feature, which is mimicked by the model, there are three general criteria animal models are expected to fulfill, namely face-, construct- and predictive validity. Face validity is given if the animal phenotype resembles the human phenotype which is aimed to be modeled. Construct validity stipulates pathobiological parallels between humans and the animal model. The criterion of predictive validity is fulfilled if manipulation of the model organism, for example via pharmacological application, achieves similar results than in humans (Neumann *et al.*, 2011).

In the field of psychiatric science and, in particular for genetic approaches, the mouse proved to be a favorable model organism. This is, on the one hand, based on the pronounced genomic homology between men and mice. On the other hand, in anatomical and physiological features of the brain as well as in the response to pharmacological treatment mice show similarity to humans. And last but not least, despite the obvious physiognomic differences between the species, the behavioral characteristics are similar, too (Tecott, 2003). The explicit advantage coming along with the mouse as a model organism is the almost infinite opportunity to manipulate the mouse genome. This can either be done by alteration of a specific locus of interest (transgenic, knockout, knockin mice) or via selective breeding approaches focusing on a trait of interest. Inbreeding strategies, on the one hand, reduce genetic heterogeneity and, on the other hand, accumulate and conserve genetic characteristics which determine the trait of interest (Cryan and Holmes, 2005; Phillips *et al.*, 2002; Tecott,

2003). This enrichment of trait relevant alleles facilitates investigation and most importantly, allows bridging the gap between genetic features and phenotypic traits. Two mouse models of affective disorders, which were generated based on selective and bidirectional breeding approaches, were used in the context of this study and will be described as follows.

### **2.9.1 The HAB/LAB mouse model reflecting extremes in trait anxiety**

Using a strictly selective and bidirectional mating protocol, a mouse model reflecting extremes in trait anxiety was generated. It comprises three mouse lines which, independent of gender, display either high anxiety-related behavior (HAB), normal (intermediate) anxiety-related behavior (NAB) or low anxiety-related behavior (LAB). The breeding paradigm is based on the degree of avoidance of the unprotected, aversive environment presented by the open arm of the elevated plus-maze (EPM) (Kromer *et al.*, 2005). HAB mice spend only about 10% of their time on the open arm, reflecting the highly anxiety-related behavioral trait of this line. LAB mice, on the contrary, spend more than 50% of their time of the open arm showing a particular low degree of avoidance behavior towards the aversive environment (Kromer *et al.*, 2005).

For this mouse model, more than 250 outbred Swiss CD-1 mice (CD-1 mice) descending from than 25 litters served as founder population. These mice were behaviorally characterized on the EPM and subsequently classified in lines spending the lowest and the most time on the open arm of the EPM, respectively. For the first eight generations, an outbreeding protocol was conducted by selectively mating mice of different litters but identical lines with each other. This initial outbreeding was performed to enhance the genomic pool of alleles determining the extremes in trait anxiety and reducing the risk of genetic drift. After generation eight, more than 40 generations of mice were selectively inbred according to their anxiety-related behavior, which involves every animal being classified at the age of seven weeks regarding its behavior on the EPM. Animals not fulfilling the breeding criterion are eliminated from the mouse model. Starting after 23 generations of HAB/LAB breeding, an intermediate control line, namely NAB mice, were generated spending about 35% of the testing time on the EPM on the open arm (Kromer *et al.*, 2005). Figure 2 displays the development of the anxiety-related behavior of particular lines over the generations.

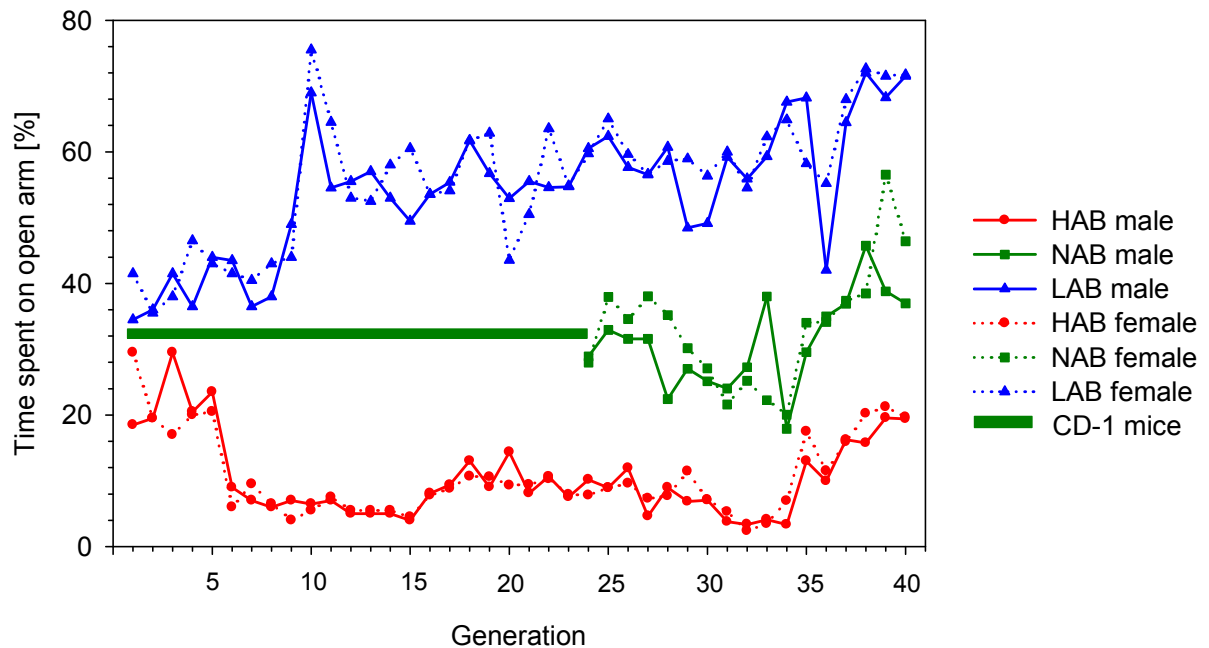


Figure 2: Graphic illustration of the development of trait anxiety over 40 generations of selective breeding of HAB and LAB mice. Trait anxiety is reflected by the percentage time animals spent on the open arm of the EPM, the parameter which served as selection criterion for selective mating. Initial differences in trait anxiety deviated further over the generations reaching kind of a steady state after about ten generations.

The HAB/LAB mouse model was used for extensive studies regarding behavioral, genetic, proteomic, cognitive, and brain physiological correlates of extremes in anxiety-related behavior. The extremes in trait anxiety were not only detected in EPM testing, but also in further behavioral paradigms testing anxiety-related behavior, like for example dark-light box tests (Kromer *et al.*, 2005). Furthermore, HAB animals display increased levels in depression-like behavior, which was shown in increased degrees of passive stress coping styles in forced swim (FST) and tail suspension (TST) tests. This co-occurrence of increased levels of anxiety-related with increased levels of depression-like behavior models the comorbidity of depressive with anxiety disorders. One major finding based on this mouse model was, for example, the identification of Glyoxalase I as a potential protein marker for trait anxiety (Hambusch *et al.*, 2010; Kromer *et al.*, 2005). Recently, combined metabolic and proteomics analyses indicated the contribution of diverging mitochondrial pathways to extremes in trait anxiety (Filiou *et al.*, 2011). As the selective breeding paradigm ensured an accumulation of genetic characteristics determining extremes in trait anxiety (Phillips *et al.*, 2002), and therefore the pronounced genetic predisposition of HAB and LAB mice towards extremes in anxiety-related

behavior predestines this model to extensively study the genetic differences between the lines in order to unravel genetic underpinnings of trait anxiety. In the study presented here, these animals were used for sequence-based analysis of loci presumably determining extremes in trait anxiety.

### **2.9.2 The stress reactivity mouse model**

The second mouse model used in this study was the stress reactivity (SR) mouse model (Touma *et al.*, 2008). The selective breeding paradigm of the SR mouse model is based on the plasma corticosterone increase after subjecting the animals to a restraint stressor, which reflects extremes in the dysregulation of the HPA axis. HPA axis dysregulation, in turn, is a key phenotype in modeling endophenotypes of MDD. In similarity to the HAB/LAB mouse model, this model consists of three separate breeding lines with distinctively different HPA axis reactivity in response to stress. The high reactivity (HR) mouse line displaying an excessive corticosterone increase and hence, a hyperreactivity of the HPA axis, the intermediate reactivity (IR) mice which, serve as standard control for physiological HPA axis reactivity, and the low reactivity (LR) mice showing sub-standard corticosterone increase caused by HPA axis hyporeactivity. In either case, two sublines were generated. In similarity to the HAB/LAB model, this mouse model was generated based on a founder population of 200 CD-1 mice. The selective and bidirectional breeding protocol was started from the first generation, but ensuring interfamilial breeding to reduce the risk of genetic drift. Figure 3 shows the development of the corticosterone increase for male and female HR, IR, and LR mice, respectively, over the first six generations. In addition to corticosterone increases after SR testing, it was found that further HPA axis parameters differed between the lines. For example, ACTH concentrations under basal conditions differed significantly between HR and LR mice with HRs showing elevated measures. Furthermore, similar to the HAB/LAB mouse model, behavioral phenotypes were investigated. In general, HR mice displayed a more active coping style when being subjected to stressful and aversive situations, whereas LR mice showed a rather passive stress coping strategy. Along this line, depression-like and anxiety-related behavioral features were observed in these animals. In summary, HR mice resembled a melancholic sub-type of depression, whereas LR mice revealed characteristics associated with atypical depression (Touma *et al.*, 2008). Furthermore, studies investigating cognitive abilities of HR, IR, and LR mice revealed memory deficits in hippocampus-dependent tasks in HRs, comprising reduced hippocampal levels of brain-derived neurotrophic factor (Knapman *et al.*, 2010a; Touma *et al.*, 2008). In addition, HRs were further shown to perform poorly in reversal learning tasks and to

display disrupted latent inhibition (Knapman *et al.*, 2010b). This seems not surprising as it is known that exposure to elevated levels of glucocorticoids is associated with cognitive impairment (McCormick and Mathews, 2010).

The heritability for this mouse model was estimated to be 40%, which is in accordance with earlier findings regarding the heritability of glucocorticoid release upon exposure to stressors in a variety of species (Touma *et al.*, 2008).

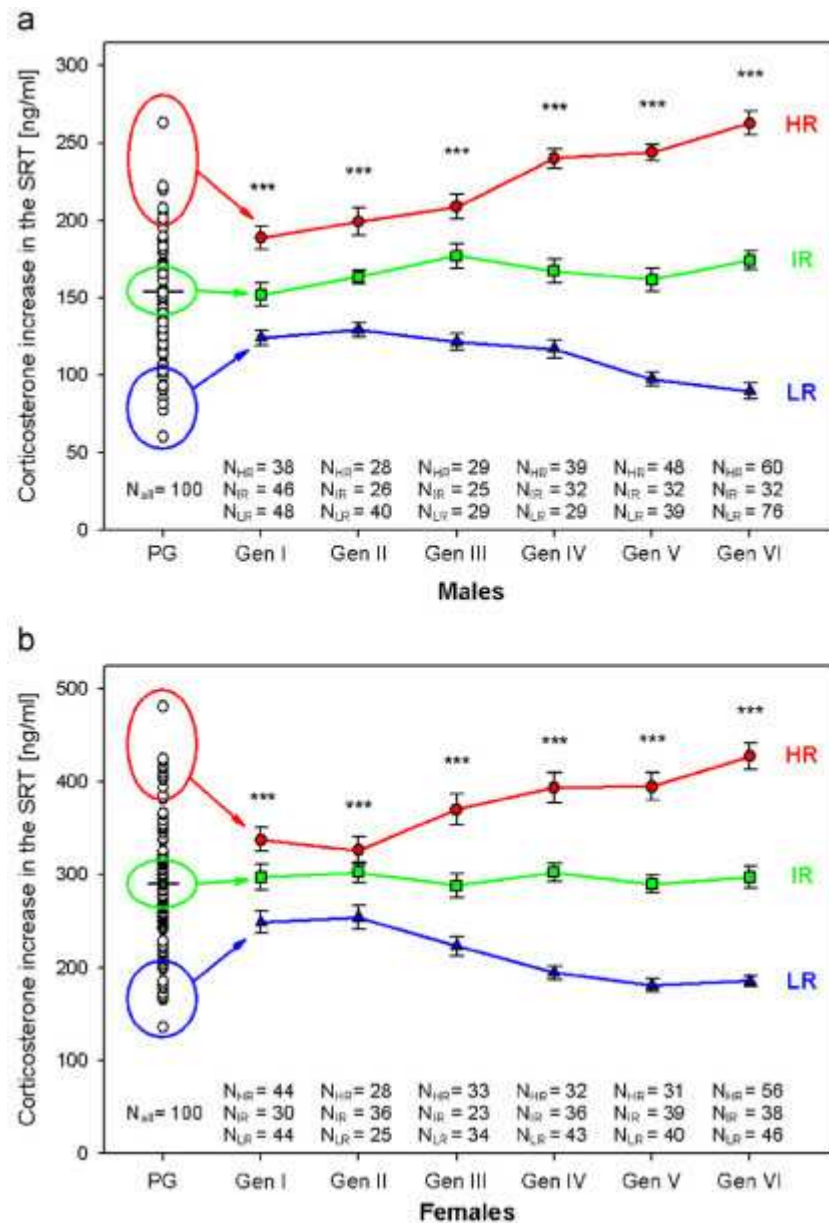


Figure 3: Graphic illustration of the corticosterone increase in male (a) and female (b) HR, IR, and LR mice after exposure to a 15 min restrain stressor. After generation four, the average corticosterone increase in males was >200 ng/ml in HRs, around 150 ng/ml in IRs, and <100 ng/ml in LR. The corticosterone increase in HR males deviated even further in the following generations to an approximate average value of 350 ng/ml in generation twelve. In female mice, the detected corticosterone increases were generally higher compared to male mice. The corticosterone increase in HR females was measured with >400 ng/ml, in IRs around 300 ng/ml, and <200 ng/ml in LR. (Figure adopted from Touma *et al.*, 2008.)

## **2.10 Technical progress in methods applied for the generation of transcriptome- and sequence-based genomic data**

In the last years, the generation of genetic data, no matter if transcriptome- or sequence-based, was eased in many ways.

To visualize this development, the generation of the first 'whole' genome sequence (whole meaning about 99% of the gene-containing regions of the human genome) was finished 2003. This 'Human Genome Project' was conducted with international scientific efforts, took about 13 years and did cost about 2.7 billion US Dollar. This was, by the way, faster and cheaper than originally expected (<http://www.genome.gov/11006929>). Today, about eight years later, the generation of a whole genome sequence via next-generation sequencing (NGS) can be achieved by one technically skilled person within two weeks for approximately 8,000 US Dollar (Peter Weber, personal communication). This comparison might appear striking, but it underlines the almost inflationary technical progress in the field.

The challenge in the field of psychiatric research is therefore not the generation of genetic data. The challenge is the attribution of functional relevance to sequence- and transcriptome-based genomic findings. The question in how far expressional profiles and variable sequences detectably infiltrate the behavioral level and determine endophenotypes needs to be answered in order to understand the multilevel and complex underpinnings of depression and associated diseases.

The contribution of both expressional differences and of sequence variations to neurobiological diseases was proven sufficiently. In this aspect, Alzheimer's disease seems like a good example. It was shown, that a mutation in the amyloid precursor protein can cause early onset of Alzheimer's disease and furthermore (Goate *et al.*, 1991), apolipoprotein E type 4 can influence the risk of late onset Alzheimer's disease in a gene dose-dependent manner (Corder *et al.*, 1993).

## **2.11 Aim and scope of this study**

The major and comprehensive aim of this study was to unravel genetic underpinnings of depression and associated diseases. The attribution of functional relevance at behavioral level to genetic data gained from two mouse models of affective disorders was intended applying a heterogeneous variety of techniques. Thereby, the impact of transcriptome- and sequence-based characteristics on behavioral endophenotypes displayed by HAB/LAB and HR/LR mice were investigated.

First, gene expressional profiling approaches were aimed to identify the pool of differentially regulated genes in the hippocampus of HR vs. LR mice. Furthermore, the

functional relevance of selected genes, detected to be differentially expressed in respect to extremes in stress reactivity of HR and LR mice, were intended to be characterized. Second, in order to be able to identify genetic markers determining the endophenotypes of HAB/LAB and HR/LR mice, a primary genome-wide association study in an outbred population of CD-1 mice was performed to detect loci associated with depression-like and anxiety-related behaviors, as well as with extremes in stress-reactivity. It was further targeted to provide the basis for the extension of this association study to a larger population of outbred CD-1 mice.



### 3 Animals, materials, and methods

#### 3.1 Experimental animals

All experimental animals used for the experiments described in this thesis were kept in type-2 Makrolon standard cages with access to food (no. 1314; Altromin GmbH, Lage) and tap water *ad libitum* in the animal facilities of the Max Planck Institute of Psychiatry. Standard housing conditions included equipment of cages with nesting and bedding material, standardized room temperature and humidity ( $23 \pm 2$  °C, 60%), and a 12-hour light/dark cycle (beginning light phase at 8 am). Before any behavioral test, a 1-hour adaptation to the light phase was allowed; behavioral tests and collection of tissue were finished the latest at 1 pm. Mice were either single or group-housed (three to five mice per cage), depending on the respective scientific context. If not indicated otherwise, mice were aged between 12 - 20 weeks when used for behavioral testing or tissue collection. In this thesis, animals of the following mouse models and mouse strains, respectively, were used: HAB/LAB mice, HR/LR mice, heterozygous Cofilin-1 knockout mice, C57BL/6 and CD-1 wild-type mice.

##### 3.1.1 Inbred mouse models

As described in the introduction, HAB and LAB mice, as well as HR and LR mice, were generated applying bidirectional and selective breeding approaches (see 2.9.1 and 2.9.2; for details see Kromer *et al.*, 2005 (HAB/LAB) and Touma *et al.*, 2008 (HR/LR)).

##### 3.1.2 Heterozygous Cofilin-1 knockout mice

Heterozygous Cofilin-1 knockout (*Cfl-1<sup>+/-</sup>*) mice (2 females, 1 male) were kindly provided by Prof. Dr. Walter Witke from the Institute of Genetics at the University of Bonn and bred with C57BL/6 wild-type mice. The breeding resulted in offspring either carrying heterozygous deletions at the Cofilin-1 (*Cfl-1*) locus or WT animals. The generation of the *Cfl-1<sup>+/-</sup>* line was described earlier (Gurniak *et al.*, 2005). Briefly, two loxP sites, both flanking exon 2 of the *Cfl-1* gene, were introduced. By excision of the lox responsive elements, the deletion of the genomic sequence enclosed by the two loxP sites was achieved, resulting in a complete deletion of exon 2 and, in addition, a frame shift mutation and a translational termination for the remaining *Cfl-1* sequence.

### **3.1.3 C57BL/6 wild-type mice**

Male and female C57BL/6 wild-type mice (WT), provided from the animal facility at the Max Planck Institute for Neurobiology in Martinsried, were used for breeding with *Cfl-1*<sup>+/-</sup> mice.

### **3.1.4 CD-1 mice**

Male outbred CD-1 mice were purchased from Charles River Laboratories (Sulzfeld) at the age of eight weeks. In this study, CD-1 mice were used for the so-called 'CD-1 panel', which involved phenotypic and genotypic characterization of mice.

## **3.2 Behavioral experiments**

All behavioral experiments were conducted with authorization of the local authorities and according to the current directives of the European Union (86/609/EEC) for animal experimentation in vertebrates.

### **3.2.1 Assessment of anxiety-related behavior**

The main principle of testing anxiety-related behavior in mice is based on subjecting animals to an approach-avoidance conflict (Bailey and Crawley, 2009). Mice have an innate exploratory drive and tend to investigate unknown territory, but at the same time they prefer a protective and familiar environment. The repellent stimulus in the unprotected environment is typically increased by illumination (Bailey and Crawley, 2009; Crawley, 1999). In the three following tests, mice were exposed to potentially challenging situations, but as well given the choice to retract to a secure environment while tracking their behavior. Mice were subjected to these tests for 5 min. In between testing animals, the apparatus was cleaned using soap water and 70% ethanol (Pharmacy Schwabinger Krankenhaus, Munich). Video tracking of animal's behavior during the test situation was done using Stoelting Any-maze software version 4.72 (Stoelting Co. West Lane, IL, USA).

#### **3.2.1.1 Open field test**

The apparatus of the open field (OF) test consisted of a round PVC barrier with a diameter of 60 cm and a height of 40 cm (Figure 4). In general, the illumination in the inner zone of the OF was brighter compared to the illumination in the outer zone creating an aversive area in the inner and a less challenging area close to the barrier. Depending on the differences in illumination between the inner and the outer zone, the OF test could

either serve as a classical test for anxiety-like behavior or, like in the context of this work, as a test to primarily assess the animals locomotion and exploratory behavior (Prut and Belzung, 2003; Walsh and Cummins, 1976); hence, the light intensity did slightly differ between the central part and the periphery of the OF arena (approximately 15 lx). The key criterion in the OF test was therefore the total distance animals travelled in the apparatus and not primarily a differentiation between the distances travelled in the inner vs. the outer zones which would have allowed a conclusion regarding the anxiety-like behavior of the animals (Crawley, 1999). Another important parameter in the OF test was the number of rearings as an indicator for the animal's explorative drive, hereby differentiating between free and wall rearings. In the beginning of a testing period, animals were placed in the center of the arena.



Figure 4: OF test apparatus with a brighter illuminated inner zone than outer zone. The inner zone, therefore, constitutes a more aversive environment compared to the outer zone.

### 3.2.1.2 Elevated plus-maze test

The elevated plus-maze (EPM) was a cross-shaped maze consisting of two closed and two open arms, which were connected via a neutral zone (Lister, 1987; Pellow *et al.*, 1985). The PVC maze was elevated by 40 cm, open arms were 30 x 5 cm, closed arms were 30 x 5 x 15 cm, and the neutral zone had an extension of 5 x 5 cm (Figure 5). The weakly illuminated closed arms (10 lx) of the maze reflected a protected environment, whereas the brighter illuminated open arms (300 lx) constituted an aversive environment for the animals (Hogg, 1996). In summary, the more time animals spent in the closed area of the EPM, the more anxious their behavior was considered. In contrary, the more time animals spend in the aversive open area of the EPM and hence followed their exploratory drive, the less anxiety-related the behavior was rated. The number of full or

partial entries into the different arms was also taken into account. In addition, the total distance travelled on the maze was considered a locomotion parameter and also contributed to the estimation of the animal's behavior. At the beginning of the EPM test, animals were placed in the neutral zone facing a closed arm.



Figure 5: Elevated plus-maze apparatus, consisting of two closed and two open arms, which are connected via a quadratic neutral zone.

### 3.2.1.3 Dark-light box test

The apparatus of the dark-light (DL) box was a rectangular PVC box with a smaller black compartment (15 x 20 x 25 cm), and a larger white compartment (30 x 20 x 25 cm; Figure 6). The two compartments were connected via a tunnel of 5 cm length. The illumination of the two compartments differed clearly, thereby creating an explicitly aversive environment in the light compartment and a secure compartment in the dark part of the box (Bourin and Hascoet, 2003; Crawley and Goodwin, 1980). The illumination of the light compartment depended on the gender of animals. Female mice were subjected to 700 lx in the light compartment, male mice to 400 lx. The illumination for mice of both genders in the dark compartment was 15 lx. Initially, animals were placed in the dark compartment of the DL box (Costall *et al.*, 1989).



Figure 6: DL box apparatus existing of a light (larger, higher illuminated) and a dark compartment (smaller, marginally illuminated).

### 3.2.2 Assessment of depression-like behavior

The conceptual basis for the assessment of depression-like behavior in mice is the comparison of an active vs. passive coping style which animals display when being exposed to a desperate, inescapable and unpredictable situation (Cryan and Holmes, 2005; Jacobson and Cryan, 2007). An animal's behavior was evaluated as depression-like when the animal showed a passive coping style in a way that it appeared to accept the desperate situation without major attempts to escape the unpleasant state. An active coping style was characterized by intensive physical efforts to get away from the desperate situation. The duration of the tests for the detection of depression-like behavior was 6 min. During testing, animals were video-tracked; the subsequent analysis of video-material was done using Eventlog 1.0 software (EMCO) by a person being blind to the experimental group of the test animal.

#### 3.2.2.1 Tail suspension test

The tail suspension test (TST) executes a haemodynamic stress to the animals (Cryan *et al.*, 2005; Steru *et al.*, 1985). Four animals at a time were subjected to the TST by suspending them at their tail tips to a metal framework (Figure 7). Their coping styles during this inescapable situation were evaluated by differentiating between mobile (active coping style) and immobile phases (passive coping style). The more immobile periods an animal displayed during this test, the more depression-like the behavior of the respective animal was rated.



Figure 7: During the TST procedure mice are suspended by their tail tips from a lever of a metal framework.

### 3.2.2.2 Forced swim test

The “Porsolt’s” forced swim test (FST) was originally published as “a primary screening test for antidepressants”, and in this way was also widely used for the screening of depression-like behavior. In the FST, a physically and mentally highly aversive stressor was provided to the animals (El Yacoubi and Vaugeois, 2007; Petit-Demouliere *et al.*, 2005; Porsolt *et al.*, 1977; Porsolt *et al.*, 1978). Mice were placed into 2 l glass cylinders which were filled with 1.75 l tempered water (23 °C). It was excluded that mice could touch the beaker’s ground with their tails, neither could they escape from the glass cylinder by climbing (Figure 8). The behavior mice showed during the test period was differentiated between struggling, swimming, floating (Steiner *et al.*, 2008; Varadarajulu *et al.*, 2011), and freezing behavior (Crawford and Masterson, 1982; Gross *et al.*, 2000). An absolute rigor, usually occurring immediately after placing the mouse mice into the water, was scored as freezing behavior. Struggling involved vehement movements of all four limbs with mostly fore-paws above the water surface. The animal’s body axis was almost horizontal during struggling periods. Swimming was scored when the mouse showed coordinated movements with all four paws under the water surface. The body axis was horizontal and the animal covered a distance when swimming. Passive periods with no movements or slight balancing movements in order to maintain the passive condition were scored as floating. Typically, in the beginning of the testing period the animals showed active coping strategies, starting with vigorously struggling and swimming, followed by passive periods of floating behavior. The total time spent floating was considered as the main parameter of the FST indicating depression-like behavior.



Figure 8: Experimental set-up of FST experiments displaying the inescapable situation for testing animals in a 2 l glass cylinder.

### 3.2.3 Assessment of stress reactivity

In order to test an animal's stress reactivity, the so-called stress reactivity test (SRT) was conducted (Touma et al., 2008). This test involved the collection of an initial blood sample from the animal's tail vessel, followed by the animal's subjection to a 15 min period of a restraint stressor and the subsequent collection of a reaction blood sample, again from the tail vessel. The initial blood sample reflected the resting condition as it was taken right after removing the mouse out the home cage. Directly after blood sampling, the mouse was placed into a 50 ml Falcon tube (Sarstedt, Nümbrecht), equipped with a hole in the ground allowing ventilation and a hole for the tail in the cap of the tube (Figure 9). After 15 min, the mouse was removed from the tube, the reaction blood sample was immediately taken and the animal was put back into the home cage. The SRT of *Cfl1*<sup>+/-</sup> and WT control mice was conducted with slight modifications, as in addition to the standard procedure described above recovery samples were collected 60 min after the reaction blood samples.

Blood samples (in each case approximately 50  $\mu$ l) were collected using heparinized capillaries (Micro haematocrit tubes, Brand GmbH and Co KG, Wertheim). Capillaries were sealed using a Haematocrit sealing compound (Brand GmbH and Co KG, Wertheim) and centrifuged for 5 min at 14,800 g to separate cellular and plasma components of the blood. Plasma was collected and stored at -20 °C for further analyses.

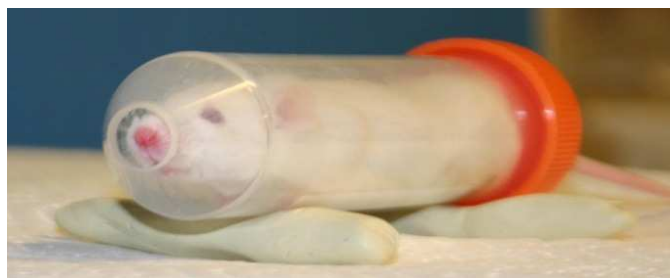


Figure 9: The restraint stressor mice are subjected to during the SRT is presented by tubing animals into a 50 ml Falcon tube. The test procedure also involves the covering of the tube with a lid.

### 3.2.4 Behavioral test batteries performed in this study

#### 3.2.4.1 Behavioral test battery conducted for phenotypic characterization of *Cfl-1<sup>+/-</sup>* vs. WT mice

At the age of eight to twelve weeks, male and female *Cfl-1<sup>+/-</sup>* and WT mice were separately subjected to a behavioral test battery. In this behavioral test battery (Figure 10), the OF was primarily chosen as a test for locomotion, followed by two paradigms for the testing of anxiety-related behavior, the FST for monitoring depression-like features, and finally the SRT to test the animal's stress reactivity. In all behavioral tests, WT littermates served as control animals.

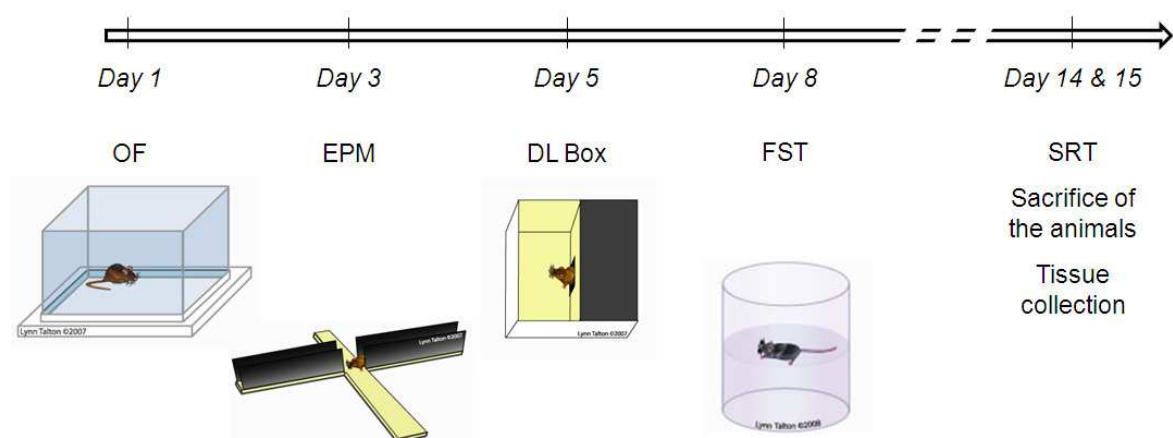


Figure 10: Illustration of the behavioral test battery *Cfl-1<sup>+/-</sup>* and WT mice were subjected to. The order of behavioral tests was arranged according to an increase of stress intensity. (Illustrations of behavioral test apparatuses were adopted from Lynn Talton available at <http://btc.bol.ucla.edu/neuroscreen.htm>.)

### 3.2.4.2 Behavioral test battery conducted for phenotypic characterization of an outbred population of CD-1 mice

384 male CD-1 mice were subjected to the 'CD-1 panel' behavioral test battery assessing locomotion, anxiety-related and depression-like behavior, as well as stress reactivity of the animals. Animals were subjected to this test battery in eight separate batches of 48 mice. After arriving from Charles River Laboratories, mice were allowed to habituate for four days before 24 mice (half the animals of a batch) were tested on the EPM and the other half in the OF. Two days later, animals, which were EPM tested already, were subjected to the OF and *vice versa*. After the FST, which followed again two days later, mice were allowed to rest for four days before they were subjected to the physically and mentally stressful SRT. The final test of the test battery was the TST. After this, mice were sacrificed and tail tips were collected for DNA extraction. The time course of the test battery is shown in Figure 11.

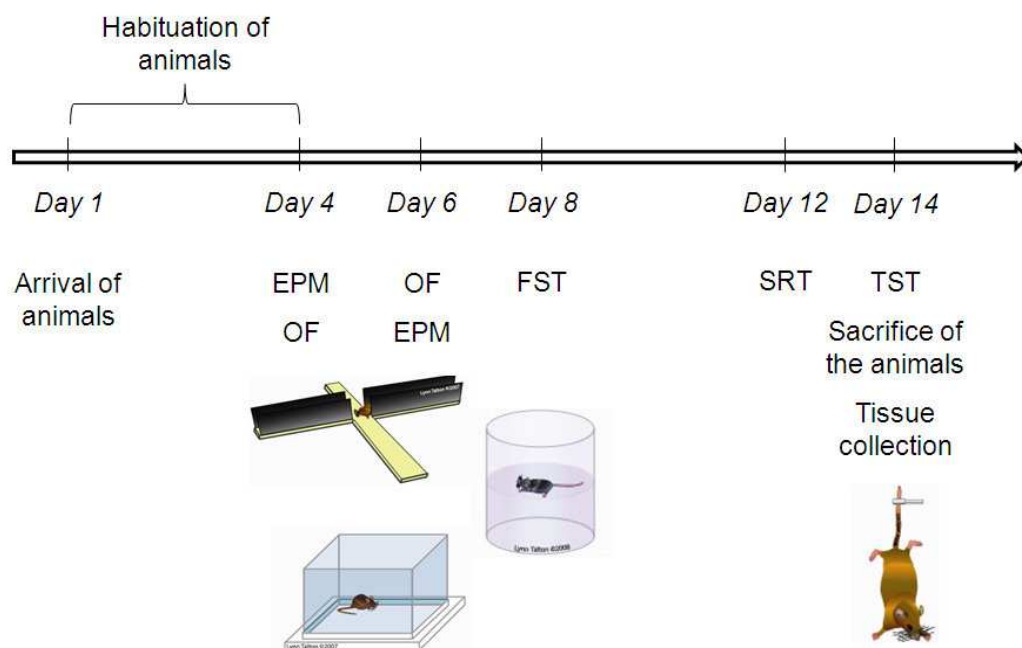


Figure 11: Graphic illustration of behavioral test battery animals of the 'CD-1 panel' were subjected to. (Illustrations of behavioral test apparatuses were adopted from Lynn Talton available at <http://btc.bol.ucla.edu/neuroscreen.htm>.)

### 3.3 Sacrifice of animals

Animals were sacrificed after administration of anesthesia. Mice were therefore placed into an inhalation chamber saturated with Isoflurane (Curamed Pharma, Karlsruhe). The anesthetized animal was immediately killed by decapitation.

### **3.4 Dissection of embryos**

Pregnant females were sacrificed on day 18 of pregnancy (ED 18). Immediately, the uterus was opened and embryos were extracted from the amniotic sacs. Embryos were promptly sacrificed by decapitation and the heads were collected in ice cold PBS (Table 3) for further extraction of the hippocampus.

### **3.5 Collection of brain and hippocampal tissue from embryonic and adult mice**

Brains were gained immediately after sacrificing the animal by opening the cranial bones along the sagittal suture, laterally removing the cranial bones and raising the brain from the base of the skull. Hippocampal tissue was collected separating the two hemispheres with a scalpel. The hemisphere was fixed at the cerebellum and the cerebrum was removed with a sliding movement using a spatula, thereby exposing the hippocampus. Hippocampal tissue was displaced from the cerebrum using curved forceps. The procedure was conducted on an iced surface. Hippocampal tissue, as well as rest brain tissue, was frozen at -80 °C for further analyses. Hippocampal tissue of embryos was collected in a cell culture plate (5 cm diameter; Nunc A/S, Roskilde, Denmark) filled with iced dissection medium containing HBSS medium, Pen/Strep, 1M HEPES, and 200 mM L-Glutamine (all from Invitrogen, Darmstadt) using a binocular microscope (Olympus U-TV0.5XC-3, Hamburg).

### **3.6 Nucleic acid based methods**

#### **3.6.1 RNA based methods**

Whenever processing RNA, protocols were conducted under a fume cupboard (Köttermann Systemlabor type 2-453-DAHD, Uetze-Hänigsen) to prevent contamination with RNAses. In addition, surfaces and equipment were treated with 0.1M NaOH (Merck, Darmstadt), followed by 70% ethanol, and pipette tips with a special security standard (Sarstedt, Nümbrecht) were used.

##### **3.6.1.1 Extraction of total RNA from hippocampal tissue**

Hippocampal tissue was thawed on ice and immediately homogenized using a pestle, fitting the conical shape of 1.5 ml Eppendorf tubes (Eppendorf, Hamburg). 1 ml TRIzol (Invitrogen) was added stepwise (Chomczynski and Sacchi, 1987). After vortexing vigorously, the homogenate was incubated at RT for 5 min. 0.2 ml chloroform (Sigma-Aldrich, Taufkirchen) per ml TRIzol were added, mixed vigorously and again incubated at

RT for 3 min. After a centrifugation step for 15 min at 21,000 g and 4 °C, the clear supernatant was transferred into a clean Eppendorf tube. 0.5 ml ice cold isopropanol (Sigma-Aldrich) per ml TRIzol were added, the sample was vortexed and incubated at -20 °C overnight. The day after, the extraction process was continued by centrifugation for 10 min at 21,000 g and 4 °C. The supernatant was discarded and 1 ml ice cold ethanol 70% per ml TRIzol was added to precipitate RNA. After vortexing and centrifuging for 5 min at 10,000 g and 4 °C, the supernatant was again discarded and the RNA pellet was air-dried for approximately 20 min. After complete vaporization of the alcohol, the RNA pellet was dissolved in 50 µl RNase-free water (Ambion, Austin, TX, USA). The amounts of this protocol were used for RNA extraction of hippocampal tissue from adult animals. If hippocampal RNA was extracted from younger mice, the measurements were adapted. For example, for the RNA extraction of hippocampi from ED 18 mice 300 µl TRIzol were used, and further amounts were reduced accordingly.

### **3.6.1.2 Control measures of RNA quality and determination of RNA concentration**

RNA was quality checked by using Agilent RNA NanoChips and the Agilent 2100 Bioanalyzer (Agilent Technologies, Böblingen). The RNA integrity number (RIN factor) was measured and taken as standard measure for RNA quality. RIN factors >7.15 were considered showing satisfactory RNA quality (Kiewe *et al.*, 2009). If RNA samples were used for microarray purposes, probes were quality checked twice, before and after amplification. Using the Bioanalyzer, concentration of RNA probes was determined simultaneously.

Alternatively, RNA concentration was detected using an Implen NanoPhotometer (Implen, München). Usually, lidfactor 50 was chosen for the determination of RNA concentrations. In case of low RNA yields, lidfactor 10 was used. The absorption ratio detected at 260 and 280 nm (A260/A280) which was automatically detected by the NanoPhotometer served as control parameter. A ratio of about 1.8 was considered showing satisfactory RNA quality. Likewise, the NanoPhotometer was also used for the determination of DNA concentrations and A260/A280 ratios.

### **3.6.1.3 Reverse transcription of RNA into cDNA**

RNA was reversely transcribed into cDNA using the High-Capacity cDNA Reverse Transcription Kit (Applied Biosystems, Darmstadt) strictly following the manufacturer's instructions. Briefly, 2.0 ml 10x RT buffer, 0.8 µl 25x dNTP mix (100 mM), 2.0 µl 10x RT random primers, 1.0 µl Multiscribe Reverse Transcriptase, 4.2 µl nuclease-free water and a total volume of 10 µl RNA were mixed on ice. A 4-step program was run (25 °C

10 min, 37 °C 120 min, 85 °C 5 min, 4 °C *ad infinitum*) in a thermal cycler (Peqlab primus 96 advanced PCR machine; Peqlab, Erlangen).

#### **3.6.1.4 RNA amplification for array analysis**

Total RNA from seven HR, and eight LR mice was processed for array analysis strictly following the instructions of the Illumina TotalPrep RNA Amplification Kit (part number AMIL1791; Ambion). In short, 250 ng total RNA were reversely transcribed into first strand cDNA using T7 oligo (dT) primers. Incubation for first strand cDNA synthesis at 42 °C and for second strand cDNA synthesis at 16 °C was done in the thermal cycler. Newly synthesized dsDNA transcription templates were purified and subsequently processed into cRNA. Therefore, incubation at 37 °C was done for 14 h in a 37 °C incubation chamber. Subsequent cRNA purification was performed using a PHMT Grant-bio thermo-shaker (Keison, Essex, UK). Assessment of purified biotin-labeled cRNA yield and quality was done via bioanalyzer analysis (see 3.6.1.2). In a direct hybridization assay, an Illumina gene expression beadchip array (type MouseWG-6\_V2\_0\_R2\_11278593\_A; Illumina, San Diego, CA, USA) was chosen for expressional profiling of cRNA. Hybridization was performed strictly following the manufacturer's instructions and using the equipment recommended by Illumina. The fluorescence based hybridization signals were detected using a BeadStation scanner and BeadStudio Gene Expression Analysis Module 3.4.0 software, both by Illumina. Statistical analysis of the microarray experiment was described under points 3.8.1.1 and 3.8.1.2.

#### **3.6.1.5 Serial analysis of gene expression**

A serial analysis of gene expression (SAGE) was conducted as an alternative transcriptome analysis. Here, pooled samples of total RNA from HR and LR animals were used for expressional profiling. The HR RNA-pool consisted of total RNA from seven HR animals in equal shares; the LR RNA-pool was prepared from eight animals accordingly.

The library was prepared following the manufacturer's instructions in the standard protocol of the Applied Biosystems SOLiD 3 System kit (Invitrogen, Paisley, UK). In short, each RNA pool contained 1 µg total RNA as starting material. The poly(A) tail of the total RNA was bound to magnetic beads and first- and second strand cDNA synthesis from the RNA-magnetic bead-hybrid was done using SuperScript III Reverse Transcriptase provided in the kit. A *Nla* III digestion step was conducted cleaving the cDNA approximately every 250 bp, providing complementary binding sequences for Adapter A ligation. The Adapter A provided a 3-terminal *Eco*P15I restriction site, and the

first priming site for later PCR amplification. Afterwards, an *EcoP15I* digestion step was carried out, as this type III restriction endonuclease served as tagging enzyme. The resulting 60 bp tag consisted of approximately 33 bp adapter sequence plus 27 bp of a specific sequence unit from a RNA transcript. The subsequent Adapter B ligation delivered the SOLiD sequencing initiation site, plus the second PCR amplification site.

Template beads were prepared according to the SOLiD 3 Systems Templated Bead Preparation full-scale protocol starting with an upscale PCR (95 °C 2 min; 95 °C 30 s, 55 °C 1 min, 72 °C 1 min, 10 cycles; 72 °C 5 min). Upscale PCR products were run on a 4% agarose gel for size separation and quality control. SAGE tag templates appeared in a 100 bp fragment, which was extracted from the gel and purified via micro columns provided with the kit. In addition, product quality was checked using High Sensitivity DNA chips (Agilent Technologies) in the Agilent 2100 Bioanalyzer. 500 pmol of the purified and controlled product were used as template in the emulsion PCR (95 °C 5 min; 93 °C 15 s, 62 °C 30 s, 72 °C 75 s, 40 cycles; 72 °C 7 min) amplifying tag library onto beads and thus preparing the clonal bead population. According to the protocol, beads were purified, enriched and modified at the 3' terminal ends.

41 million beads per pool were deposited as octets on the slide and sequenced accordingly using the Applied Biosystems SOLiD Analysis Tool (SAT) v3.5 (Applied Biosystems, Carlsbad, CA, USA). The statistical analysis of the SAGE experiment was described under point 3.8.2.

### **3.6.2 DNA based methods**

#### **3.6.2.1 DNA extraction from mouse tissue**

Genomic DNA was extracted from either tail tips or brain tissue using the Genomic DNA from Tissue Nucleospin Tissue kit (Machery-Nagel, Düren). DNA extraction from brain tissue was carried out following the manufacturer's instructions of the standard protocol for human or animal tissue and cultured cells. Briefly, around 25 mg homogenized brain tissue was incubated in 180 µl buffer T1 and 25 µl Proteinase K at 56 °C overnight to digest and lyse the tissue using a thermo-shaker (Thermomixer 5436, Eppendorf, Hamburg). The day after, 200 µl lysis buffer B3 were added, and DNA was precipitated by adding 210 µl ethanol 96%. Further on, samples were loaded onto a Nucleospin tissue column and DNA was collected in the silica membrane of the column by centrifugation for 1 min at 11,000 rpm. After a first washing step with 500 µl buffer BW, followed by centrifugation for 1 min at 11,000 rpm and a second wash step with 600 µl buffer B5 and again centrifugation for 1 min at 11,000 rpm, the silica membrane was

dried, and DNA was eluted in 100 µl pre-warmed elution buffer. Extraction of genomic DNA from tail tips was performed according to the support protocol for mouse or rat tails which requires an extra centrifugation step after the overnight incubation. Here, samples were centrifuged for 5 min at high speed to pellet undigested tissue. 200 µl of the clear supernatant were collected and the protocol was continued as described above. Determination of DNA concentration and quality was done in analogy to the determination of RNA concentration and quality as described under point 3.6.1.2.

### **3.6.2.2 Polymerase-chain reactions and gel electrophoresis**

Polymerase-chain reactions (PCRs) were performed to amplify a DNA fragment of interest and subsequently visualize the amplicon in a gel electrophoresis. PCRs were conducted to genotype embryos regarding gender and to differentiate between mice being either heterozygous knockout or WT at the *Cfl-1* locus. All PCRs were prepared in ice and were run using a thermal cycler.

#### **PCR for specific amplification of the *Sry* locus**

A PCR specifically amplifying the *Sry* locus (*Sry* PCR) on chromosome Y was conducted to distinguish between male and female mice gained at ED 18. The detection of the *Sry* gene in this PCR was taken as a marker for a male genotype, whereas the absence of the *Sry* gene displayed a female genotype. The PCR mix for one sample contained 5 µl 10x DreamTaq buffer, 5 µl dNTP mix (2 mM each), 1 µM upstream primer, 1 µM downstream primer, 1 µg genomic DNA, 1.25 u DreamTaq DNA polymerase and nuclease-free water up to a total volume of 50 µl (Fermentas, St. Leon-Rot; oligonucleotide sequences see Table 1). DNA of adult male and female mice served as positive and negative controls, respectively. In addition, water controls containing water instead of DNA were prepared. The PCR was run in a touch-down program (95 °C 4 min; 95 °C 1 min, 66 °C 1 min, 72 °C 1 min, 5 repeats; 95 °C 1 min, 64 °C 1 min, 72 °C 1 min, 5 repeats; 95 °C 1 min, 62 °C 1 min, 72 °C 1 min, 5 repeats; 72 °C 10 min).

#### **PCR for genotyping of the *Cfl-1* locus**

The genotyping of the *Cfl-1* locus was done by PCR (*Cfl-1* PCR) using a set of three primers (A, B, and C primer; oligonucleotide sequences see Table 1). Amplification of DNA from mice carrying two WT alleles at the *Cfl-1* locus resulted in one distinct amplicon with a fragment size of 380 bp. DNA of mice carrying a heterozygous knockout at the *Cfl-1* locus showed one WT amplicon and, in addition, a 170 bp fragment, which is

the PCR product of the truncated *Cfl-1* allele. The PCR reaction for one sample contained 10 µl 5x Colorless GoTaq reaction buffer, 5 µl MgCl<sub>2</sub> 25 mM, PCR Nucleotide Mix 10 mM 1 µl, 1 µM of each primer, GoTaq DNA polymerase (5u/µl) 0.25 µl, 1 µg genomic DNA and nuclease-free water up to 50 µl (Promega, Madison, WI, USA). Genotyping strategy, primer sequences and PCR conditions (94 °C 2 min; 94 °C 30 s, 58 °C 30 s, 68 °C 40 s, 35 repetitions; 68 °C 5 min) were kindly provided by Christine Gurniak (Gurniak *et al.*, 2005).

### **3.6.2.3 Gel electrophoresis**

PCR products were controlled and visualized via gel electrophoresis. Therefore, 1.5% agarose (UltraPure, Invitrogen) in TAE buffer (10.8 g TRIS (Roth, Karlsruhe), 5.5 g boric acid (Sigma, Taufkirchen), 0.7 g EDTA (Sigma), ddH<sub>2</sub>O *ad* 1 l; pH = 8.0) were microwave heated until all solid particles were dissolved. 5 µl ethidiumbromide (Roth) per 100 ml gel were added. After gel polymerization, 12 µl PCR product together with 2 µl 6x DNA loading dye (Fermentas) were loaded. ZipRuler Express DNA ladder 1 (Fermentas) served as DNA standard ladder. The gels were run at 110 V for 1 h in TAE buffer. After gel electrophoresis, DNA signals were visualized under UV light (BioDoc II Transilluminator; UVP, Upland, CA, USA) and documented using a digital graphic printer (UP-D860E; Sony, New York, NY, USA).

### **3.6.2.4 Precipitation of cDNA**

After reverse transcription of RNA into cDNA, genomic DNA fragments were precipitated via ethanol-based precipitation. Therefore, 20 µl cDNA were mixed with 2 µl sodium acetate 3 M (Sigma), 40 µl ethanol 96%, and 2 µl glycogen 10 mg/ml (Roth). The samples were vortexed and shock frozen in liquid nitrogen (Air Liquide, München). After centrifugation for 30 min at 21,000 g and 4 °C, supernatant was discarded and 300 µl ethanol 70% were added. After a second centrifugation step for 5 min at 21,000 g and 4 °C, the supernatant was again discarded and the samples were dried at 65 °C in the thermo block for 15 min, followed by 20 min at room temperature. cDNA pellets were dissolved in the appropriate volume of nuclease-free water; for example, 50 µl nuclease-free water were used for dissolving of cDNA from a whole hippocampus of an adult animal.

### 3.6.2.5 Quantitative real-time PCR

The principle behind quantitative real-time PCR (qPCR) analysis is a simultaneous amplification and quantification of PCR products allowing quantitative conclusions regarding a target gene's expressional activity (Higuchi *et al.*, 1993). Sybr Green was used as a fluorescent reporter signal. The fluorescence signal of a target gene was standardized to the fluorescence signal of a housekeeping gene and the result was seen as a relative expression value of the target vs. the housekeeping gene. The housekeeping gene used for qPCRs presented in this study was beta-2 microglobulin (*B2m*, Becker *et al.*, 2004). qPCR runs were analyzed using the absolute quantification fit point function of the LightCycler Software 4.05 and the LightCycler 2.0 instrument (Roche Diagnostics, Mannheim), thereby standardizing thresholds and noise bands of target and housekeeping genes to equal values. Crossing points (CPs) were transformed into fold changes (FCs) using the  $2^{-\Delta\Delta CT}$  algorithm (Livak and Schmittgen, 2001). As internal control, a pooled standard dilution series was prepared. Error rates below 0.05 and efficiencies of 2.0 were aimed. Samples as well as standards were measured in duplicates. CPs of duplicates deviating more than one CP were excluded from the analyses. Water controls (containing water instead of cDNA) and RT controls (containing negative sample of the RT instead of cDNA) were measured as well. The melting temperature ( $T_m$ ) of the amplicon was detected and equal  $T_m$ s were taken as a control measure for primer specificity.

qPCR primers were designed to be intron-spanning to guarantee the amplification of cDNA only (oligonucleotide sequences see Table 1). Primer pairs not fulfilling control parameters were discarded and redesigned.

Samples were prepared using QuantiFast Sybr Green PCR mastermix (Qiagen, Hilden) containing 5  $\mu$ l QuantiFast Sybr Green, 1  $\mu$ l forward primer 10 pM, 1  $\mu$ l reverse complementary primer 10 pM, 2  $\mu$ l cDNA and 1  $\mu$ l nuclease-free water. The conditions of the LightCycler program (95 °C 10 min; 95 °C 10 s, 60 °C 30 s, 40 repetitions; generation of melting curve: 50 - 95 °C with 0.1 °C/s temperature increase) were adjusted to the recommendations of the QuantiFast Sybr Green PCR mastermix.

### 3.6.2.6 Table of oligonucleotides

Table 1: List of oligonucleotids ('primers') used for experiments presented in this study. All primers were purchased from Sigma Aldrich.

Primer Table					
I. qPCR Primer					
Target gene	Forward sequence	T <sub>m</sub> [°C]	Reverse complementary sequence	T <sub>m</sub> [°C]	Product length [bp]
<i>Accn2</i>	AGT GCT ACA CAT TCA ACT CGG	61.72	CTC GTC CTG ACT GTG GAT CT	61.93	185
<i>Acot1</i>	AAG AAG CCG TGA ACT ACC TG	60.85	CTC ATC CTT GTA GGA GAT GGT	59.56	185
<i>Acot11</i>	ACA GCC TCT ATG GAT GAC ATC	60.53	CTG CTT CTC AGA GCA CAG AT	59.89	147
<i>Acot13</i>	AGA GTT CAT TCT CGC AGA GC	61.28	CTT CCA CCT TCA TCT CAC AGA	61.85	180
<i>Adam11</i>	CAG TGT CAC CTT CTA CCA CCA	62.64	AGA TCC TTC GCT CTC CAC TT	61.89	197
<i>Adam22</i>	CAC CCA CTT TCC TCA CAA T	59.96	TTC CTA AGA TGA GGG CCA G	61.72	128
<i>Aldh1l1</i>	GCT GGC TGG TGT GAT AAG AT	61.67	TTC CAG GAC AGC ATC ATT AAG	61.58	149
<i>Ash1l</i>	TTC AGA ACA TAA GAA GGG GGT	61.25	AGC ACA GGT TGC AAG GTA TT	61.12	195
<i>B2m</i>	CTA TAT CCT GGC TCA CAC TGA	59.30	CAT CAT GAT GCT TGA TCA CAT	60.96	130
<i>Bdnf</i>	TTC CAC CAG GTG AGA AGA GT	61.30	CAT TCA CGC TCT CCA GAG T	60.60	163
<i>Cfl-1</i>	ATG ATC TAT GCC AGC TCC AAG	63.01	CGC TGC CAC CTA GTT TCT CT	63.38	127
<i>Cntn6</i>	GAA TGC ATC GCA GGT AAC C	63.04	GTG TTG AGA CGT TGA CCA TTC	62.02	194
<i>Crtac1</i>	ATC TAC AGA TGA GTG CTC ACG	59.48	TTC TGT AGG CAA TGT TGT TGA	60.72	150
<i>Cyp4f13</i>	ATG TTC TCT TGA TGG CTG AG	59.39	TCG CCA GGT TGT AGA GAA T	59.82	138
<i>Cyp4f14</i>	ATA GCA CCA ACA TCA TGC AC	61.01	CCA GGA TGG CAG CAA TAT AT	61.25	174
<i>Cyp4f15</i>	ACA TCA TTC GAT CTG TTC TCA	59.67	CTC CAC TTG TCA CCA TCA CT	60.18	121
<i>Cyp4f16</i>	ATG TGC ATC AAG GAG AGT CTG	61.88	GATGCTGATGACA CAGATGTT	60.16	126
<i>Dap3</i>	GAG CTT CTG GGC TAC CTG A	62.11	AGC ATC TGG GAT ATG CAG AAT	62.31	156
<i>Fam116b</i>	AAC TCA TGC TTC TTG GGG A	62.22	GCT CCT TGA ACT CAC TGT CAT	60.89	156
<i>Fam123a</i>	ACA GGT GAC GTT CCG ATA AA	61.92	TTC AGT GAA GTC ACG TCA GAA	61.08	155
<i>Gabrg2</i>	TGC TCC TGC TAT CGC TCT A	61.40	TTG TCA TAC CCT TCC AGC A	61.7	184
<i>Hmgn3</i>	AGG TGC TAA GGG GAA GAA GG	63.30	GTC CCG AGA GGT ACG TGA AA	64.00	171
<i>Hsp90ab1</i>	CCT GAG GAA GTG	61.34	CAA TTT TCA GCT	62.42	217

	CAC CAT		CTT TCC CAC		
<b>Mthfd1</b>	AAG ACT GCC AAT CTG GAC AAG	63.13	CTG GAA CAT AAT TGA TCC CAC A	63.34	136
<b>Prodh</b>	ACA ATG TGA CCT TGG ATA TGG	61.06	ACA TAG TTA AGG CAC CTG TGG T	61.23	181
<b>Pvalb</b>	ACA TCA AGA AGG CGA TAG GA	61.18	GAG GAG AAG CCC TTC AGA AT	61.28	187
<b>Rgl1</b>	ACA CAC AGT CAG TCA GTA CGA G	59.46	AGC TCC AGC ACT TCC TTA GT	59.64	171
<b>Rps6ka5</b>	CGG TCT GAG TAA GGA GTT TGT	59.79	AAC ACC TAA GCT CCA CCA GT	60.19	142
<b>Sh3gl2</b>	ATG ATT GCA ACT TTG GTC CT	60.93	CAG ATC CTT GTC ATG AAG ATT CT	61.03	137
<b>Ssh1</b>	CAA GTG ATG ATC AAC CTC CT	59.08	GTC AAC TCC CAG CAG AAT ATT	59.59	150
<b>Tesk1</b>	GAG ACC TCA CAT CCA AGA ACT	59.72	GCC TTC TCA TCA TAC AGC TCT	60.01	193
<b>Timp4</b>	TCC AGT GAG AAG GTA GTC CCT	61.64	ATA CTG CTT GTG ACT GTT GGT TT	61.38	188
<b>Tmem106c</b>	ACC GCG GTA TAA ACA TTG AG	61.30	CTT CAC TGC TAA CCA ATC CAT	60.54	178
<b>Tmem132d</b>	CAT CCC TTC TTC AGC CAG AG	63.80	AGT GAG AAC CGC TGA ATG CT	63.90	187
<b>Ttbk1</b>	ATC AGT GTG TCC ATG CCT GT	63.20	ACT GTT TGG GAC GGA GGT C	64.00	148
<b>Usp38</b>	ACT GGC AGC TGT TCA GAA G	60.79	GCA GCA TAT GAG AGA GGA CTG	61.55	128
<b>II. Sry PCR</b>					
<b>Sry</b>	TGT TTC TCT TTG CAT CAC ATC TCT GTC	68.22	GTC CCA CTG CAG AAG GTT GTA CA	67.22	482
<b>III. Cfl-1 PCR</b>					
<b>deleted Cfl-1 allele (A and B primer)</b>	CGC TGG ACC AGA GCA CGC GGC ATC	82.31	CTG GAA GGG TTG TTA CAA CCC TGG	70.00	170
<b>Cfl-1 WT allele (C and B primer)</b>	CAT GAA GGT TCG CAA GTC CTC AAC	69.63	CTG GAA GGG TTG TTA CAA CCC TGG	70.00	380

### **3.7 Protein based methods**

#### **3.7.1 Mitochondrial proteomics**

##### **3.7.1.1 Preparation of mitochondrial protein lysates**

Mitochondrial protein lysates from hippocampal tissue of adult HR and LR mice were gained according to the subcellular fractionation and protein extraction protocol described by Cox and Emili in Nature Protocols (Cox and Emili, 2006). According to this, hippocampal tissue (around 30 mg) was slowly thawed from -80 °C and homogenized on ice using a plastic pestle tightly fitting a 1.5 ml Eppendorf tube. After homogenization, 180 µl 250-STMDPS buffer (Table 2) were added to the hippocampal tissue and the tissue homogenate was dissolved in the buffer by slightly grinding for 3 min. The completely dissolved homogenate was centrifuged for 15 min at 80 g, supernatant was collected and stored on ice. The pellet (volume around 80 µl) was dissolved in 640 µl 250-STMDPS buffer and rehomogenized for 1 min using the plastic pestle. A second centrifugation step for 15 min at 80 g followed and the supernatant was collected again, the pellet was discarded. To pellet the mitochondrial protein fraction, the first and the second supernatant from one hippocampal tissue sample were collected and centrifuged in separate tubes for 15 min at 4,500 g. The mitochondrial pellets from one sample were resuspended in 100 µl 250-STMDPS buffer, centrifuged for 15 min at 4,500 g to repellet the mitochondrial fraction. After resuspension of the pellet in 100 µl HDP buffer (Table 2), the suspension was incubated on ice for 30 min. Samples were sonicated on ice using five bursts each of the Branson Sonifier Cell Disruptor B15 (Hielscher Ultrasonics, Teltow) to support protein lyses. After spinning the samples for 30 min at 10,000 g, the supernatant containing the soluble fraction of the mitochondrial matrix proteins was collected. In order to achieve an extraction of mitochondrial membrane proteins, the pellet was resuspended in 100 µl ME buffer (Table 2) and incubated for 30 min at 4 °C while gently rocking the samples using an Elmi Rotamix RM1 (ELMI, Riga, Latvia). A final centrifugation step was conducted for 30 min at 10,000 g. The resulting supernatant contained the fraction of mitochondrial membrane proteins. Both mitochondrial proteins fractions, the matrix protein fraction and the mitochondrial membrane proteins, were merged and protein concentration was determined via a Bradford assay.

### **3.7.1.2 Bradford assay**

5  $\mu$ l of the mitochondrial protein sample were mixed with 795  $\mu$ l ddH<sub>2</sub>O. A standard curve consisting of a BSA dilution series (2, 4, 6, 8, and 10  $\mu$ g/ml) was pipetted, and both the diluted protein samples and the BSA standards were mixed with 200  $\mu$ l Bradford reagent (Bio-Rad Laboratories, München). Absorption was detected within 30 min at 595 nm using a Beckman DV640 Spectrophotometer (Beckman Coulter, Krefeld). Samples as well as standards were measured in duplicated and mean values were used for further calculations.

### **3.7.1.3 Two-dimensional gel electrophoresis**

After determination of protein concentrations, 200  $\mu$ g mitochondrial protein lysates were diluted in IEF buffer (Table 2) to a total volume of 250  $\mu$ l. The mitochondrial protein samples were centrifuged for 20 min at 24,000 g and subsequently loaded on a ReadyStrip IPG Strip (Bio-Rad Laboratories, Hercules, CA, USA). 200  $\mu$ l of the samples were loaded on an IPG strip and incubated for 1 h before overlaying it with 3 ml mineral oil (Bio-Rad). After rehydrating the IPG strips in the IEF-tray (Bio-Rad) for 12 h, wicks (Bio-Rad), which were humidified with 20  $\mu$ l ddH<sub>2</sub>O, were placed between IPG strips and electrodes to absorb excess salt. The first dimension, which separates the proteins contained in the lysate according to the isoelectric point of the proteins, was run for 8 - 9 h with a final voltage of 8,000 V.

In the second dimension, the proteins already separated along the isoelectric gradient, were additionally segregated along a size gradient. One criterion gel per sample was therefore prepared using a 12% separating gel consisting of 12 ml acrylamide/bis-acrylamide (37.5:1; Serva Electrophoresis, Heidelberg), 1.5 M Tris-HCl 7.5 ml, 10% SDS 300  $\mu$ l, Temed 15  $\mu$ l, 10% APS 150  $\mu$ l (all Bio-Rad), 10.06 ml ddH<sub>2</sub>O and a 4% stacking gel consisting of acrylamide/bis-acrylamide (37.5:1) 1.98 ml, 0.5 M Tris-HCl 3.78 ml, 10% SDS 150  $\mu$ l, Temed 15  $\mu$ l, 10% APS 75  $\mu$ l and 9 ml ddH<sub>2</sub>O. During polymerization of criterion gels, IPG strips were equilibrated for 15 min in equilibration buffer I and subsequently for 10 min in equilibration buffer II. After equilibration, IPG strips were overlaid with running buffer, inserted between the spacer glass plates above the stacking phase of the criterion gel, and additionally covered with pre-warmed 0.5% low-melting agarose solution (Bio-Rad). A placeholder for the protein ladder (Precision Plus Protein Standard; Bio-Rad) was formed. The gel was initially run at 80 V, voltage was increased to 120 V after 10 min for approximately 1.5 h.

For protein staining in colloidal coomassie, the gel was fixed in 100 ml 30% ethanol containing 2% phosphoric acid (Merck) overnight and afterwards washed in ddH<sub>2</sub>O three

times for 1 h, and incubated in 120 ml staining solution for 1 h. The two-dimensional (2D) gels were left in the colloidal coomassie staining solution (Table 2) rocking for three days on a Rotamax 120 shaker (Heidolph Instruments, Schwabach).

Table 2: List of buffers and staining solutions used for protein based protocols.

<b>Buffer</b>	<b>Function</b>	<b>Composition (filter-sterilized, stored at 4 °C)</b>
<b>250-STMDPS</b>	Initial homogenization	1 mM DTT (Bio-Rad) 25 µg ml <sup>-1</sup> spermine (Sigma) 25 µg ml <sup>-1</sup> spermidine (Sigma) PMSF as per manufacturer's specifications (Sigma) Complete Protease Inhibitor Cocktail Tablets (Roche) according to manufacturer's instructions
<b>HDP</b>	Extraction of soluble mitochondrial proteins	10 mM HEPES (pH = 7.9; Sigma) 1 mM DTT 1 mM PMSF
<b>ME</b>	Extraction of mitochondrial membrane proteins	20 mM Tris-HCl (pH 7.8; Bio-Rad) 0.4 M NaCl (Merck) 15% glycerol (Merck) 1 mM DTT 1 mM PMSF 1.5% Triton-X-100 (Sigma)
<b>Rehydration buffer</b>	Rehydration of IPG strips	7 M urea (Bio-Rad) 2 M thiourea (Sigma) 0.2% biolytes 3 - 10 (Bio-Rad) 2% CHAPS (Bio-Rad) 100 mM DTT
<b>IEF</b>	Sample buffer during first dimension	Rehydration buffer including 25x Complete Protease Inhibitor (Roche) 100 mM PMSF 100x Pepstatin (Roche)
<b>2D running buffer</b>	Running buffer during electrophoresis	10 x TGS (Bio-Rad) ddH <sub>2</sub> O
<b>Equilibration buffer I</b>	First equilibration of IPG strip	180 g urea 20% SDS 50 ml (Bio-Rad) 1.5 M Tris (pH 8.8; Bio-Rad) 87% glycerol 115 ml (Merck) 2% DTT ddH <sub>2</sub> O up to 500 ml
<b>Equilibration buffer II</b>	Second equilibration of IPG strip	180 g urea 20% SDS 50 ml 1.5 M Tris (pH = 8.8) 87% glycerol 115 ml 2.5% IAA (Bio-Rad) ddH <sub>2</sub> O up to 500 ml
<b>Colloidal coomassie</b>	Gel staining solution	17% ammonium sulfate (Merck) 2% phosphoric acid 34% methanol (Merck)

Destaining was done by washing the 2D gels in ddH<sub>2</sub>O for 1 h until background signals were minimal and protein signals were precise. Finally, gels were scanned using a gel scanner (GS-800 Calibrated Densitometer; Bio-Rad).

### 3.7.2 Cytochrome c immunoassay

The release of cytochrome c from the mitochondrial membrane into the cytoplasm was considered a marker for apoptotic activity in the cell (Huttemann *et al.*, 2011). To determine potential differences in apoptosis between HR and LR mice, a Quantikine rat/mouse cytochrome c Immunoassay (R&D Systems, Abingdon, UK) was performed.

The protein extraction from hippocampal tissue was conducted as described in a publication of Carboni and colleagues (Carboni *et al.*, 2005). Therefore, hippocampi were homogenized in a 1.5 ml Eppendorf tube using a tightly fitting plastic pestle. 1 ml of ice-cold lysis buffer containing 210 mM mannose (Merck), 250 mM sucrose (Sigma), 10 mM HEPES-NaOH (pH = 7.4), 10 mM KCl (Merck), 1.5 mM MgCl<sub>2</sub> (Merck), 1 mM EDTA, 1 mM EGTA (both Sigma), 1 mM DTT and Complete Protease Inhibitor (Roche) was added. Homogenized lysates were centrifuged for 10 min at 60 g and 4 °C, supernatant was collected and recentrifuged for 30 min at 1,100 g and 4 °C. After recentrifugation, the supernatant was collected as the cytosolic protein phase, the pellet as the mitochondrial protein fraction. The pellet was resuspended in 100 µl lysis buffer and stored at -80 °C for further analyses. The concentration of the cytosolic protein fraction was determined by a Bradford-Assay and subsequently standardized to 0.3 µg cytosolic protein per µl lysate. Following, lysates were 1:10 diluted with PBS to decrease the DTT concentration of the samples below 0.1 mM, and then to a final dilution factor of 1:30 with RD5-18 calibrator diluent to ensure that the absorption values of the cytosolic protein samples were within the same range than the absorption values of the standard curve.

The Quantikine assay is a sandwich enzyme immunoassay which allows the quantitative determination of rat/mouse cytochrome c concentrations in lysates of whole cells and subcellular fractions. It was conducted according to the manufacturer's instructions, which was in short the application of 75 µl rat/mouse cytochrome c conjugate to each well of a 96-well plate, followed by the application of 50 µl cytosolic protein lysate, standard sample or control probe. The solutions were mixed by gently rocking the plate for 1 min and incubation for 2 h at room temperature. Following the incubation period, the plate was emptied and washed five times with 400 µl wash buffer per well and per wash step. 100 µl substrate solution per well were added and the plate was incubated for 30 min at room temperature while protecting it from light. The reaction was stopped by

adding 100 µl stop solution per well and gentle mixing of the reagents. The optical density of the assay was determined at 450 nm using an absorbance reader (GENios Pro; Tecan, Crailsheim). Wavelength correction was set to 540 nm. All standard and cytosolic protein samples were measured in triplicates. Mean values of the three absorption values were calculated and a standard curve was generated based on the absorption values of the standard dilution series. The cytochrome c concentration of the cytosolic protein lysates were calculated based on the equation of the standard line.

### **3.7.3 Cytochrome c oxidase staining**

Cytochrome c oxidase (CO) staining was performed as a marker staining for neuronal and metabolic activity (Hu *et al.*, 2005). Therefore, dissected brains of HR and LR female mice were sliced into 20 µm thick coronal brain slices using a Microm HM 560 cryostat (Thermo Fisher Scientific, Schwerte) and mounted on Superfrost Plus microscope slides (Gerhard Menzel, Braunschweig). Brains were collected beginning approximately 100 µm anterior of the hypothalamic paraventricular nucleus and ending directly posterior of the ventral hippocampus. Immediately after slicing, slides were heated up to 60 °C for 1 min and afterwards stored at -20 °C until CO staining was carried out.

As a standard, liver tissue was homogenized as previously described with slight modifications (Riddle and Forbes, 2005). Approximately 2 ml of the liver homogenate were centrifuged at 8 g to remove residual air bubbles and frozen at -20 °C in cubic plastic gauges. Frozen homogenates were sliced, heated, and stained like brain slices.

CO staining was carried out in glass staining chambers while gently rocking during the whole protocol. The staining solution was required to be freshly prepared immediately before the staining by tempering the solution to 40 °C for 30 min and filtering before use. Each staining chamber contained next to the brain slices two slides with liver homogenates. The staining protocol started with tissue fixation for 5 min in acetone (Sigma-Aldrich) and washing in 0.1 M sodium phosphate buffer three times for 5 min, both at 4 °C. After this, slices were incubated in CO staining solution for 20 min at 37 °C, staining was stopped by transferring the slides in 0.1 M sodium phosphate buffer at 4 °C, followed by two washing steps in 0.1 M sodium phosphate buffer for 5 min. Post-fixation was achieved by incubation of the stained slices in 4% PFA for 30 min. The washing step in 0.1 M sodium phosphate buffer was repeated twice before drying the tissue sections in an ethanol dilution series of 70%, 80%, and 99% ethanol (5 min each), followed by 2 min in isopropanol. Finally, slides were cover-slipped with Roti Histokitt (Carl Roth, Karlsruhe).

Digitalization of stained tissue sections was done using an AxioCam MR05 (Leica Camera, Solms). Regions of interests were marked using a Bamboo paint tablet (Wacom, Krefeld) and subsequent densitometric quantification was done via ImageJ (version 1.43u) freeware.

For standardization, densitometric values of brain tissue slices were normalized to densitometric values of simultaneously stained of liver homogenates.

Table 3: Composition of buffers and solutions used for the CO staining protocol.

Buffer	Function	Composition
<b>0.1 M Sodium phosphate solution</b>	Wash buffer	10.6 g Na <sub>2</sub> HPO <sub>4</sub> x 2 H <sub>2</sub> O (Merck) 56 g K <sub>2</sub> HPO <sub>4</sub> (Merck) ddH <sub>2</sub> O up to 1 l (pH = 7.2)
<b>CO staining solution</b>	Cytochrome c oxidation	45 g sucrose 3% DAB (Sigma) 50 mg cytochrome c (Sigma) 100 mg Ni(NH <sub>4</sub> ) <sub>2</sub> (SO <sub>4</sub> ) <sub>2</sub> x 6 H <sub>2</sub> O 0.1 M (Merck) sodium phosphate solution up to 1 l
<b>4% PFA</b>	Post-fixation	2 g paraformaldehyde (Roth) 0.1 M PBS (pH = 7.2) up to 1 l
<b>0.1 M PBS</b>	Preparation of 4% PFA	14.4 g NaCl 0.1 M sodium phosphate solution 400 ml, ddH <sub>2</sub> O 1.2 l (pH = 7.2)

### 3.7.4 Quantification of plasma corticosterone via radioimmunoassays

Plasma corticosterone values of SRT blood samples were measured via corticosterone (rat/mouse) radioimmunoassays (RIAs; DRG Instruments, Marburg) according to the manufacturer's instructions but with slight modifications. In this competitive binding assay the quantitation of corticosterone molecules in the plasma was achieved using radioactively labeled corticosterone and an antibody-based detection of bound radioisotopes.

Initial plasma samples were diluted 1:13.5, reaction and recovery plasma samples 1:100, other than recommended in the kit. Initial plasma samples were measured once, reaction and recovery blood samples were detected in duplicates. In case the detected concentrations of the duplicate samples deviated more than 10%, the plasma of the respective sample was rediluted and measured again. Mean values from double detections were used for further calculations. The difference between the corticosterone concentration of a reaction and an initial sample was considered the corticosterone increase during the SRT, the difference between a reaction and a recovery sample was regarded the corticosterone decrease. Pooled plasma samples with a corticosterone concentration in the average range of an initial and of a reaction corticosterone

concentration were prepared and placed in the beginning and at the end of the assay to exclude intra-assay variations. A 6-fold standard dilution series with known corticosterone concentrations was used to calculate the corticosterone concentration of the probes accordingly.

### **3.8 Statistical and bioinformatical methods**

#### **3.8.1 Statistical analyses of microarray experiment**

##### **3.8.1.1 Univariate analysis**

The raw fluorescence data or signal intensities, based on the degree of hybridization of cRNA to beads with the corresponding probe sequences, was exported by the Illumina BeadStudio software (version 3.4.0), based on the optical scan signals from the arrays. These data were further processed using various functions of the R; for example, the `vs` function was used for data normalization, and the LIMMA package was applied for differential expression analyses. The ranking of significantly different expressed genes was achieved via an empirical Bayes method considering the correlation structure within the samples, and therefore increasing the validity of analysis. Genes not showing any expression signal were excluded from further evaluation to not fail the variances in the Bayesian correlation. These expression values were assorted according to the respective line of the animals which resulted in a design matrix. A false discovery rate approach was employed to correct for multiple testing, yielding adjusted p-values of differential expression.

##### **3.8.1.2 Multivariate analysis**

Based on normalized microarray raw data of HR and LR animals, multivariate analyses using support vector machines with recursive feature elimination (SVM-RFE) and random forest (RF) classifiers were performed in addition to the univariate analysis.

For SVM-RFE, the algorithm developed by Augustin and colleagues according to Zhou was applied (Augustin *et al.*, 2011; Trumbach *et al.*, 2010; Zhou and Tuck, 2007), at which for SVM prediction the `svm` function from the `e1071` package in R statistical software (<http://www.r-project.org/>) was used. The function `svm` was used with default settings except the parameters `type = 'C-classification'`, `kernel = 'linear'`, `cost = 0.1`. SVM-RFE algorithm was applied 40 times on different subsets of the original dataset and finally 40 different gene selections, each consisting of the best 1,000 genes for

classifying according to the cost function of the SVM classifier, were obtained. The frequency of each gene occurring in all the gene selections was computed to identify the most important genes. Finally, genes persisting more than 30 recursive feature eliminations were considered significantly different regulated.

Supervised clustering with the ensemble classifier RF was performed 50 times (Trumbach *et al.*, 2010); candidates occurring among the top 200 after ranking according to the mean decrease accuracy in each analysis were considered significantly differential expressed between the lines. For RF analysis, the function `randomForest` in R was applied by setting the number of trees `ntree` = 15,000, the number of input variables tried at each split `mtry` = 500 and otherwise default parameters. The candidate gene expressions were compared between the SVM-RFE and the RF method.

### **3.8.2 Statistical analyses of the SAGE experiment**

The pre-processing of the reads prior to quality controls involved the removal of the first primer base (T) which occurred as an adapter artifact and the first color. The actual quality control step was based on the phred-like scores for each color which was provided by the ABI SOLiD sequencer. More precisely, the quality control was done by computing a linear function of the phred scores of the complete read as well as the scores of the first 20 colors of the read. As a next step, identification of the adaptor sequence and the restriction enzyme binding site was carried out via dynamic programming allowing a maximum of two color mismatches to the standardized color sequence. Identifiable patterns were trimmed after identification of the target sequence (CAGT) representing the restriction enzyme binding site. Terminating element was the adapter sequence. Reads were standardized to a length of 23 colors if this sequence element could not be identified. Computation of the alignments was done using the BWA algorithm allowing a maximum of two color mismatches (Li and Durbin, 2009). The UCSC mRNA database served as a reference sequence for the alignment of remaining reads. In order to increase accuracy of the alignments, the mRNA reference sequences were trimmed to the fragments that can theoretically be produced by the 3' SAGE protocol. Following the alignment step, the mRNA reference IDs were mapped to gene symbols.

For the comparison of expressional profiles Z-scores were calculated based on the logarithm of the HR vs. LR counts for each gene symbol. Z-score values  $\geq 2$  were indicative for significantly differential expression.

### **3.8.3 Cluster analyses of differentially regulated genes**

#### **3.8.3.1 Database for annotation, visualization, and integrated discovery**

Cluster analyses with candidate genes detected as differentially expressed in the hippocampus of HR vs. LR animals by microarray and SAGE experiments were done to systematically screen the set of regulated genes for functional enrichment. The database for annotation, visualization, and integrated discovery (DAVID), an integrative tool for the analysis of large sets of gene and protein lists, was employed for mapping of regulated genes to associated biological annotations and for subsequent statistical analyses of enriched gene sets (<http://david.abcc.ncifcrf.gov/>). Thereby, the protocol for the analyses of large gene lists described in the publication of Huang et al. was strictly followed (Huang da *et al.*, 2009). In short, the lists of regulated genes, detected in the microarray and in the SAGE experiments, were submitted to DAVID bioinformatics tool. Functional annotation clustering, chart and table were generated applying medium classification stringency. Detected clusters with enrichment scores  $\geq 1.3$  were considered reflecting functional clusters indicating a significant biological impact in the sets of regulated genes. Benjamini correction was applied to correct for multiple testing.

#### **3.8.3.2 Gene ontology analyses**

Pathway studio (version 8.0) was used to perform gene ontology (GO) analysis of genes found to be regulated in hippocampal tissue of HR and LR mice by means of the microarray study. The set of genes which was detected in the SVM-RFE evaluation to differ the most in the expression was used for these additional annotation analyses regarding common biological processes, common cellular components, and common molecular functions. The resulting adjusted p-values were corrected for multiple testing according to Benjamini-Hochberg (Benjamini *et al.*, 2001).

### **3.8.4 High-density screening for single-nucleotide polymorphisms and detection of segmental copy number variants by means of the Jax Mouse Diversity Genotyping array**

The Jax Mouse Diversity Genotyping array is a high-through-put genotyping array for the mouse simultaneously detecting 623,124 single-nucleotide polymorphisms (SNPs) and 916,269 invariant genomic probes. It resembles therefore the Affymetrix Human 6.0 array. The invariant genomic probes were targeted to functional elements and regions known to harbor segmental duplications (Yang *et al.*, 2009). The Mouse Diversity

Genotyping array was built on an Affymetrix platform and contains SNPs from either source, mice derived from the wild and known inbred-strains commonly used in research.

The performance of the assay was offered by The Jackson Laboratories (Bar Harbor, ME, USA) as a service feature, beginning with the extraction of high-molecular weight DNA from tail tip tissue via computational analyses of raw data until customized analyses adapted to individual scientific demands. Therefore, roughly 0.5 cm of tail tip tissue from CD-1 mice were sent to The Jackson Laboratories. After processing of the assay, data from basic analyses as well as from custom analyses were submitted via Accellion Secure File Transfer.

#### **3.8.4.1 Detection of segmental copy number variation based on data from Jax Mouse Diversity Genotyping array**

Segmental duplications and copy number variants (CNVs) were identified in HAB vs. LAB and HR vs. LR animals based on invariant genomic probes of the JAX Mouse Diversity Genotyping array following the 'Simple CNV' instructions of the MouseDivGeno Vignette (version 1.0.0) by Yang and Sheppard (obtained from <http://genomedynamics.org/tools/MouseDivGeno>). Therefore, the MouseDivGeno together with the HiddenMarkov R packages were installed. One animal from each mouse model was needed to be defined as 'reference animal'. Hence, invariant genomic probes raw data of the other animal from the same mouse model were analyzed in respect to the data of the 'reference animal'. For the HAB/LAB comparison, data gained from the LAB mouse served as reference; in case of the HR/LR comparison, sequences obtained from the LR mouse were chosen as reference. As a consequence, 'gains' and 'losses' detected in HAB and HR mice, respectively, were 'gains' and 'losses' in respect to the particular reference sequences.

#### **3.8.5 Principle component analyses of phenotypic features**

Principal component analyses (PCA) were conducted to structure phenotypes collected in the behavioral test battery of the so-called 'CD-1 panel'. Detected behavioral variables were condensed and arranged in a multidimensional scaling following an orthogonal varimax rotation maintaining variables with an eigenvalue >1 (Henderson *et al.*, 2004). The PCA and the varimax rotation were accomplished using the open-source statistical software package R.

### **3.8.6 Calculation of association via WG-Permer**

Associations between genotypes resulting from the Jax Mouse Diversity Genotyping array and phenotypes detected in the behavioral test battery of the 'CD-1 panel' were tested using WG-Permer freeware (version 0.9.9; obtained from <http://www.wg-permer.org/>). Settings were defined as follows. The level of significance was set to nominal p-values <0.05, Chi-square-test was performed for quality controls, the number of permutations was set to 10,000, the permuted Fisher product-combination-method was applied over all selected models, and point-wise empirical p-values were calculated accordingly. Correction for permutation-based multiple testing was done via the minP method of Westfall and Young (WY-corrections).

### **3.8.7 Generation of CD-1 strain-specific haplotype map**

Genotypes gained from high-throughput SNP screening of 32 CD1 mice were used for the generation of a strain-specific haplotype map. Therefore, genotypes of heterozygous and opposite homozygous SNPs were transferred into a PLINK file using PLINK freeware (version 1.07; <http://pngu.mgh.harvard.edu/~purcell/plink/>). Linkage disequilibrium (LD) parameters were calculated for every possible SNP combination (conservative clustering) within a sliding window of 5 mb applying a greedy algorithm. The maximal marker density within a sliding window was set to 1,000 SNPs. This iterative tagging resulted in the calculation of a correlation coefficient ( $R^2$ ) for every potential marker combination.  $R^2$  values  $\geq 0.8$  within a sliding window were filtered and considered reflecting strong LD clustering. The SNP with the highest  $R^2$  value which is thus predicting the most genotypes of SNPs within the sliding window was considered the tagging SNP of the respective LD cluster.

### **3.8.8 Statistical data analyses, graphical illustration, and common bioinformatical processes**

Statistical calculations for two or more group comparisons were done using SPSS software (version 16.0). Converging normal distribution, behavioral data sets were analyzed via parametric statistics (independent samples T-test; IST); non-parametric statistics (Mann-Whitney-U test; MWU) was applied for statistical analyses of molecular biological data sets. For statistical analysis of qPCR data, prior to MWU testing descriptive statistics was applied and separate values in the range of upper and lower whiskers were considered methodological artifacts rather than reflecting biological variance and were, therefore, excluded from the analysis.

Comparative illustrations of data were created by the use of SigmaPlot 16.0. Respective data are provided in box plots showing medians as lines in the boxes and 25% and 75% percentiles (boxes). 10% and 90% percentiles are shown by the whiskers.

Common bioinformatical processes, such as comparison of large data tables, were conducted by making use of the open-source statistical software package R (<http://www.r-project.org/>). Furthermore, diverse functions of the Microsoft Office 2007 package were employed.

## 4 Results

### 4.1 Gene expressional profiling of the SR mouse model

#### 4.1.1 Differentially expressed genes according to univariate analysis of the microarray experiment

Applying univariate analysis, microarray-based gene expression profiling of hippocampal tissue from HR and LR animals revealed 330 probes to be significantly different regulated (adjusted p-values  $\leq 0.05$ ), identifying a total of 297 differentially regulated genes between the lines. Out of these 297 differentially regulated genes, 27 candidates were detected with more than one hybridization probe. *Tpmt* was identified with two different probes showing contradictory fold changes; the gene was therefore not considered for further analysis. Minor discrepancies in the number of regulated genes noted in further analyses appeared due to variations in genome build and gene alignment versions. Identified candidates are listed in Table S1 of the supplementary data.

Supplementary data are provided on the external data source which was attached to the thesis; respective Tables and Figures were marked with 'S' before serial numbers.

#### 4.1.2 Genes detected as differentially expressed in the SAGE experiment

A total of 709 genes were identified to differ significantly in their expression in the hippocampus of HR vs. LR mice (Z-score  $\geq 2$ ). Detected candidates, respective fold changes, and Z-scores are summarized in Table S2.

#### 4.1.3 Overlapping pool of genes detected as differentially expressed in both gene expression profiling approaches

Combining the gene pools detected in the microarray and in the SAGE experiment, a total number of 1,007 genes was found to differ significantly in hippocampal expression. 25 genes (2.48%) were detected by either approach (Table 4). The resulting combined gene pool, therefore, consists of 982 genes.

Table 4: Combined pool of 25 genes detected as differentially expressed in the microarray and in the SAGE experiment. Genes are listed in alphabetical order. Respective significance values are shown (adjusted p-value for microarray candidates, Z-score for SAGE candidates). In either case, positive fold change values indicate higher expression in HR, negative fold changes higher expression in LR mice.

Gene symbol	Fold changes in	
	Microarray	SAGE
<i>Aars2</i>	-1.303	-2.565
<i>Abcb1b</i>	1.926	6.939
<i>Acot1</i>	1.283	2.611
<i>Adora2b</i>	-1.922	-1.813
<i>Akr1e1</i>	-1.934	-2.267
<i>Aldh1l1</i>	2.027	2.488
<i>Rrp36</i>	1.344	-4.600
<i>Brf2</i>	-1.966	-1.615
<i>Cyp4f14</i>	2.296	5.039
<i>Cyp4f15</i>	2.515	7.739
<i>Cyp4f16</i>	1.664	2.582
<i>Dap3</i>	1.956	2.276
<i>Fbxo6</i>	-1.341	-1.427
<i>Hhat1</i>	-1.759	-1.807
<i>Hist1h2be</i>	-1.870	-2.845
<i>Kars</i>	1.251	4.410
<i>Ldb3</i>	-1.692	-2.500
<i>Rgl1</i>	4.263	1.661
<i>Sap130</i>	1.328	1.936
<i>Sh3gl2</i>	1.447	1.644
<i>Slc25a34</i>	1.806	3.002
<i>Slc35b2</i>	1.375	7.649
<i>Spast</i>	1.377	2.207
<i>Timp4</i>	1.336	1.924
<i>Tmf1</i>	-1.482	-1.450

*Rrp36* (*Rrp36* ribosomal RNA processing 36 homolog) was detected by either gene expression profiling approach to differ significantly in its expression, but with contradictory fold changes. The gene was therefore not considered in further analyses, reducing the number of genes in the combined gene pool of differentially expressed genes to 981.

#### 4.1.4 Univariate vs. multivariate analysis of microarray data

In addition to univariate analysis, two different multivariate algorithms were applied for microarray analysis. Using SVM-RFE, 368 hybridization probes were identified with frequencies between 30 and 40 after 40 iterations and were therefore rated to differ significantly in their expression. These 368 hybridization probes identified 337 genes. RF analysis resulted in the identification of 108 probes and 103 genes, respectively. A

comparison of genes identified to differ significantly in their expression in the hippocampus of HR vs. LR animals according to applied algorithms is assembled in Table S3. The SVM-RFE algorithm identified 74.07% (= 220 genes) of the genes already detected in the univariate analysis; the RF algorithm 30.3% (= 90 genes). The number of candidates exclusively detected as differentially expressed according to SVM-RF was 109, using the RF algorithm five. The overlapping pool of genes detected as differentially expressed exclusively applying the multivariate algorithms yielded eight genes (Table S4).

#### **4.1.5 Cluster analyses of differentially expressed genes**

Annotational cluster analyses were performed to investigate functional relevance of candidates detected as differentially expressed in the microarray and in the SAGE experiments.

##### **4.1.5.1 Identification of significant gene clusters in microarray candidates using the DAVID Bioinformatics Database**

Submitting the list of genes detected as differentially expressed in the microarray study according to univariate analysis to the DAVID Bioinformatics Database for functional annotation clustering, five significantly enriched gene clusters were identified (Table 5). In order to assign a functional meaning to detected gene clusters, common denominators of assigned gene functions were defined and the clusters named accordingly.

The first cluster contained 41 genes, all of them contributing to the various functions of the mitochondrion. Genes in the so-called 'mitochondrial cluster' are genomically encoded and cannot be ascribed to a specific mitochondrial function or pathway. The second enriched cluster comprised 25 genes which are specifically involved in functions along the mitochondrial membranes and the inter-membrane space. It is therefore called 'mitochondrial envelope' cluster and depicts an envelope-associated fraction of genes already assigned to the mitochondrial cluster. The third significantly enriched cluster includes four genes, all of them annotated with esterase functions. The fourth functional group of genes, the 'cofactor cluster', contains eight genes, all of them fulfilling metabolic and biosynthetic cofactor and coenzyme functions, respectively in various biochemical processes. The fifth enriched cluster counts five genes, all involved in the metabolism of xenobiotics. With exception of *Ugt1a10*, the genes contained in this cluster are also involved in the glutathione pathway.

Table 5: Summary of significantly enriched gene clusters detected using DAVID Bioinformatics tool. In total, five clusters were significantly enriched (enrichment score  $\geq 1.3$ ). Genes contained in the particular clusters are listed in alphabetical order. The '%' column indicates the proportion of genes contributing to the respective cluster among the 297 genes differentially expressed according to univariate analysis.

No.	Functional assignment	Enrichment score	List of genes	%
1	Mitochondrion	2.2	<i>1810049H13Rik, Aars2, Abcb1b, Acaa2, Acot1, Acot13, Acss1, Aldh111, Brf2, Ccbl2, Cdc5l, Dap3, Dbt, Gcdh, Gm5512, Gstk1, Gstz1, Hey2, Hsp90ab1, Kars, Krr1, LOC100047937, Mff, Mobp, Mrpl10, Mrpl3, Mtus1, Nfya, Nipsnap1, Nt5dc3, Pdk2, Prodh, Prosc, Rmnd1, Rpain, Rpl10a, Sdhaf1, Slc25a17, Slc25a34, Top1mt, Ugt1a10</i>	13.8%
2	Mitochondrial envelope	1.4	<i>Aars2, Abcb1b, Acaa2, Acss1, Alox5ap, Ankle2, Atp6v1g1, Chst5, Dap3, Dbt, Gcdh, Gstk1, Mff, Mrpl10, Mrpl3, Nipsnap1, Pdk2, Pex6, Prodh, Rep15, Sdhaf1, Slc25a17, Slc25a34, Tmf1, Ugt1a10</i>	8.4%
3	Esterases	1.4	<i>Acot1, Acot11, Acot13, Usp38</i>	1.3%
4	Cofactors	1.3	<i>Acot1, Acss1, Aldh111, Dbt, Dcxr, Gstk1, LOC100047937, Pank3</i>	2.7%
5	Xenobiotic metabolism	1.3	<i>Gstk1, Gstm1, Gstz1, Oplah, Ugt1a10</i>	1.7%

#### 4.1.5.2 Identification of significant gene clusters in SAGE candidates using DAVID Bioinformatics Database

Genes, detected as differentially expressed in the SAGE study, were in analogy to microarray candidates submitted for functional annotation analysis to the DAVID Bioinformatics Database, resulting in 14 significantly enriched gene clusters (Table 6). The gene cluster achieving the highest enrichment score was, in similarity to the functional annotation analysis of microarray candidates, a cluster containing genes which contribute in various ways to mitochondrial functions. 49 genes were assorted to this cluster, resulting in an explicitly significant enrichment score of 3.1. The second cluster counting 111 genes is the largest of all detected clusters and contained genes involved in the energy metabolism of the brain; for example, six genes encoding for different subunits of the ATP synthase, the proton transporting enzyme which is integrated into the mitochondrial F1 complex (Chinopoulos, 2011). Therefore, the cluster was entitled 'energy metabolism'. The third enriched cluster based on the SAGE gene pool was

ascribed as 'iron metabolism' cluster. It included nine genes, all of them fulfilling metabolic functions around iron homeostasis. The fourth cluster contained, similarly to the second cluster detected based on the microarray candidates, genes encoding for protein products which are fulfilling functions in the mitochondrial bilayer and the inner-membrane space. In total, 36 genes were attributed to this 'mitochondrial envelope' cluster. The fifth cluster, the so-called 'protein synthesis' cluster, comprised 49 genes involved in ribosomal protein synthesis. A further accumulation of functionally associated genes counted 21 candidates, all of them related to flavin adenine dinucleotide (FAD) and therewith linked with cellular redox reactions, was called 'FAD' cluster. The next cluster contained 32 genes with the functional similarity that all of them contribute to the respiratory chain. The eight genes counting to the eighth annotational cluster participate in a broad spectrum of metabolic processes, as they are involved in lipid, carbohydrate, and amino acid synthesis and degradation. The next cluster counting 56 genes was identified as a functional accumulation of genes involved in enzymatic processes along with cytochrome P450 activities. The common denominator of the next annotational cluster is the generation of energy. It contains 18 genes which all are involved in energy generation, for example via cellular or aerobic respiration, as well as via the tricarboxylic acid cycle. The eleventh cluster comprised 45 genes involved in immunological processes. The twelfth cluster, which contained four genes, was assembled based on shared sequence domains. According to UniProt sequence annotation features, integrins and sodium channels contained in this cluster have repeated sequence motifs in common. 20 genes were assorted to cluster thirteen, all of them fulfilling diverse functions in protein assembly. The last cluster contained 14 genes involved in the regulation of lipase activities.

Table 6: Overview over annotational enrichment clusters resulting from genes detected in the SAGE study to be differentially expressed in the hippocampus of HR vs. LR mice. Genes assorted in respective functional clusters are listed in alphabetical order. The '%' column is giving the percentage of genes assigned to the respective cluster based on the 709 genes detected in the SAGE experiment.

No.	Functional assignment	Enrichment score	List of genes	%
1	Mitochondrion	3.1	<i>1110032A13Rik, 2310061104Rik, Acadsb, Acot1, Acot3, Aldh18a1, Aldh111, Atp5e, Atp5g1, Atp5g3, Atp5h, Atp5j, Atp5o, Cac, Cat, Efhd1, Etfb, Ethe1, Fdx1, Fh1 Flnb, G6pd2, Glyat, Gm16517, Gm5436, Gm6419, Gm6419, Gm6419, Gng5, Gpd2, Hcrt, Mcee, Mip, Mosc2, Mrpl39, Mrpl42, Ndufb11, Ndufs1, Nt5dc3, Oxct1, Pgam5, Pgs1, Ppox,</i>	6.9%

			<i>Rbfa, Sdhaf1, Trpv6, Tusc3, Usp30, Uxs1</i>	
2	<b>Energy metabolism</b>	2.4	<i>1110032A13Rik, 1500035H01Rik, 3000002C10Rik, Aars2, Abca4, Abcb1b, Abcb4, Abcd1, Acadsb, Aco2, Aifm3, Aldh18a1, Ampd2, Ap1p2, Aqp1, Atic, Atp5e, Atp5g1, Atp5g3, Atp5h, Atp5j, Atp5o, Atp6v0d1, Atp6v1a, Atp6v1d, Atp9a, Bcap31, Cacnb3, Casp12, Cat, Cbx3, Clcn4-2, Cyba, Dap3, Efhd1, Etfb, Ethe1, Fdx1, Fdx1l, Fdxr, Fh1, Ftl1, Gipc1, Gm6498, Gpd2, Grin2b, H47, Hmgcs2, Isca1, Kcne2, Kcnh3, Kcnh4, Kcnq2, Kctd8, LOC654426, Lpl, Mcee, Mfsd6, Mgat1, Mosc2, Mrpl39, Mrpl42, Msh2, Ndufa12, Ndufa4, Ndufa7, Ndufb11, Ndufs1, Ndufv3, Nfu1, Nmnat2, Nos1, Oat, Oxct1, Paics, Park2, Pdpn, Pgam1, Pgam5, Pgs1, Polr2d, Ppox, Prlr, Ptgds, Rpl38, Ryr2, Scn4a, Scn9a, Sdhaf1, Sdhc, Slc12a2, Slc25a34, Slc2a13, Slc35b1, Slc35b2, Slc37a2, Slc38a3, Slc40a1, Slc5a5, Slc6a3, Spast, St6galnac5, Suclg1, Syt1, Tes, Tgm2, Tmf1, I15, Tusc3, Uchl1, Usp30</i>	15.7%
3	<b>Iron metabolism</b>	2.4	<i>Aco2, Aifm3, Fdx1, Fdx1l, Isca1, Mrpl39, Ndufs1, Nfu1, Xdh</i>	1.3%
4	<b>Mitochondrial envelope</b>	2.2	<i>Aars2, Acadsb, Aifm3, Aldh18a1, Atp5e, Atp5g1, Atp5h, Atp5j, Atp5o, Dap3, Efhd1, Etfb, Ethe1, Fdx1, Fdx1l, Fdxr, Gpd2, Hmgcs2, LOC654427, Mosc2, Mrpl39, Ndufa12, Ndufa4, Ndufa7, Ndufb11, Ndufs1, Ndufv3, Nos1, Oat, Oxct1, Ppox, Sdhaf1, Sdhc, Slc25a34, Suclg1, Usp30</i>	5.1%
5	<b>Protein synthesis</b>	2.2	<i>Aars2, Aarsd1, Cldn11, Cldn2, Crnk1l, Cwc15, Dap3, Eef1b2, Eef1d, Eftud2, Eif2b1, Eif3h, Eif4b, Eif4g3, Eprs, Gm15427, Gm15772, Gm4987, Gm6402, Gm6548, Isca1, Kars, Krr1, Lsm14b, Lsm4, Mrpl39, Mrpl42, Nell2, Nol6, Plp1, Ppwd1, Prpf8, Rbm3, Rbm8a, Rpl11, Rpl26, Rpl38, Rpl5, Rps25, Rps29, Rps4x, Rps6, Rps6ka2, Sf3b1, Snora65, Snrpc, Srp9, Tuba3a, Tuba4a</i>	6.9%
6	<b>FAD</b>	2.1	<i>3000002C10Rik, Acadsb, Aifm3, Bdh2, Etfb, Fdxr, Gad1, Gad1l, Gm6498, Gpd2, Kdm1a, Mosc2, Nos1, Oat, Pnpo, Ppox, Prlr, Sqle</i>	3.0%

7	<b>Respiratory chain</b>	2.0	<i>Txnrd1, Uxs1, Xdh, Aco2, Aifm3, Atp5e, Atp5g1, Atp5g3, Atp5h, Atp5j, Atp5o, Atp6v0d1, Atp6v1a, Atp6v1d, Cat, Cyba, Etfb, Fdx1, Fdx1l, Fdxr, Fh1, Gm6498, LOC654426, Msh2, Ndufa12, Ndufa4, Ndufa7, Ndufb11, Ndufs1, Ndufv3, Pgam1, Sdhc, Slc37a2, Suclg1, Txnrd1</i>	4.5%
8	<b>Diverse metabolic processes</b>	1.6	<i>Acadsb, Akr1e1, Bdh2, Gad1, Hmgcs1, Hmgcs2, Mcee, Oxct1</i>	1.1%
9	<b>Cytochrome P450</b>	1.6	<i>Acadsb, Aco2, Aifm3, Akr1e1, Aldh18a1, Aldh1a2, Aldh1l1, Aldh3a1, Bdh2, Cat, Cyba, Cyp2e1, Cyp4f14, Cyp4f15, Cyp4f16, Cyp4f18, Cyp4f40, Etfb, Fdx1, Fdx1l, Fdxr, Fibp, Ftl1, Gm6498, Gpd2, Hbb-b2, Isca1, Kdm1a, Kdm4d, Mosc2, Ndufa12, Ndufa4, Ndufa7, Ndufb11, Ndufs1, Ndufv3, Nfu1, Nos1, Pdcd6, Plod3, Pnpo, Pon1, Ppox, Ppp4c, Ptgds, Ptgs2, Sdhc, Slc37a2, Slc40a1, Sord, Sqle, Trf, Txnrd1, Vkorc1, Xdh, Ywhab</i>	7.9%
10	<b>Energy generation</b>	1.5	<i>Aco2, Acot1, Aldh1l1, Cat, Fh1, Folr1, Isca1, Mthfs, Ndufa7, Ndufs1, Nfu1, Nmnat2, Pdss2, Ppox, Sdhc, Slc37a2, Suclg1, Vkorc1</i>	2.5%
11	<b>Immunological processes</b>	1.5	<i>Actb, Cd180, Cd74, Cldn11, Cldn2, Eif4g3, Gad1, Git1, Gm16379, H2-Ab1, H2-D1, H2-Eb1, H2-K1, H2-Q6, H2-Q8, H2-T9, Il1r1l, Islr, Itgb4, Lax1, LOC547349, Mafk, Masp2, Mfsd6, Mif, Mpzl2, Myh3, Myh4, Pcp4, Pira6, Psg23, Psg27, Psmb8, Robo1, Runx1, Sema3f, Serpina3g, Sh3gl2, Siglec1, Speg, Stbd1, Tgm2, Thy1, Tlr1, Tlr12</i>	6.3%
12	<b>Repeated sequence motifs</b>	1.4	<i>Itgb4, Itgb6, Scn4a, Scn9a</i>	0.6%
13	<b>Protein assembly</b>	1.4	<i>Anxa5, Brf2, C1qtnf7, Caly, Cd74, Crnk1l, Gsn, H2-D1, Hist1h2bc, Hp1bp3, Pdss2, Psmg2, Sdhaf1, Spast, Synj1, Taf10, Tes, Tgm2, Tuba3a, Tuba4a</i>	2.8%
14	<b>Regulation of lipase activity</b>	1.4	<i>Adora2b, Aifm3, Bat2, Car8, Foxj1, Ghrh, Gnai2, Gng13, Hcrtr2, Pdcd6, S1pr1, Synj1, Tgm2, Thy1</i>	2.0%

#### 4.1.6 GO analyses of differentially expressed genes detected in the microarray study

In addition to annotational cluster analyses via the DAVID Bioinformatics Database, GO analyses were done based on candidates detected as differentially expressed in the microarray study. Genes were screened regarding overlapping entities in terms of cellular components, biological processes, and molecular functions. In total, 22 overrepresented GO categories among cellular components were identified. Out of these, four significantly overrepresented categories were attributed to the mitochondrion (Table 7).

Table 7: Summary of overrepresented GO categories which involved the mitochondrion and mitochondrial components, respectively.

Cellular component	List of genes	p-value	FDR
<b>Mitochondrion</b>	<i>Mrpl3, Ttc19, Slc25a34, Abcb1b, Rpl10a, Hsp90ab1, Mthfd1, Elac2, Gstz1, Prodh, Dap3, Aldh111, Mff, Acaa2, Gstk1, Ccbl2, Gcdh, Nt5dc3, Mrpl10</i>	$5.6 \times 10^{-4}$	0.071
<b>Mitochondrial matrix</b>	<i>Prodh, Dap3, Acaa2, Gstk1, Gcdh</i>	$2.7 \times 10^{-3}$	0.172
<b>Mitochondrial large ribosomal subunit</b>	<i>Mrpl3, Mrpl10</i>	$7.4 \times 10^{-3}$	0.202
<b>Mitochondrial inner membrane</b>	<i>Slc25a34, Prodh, Acaa2, Gstk1, Gcdh</i>	$4.6 \times 10^{-2}$	0.266

In the GO analyses of biological processes, 174 significantly enriched categories were identified. An overview of the category 'Central nervous system development', which was further pursued in this study, is given in Table 8. In addition, 80 significantly enriched molecular functions were clustered. The complete lists of all significant clusters are provided in Tables S5 (cellular components), S6 (biological processes), and S7 (molecular functions).

Table 8: Summary of the overrepresented GO category 'Central nervous system development'.

Biological process	List of genes	p-value	FDR
Central nervous system development	<i>Timp4, Sh3gl2, Adam22</i>	$1.4 \times 10^{-2}$	0.075

#### 4.1.7 Insufficient yield of mitochondrial protein lysate for 2D gel analysis

2D gel analysis of mitochondrial protein fractions gained from hippocampi of HR and LR mice delivered no detectable protein spots. The amount of protein load extractable from the mitochondrial protein fraction of a whole hippocampus was too low for the reliable detection of analyzable protein signals on 2D gels.

#### 4.1.8 No differences in cytochrome c release from mitochondrial bilayer into cytoplasm in HR vs. LR mice

In cytosolic protein fractions gained from hippocampal tissue of six HR and eight LR mice, no differences in the cytochrome c release from the mitochondrial bilayer into the cytoplasm were measured. The mean cytochrome c concentration in HR mice was 4.41 ng/ml (SEM  $\pm 1.80$ ), in LR mice 5.57 ng/ml (SEM  $\pm 1.97$ ; MWU p-value = 0.156). Detected ODs were within the linear scope of the standard curve. The cytochrome c concentration of the positive control provided with the Quantikine kit was measured as 1.44 ng/ml and, thus, within the range indicated in the kit.

#### 4.1.9 Cytochrome c oxidase activity in the hippocampus of HR vs. LR female mice

Standardized values of densitometric quantification from CO stained hippocampal slices are summarized in Table 9. Comparison of CO activity in the whole hippocampus of twelve HR vs. eleven LR females marginally failed a statistical trend (MWU p-value = 0.103). Densitometric quantification of both hemispheres as well as separate analyses of the right and the left hemisphere showed an increased CO activity in the dorsal hippocampus of HR female mice, resulting in statistical trends (MWU p-value<sub>both</sub> = 0.074, p-value<sub>right</sub> = 0.074, p-value<sub>left</sub> = 0.097). No differences were detected in intermediate and ventral parts of the hippocampus.

Table 9: Summary of densitometric quantification values after CO staining from hippocampal slices of HR vs. LR female mice. While quantifying CO activity, it was distinguished between the dorsal, the intermediate, and the ventral hippocampus, and between hemispheres. Values given in the HR and LR column were calculated as standardized mean values of the respective lines in the hippocampal areas indicated in the Table.

Hippocampal region	Hemisphere	HR means SEM	LR means SEM	p-value
Dorsal	Both	1.488 ±0.43	1.338 ±0.40	0.074
	Right	1.506 ±0.43	1.352 ±0.40	0.074
	Left	1.471 ±0.44	1.323 ±0.41	0.097
Intermediate	Both	1.438 ±0.42	1.289 ±0.39	0.110
	Right	1.454 ±0.41	1.299 ±0.39	0.110
	Left	1.423 ±0.42	1.279 ±0.39	0.140
Ventral	Both	1.373 ±0.39	1.249 ±0.38	0.176
	Right	1.382 ±0.39	1.261 ±0.37	0.196
	Left	1.365 ±0.40	1.236 ±0.38	0.157
<b>Total</b>		1.444 ±0.42	1.300 ±0.39	0.103

#### 4.1.10 Confirmation of microarray candidates via qPCR analyses

Selected candidates detected as differentially expressed in the microarray study were chosen for qPCR analysis in order to confirm the differential expression. In addition to microarray candidates, several genes, however interesting in the context of the stress reactivity mouse model, were tested for differential expression using qPCR as well. The results of qPCR analyses are summarized in Table 10. From 22 genes tested regarding their expression levels in the hippocampus of HR vs. LR mice, 18 genes were chosen based on their adjusted p-values in the microarray study. For these genes, the differential expression detected in the microarray was confirmed via qPCR in seven cases. In 11 cases, the microarray result could not be confirmed, whereas for *Mthfd1* a significant, but contradictory expressional difference and for *Tmem132d* a contradictory trend was measured in the qPCR. Expressional analyses of the additional four genes of interest (*Bdnf*, *Cfl-1*, *Hmgn3*, and *Rps6ka5*) resulted in the detection of significant up-regulations in HR vs. LR mice.

Table 10: Summary of qPCR analyses. Genes are listed in alphabetical order. ddCT values were standardized by setting LR ddCT group mean to 1.00; the HR ddCT group mean was calculated accordingly. Positive fold changes in the microarray indicate up-regulation in HR vs. LR; negative fold changes show up-regulation in LR vs. HR. Fold changes of genes detected with more than one probe are shown as mean values. Respective genes were marked with ‘#’ ( $n_{(HR)} = 8, n_{(LR)} = 10$ ); ‘+’ ( $n_{(HR)} = 5, n_{(LR)} = 6$ ); ‘°’ ( $n_{(HR/LR)} = 6$ ); n. s. = not significant, T = p-value <0.1, \* = p-value <0.05, \*\* = p-value <0.01, \*\*\* = p-value <0.001; FC = fold change; MA = microarray; Sign. = significance).

Gene	HR mean SEM	LR mean SEM	p-value qPCR	Sign.	FC MA	MA result
<i>Acot1</i> <sup>#</sup>	1.39 ± 0.32	1.00 ± 0.16	0.329	n. s.	1.28	Not confirmed
<i>Acot11</i> <sup>#</sup>	2.19 ± 0.22	1.00 ± 0.14	0.002	**	1.21	Confirmed
<i>Acot13</i> <sup>#</sup>	0.71 ± 0.15	1.00 ± 0.19	0.283	n. s.	-1.38	Not confirmed
<i>Aldh11</i> <sup>#</sup>	4.33 ± 0.97	1.00 ± 0.17	0.015	*	2.03	Confirmed
<i>Bdnf</i> <sup>+</sup>	1.00 ± 0.20	1.00 ± 0.11	0.715	n. s.	n. a.	n. a.
<i>Cfl-1</i> <sup>#</sup>	1.70 ± 0.22	1.00 ± 0.13	0.021	*	n. a.	n. a.
<i>Cyp4f13</i> <sup>#</sup>	1.06 ± 0.25	1.00 ± 0.15	0.689	n. s.	-1.33	Not confirmed
<i>Cyp4f14</i> <sup>#</sup>	4.35 ± 0.65	1.00 ± 0.11	0.001	***	2.3	Confirmed
<i>Cyp4f15</i> <sup>#</sup>	4.67 ± 1.04	1.00 ± 0.16	0.002	**	2.5	Confirmed
<i>Cyp4f16</i> <sup>#</sup>	1.43 ± 0.35	1.00 ± 0.23	0.329	n. s.	1.66	Not confirmed
<i>Dap3</i> <sup>°</sup>	1.27 ± 0.15	1.00 ± 0.11	0.297	n. s.	1.96	Not confirmed
<i>Gabrg2</i> <sup>**</sup>	1.72 ± 0.39	1.00 ± 0.06	0.028	*	2.58	Confirmed
<i>Hmgn3</i> <sup>+</sup>	1.92 ± 0.43	1.00 ± 0.13	0.042	*	n. a.	n. a.
<i>Hsp90ab1</i> <sup>°</sup>	1.29 ± 0.12	1.00 ± 0.15	0.229	n. s.	3.13	Not confirmed
<i>Mthfd1</i> <sup>+</sup>	1.68 ± 0.34	1.00 ± 0.10	0.027	*	-2.56	Conflicting
<i>Prodh</i> <sup>**</sup>	1.94 ± 0.47	1.00 ± 0.13	0.027	*	1.33	Confirmed
<i>Rgl1</i> <sup>°</sup>	1.13 ± 0.11	1.00 ± 0.17	0.631	n. s.	4.26	Not confirmed
<i>Rps6ka5</i> <sup>#</sup>	0.89 ± 0.11	1.00 ± 0.15	0.810	n. s.	n. a.	n. a.
<i>Tesk1</i> <sup>#</sup>	1.83 ± 0.44	1.00 ± 0.18	0.159	n. s.	4.01	Not confirmed
<i>Tmem132d</i> <sup>#</sup>	1.59 ± 0.22	1.00 ± 0.14	0.051	T	-2.20	Conflicting
<i>Ttbk1</i> <sup>#</sup>	2.7 ± 0.49	1.00 ± 0.16	0.006	**	6.17	Confirmed
<i>Usp38</i> <sup>#</sup>	1.61 ± 0.44	1.00 ± 0.19	0.283	n. s.	-2.46	Not confirmed

Furthermore, in order to test for the reliability of the microarray analysis, four genes (*Accn2*, *Fam116b*, *Tmem106c*, and *Pvalb*) that should show no expressional differences according to the microarray results were tested in the qPCR. For these four genes, non-regulation in the hippocampus of HR vs. LR mice was confirmed in the qPCR. The results are listed in Table 11.

Table 11: Summary of qPCR and microarray results from genes, which were detected as not regulated between the lines in the microarray. ( $n_{(HR)} = 8$ ,  $n_{(LR)} = 10$ ; FC = fold change; MA = microarray; Sign. = significance)

Gene	HR mean SEM	LR mean SEM	p-value qPCR	Sign.	FC MA
<i>Accn2</i>	1.16 ± 0.16	1.00 ± 0.16	0.374	1.00	Confirmed
<i>Fam116b</i>	1.28 ± 0.12	1.00 ± 0.16	0.178	1.00	Confirmed
<i>Tmem106c</i>	1.03 ± 0.16	1.00 ± 0.09	0.916	-1.02	Confirmed
<i>Pvalb</i>	0.87 ± 0.09	1.00 ± 0.11	0.596	1.00	Confirmed

#### 4.1.11 Neurodevelopmental study

##### 4.1.11.1 Expressional profiling of neurodevelopmentally expressed genes in hippocampal tissue of adult animals

In addition to qPCR analyses of microarray candidates already described in Table 10, a further set of nine genes, all of them known to have diverse functions in neurogenesis and neurodevelopment, respectively, were chosen to be analyzed for expressional differences by qPCR. cDNA generated from hippocampal tissue of male embryos (ED 18), pups (PND 7), and adolescent animals (PND 28) was used to test for differences in gene expression at earlier stages of the development. In addition to neurodevelopmental genes detected in the microarray, further genes interesting in the context of the SR mouse model and known to be expressed during neurodevelopment, were included in the analysis.

In adult mice, a significantly different expression was detected for *Adam11*, *Ash1l*, *Crtac1*, *Sh3gl2*, and *Ssh1* in the qPCR. For *Fam123a*, a statistical trend was detected. *Adam22*, *Cntn6*, and *Timp4* were not differentially expressed in adult HR vs. LR according to qPCR and, hence, these genes were not pursued in cDNA gained from earlier stages of the development. Results are summarized up in Table 12.

Table 12: Summary of qPCR results conducted using cDNA of adult mice. Genes are assorted in alphabetical order. Group means of LR ddCTs are normalized to 1.00, group means of HR ddCTs were calculated accordingly. ( $n_{(HR)} = 5$ ,  $n_{(LR)} = 6$ ; n. s. = not significant, T = p-value <0.1, \* = p-value <0.05, \*\* = p-value <0.01; Sign. = significance)

Gene	HR mean SEM	LR mean SEM	p-value qPCR	Sign.
<i>Adam11</i>	2.24 ± 0.39	1.00 ± 0.14	0.018	*
<i>Adam22</i>	1.33 ± 0.17	1.00 ± 0.09	0.143	n. s.
<i>Ash1l</i>	2.29 ± 0.69	1.00 ± 0.15	0.028	*
<i>Cntn6</i>	0.74 ± 0.08	1.00 ± 0.25	0.711	n. s.
<i>Crtac1</i>	2.24 ± 0.35	1.00 ± 0.13	0.006	**
<i>Fam123a</i>	1.44 ± 0.19	1.00 ± 0.13	0.085	T
<i>Sh3gl2</i>	2.11 ± 0.48	1.00 ± 0.16	0.045	*
<i>Ssh1</i>	1.46 ± 0.15	1.00 ± 0.11	0.033	*
<i>Timp4</i>	1.17 ± 0.17	1.00 ± 0.09	0.410	n. s.

#### 4.1.11.2 Expressional profiling of neurodevelopmental genes in hippocampal tissue of ED 18 mice

Pursuing gene expression levels of neurodevelopmental genes in male ED 18 HR and LR mice, genes detected as differentially expressed in adults (Table 9) were tested in addition to further candidates confirmed to be differentially expressed earlier (*Aldh1l1*, *Cfl-1*, *Hmgn3*, *Prodh*; Table 7). Preceding qPCR analyses, the gender of the embryos was determined via SRY PCR. The only candidate detected to be significantly different expressed at ED 18 was *Prodh*. This gene was detected with a 1.49-fold up-regulation in HR vs. LR mice. Detailed results of qPCRs using cDNA of ED 18 mice are summarized in Table 13.

Table 13: Summary of qPCR results conducted using cDNA of ED 18 mice. Genes are assorted in alphabetical order. Group means of LR ddCTs are normalized to 1.00, group means of HR ddCTs were calculated accordingly. ( $n_{(HR/LR)} = 6$ ; n. s. = not significant, \* = p-value <0.05; Sign. = significance )

Gene	HR mean SEM	LR mean SEM	p-value qPCR	Sign.
<b><i>Adam11</i></b>	0.91 ± 0.22	1.00 ± 0.25	0.810	n. s.
<b><i>Aldh1l1</i></b>	0.83 ± 0.28	1.00 ± 0.22	0.522	n. s.
<b><i>Ash1l</i></b>	0.71 ± 0.37	1.00 ± 0.42	0.522	n. s.
<b><i>Cfl-1</i></b>	0.70 ± 0.25	1.00 ± 0.26	0.200	n. s.
<b><i>Crtac1</i></b>	1.01 ± 0.39	1.00 ± 0.19	0.575	n. s.
<b><i>Hmgn3</i></b>	0.85 ± 0.26	1.00 ± 0.41	0.873	n. s.
<b><i>Prodh</i></b>	1.49 ± 0.15	1.00 ± 0.12	0.040	*
<b><i>Sh3gl2</i></b>	0.89 ± 0.14	1.00 ± 0.29	0.715	n. s.
<b><i>Ssh1</i></b>	0.78 ± 0.28	1.00 ± 0.18	0.337	n. s.

#### 4.1.11.3 Expressional profiling of neurodevelopmental genes in hippocampal tissue of PND 7 mice

Independent of the results gained in hippocampal tissue from ED 18 mice, the same nine gene candidates were tested in hippocampal tissue from PND 7 animals which were identified as male mice using SRY PCR. The only gene detected to differ in the expression between the lines was *Prodh* with an up-regulation close to 2-fold in LR vs. HR mice, resulting in a statistical trend. The other candidates were not differentially expressed between the lines. Data gained from PND 7 mice are summarized in Table 14.

Table 14: Summary of qPCR results conducted using cDNA of PND 7 mice. Genes are listed in alphabetical order. Group means of LR ddCTs are normalized to 1.00, group means of HR ddCTs are calculated accordingly. ( $n_{(HR/LR)} = 6$ ; n. s. = not significant, T = p-value <0.1; Sign. = significance)

Gene	HR mean SEM	LR mean SEM	p-value qPCR	Sign.
<i>Adam11</i>	0.79 ± 0.25	1.00 ± 0.18	0.150	n. s.
<i>Aldh1l1</i>	1.23 ± 0.48	1.00 ± 0.17	1.00	n. s.
<i>Ash1l</i>	1.15 ± 0.39	1.00 ± 0.18	1.00	n. s.
<i>Cfl-1</i>	0.89 ± 0.26	1.00 ± 0.12	0.297	n. s.
<i>Crtac1</i>	0.83 ± 0.22	1.00 ± 0.15	0.200	n. s.
<i>Hmgn3</i>	1.10 ± 0.19	1.00 ± 0.11	0.715	n. s.
<i>Prodh</i>	0.47 ± 0.10	1.00 ± 0.16	0.055	T
<i>Sh3gl2</i>	0.87 ± 0.19	1.00 ± 0.15	0.465	n. s.
<i>Ssh1</i>	0.74 ± 0.22	1.00 ± 0.10	0.201	n. s.

#### 4.1.11.4 Expressional profiling of neurodevelopmental genes in hippocampal tissue of PND 28 mice

The same genes were tested in tissue of adolescent HR and LR mice (PND 28), resulting in the detection of a significant up-regulation of *Hmgn3* in LR vs. HR mice. The other candidates were quantified as not differentially expressed between the lines. qPCR results are summarized in Table 15.

Table 15: Summary of qPCR results conducted using cDNA of PND 28 mice. Genes are listed in alphabetical order. Group means of LR ddCTs are normalized to 1.00, group means of HR ddCTs were calculated accordingly ( $n_{(HR/LR)} = 6$ ; n. s. = not significant, \* = p-value <0.05; Sign. = significance).

Gene	HR mean ±SEM	LR mean ±SEM	p-value qPCR	Sign.
<i>Adam11</i>	0.67 ± 0.12	1.00 ± 0.23	0.337	n. s.
<i>Aldh1l1</i>	0.92 ± 0.17	1.00 ± 0.22	0.936	n. s.
<i>Ash1l</i>	1.13 ±0.24	1.00 ± 0.15	0.855	n. s.
<i>Cfl-1</i>	0.96 ±0.18	1.00 ± 0.15	0.670	n. s.
<i>Crtac1</i>	0.80 ± 0.15	1.00 ± 0.19	0.337	n. s.
<i>Hmgn3</i>	0.47 ± 0.08	1.00 ± 0.17	0.037	*
<i>Prodh</i>	0.82 ± 0.12	1.00 ± 0.18	0.378	n. s.
<i>Sh3gl2</i>	0.81 ± 0.15	1.00 ± 0.13	0.465	n. s.
<i>Ssh1</i>	0.87 ± 0.22	1.00 ± 0.17	0.522	n. s.

## 4.2 From gene expressional profiling to behavior – tracking one candidate gene to a behavioral phenotype

### 4.2.1 Non-detection of differential expression of *Cfl-1* in hippocampal tissue of HR vs. LR mice in microarray study

The differential expression of the *Cfl-1* gene in HR vs. LR mice was shown using qPCR analysis (Table 10), but the up-regulation of the gene was not detected in the microarray experiment. This non-detection was due to the obsolete design of the microarray probe for this gene. According to the current annotation of *Cfl-1* (genome build version 37.2; chr. 19: 5,489,915 - 5,494,563) the microarray probe (chr. 19: 5,494,951 - 5,495,000) would have bound to genomic coordinates at least 388 bp after the 3'-terminal end of the target gene. The microarray probe, therefore, presents the complementary sequence of a genomic fragment in the intergenic region between *Cfl-1* and *Snx32*, the gene located down-stream of *Cfl-1*. This excludes the correct detection of *Cfl-1* expression levels in the mRNA-based expressional assay used for this study.

### 4.2.2 Behavioral phenotype in heterozygous *Cfl-1*<sup>+/-</sup> mice

*Cfl-1*<sup>+/-</sup> and WT controls were subjected to the behavioral test battery described on under point 3.2.4.1.

#### 4.2.2.1 No distinct behavior of *Cfl-1*<sup>+/-</sup> vs. WT mice in the OF

None of the parameters tested in the OF differed between *Cfl-1*<sup>+/-</sup> and WT controls, neither in male, nor in female mice. This applied to the key parameters indicating anxiety-like and locomotive behavior, like the total distance travelled and the time spent in the inner zone, as well as to additional parameters tested, like free and wall rearings which were taken as indicators for explorative behavior. In male mice, the mean distance travelled in the OF for *Cfl-1*<sup>+/-</sup> mice was 12.46 m (SEM ±1.06), for WT littermates 11.66 m (SEM ±0.82; IST p-value = 0.549). On average, *Cfl-1*<sup>+/-</sup> mice spent 89.63 s (SEM ±15.94) in the inner zone of the OF apparatus, WT mice 91.49 s (SEM ±13.51; IST p-value = 0.93). In female mice, the mean total distance travelled of *Cfl-1*<sup>+/-</sup> mice was 13.08 m (SEM ±1.31) and 15.53 m in WT littermates (SEM ±0.89; IST p-value = 0.155). The time spent in the inner zone of *Cfl-1*<sup>+/-</sup> females was measured with 93.94 s (SEM ±18.26), for female WT littermates 101.34 s (SEM ±12.08; IST p-value = 0.749). These two parameters were depicted in Figure 12, exemplarily for all the other features tested in the OF but not differing between groups.

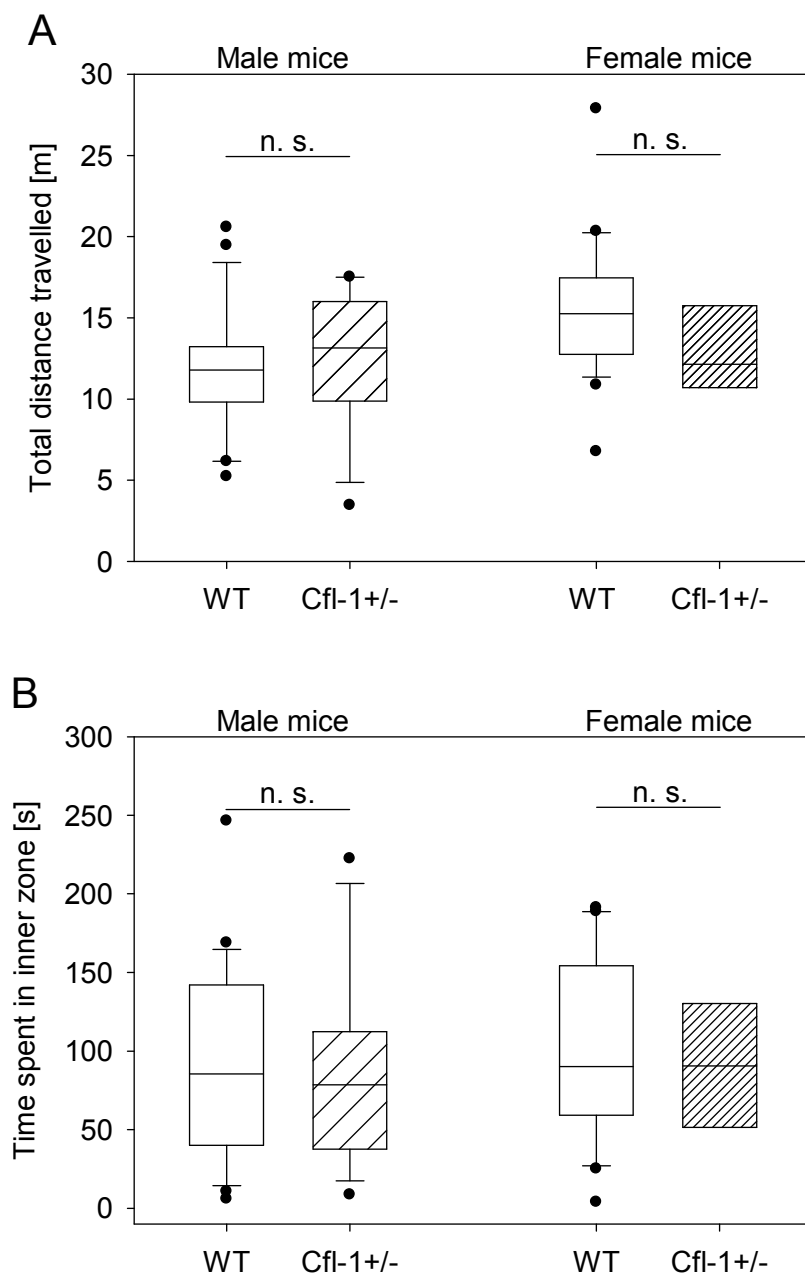


Figure 12: Results of the OF parameters 'total distance travelled' (A) and 'time spent in the inner zone' (B) in *Cfl-1<sup>+/-</sup>* vs. WT male and female mice (Males:  $n_{(Cfl-1+/-)} = 16$ ,  $n_{(WT)} = 22$ ; females:  $n_{(Cfl-1+/-)} = 8$ ,  $n_{(WT)} = 22$ ; n. s. = not significant).

#### 4.2.2.2 Anxiety-related behavior in *Cfl-1<sup>+/-</sup>* vs. WT mice on the EPM

The behavior of animals on the EPM indicated an anxiety-related phenotype in *Cfl-1<sup>+/-</sup>* mice compared to WT controls. This applied to both genders, although the anxiety-related features were more pronounced in female mice. In males, the total distance travelled on the EPM did not differ between the test groups, again implying equal locomotor activity between *Cfl-1<sup>+/-</sup>* and WT males. On average, male *Cfl-1<sup>+/-</sup>* mice

travelled 4.91 m (SEM  $\pm$ 0.83) on the EPM, WT males 4.63 m (SEM  $\pm$ 0.54; IST p-value = 0.769). Also, for the time spent immobile on the EPM no differences were detected between the groups (mean value *Cfl-1<sup>+/-</sup>* mice 80.71 s, SEM  $\pm$ 13.21; WT 82.11 s, SEM  $\pm$ 11.24; IST p-value = 0.936). Differences between the groups though were measured in the time spent on the open arm. *Cfl-1<sup>+/-</sup>* males spent 28.20 s (SEM  $\pm$ 9.86) on the open arm, WT controls spent more than twice as much time on the open arm (67.24 s, SEM  $\pm$ 20.39; IST p-value = 0.095). The distances *Cfl-1<sup>+/-</sup>* males travelled on the open arm did not differ significantly in comparison to WT males, neither did the number of entries into the open arm (mean distance travelled on the open arm: *Cfl-1<sup>+/-</sup>* 0.58 m, SEM  $\pm$ 0.17 vs. WT 1.17 m, SEM  $\pm$ 0.34; IST p-value = 0.135; mean open arm entries: *Cfl-1<sup>+/-</sup>* 6.94, SEM  $\pm$ 1.61 vs. WT controls 6.64, SEM  $\pm$ 1.26; IST p-value = 0.882). In females, the total distance travelled on the maze differed significantly (*Cfl-1<sup>+/-</sup>* 0.39 m, SEM  $\pm$ 0.17 vs. WT controls 6.91 m, SEM  $\pm$ 0.66; IST p-value  $<$ 0.001). The time animals spent immobile on the EPM also varied (*Cfl-1<sup>+/-</sup>* 68.1 s, SEM  $\pm$ 11.14 vs. WT controls 43.12 s, SEM  $\pm$ 7.11), resulting in a statistical trend (IST p-value = 0.077). The time *Cfl-1<sup>+/-</sup>* females spent on the open arm was measured with 22.76 s (SEM  $\pm$ 10.19), WT controls spent more than three times more time on the open arm (75.11 s, SEM  $\pm$ 20.47; IST p-value = 0.03). Correspondingly, the distance travelled on the open arm differed as well (*Cfl-1<sup>+/-</sup>* 0.39 m, SEM  $\pm$ 0.17 vs. 1.57 m, SEM  $\pm$ 0.38; IST p-value = 0.008). The number of open arm entries of *Cfl-1<sup>+/-</sup>* females was counted with 8.13 (SEM  $\pm$ 2.09), for WT controls 10.55 (SEM  $\pm$ 1.91; IST p-value = 0.486). Exemplary EPM data of male and female mice were depicted in Figures 13 and 14.

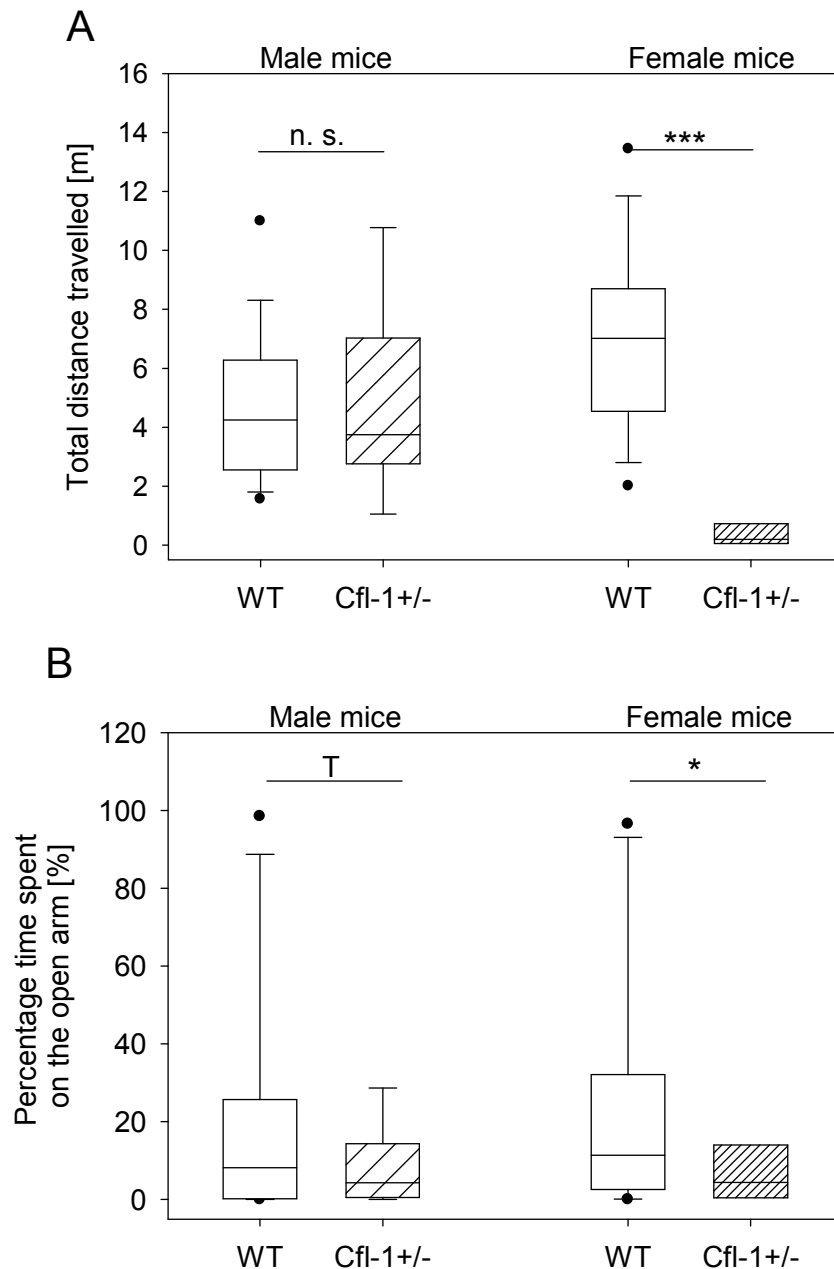


Figure 13: Comparison of the EPM parameters 'total distance travelled' (A) and 'percentage time spent on the open arm' (B) between male and female *Cfl-1<sup>+/-</sup>* and WT controls (Males:  $n_{(Cfl-1+/-)}$  = 16,  $n_{(WT)}$  = 22; females:  $n_{(Cfl-1+/-)}$  = 8;  $n_{(WT)}$  = 22; n. s. = not significant, T = p-value <0.1, \* = p-value <0.05, \*\*\* = p-value <0.001).

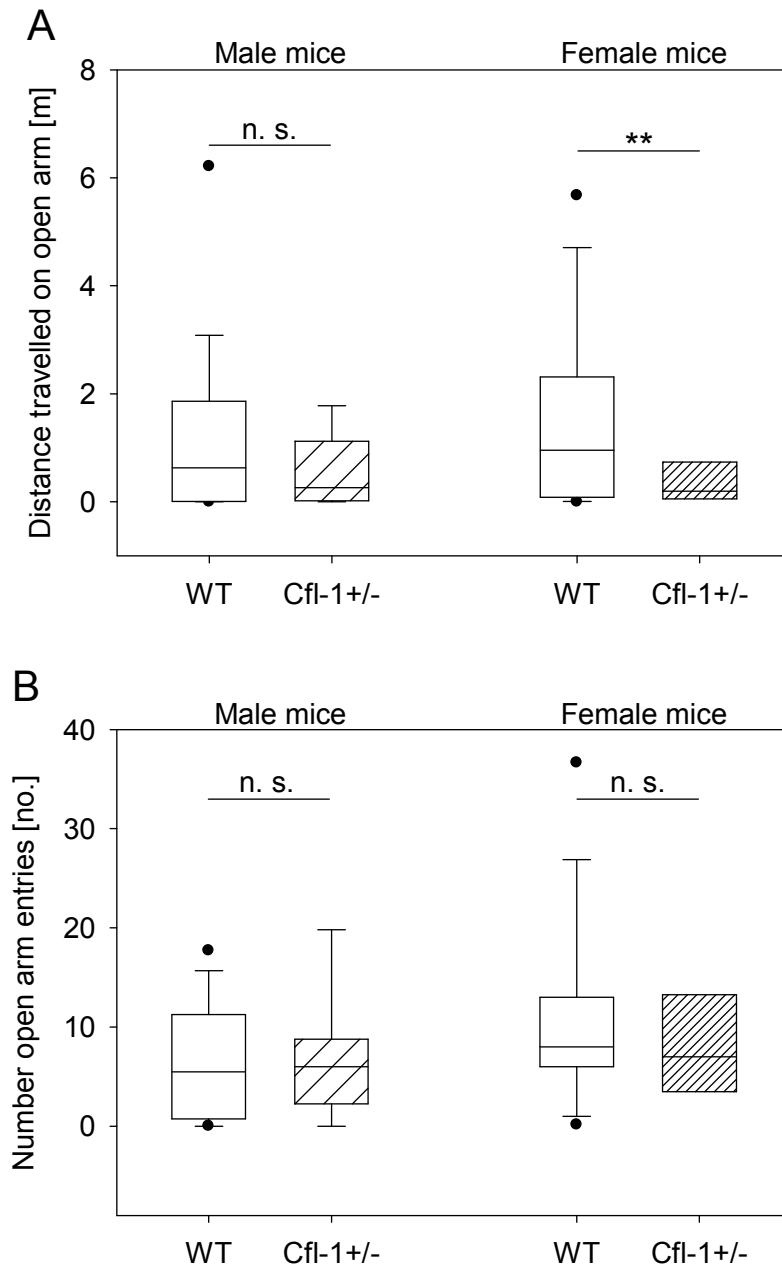


Figure 14: Comparison of EPM parameters 'distance travelled on the open arm' (A) and 'open arm entries' (B) between male and female *Cfl-1<sup>+/-</sup>* and WT mice (Males:  $n_{(Cfl-1+/-)} = 16$ ,  $n_{(WT)} = 22$ ; females:  $n_{(Cfl-1+/-)} = 8$ ;  $n_{(WT)} = 22$ ; n. s. = not significant, \*\* = p-value <0.01).

#### 4.2.2.3 Detection of increased anxiety-related behavior in female *Cfl-1<sup>+/-</sup>* vs. WT mice in the DL box

In male *Cfl-1<sup>+/-</sup>* vs. WT mice, none of the parameters tested in the DL box differed between the groups. In females, the total distance travelled showed a significantly shorter distance for *Cfl-1<sup>+/-</sup>* compared to WT mice (8.10 m, SEM  $\pm 0.76$  vs. 13.1 m, SEM  $\pm 1.24$ ; IST p-value = 0.002). In the time animals spent in the light compartment no

difference was detected ( $Cfl-1^{+/-}$  44.54 s, SEM  $\pm$ 16.92 vs. 64.52 s, SEM  $\pm$ 14.31; IST p-value = 0.427), but the distance females travelled in the light compartment was measured as significantly shorter compared to WT controls (1.79 m, SEM  $\pm$ 0.61 vs. 4.25 m, SEM  $\pm$ 0.62; IST p-value = 0.026). Furthermore, the number of entries into the light compartment was clearly reduced in  $Cfl-1^{+/-}$  females ( $Cfl-1^{+/-}$  1.88, SEM  $\pm$ 0.69 vs. 4.79, SEM  $\pm$ 0.68; IST p-value = 0.018; Figures 15 and 16).

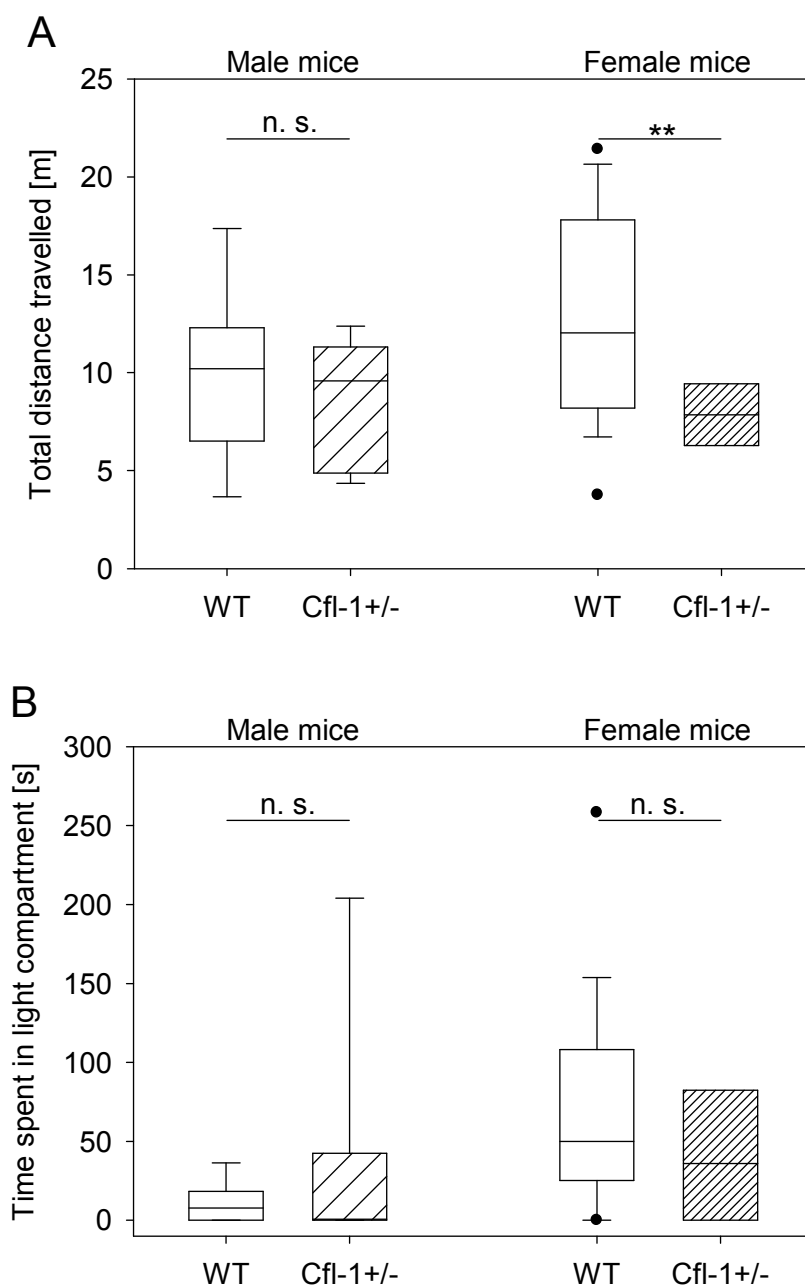


Figure 15: Comparison of DL box parameters 'total distance travelled' (A) and 'time spent in the light compartment' (B) (Males:  $n_{(Cfl-1^{+/-})} = 13$ ,  $n_{(WT)} = 17$ ; females:  $n_{(Cfl-1^{+/-})} = 8$ ;  $n_{(WT)} = 19$ ; n. s. = not significant, \*\* = p-value <0.01).

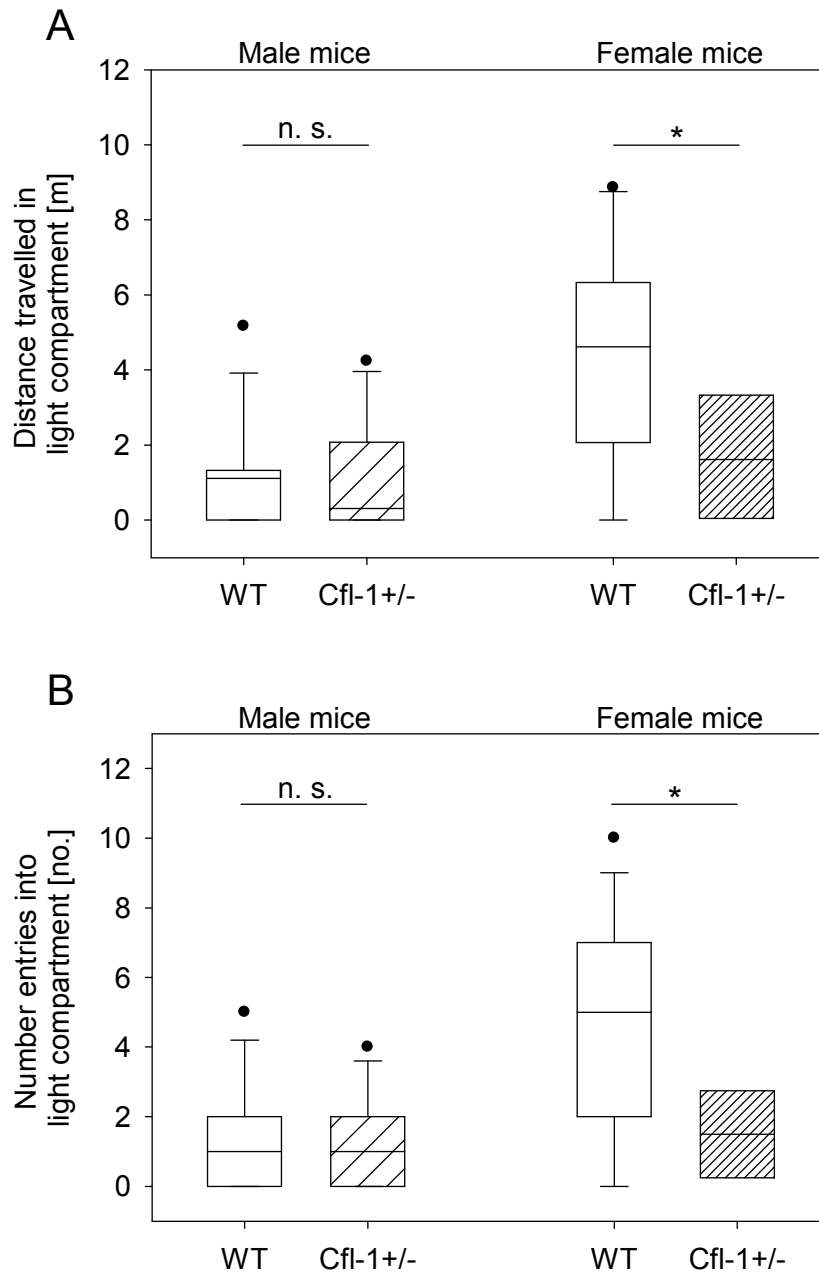


Figure 16: Comparison of DL box parameters 'distance travelled in the light compartment' (A) and 'number of entries into light compartment' (B) (Males:  $n_{(Cfl-1+/-)} = 13$ ,  $n_{(WT)} = 17$ ; females:  $n_{(Cfl-1+/-)} = 8$ ,  $n_{(WT)} = 19$ ; n. s. = not significant, \* = p-value < 0.05).

#### 4.2.2.4 FST data indicate more active stress-coping style of female *Cfl-1<sup>+/-</sup>* vs. WT mice

None of the parameters tested in the FST differed in male *Cfl-1<sup>+/-</sup>* vs. WT mice. In females, struggling time as well as the struggling frequency were significantly different in *Cfl-1<sup>+/-</sup>* compared to WT mice (struggling time *Cfl-1<sup>+/-</sup>* 59.61 s, SEM  $\pm$ 5.90 vs. in WT 39.3 s, SEM  $\pm$ 3.32; IST p-value = 0.004; struggling frequency *Cfl-1<sup>+/-</sup>* 6.88 s, SEM  $\pm$ 0.97 vs. in WT 10.05, SEM  $\pm$ 0.81; IST p-value = 0.039). The average swimming frequency counted in *Cfl-1<sup>+/-</sup>* females was significantly decreased in comparison to WT controls (27.63, SEM  $\pm$ 3.68 vs. 35.27, SEM  $\pm$ 1.62; IST p-value = 0.036). FST data are depicted in Figures 17 and 18.

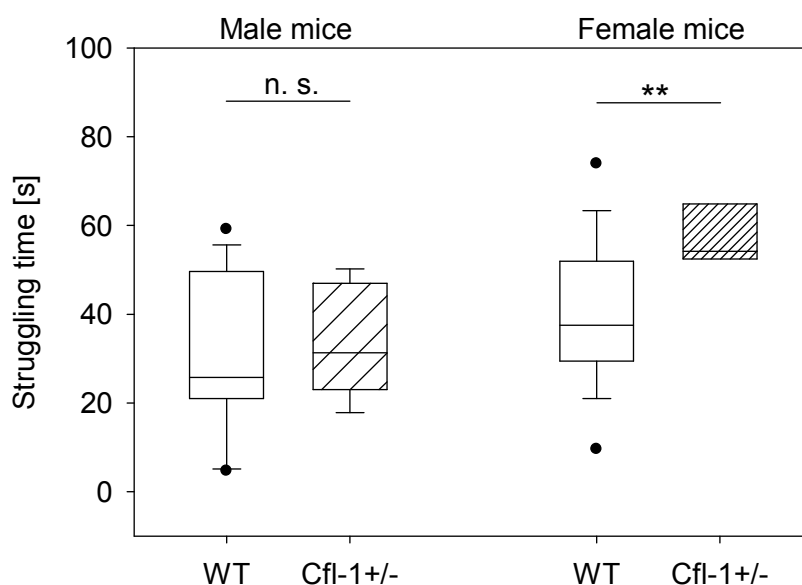


Figure 17: Results of FST scoring. Significant differences in the time struggling were detected in females only (Males:  $n_{(Cfl-1+/-)}$  = 16,  $n_{(WT)}$  = 22; females:  $n_{(Cfl-1+/-)}$  = 8,  $n_{(WT)}$  = 22; n. s. = not significant, \*\* = p-value < 0.01).

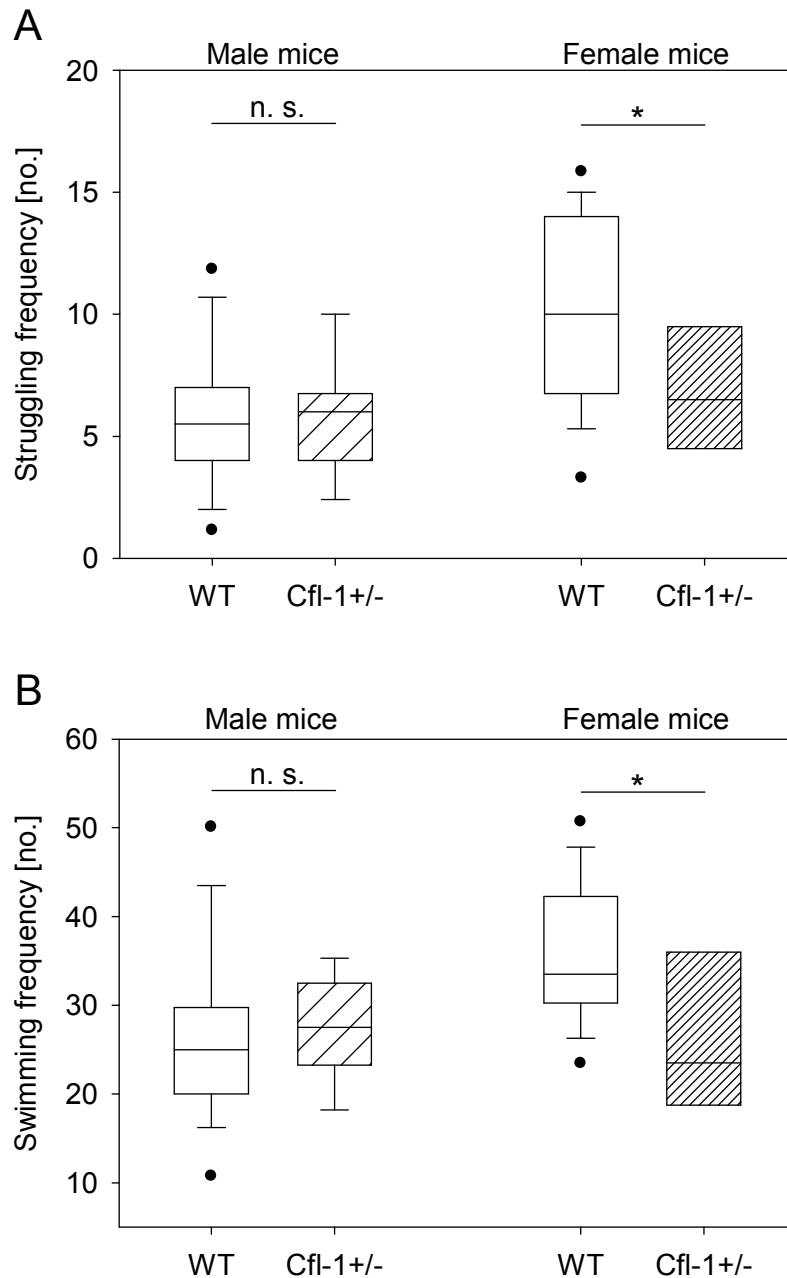


Figure 18: Results of FST scoring. Significant differences in struggling (A) and swimming (B) frequencies were detected in females only (Males:  $n_{(Cfl-1^{+/-})} = 16$ ,  $n_{(WT)} = 22$ ; females:  $n_{(Cfl-1^{+/-})} = 8$ ;  $n_{(WT)} = 22$ ; n. s. = not significant, \* = p-value < 0.05).

#### 4.2.2.5 Increased stress reactivity in *Cfl-1<sup>+/-</sup>* vs. WT mice

As detected in the SRT, the initial corticosterone concentrations in the plasma of male and female *Cfl-1<sup>+/-</sup>* vs. WT mice did not differ (males: *Cfl-1<sup>+/-</sup>* 7.49 ng/ml, SEM  $\pm 2.57$  vs. in WT 5.08 ng/ml, SEM  $\pm 0.87$ ; MWU p-value = 0.885; females: *Cfl-1<sup>+/-</sup>* 14.67 ng/ml, SEM  $\pm 4.61$  vs. in WT 13.62 ng/ml, SEM  $\pm 3.93$ ; MWU p-value = 0.453). The corticosterone

concentrations in the plasma of reaction samples differed significantly independent of gender (males: 268.42 ng/ml, SEM  $\pm$ 18.02 vs. in WT 224.57 ng/ml, SEM  $\pm$ 14.06; MWU p-value = 0.043; females: 453.45 ng/ml, SEM  $\pm$ 26.25 vs. in WT 387.15 ng/ml, SEM  $\pm$ 14.15; MWU p-value = 0.028), suggesting that the stress reactivity of tested animals is influenced by the genotype at the *Cfl-1*<sup>+/-</sup> locus. The same applied to the corticosterone increase. The increase calculated between the initial and the reaction plasma corticosterone concentration showed as a statistical trend in male mice (*Cfl-1*<sup>+/-</sup> 260.92 ng/ml, SEM  $\pm$ 17.66 vs. in WT 219.50 ng/ml, SEM  $\pm$ 14.11; MWU p-value = 0.055) and differed significantly in female mice (*Cfl-1*<sup>+/-</sup> 438.78 ng/ml, SEM  $\pm$ 26.08 vs. in WT 373.53 ng/ml, SEM  $\pm$ 11.84; MWU p-value = 0.039). In addition, the recovery value as well as the corticosterone decrease between the reaction and the recovery sample did not show any statistically relevant differences in male mice (mean recovery value *Cfl-1*<sup>+/-</sup> 33.28 ng/ml, SEM  $\pm$ 7.29 vs. in WT 31.11 ng/ml, SEM  $\pm$ 4.87; MWU p-value = 0.773; mean decrease value *Cfl-1*<sup>+/-</sup> 244.15 ng/ml, SEM  $\pm$ 23.47 vs. in WT 226.69 ng/ml, SEM  $\pm$ 22.76; MWU p-value = 0.564). In females, the corticosterone concentration in the recovery plasma sample was still increased in *Cfl-1*<sup>+/-</sup> compared to WT mice (*Cfl-1*<sup>+/-</sup> 40.05 ng/ml, SEM  $\pm$ 8.90 vs. in WT 18.12 ng/ml, SEM  $\pm$ 2.80; MWU p-value = 0.064). This statistical effect did not show in the corticosterone decrease, as the reaction and the recovery sample were increased at equal measures (*Cfl-1*<sup>+/-</sup> 405.29 ng/ml, SEM  $\pm$ 45.70 vs. in WT 354.50 ng/ml, SEM  $\pm$ 30.72; MWU p-value = 0.28). In general, the corticosterone concentrations measured in female mice were considerably increased compared to male mice, independent of the genotype at the *Cfl-1* locus. The results of SRT data are summarized in Figures 19, 20, and 21.

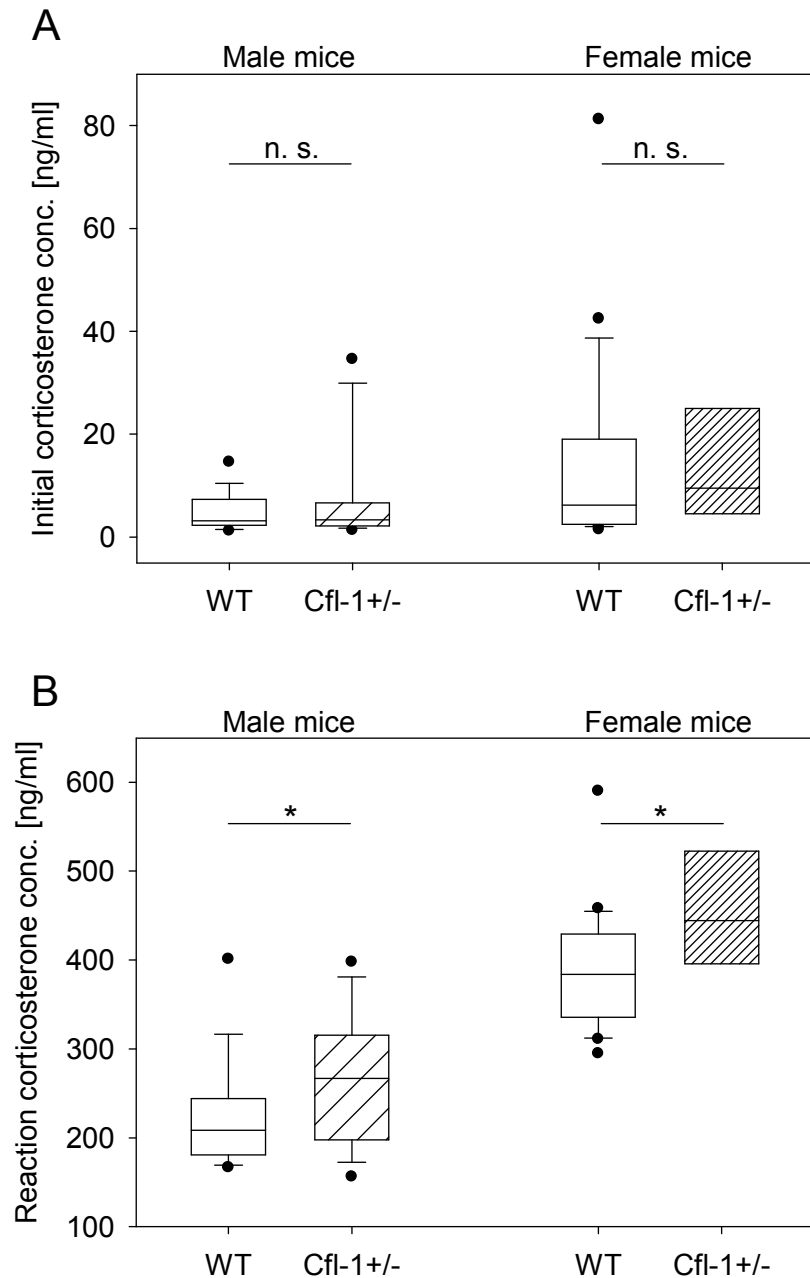


Figure 19: Results of the SRT. Independent of gender, initial corticosterone concentrations (A) did not differ between the lines, reaction corticosterone concentrations (B) differed significantly between *Cfl-1*<sup>+/-</sup> and WT mice (Males:  $n_{(Cfl-1+/-)} = 15$ ,  $n_{(WT)} = 18$ ; females:  $n_{(Cfl-1+/-)} = 8$ ,  $n_{(WT)} = 22$ ; n. s. = not significant, \* = p-value < 0.05).

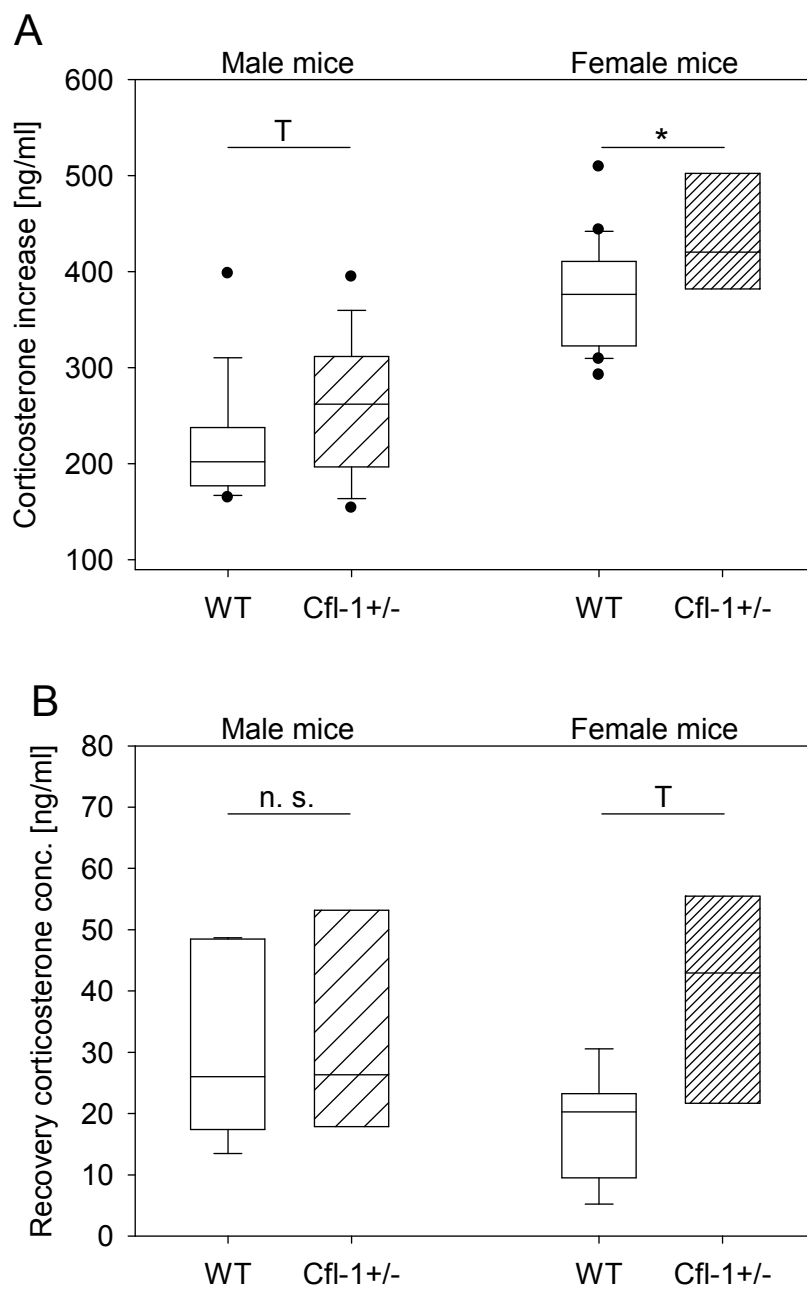


Figure 20: Results of the SRT. Corticosterone increase values (A) and recovery corticosterone concentrations (B) gender-dependently differed between *Cfl-1*<sup>+/-</sup> and WT mice (Corticosterone increase males:  $n_{(Cfl-1+/-)} = 15$ ,  $n_{(WT)} = 18$ ; females:  $n_{(Cfl-1+/-)} = 8$ ,  $n_{(WT)} = 22$ ; recovery corticosterone concentrations males;  $n_{(Cfl-1+/-)} = 8$ ,  $n_{(WT)} = 9$ ; females:  $n_{(Cfl-1+/-)} = 4$ ,  $n_{(WT)} = 9$ ; n. s. = not significant, T = p-value <0.1, \* = p-value <0.05).

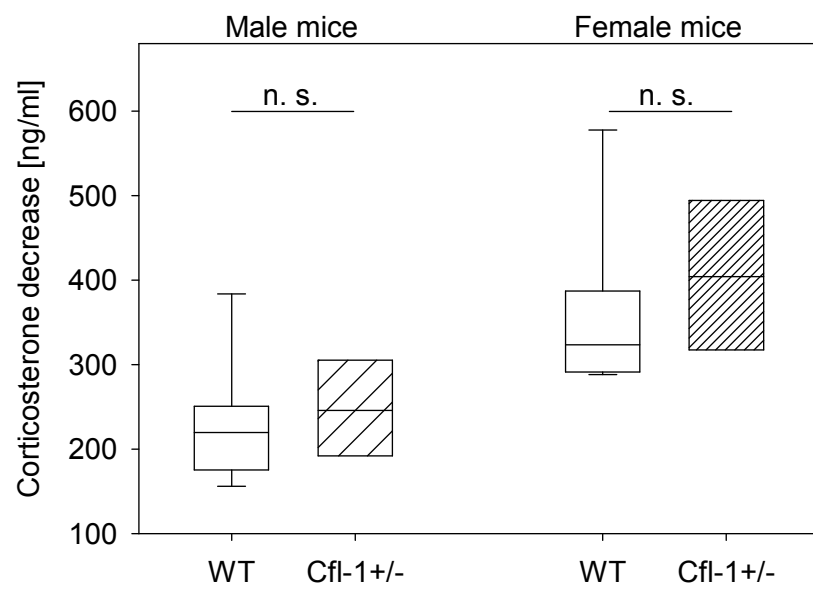


Figure 21: Results of the SRT. Corticosterone decrease values did not differ between *Cfl-1<sup>+/-</sup>* and WT mice (Males:  $n_{(Cfl-1+/-)} = 8$ ,  $n_{(WT)} = 9$ ; females:  $n_{(Cfl-1+/-)} = 4$ ;  $n_{(WT)} = 9$ ; n. s. = not significant).

### **4.3 Segmental copy number variation and SNP profiling of HAB vs. LAB and HR vs. LR mice**

#### **4.3.1 Regions of segmental copy number variation in DNA copy numbers differing in HAB vs. LAB and in HR vs. LR mice**

The Jax Mouse Diversity Genotyping array disclosed 180 regions harboring segmental copy number variations between HAB and LAB mice, fragment sizes ranging from 2 to 7,383,756 bp. Among these 180 regions, 137 CNVs (>1 kbp) and 43 segmental changes (<1 kbp) were identified covering in total 14,731,644 bp of the HAB/LAB genome. Having taken the LAB sequence as reference sequence, 62 losses and 118 gains were identified in the HAB sequence in relation to the reference sequence. The comparison of HR and LR sequences resulted in the detection of 154 segmental copy number variations, the shortest segmental variation counted 9 bp, the longest 1,115,056 bp. Among these, 115 CNVs and 39 segmental changes were revealed, which covered in total 5,445,908 bp of the HR/LR genome. In this comparison, the LR sequence served as reference sequence. Thus, 108 gains and 46 losses were detected in the HR sequence in respect to the LR sequence. A rather general observation applying to both mouse models was the accumulation of segmental variations in proximate vicinity. A detailed summary of the detected segmental variation in DNA copy numbers is provided in Tables S8 (HAB/LAB) and S9 (HR/LR). Figures 22 (HAB vs. LAB) and 23 (HR vs. LR) depict the genomic location of segmental variations in both mouse models. Independent of the fragment size, segmental changes are further on referred to as CNVs.

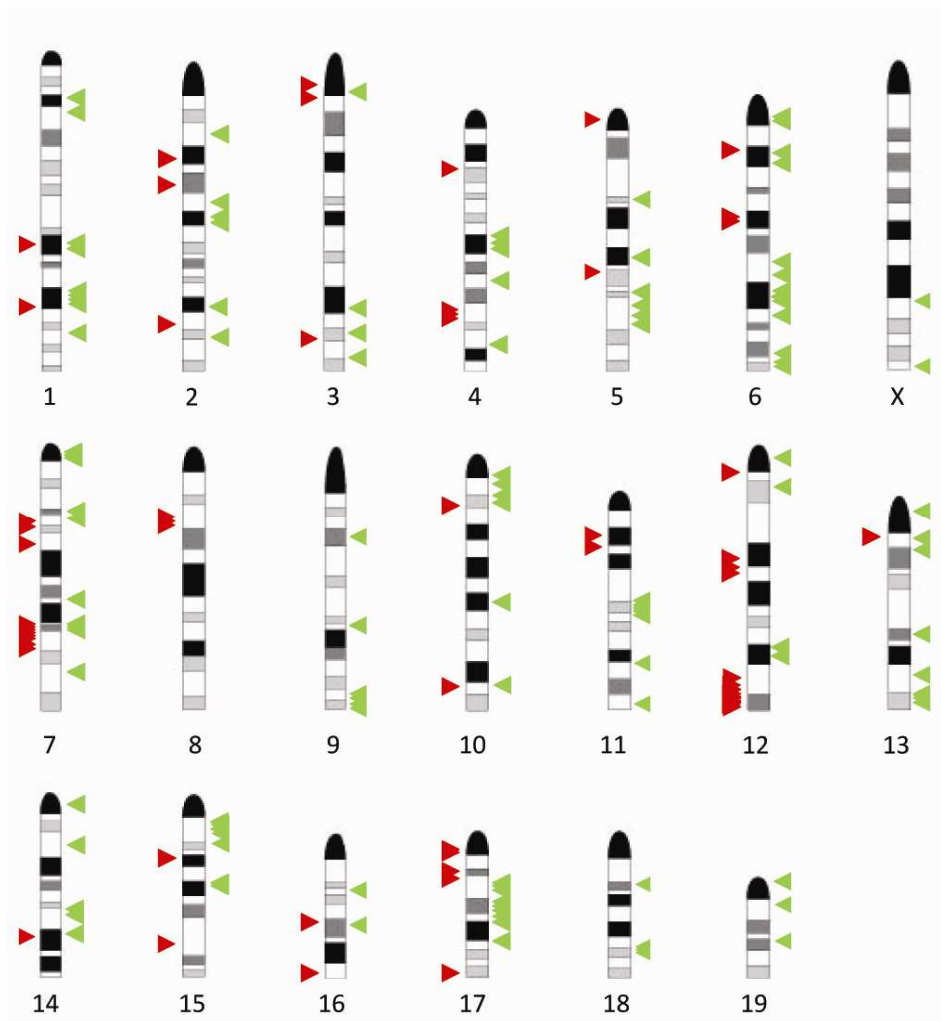


Figure 22: Locations of segmental copy number variations in the genome of HAB vs. LAB mice. Relative gains are indicated with green, relative losses with red arrows.

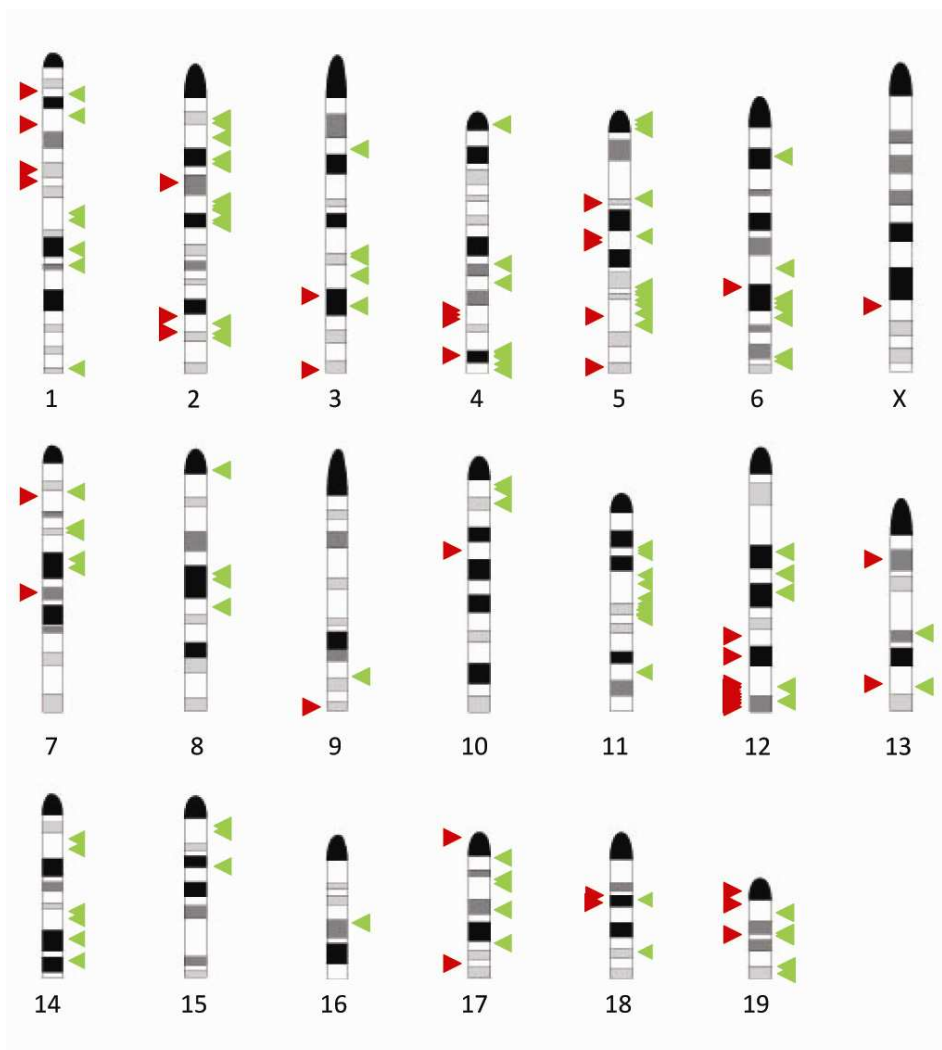


Figure 23: Locations of segmental copy number variations in the genome of HR vs. LR mice. Relative gains were indicated with green, relative losses with red arrows.

#### 4.3.2 Influence of segmental variation in DNA copy numbers on gene expression in the hippocampus of HR and LR mice

A regulatory effect of segmental copy number variation on gene expression in the hippocampus of HR and LR mice was found based on CNV data derived from the Jax Mouse Diversity Genotyping array and the pool of genes detected to be differentially regulated in the microarray experiment ( $p$ -value = 0.042). For this analysis, a two-proportion Z-test was performed comparing the proportion of probes covering regions of segmental variation in all probes not showing expressional differences with the proportion of probes covering regions of segmental variations in all probes that were shown to be differentially expressed. Numbers underlying this calculation are summarized in Table 16.

Table 16: Numbers underlying the calculation of the two-proportion Z-test based on the microarray study.

<b>No. of</b>	<b>HR vs. LR</b>
Regulated genes	300
Segmental variation in DNA	154
Total microarray probes	45,281
Detectable probes	20,154
Differentially expressed probes	248
Probes in CNVs	735
Differentially expressed probes in segmental variation	15
<b>p-value</b>	<b>0.042</b>

To overcome the limitation coming along with non-detectable probes in the microarray study, the identical calculation was repeated with genes detected to be differentially expressed in the hippocampus of HR vs. LR mice according to the SAGE study. This NGS-based transcriptome analysis was chosen as a probe-independent approach which did not entail the identification of a delimited pool of regulated genes only. Thus, the two-proportion Z-test compared the proportion of genes encoded for in regions of segmental variation in the total of non-differentially expressed genes genome-wide with the proportion of those genes in segmental variations in the total of differentially expressed genes.

In either case, protein coding genes only were taken into account. The number of protein coding genes in the mouse was according to the UCSC genome browser assessed with 25,071 (<http://genome.ucsc.edu/>). The two-proportion Z-test resulted in a p-value of 0.043 and, thus, very much resembled the p-value calculated based on the microarray gene pool. The data underlying the two-proportion Z-test are shown in Table 17.

Table 17: Numbers underlying the calculation of the two-proportion Z-test based on the SAGE study.

<b>No. of</b>	<b>HR vs. LR</b>
Differentially expressed protein coding genes	662
Protein coding genes in regions harboring segmental variation	795
Differentially expressed protein coding genes in segmental variation	30
<b>p-value</b>	<b>0.043</b>

#### 4.3.3 SNP profiling of HAB vs. LAB and HR vs. LR animals using the JAX Mouse Diversity Genotyping array

The SNP profiling of one representative animal ('master animal') per line resulted in the identification of 60,077 heterozygous SNPs to differ between HAB and LAB which equals 9.64% of SNPs tested in the Jax Mouse Diversity Genotyping array. A total of 47,470

SNPs was detected to diverge between the HR and LR sequences, which equals 7.62% of all SNPs tested in the array. According to their location, SNPs were classified in intragenic (coding non-synonymous, coding, UTR, intronic) and intergenic SNPs. The exact numbers are summarized in Table 18. In addition, complete lists of all heterozygous SNPs between HAB and LAB and between HR and LR assorted according to their chromosomal location (genome build version 37) including information regarding the locus symbols of intragenic SNPs and type of SNP are provided in Table S8 (HAB vs. LAB) and S9 (HR vs. LR; excel-files).

Table 18: Summary of heterozygous SNPs differing between the lines of the inbred mouse models detected in the Jax Mouse Diversity Genotyping array.

<b>No. of SNPs</b>	<b>HAB vs. LAB</b>	<b>HR vs. LR</b>
Intragenic	23,248	18,758
Coding non-synonymous	299	213
Coding	603	526
UTR	533	471
Intronic	21,813	17,548
Intergenic	36,829	28,712
<b>Total</b>	<b>60,077</b>	<b>47,470</b>

Based on the SNP profiling of the two mouse models, an overlapping pool of SNPs was created containing heterozygous SNPs differing between HAB and LAB and at the same time between HR and LR mice. This overlapping SNP pool contained 17,722 SNPs, 7,374 intragenic (96 coding non-synonymous, 189 coding, 171 UTR, 6,918 intronic) and 10,348 intergenic SNPs. A complete list of SNPs of the overlapping pool was prepared in Table S10 (excel-file). This file contains information regarding SNP genotypes, chromosomal coordinates (genome build version 37), locus symbols of intragenic SNPs and the type of SNPs. This overlapping SNP pool served as basis for the design of two customized Illumina SNP genotyping chips.

#### **4.4 Phenotypic characterization of an outbred population of CD-1 male mice**

##### **4.4.1 Results of behavioral testing of 384 CD-1 male mice**

384 CD-1 male mice were batch-wise subjected to the 'CD-1 panel' behavioral test battery described under point 3.2.4.2.

##### **4.4.1.1 Results of EPM testing**

First, it was excluded that there were relevant differences in the behavior of animals on the EPM between the eight test batches assuring the comparability of separate batches. The means values did not differ significantly between the batches. The majority of animals displayed an intermediate level of anxiety-related behavior, though extreme traits towards both directions were collected as well. The mean values per batch including SEMs of the total distance travelled on the EPM, the percentage time spent on the open arm, and the numbers of open arm entries are provided in Table 19. In addition, the distribution of the three EPM parameters named above over the eight test batches is provided in Figures 24 and 25 A. Furthermore, the distribution of the percentage time animals spent on the open arm of the EPM among the 384 animals tested is shown in Figure 25 B. The percentage time animals spent on the open arm was therefore plotted against the number of animals displaying the respective time. This graph reflects the continuum of the anxiety-related behavior present in the outbred population. The majority of animals displayed an intermediate anxiety-related phenotype by spending roughly 20 - 60% of their time on the open arm of the EPM. Animals displaying around 10% of their time on the maze on the open arm represent the fraction of the CD-1 population displaying extremes in the anxiety-related behavior and, therefore, resemble to HAB mice in that aspect. Also, extremely non-anxious mice spending approximately 90% of their time on the EPM on the open arm were observed in the CD-1 population, resembling to the behavior of LAB mice.

Table 19: Summary of data collected from EPM core parameters including mean values and the respective SEMs for the eight different test batches and the total of animals tested.

Batch	Total distance travelled [m]	Percentage time spent on open arm [%]	Open arm entries [no.]
	Batch means $\pm$ SEM	Batch means $\pm$ SEM	Batch means $\pm$ SEM
1	9.52 $\pm$ 0.35	34.16 $\pm$ 1.76	32.02 $\pm$ 1.22
2	9.52 $\pm$ 0.32	35.43 $\pm$ 1.85	30.65 $\pm$ 1.15
3	9.58 $\pm$ 0.31	37.71 $\pm$ 2.03	28.81 $\pm$ 1.16
4	10.15 $\pm$ 0.34	35.02 $\pm$ 1.44	31.13 $\pm$ 1.13
5	9.67 $\pm$ 0.32	35.98 $\pm$ 1.84	30.19 $\pm$ 1.52
6	10.02 $\pm$ 0.32	35.34 $\pm$ 1.57	28.65 $\pm$ 1.12
7	8.84 $\pm$ 0.30	31.13 $\pm$ 1.71	29.81 $\pm$ 1.13
8	9.97 $\pm$ 0.25	37.30 $\pm$ 1.52	28.73 $\pm$ 1.23
<b>Total</b>	<b>9.66</b> <b><math>\pm</math>0.11</b>	<b>35.26</b> <b><math>\pm</math>0.61</b>	<b>29.00</b> <b><math>\pm</math>0.43</b>

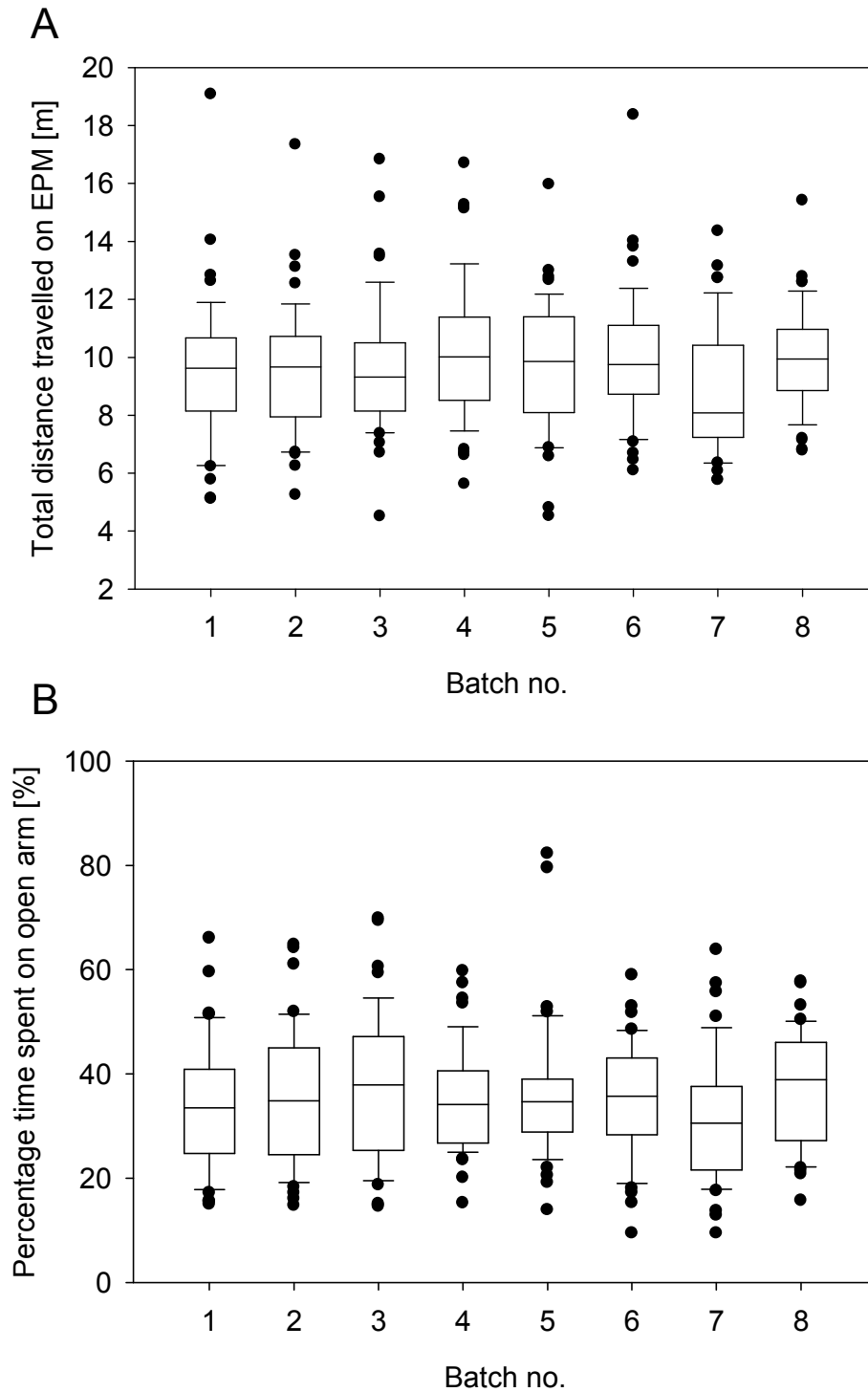


Figure 24: Graphic comparison of EPM data. The total distance travelled on the EPM (A) and the percentage time animals spent on the open arm of the EPM (B) did not significantly differ between the eight test batches.

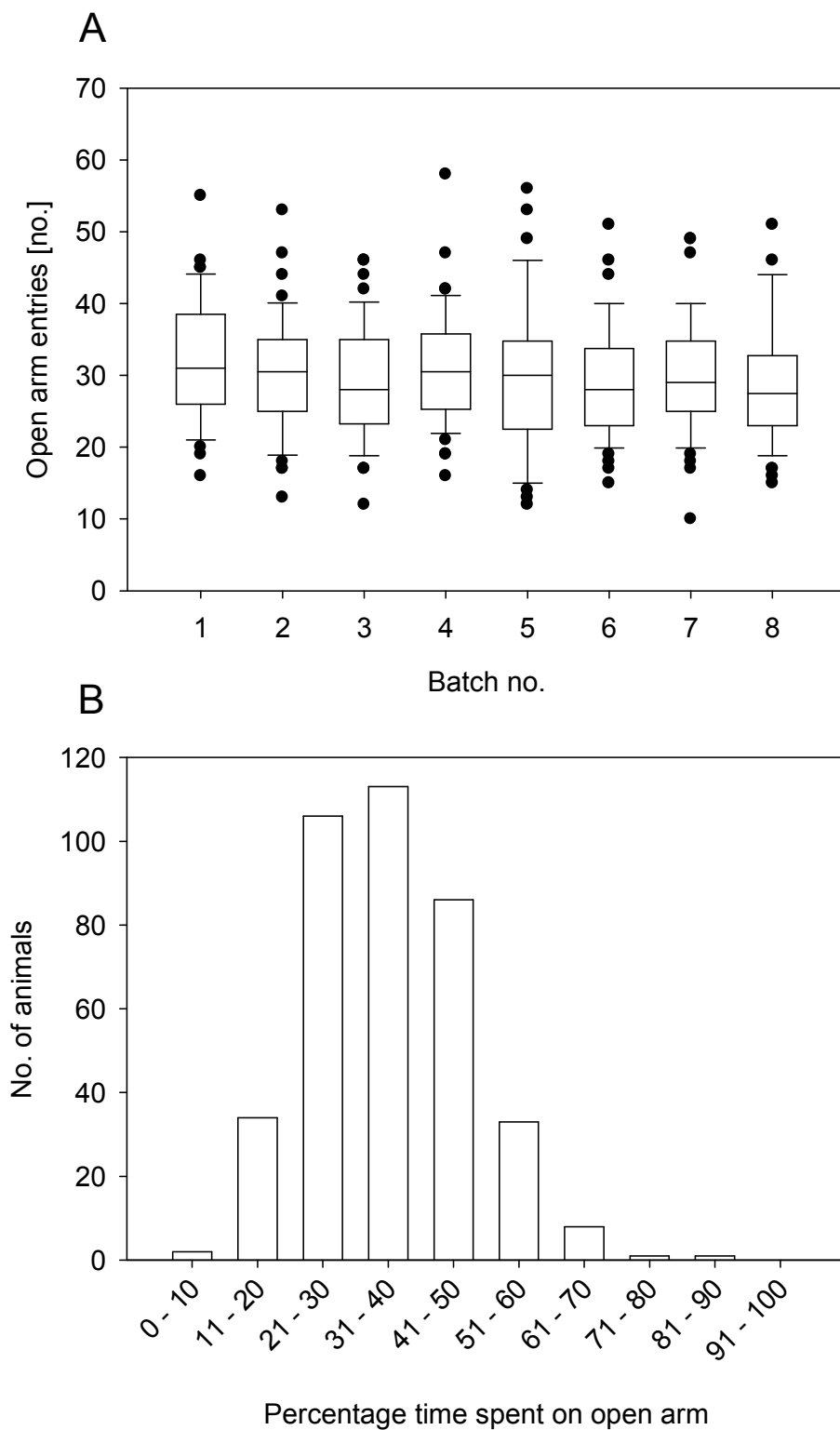


Figure 25: Graphic comparison of EPM data. The number of open arm entries on the EPM did not significantly differ between the eight test batches (A) and furthermore, the distribution of the EPM parameter 'percentage time spent on the open arm' in the 384 animals (B) is provided.

#### 4.4.1.2 Results of OF testing

In similarity to data collected from EPM testing, considerable differences in the behavior of mice in the OF from different batches were excluded. A summary of the results of the OF key parameters 'total distance travelled in the OF', 'time spent in the inner zone', and 'the distance travelled in the inner zone' is compiled in Table 20. In Figures 26 and 27 A graphic illustrations of these OF key parameters are provided. According to this, the majority of CD-1 mice tested displayed an intermediate trait anxiety in the OF, though, extremes towards both directions were observed as well. In addition, in Figure 27 B the distribution of the parameter 'total distance travelled in the OF' is plotted against the respective number of animals displaying the trait. This graph reflects the continuum of anxiety-related behaviors presented in the CD-1 population. The majority of mice travelled between 16 and 40 m in the OF apparatus. Individuals displaying extremes of trait anxiety were observed as well. Data of EPM and OF testing were also analyzed regarding a potential influence of the test order – EPM testing first vs. OF testing first. An influence of the test order on the behavior of the animals was excluded. This is exemplarily shown for the total distance animals travelled on the EPM in Figure 28.

Table 20: Summary of OF key parameters from different test batches and from the total number of animals tested. Batch mean values and SEMs are provided for the three key parameters.

Batch	Total distance travelled [m]	Time spent in inner zone [s]	Distance travelled inner zone [m]
	Batch means ±SEM	Batch means ±SEM	Batch means ±SEM
1	23.98 ±1.03	22.84 ±2.59	2.26 ±0.22
2	25.97 ±0.98	25.71 ±2.25	2.86 ±0.23
3	25.58 ±0.85	23.85 ±2.31	2.53 ±0.24
4	27.55 ±1.07	24.21 ±2.15	2.96 ±0.28
5	27.94 ±0.80	24.89 ±2.02	2.98 ±0.22
6	25.88 ±0.88	15.89 ±1.58	1.99 ±0.19
7	25.36 ±0.79	25.09 ±1.95	2.60 ±0.27
8	27.35 ±0.87	22.47 ±1.53	2.73 ±0.21
<b>Total</b>	<b>26.20 ±0.33</b>	<b>23.12 ±0.74</b>	<b>2.62 ±0.08</b>

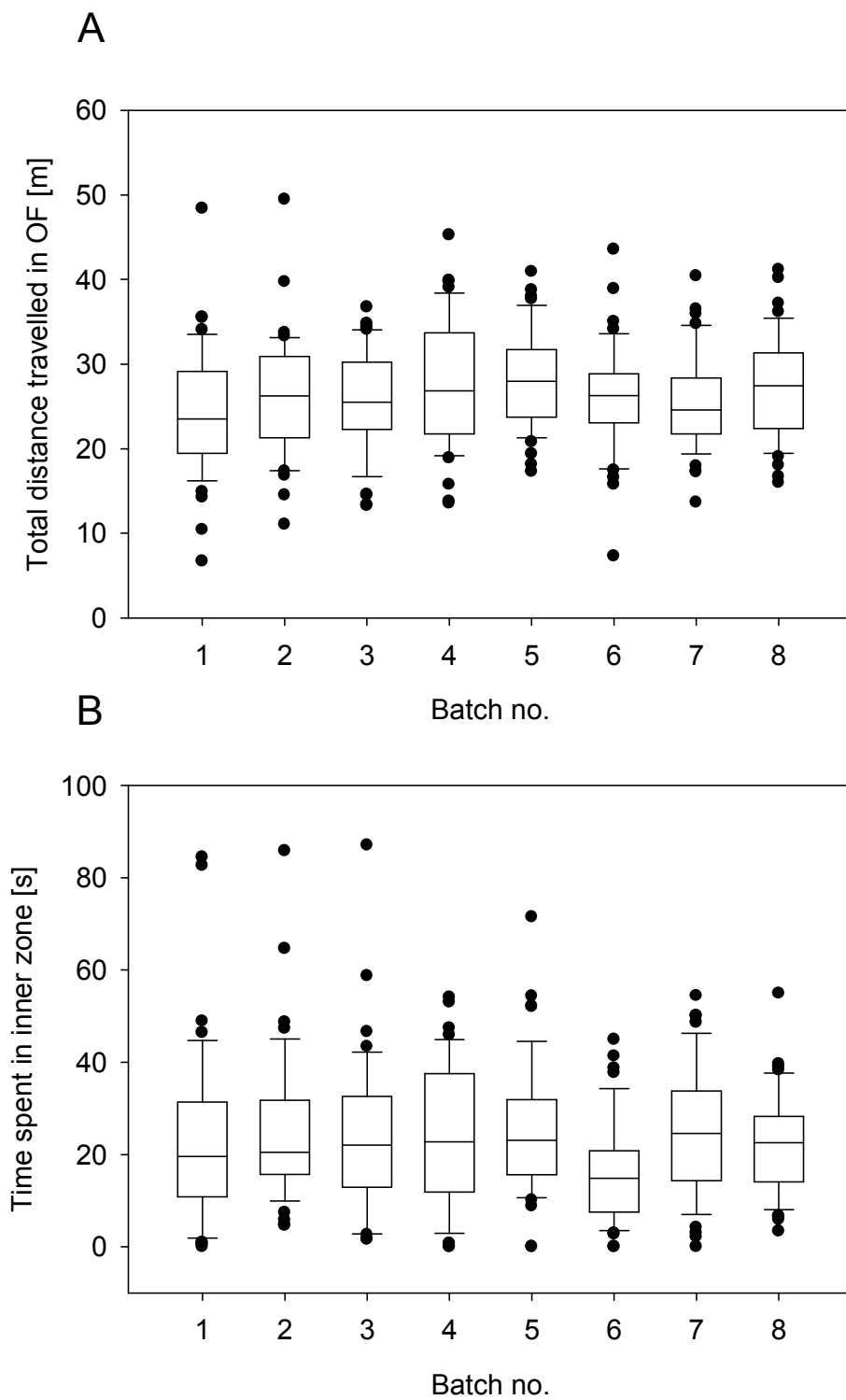


Figure 26: Graphic comparison of OF data. The mean distances travelled (A) and the time animals spent in the inner zone of the OF (B) did not differ substantially between the eight separate test batches.

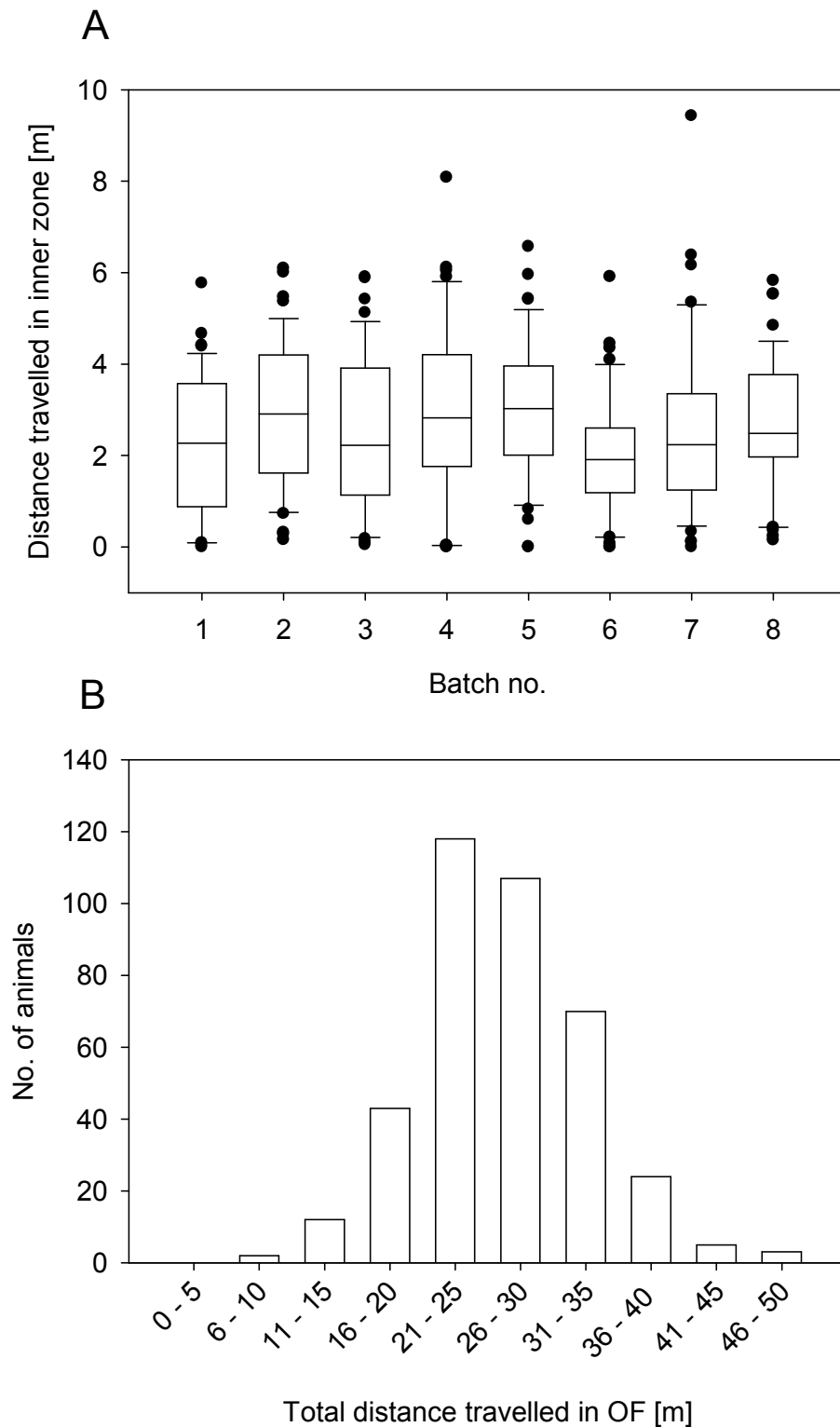


Figure 27: Graphic comparison of OF data. The distance travelled in the inner zone of the OF (A) did not significantly differ between the eight test batches and furthermore, the distribution of the OF parameter 'total distance travelled in OF' among the 384 animals tested is shown (B).

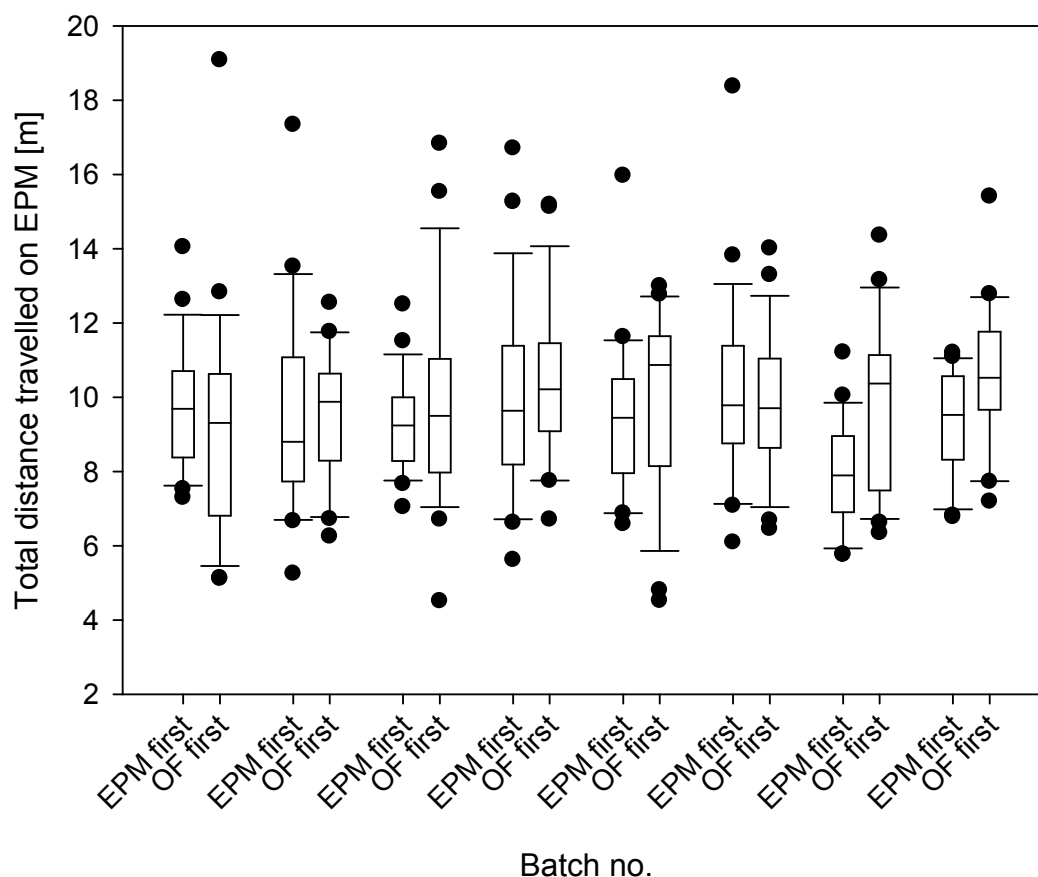


Figure 28: Graphic illustration of the total distances animals travelled on the EPM. The alternating order of EPM and OF testing did not influence the behavior of animals in the tests for anxiety-related behavior.

#### 4.4.1.3 Results of FST

An overview over data from FST key parameters 'time swimming', 'time floating', and 'floating latency' is provided in Table 21 and in Figures 29 and 30 A. In similarity to the behavioral tests reflecting anxiety-related behavior, also in the FST no significant differences between the batches were observed. Furthermore, the majority on CD-1 mice displayed an intermediate depression-like behavior but also extreme traits towards both directions were observed. The continuum of depression-like behaviors in the CD-1 outbred population is shown in Figure 30 B. The total immobility time which comprises the time animals spent floating and freezing during FS testing, was therefore plotted against the number of animals showing the respective immobility time. According to this, the majority on CD-1 mice spent 151 to 299 s immobile during the FST period.

Table 21: Summary of FST key parameters from different test batches and from the total of animals tested. Mean values and SEMs are provided for the three key parameters.

Batch	Time swimming [s]	Time floating [s]	Floating latency [s]
	Batch means ±SEM	Batch means ±SEM	Batch means ±SEM
1	102.5 ±8.58	200.34 ±8.95	85.06 ±5.11
2	83.69 ±6.18	216.2 ±6.80	70.81 ±3.25
3	78.79 ±5.84	234.86 ±7.10	67.29 ±3.41
4	80.28 ±4.82	235.52 ±4.96	62.97 ±2.91
5	89.54 ±5.62	230.74 ±5.94	56.26 ±3.22
6	94.74 ±5.88	230.57 ±5.45	66.15 ±2.58
7	85.41 ±5.17	225.56 ±5.88	64.75 ±3.10
8	73.60 ±4.54	235.96 ±5.58	63.61 ±3.57
<b>Total</b>	<b>86.07</b> <b>±2.13</b>	<b>226.22</b> <b>±2.33</b>	<b>68.24</b> <b>±1.26</b>

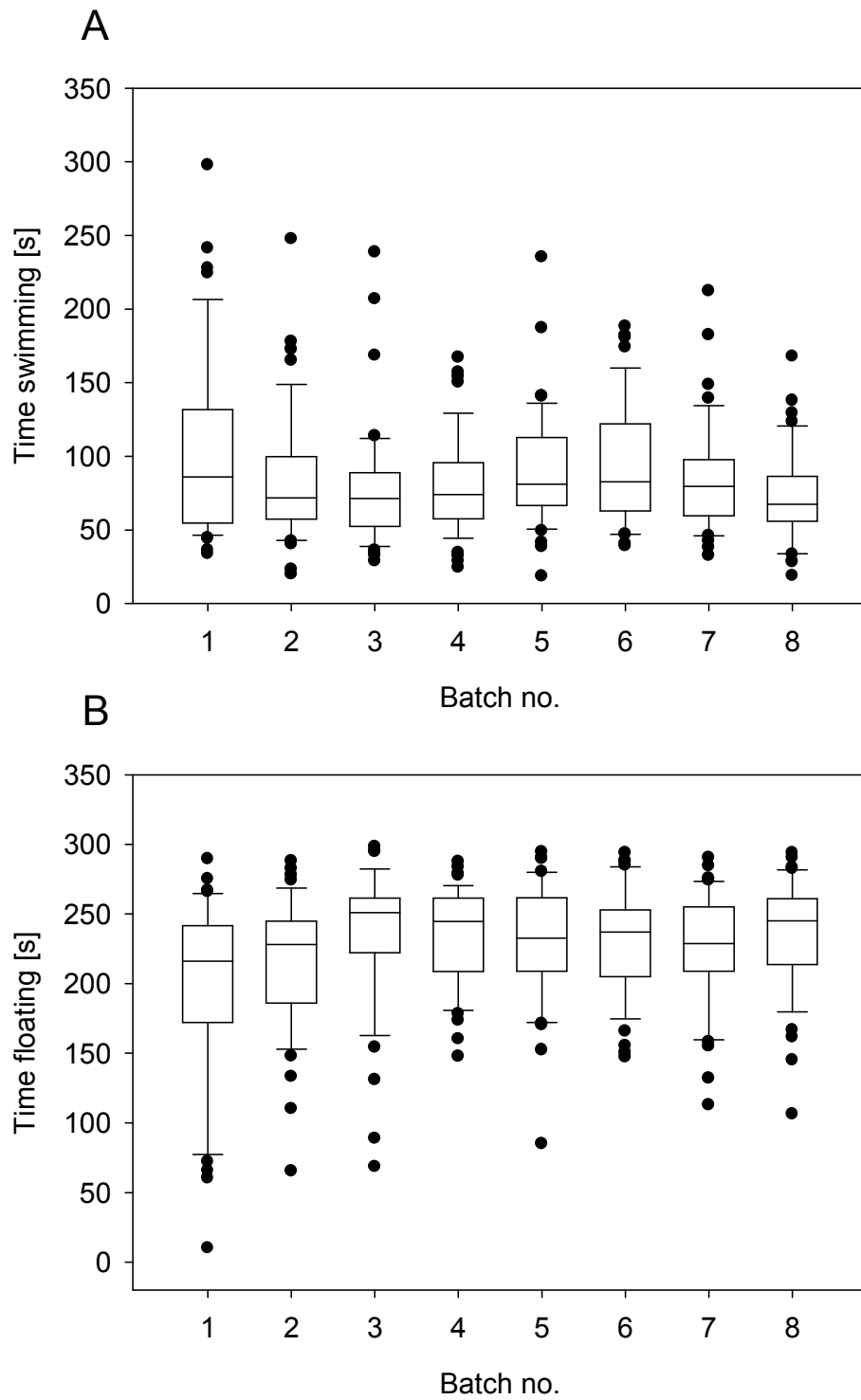


Figure 29: Graphic comparison of FST data. The times animals spent swimming (A) and floating (B) did not differ significantly between the eight test batches.

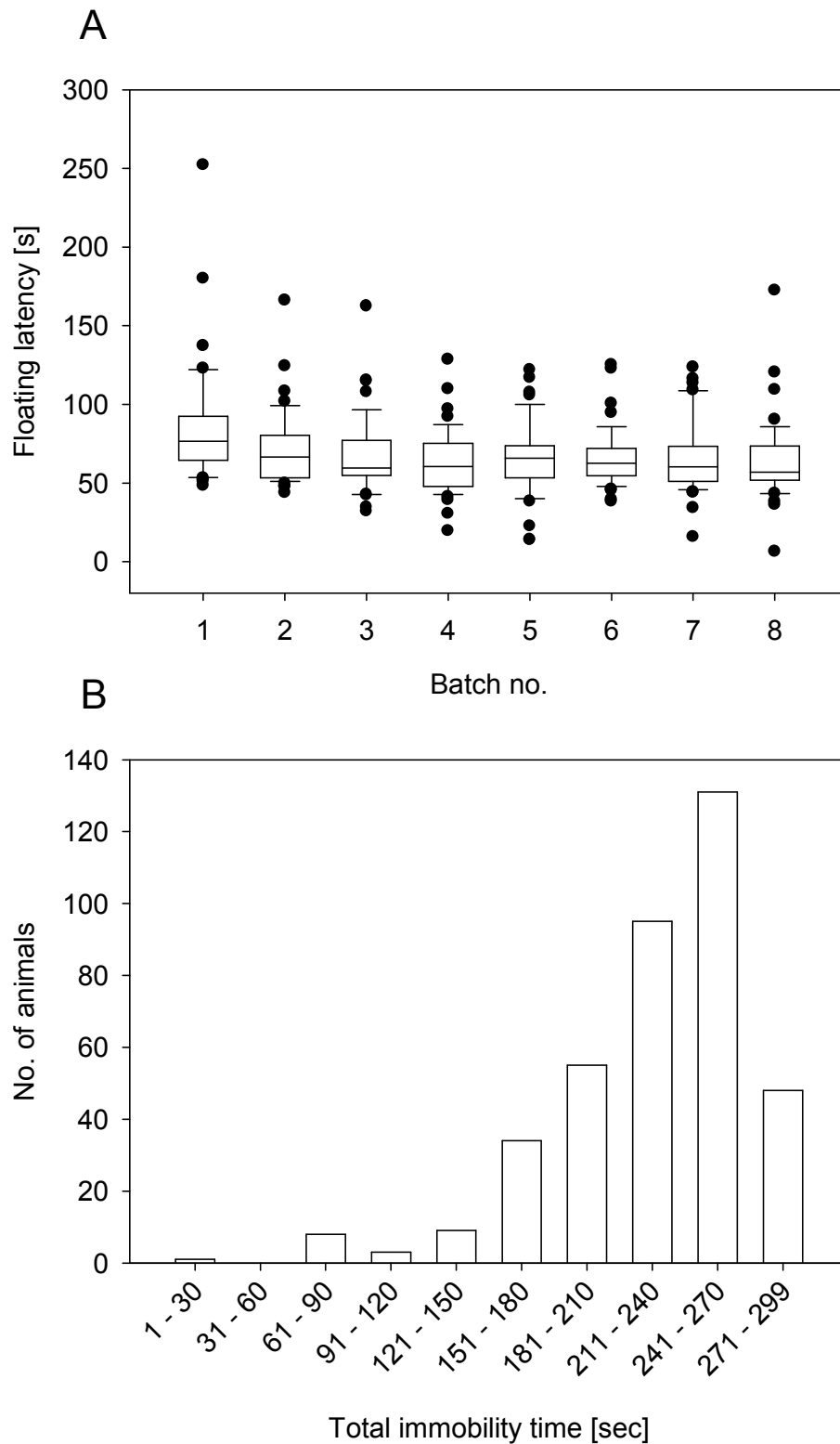


Figure 30: Graphic comparison of FST data. The floating latency (A) did not differ significantly between the eight test batches and furthermore, the distribution of the total immobility time is shown (B).

#### 4.4.1.4 Results of SRT

The plasma corticosterone concentrations measured in initial and reaction probes, as well as the corticosterone increase which was calculated based on these measures, are shown as mean values of the test batches including the respective SEMs in Table 22. In Figures 31 and 32 A graphical illustrations of the data shown in Table 22 are provided. Also in the SRT, major differences between the separate test batches were excluded. Furthermore, a broad range of corticosterone increased was detected in the CD-1 outbred population (Figure 32 B). The majority of animals displayed an intermediate corticosterone increase, ranging from 121 to 240 ng/ml. Though, animals showing extremes in stress reactivity were observed. CD-1 mice showing a sub-standard corticosterone increase (about 100 ng/ml) resemble to LR mice in this aspect, whereas animals displaying a corticosterone increase by about 250 ng/ml and higher resemble the stress reactivity observed in HR mice.

Table 22: Summary of corticosterone measures detected after the SRT. Mean corticosterone concentrations per batch including SEMs are provided as well as for the total number of animals tested.

Batch	Initial corticosterone conc. [ng/ml]	Reaction corticosterone conc. [ng/ml]	Corticosterone increase [ng/ml]
	Batch means $\pm$ SEM	Batch means $\pm$ SEM	Batch means $\pm$ SEM
1	8.0 $\pm$ 2.31	199.6 $\pm$ 9.02	191.6 $\pm$ 8.33
2	6.8 $\pm$ 1.23	182.3 $\pm$ 6.04	175.4 $\pm$ 5.45
3	7.0 $\pm$ 1.57	193.4 $\pm$ 7.0	186.5 $\pm$ 6.53
4	11.2 $\pm$ 2.63	223.7 $\pm$ 8.17	212.5 $\pm$ 7.08
5	5.4 $\pm$ 1.28	191.3 $\pm$ 7.27	185.9 $\pm$ 6.86
6	10.1 $\pm$ 3.54	208.5 $\pm$ 10.03	198.4 $\pm$ 9.89
7	16.0 $\pm$ 5.18	226.6 $\pm$ 10.07	210.5 $\pm$ 8.25
8	4.8 $\pm$ 1.19	180.6 $\pm$ 7.57	175.8 $\pm$ 6.89
<b>Total</b>	<b>8.8 <math>\pm</math>1.00</b>	<b>201.3 <math>\pm</math>3.04</b>	<b>192.5 <math>\pm</math>2.74</b>

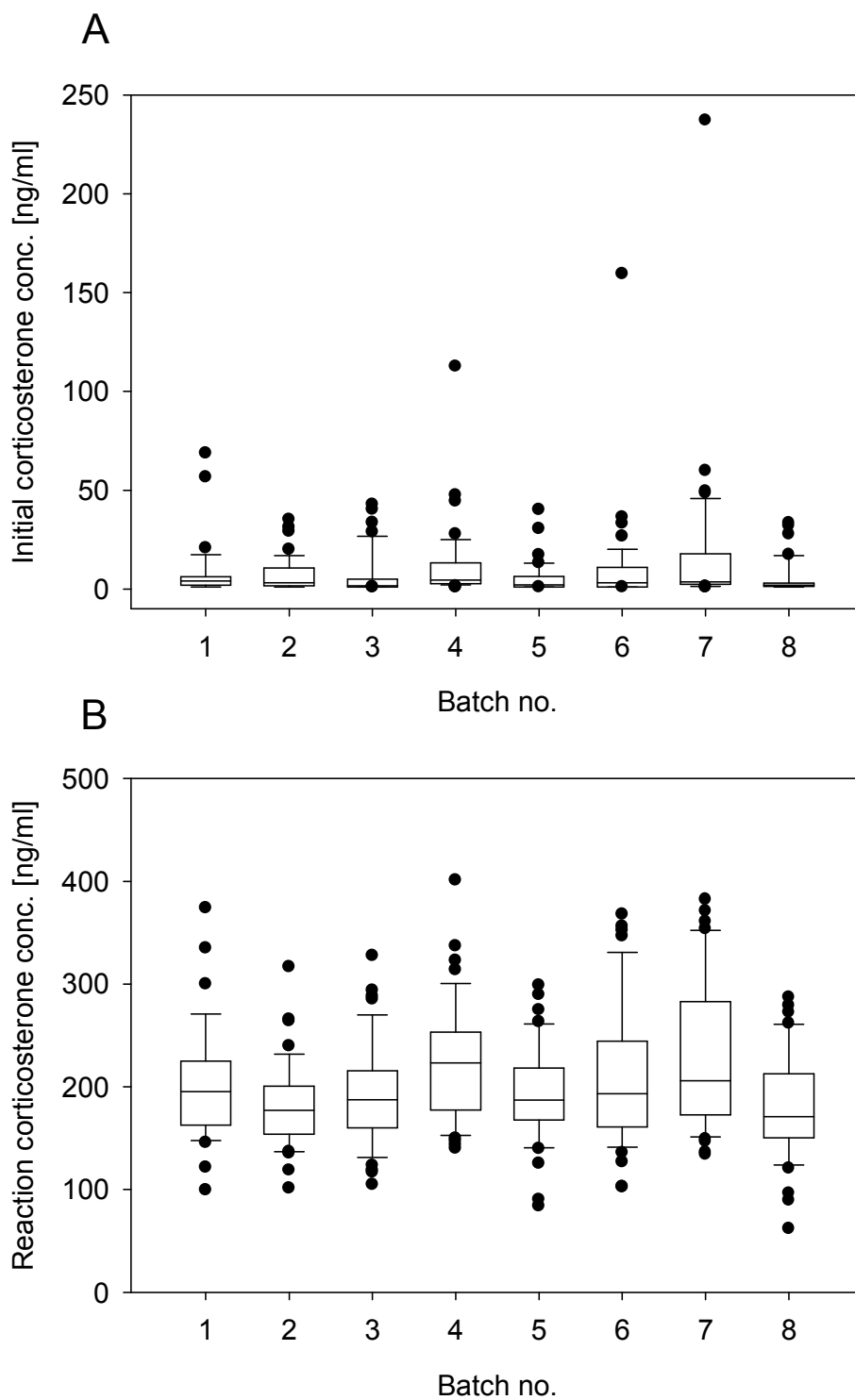


Figure 31: Graphic illustration of SRT data. Initial (A) and reaction (B) corticosterone concentrations are shown. No major differences were observed between the different test batches.

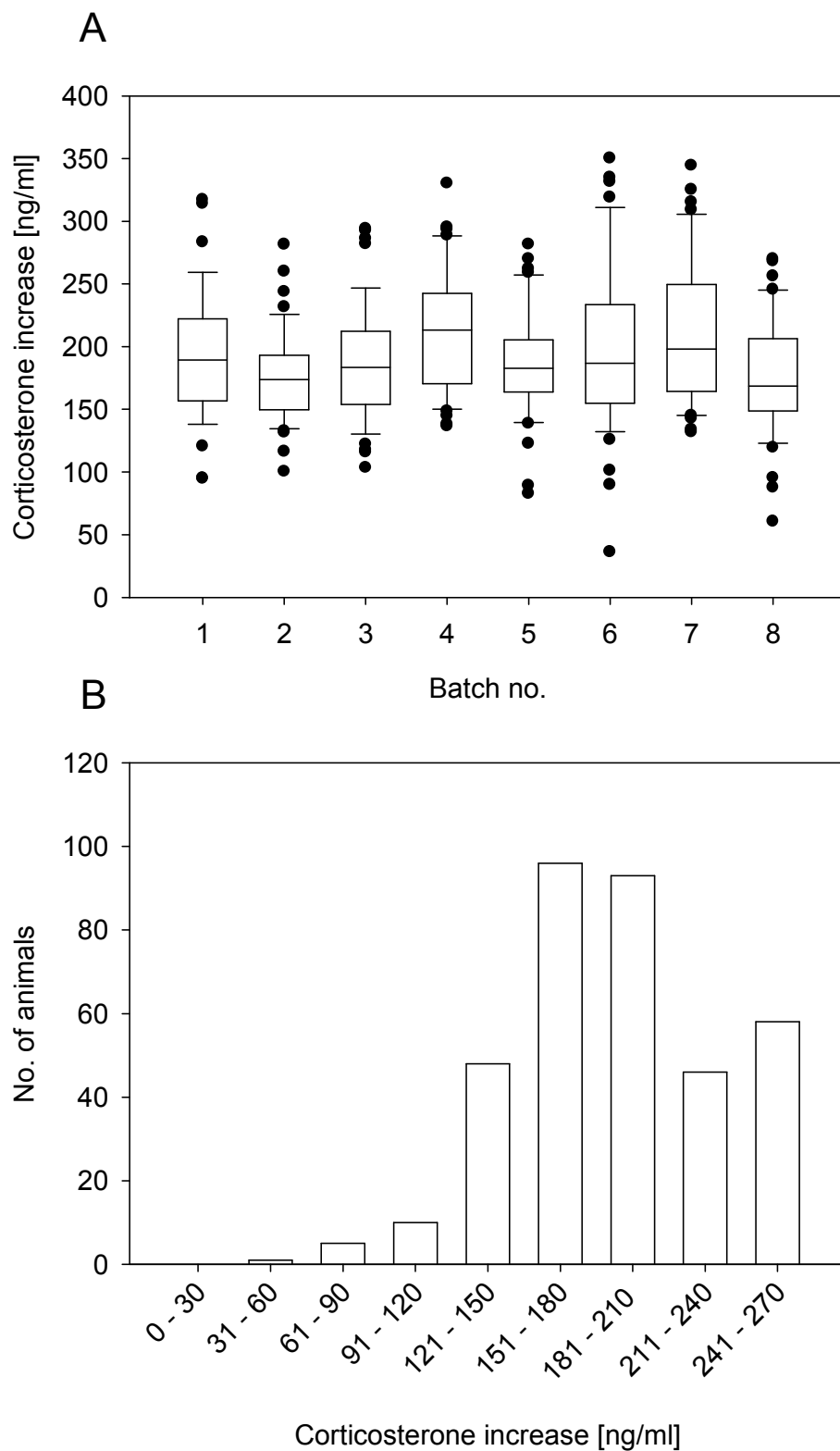


Figure 32: Graphic illustration of SRT data. The corticosterone increase (A) did not significantly differ between the test batches and furthermore, the distribution of the corticosterone increases (B) among the 384 CD-1 mice is shown.

#### 4.4.1.5 Results of TST

The results of the TST are summarized in Table 23 and Figure 33 A. Major differences in the depression-like behavior between the test batches were excluded. The majority of mice displayed an intermediate time immobile in the TST reflecting intermediate depression-like behavior. Figure 33 B depicts the distribution of the time immobile observed among the 384 CD-1 mice tested and reflects the continuum of depression-like features presented by the CD-1 outbred population. The majority of mice showed immobile phases between 0 and 150 s.

Table 23: Summary of data collected in the TST. The mean values including the respective SEMs of the total immobility time, the immobility frequency, and the latency to the first immobile phase are shown for the eight different batches and the total of all animals tested.

Batch	Immobility time [s]	Immobility frequency [no.]	Immobility latency [s]
	Batch means ±SEM	Batch means ±SEM	Batch means ±SEM
1	77.61 ±7.28	5.55 ±0.51	114.04 ±11.51
2	59.56 ±6.64	4.77 ±0.45	145.01 ±12.48
3	66.91 ±6.74	5.81 ±0.52	143.64 ±11.93
4	73.99 ±6.77	4.87 ±0.41	131.25 ±10.47
5	88.10 ±6.74	5.96 ±0.39	126.40 ±8.93
6	72.18 ±7.83	5.17 ±0.52	130.98 ±11.80
7	60.77 ±6.46	4.70 ±0.42	139.85 ±13.07
8	61.37 ±7.88	4.50 ±0.43	122.94 ±12.71
<b>Total</b>	70.21 ±2.51	5.18 ±0.16	131.96 ±4.12

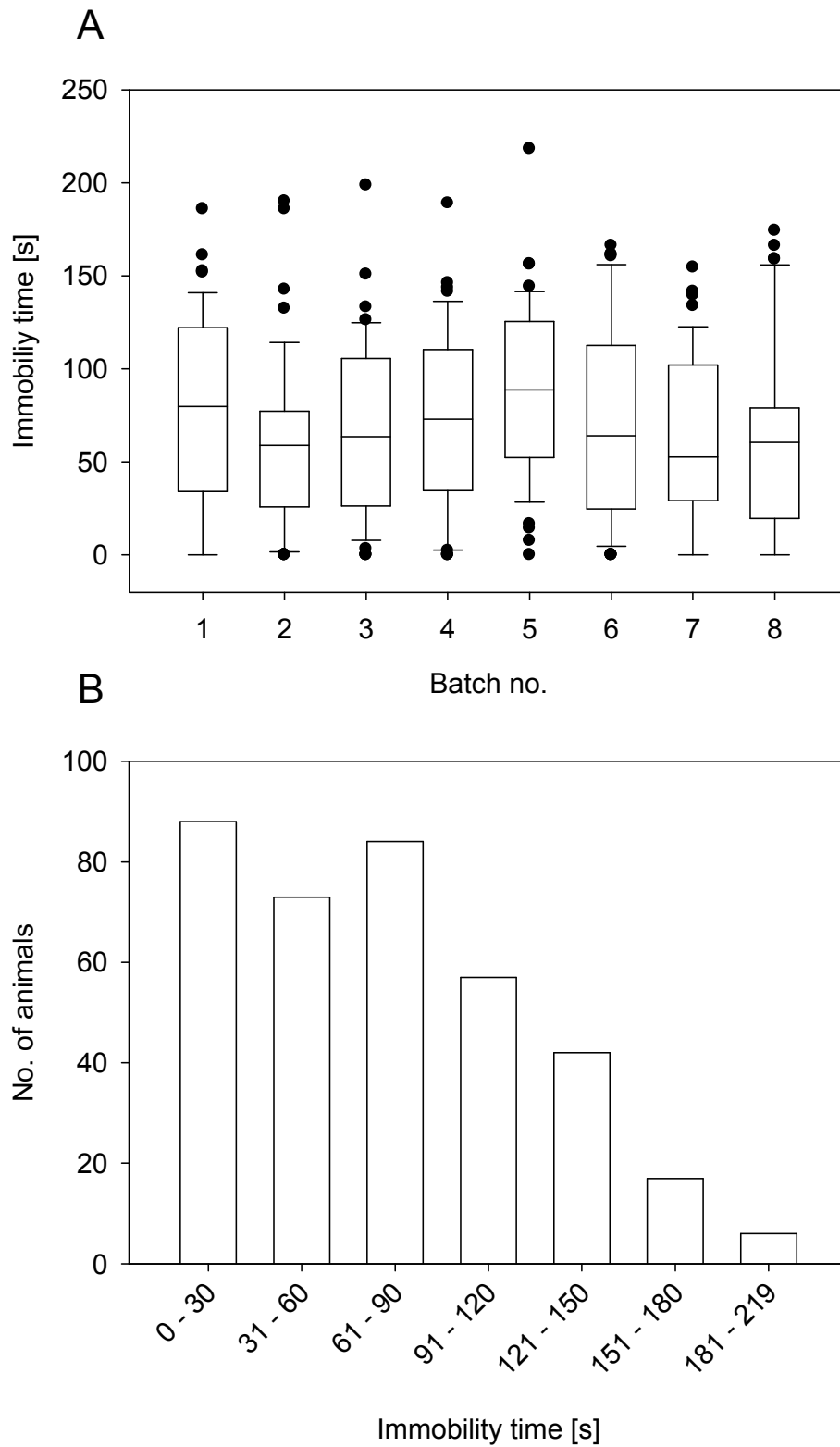


Figure 33: Graphic illustration of TST results. The immobility time did not differ significantly between the eight batches (A) and furthermore, the immobility time was plotted against the number of animals displaying the respective time immobile (B).

#### 4.4.1.6 No correlation between phenotypes collected in behavioral experiments of the 'CD-1 panel'

The PCA revealed no significant correlation of phenotypes collected in the behavioral test battery of the 'CD-1 panel'. As shown in Figure 34, the only correlated features were the ones implicated by the experimental set-up as, for example, mice can spend their time either in the inner or in the outer zone of the OF. The resulting inverse correlation is, thus, reflecting the experimental design and no biological correlation. A correlation of biological relevance, like for example the time spent floating in the FST and the immobility time in the TST, was not detected. Co-segregating phenotypes were, thus, not identified.

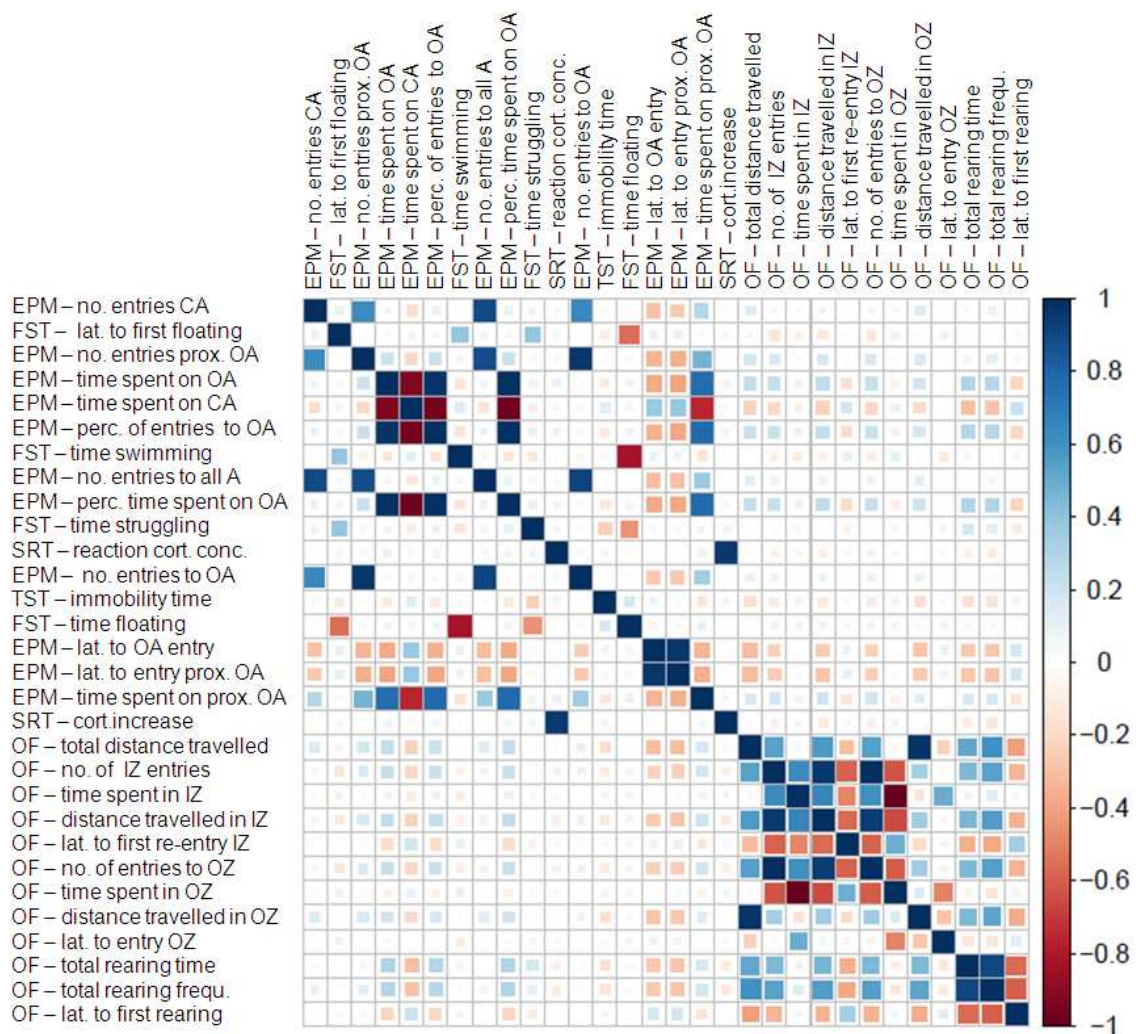


Figure 34: Graphical illustration of PCA results for phenotypes collected in the 'CD-1 panel'. Red bars show negative correlations, blue bars indicate positive correlations. The only correlations detected in the PCA are those implied by the experimental set-up (lat. = latency, prox. = proximal, OA = open arm, CA = closed arm, perc. = percentage, cort. = corticosterone, IZ = inner zone, OZ = outer zone, frequ. = frequency).

## **4.5 Association study – attribution of functional relevance to SNPs**

### **4.5.1 Selection of 32 phenotypically characterized CD-1 mice based on behavioral data**

The Jax Mouse Diversity Genotyping array was used to SNP- and CNV genotype 32 male CD-1 mice which were prior to that behaviorally characterized regarding anxiety-related and depression-like behavior, as well as regarding stress reactivity in the context of the 'CD-1 panel'. The selection of the 32 CD-1 mice was done by choosing the twelve most 'HAB-like' mice, the twelve most 'LAB-like' mice and eight animals displaying intermediate behaviors in the respective behavioral traits. As selection criterion for the determination of the anxiety-related behavior the time animals spent on the open arm of the EPM was taken. As key indicator for depression-like behavior served the time floating in the FST and the corticosterone increase after the SRT was chosen as the parameter reflecting the animal's stress reactivity. In order to simulate the behavioral patterns of the inbred mouse models in the 32 selected CD-1 mice, the most anxious mice showing the strongest depression-like feature and at the same time the lowest stress reactivity were considered as 'HAB-like'. Mice selected as 'LAB-like' fulfilled opposite criteria. Animals were ranked regarding each of the above named behavioral feature. Individuals reaching the highest, the lowest and the most intermediate mean ranking values among the population of 384 CD-1 mice were selected for array analysis. A complete list containing all behavioral features detected in the behavioral test battery of these 32 selected mice is provided in Table S13.

#### **4.5.1.1 PCA of quantitative behavioral traits confirmed correlation of phenotypes which served as selection criterion**

In addition to the PCA conducted with phenotypic data from the entire 'CD-1 panel' population, a separate PCA was calculated based on 31 phenotypic parameters collected from the 32 selected CD-1 mice. The PCA resulted in the formation of nine components which describe the phenotypic entity of these 32 mice to 84% (summation of proportion of variances, Table S14). For example, the first phenotypic component comprising six phenotypic parameters described the phenotypic variances to 19%. This component contained the three key parameters which served as ranking criteria for the selection of the 32 mice. The parameters were correlated as expected as the time animals spent on the open arm of the EPM and the corticosterone increase were negatively correlated within this cluster (-0.84 and -0.94) and the time animals spent floating in the FST was positively correlated (0.81). In addition to that, there were further

components comprising loadings of biological relevance. For example, component six which showed the positive correlation of the struggling frequency in the FST and an inverse correlation for the time spent immobile in the TST. A high struggling frequency which is reflecting an active stress coping style would most likely go along with a shorter period spent immobile in the TST, as immobility during TS testing indicates a passive stress coping style. Therefore, the grouping of those two loadings with inverse algebraic signs within the identical component reflected the conflicting stress coping styles detected by the respective behavioral phenotypes.

#### **4.5.1.2 Polymorphic SNPs detected in 32 selected CD-1 mice**

In the Jax Mouse Diversity Genotyping array, samples were screened regarding 623,124 SNPs positions. Out of these 623,124 SNPs, a recall of 549,665 SNPs per sample was achieved which made a total of 17,589,280 recalls in the 32 selected CD-1 mice. Deleting SNP positions non-polymorphic among the animals, a SNP-pool of 176,291 heterozygous or opposite homozygous SNPs remained and was employed for first, the generation of a CD-1 specific haplotype map and second, for the calculation of primary associations between SNP genotypes and phenotypic traits of selected animals. Polymorphic SNPs recalls are provided in Table S15 (text-file).

#### **4.5.1.3 Generation of the first CD-1 specific haplotype map**

The calculation of a CD-1 strain-specific haplotype map revealed a genome-wide coverage of 78.6% with 138,652 of the original 176,291 positions polymorphic among the 32 selected CD-1 mice with  $R^2 \geq 0.8$ . The remaining 21.4% of polymorphic marker positions could not be tagged. Based on the LD clustering of the tag-SNP-pool, a selection of 6,000 SNPs could cover these 138,652 polymorphic positions. Hence, 78.6% of the CD-1 genome could be tagged choosing 6,000 SNPs in respect to the CD-1 strain-specific LD clustering. In Table S16, the list of 138,652 SNPs which could be reliably tagged with 6,000 tag-SNPs is provided (text-file).

#### **4.5.1.4 Primary associations identified between genotypes and phenotypes of selected CD-1 mice**

Before the analyses of associated loci seven phenotypes were excluded from the analyses to ensure a certain data distribution in the down-sized population of 32 mice. Phenotypic traits were therefore clustered against the respective frequency of animals displaying the trait to the respective extend. If histograms did not reveal a minimum

distribution over three clusters with a minimum animal number of five animals in at least two of these clusters, the respective phenotype was excluded from further analysis. Phenotypic parameters, therefore, disqualified from the association study were the latency to the first closed arm entry on the EPM, the freezing and struggling latency in the FST, the free rearing frequency, latency, and time in the OF, as well as the latency to the first outer zone entry in the OF.

### **Detection of the internal calibrator *Tmem132d* to be significantly associated**

The detection of the *Tmem132d* locus as associated locus was expected and served as internal quality standard for the entire approach. This gene was chosen as internal calibrator as it was shown in humans and in mice to be associated with anxiety severity and a 3.5-fold expressional up-regulation in the cingulate cortex of HAB vs. LAB mice was reported (Erhardt *et al.*). In the mouse, *Tmem132d* is encoded on the negative strand of chromosome 5 (-129,039,800 : -128,162,202). In this study, the *Tmem132d* locus was identified with 17 SNPs (most up-stream coordinate at bp 128,210,585 and most down-stream coordinate at bp 128,324,243). The locus was identified to be associated with the time spent freezing in the FST (mean nominal p-value =  $1.48 \times 10^{-6}$  and mean empiric p-value = 0.018) and the latency to wall rearings in the OF (mean nominal p-value =  $3.0 \times 10^{-5}$ , mean empiric p-value = 0.029).

### **Detection of second calibrator locus *PPARGC1A***

The detection of a second calibrator locus which was recently published as a result of an association study in humans and mice after diverse levels of locus filtering and prioritizing (Hettema *et al.*, 2011) was also taken as quality measure in testing the validity of the association study presented in this study. Hettema and colleagues detected the locus to be associated with anxiety-spectrum disorders. The *Ppargc1a* locus identified in this study comprised in total 16 markers (nominal and empiric p-values  $\leq 0.05$ ), all of them associated with at least two different phenotypes. Among the associated phenotypes were the corticosterone concentration detected in reaction samples as well as the corticosterone increase, the time immobile in the EPM, which was considered a parameter reflecting locomotor activity, three OF phenotypes indicating anxiety-related behavior (inner zone distance and time, as well as outer zone time) and the wall rearing time in the OF as a parameter for explorative behavior.

#### **4.5.1.5 Identified associations between genotypes and phenotypes of selected CD-1 mice**

Significantly associated loci were identified using WG-Permer software. Associated loci were analyzed focusing on phenotypes most interesting in the context of the two inbred mouse models. Therefore, to evaluate loci associated with the locomotor activity of animals, the anxiety-related and the depression-like behavior as well as with the stress reactivity, key parameters reflecting respective traits were analyzed by identifying in each case the ten best associated loci.

As key parameters for locomotor activity the number of entries into the closed arm of the EPM and total distance travelled in the OF were considered; for anxiety-related behavior the percentage of time spent on the open arm of the EPM and the time spent in the inner zone of the OF; for depression-like behavior the time spent floating in the FST and the time spent immobile in the TST; for stress reactivity the corticosterone increase after the SRT. In Table 24 - 30, the ten top associated loci for these phenotypes are summarized in the same order named above. All loci detected were identified with a multitude of markers. The SNPs listed in the Tables were the markers of the respective locus associated with the lowest nominal p-value. If this marker was located in a protein coding sequence, the encoded gene is provided under locus information.

For graphical illustrations, the chromosomal coordinates of every single marker were plotted against the logarithmized value of the nominal p-value. Resulting peaks were used for the identification of the ten best associated loci per key phenotype. This is exemplarily shown in Figure 35 for the associations of the total distance travelled in the OF on chromosome 4. In a separate folder of the supplementary data, graphic illustrations of associations between nominal p-values of all SNPs which were plotted against the chromosomal coordinates of the particular marker for every key phenotype named above are provided.

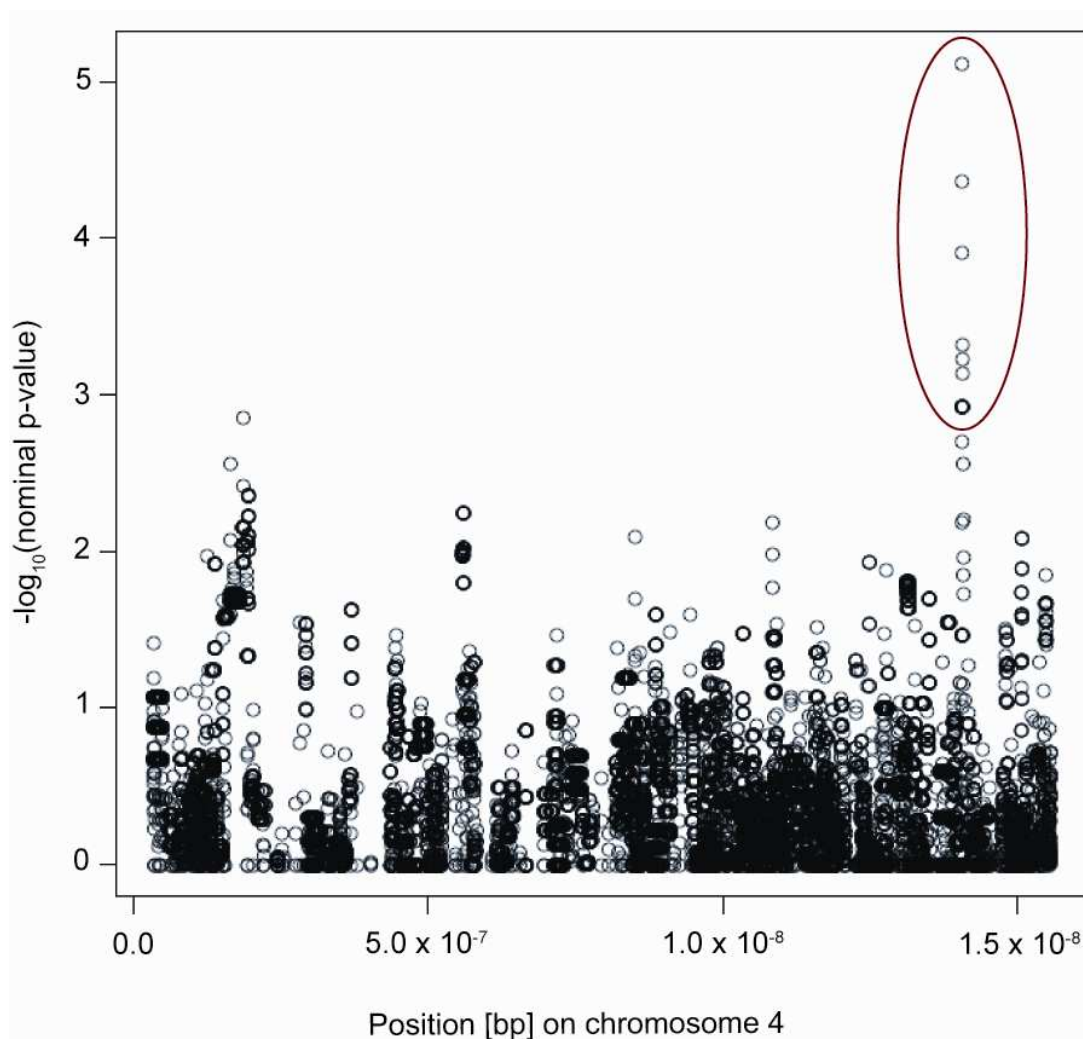


Figure 35: Markers on chromosome 4 are plotted against the  $-\log_{10}$  value of the nominal p-values. The marked peak (roughly at 140 Mb) identifies a significantly associated marker for the total distance travelled in the OF.

Table 24: Top ten loci associated with the total distance travelled in the OF, the first key parameter reflecting locomotor activity of tested mice. Loci are assorted according to ascending nominal p-values (Chr. = chromosome).

SNP identifier	Chr.	Mapping position [bp]	p-value nominal	p-value empiric	Locus information
JAX00626778	6	133,988,869	$3,50 \times 10^{-5}$	$3,00 \times 10^{-4}$	<i>Etv6</i>
JAX00617278	6	90,542,520	$8,80 \times 10^{-5}$	$1,60 \times 10^{-3}$	<i>Aldh111</i>
JAX00140826	6	50,294,630	$1,53 \times 10^{-4}$	$9,90 \times 10^{-3}$	<i>Osbp13</i>
JAX00568919	4	140,500,033	$1,24 \times 10^{-4}$	$2,20 \times 10^{-3}$	<i>Padi2</i>
JAX00450828	18	4,655,562	$2,81 \times 10^{-3}$	$1,25 \times 10^{-2}$	<i>9430020K01Rik</i>
JAX00087163	19	15,019,345	$1,23 \times 10^{-4}$	$6,00 \times 10^{-4}$	-
JAX00149816	7	31,508,107	$3,81 \times 10^{-4}$	$1,10 \times 10^{-3}$	<i>Atp4a</i>
JAX00701915	9	92,808,477	$2,34 \times 10^{-4}$	$2,40 \times 10^{-3}$	-
JAX00031647	11	108,977,709	$2,06 \times 10^{-4}$	$1,20 \times 10^{-3}$	-
JAX00038958	12	92,061,749	$3,81 \times 10^{-4}$	$1,30 \times 10^{-3}$	-

Table 25: Top ten loci associated with the number of entries to the closed arm of the EPM, the second key parameter reflecting locomotor activity of tested mice. Loci are assorted according to ascending nominal p-values (Chr. = chromosome).

SNP identifier	Chr.	Mapping position [bp]	p-value nominal	p-value empiric	Locus information
JAX00075625	17	39,714,123	$7.30 \times 10^{-5}$	$3.10 \times 10^{-3}$	-
JAX00245014	1	26,142,536	$7.40 \times 10^{-5}$	$3.50 \times 10^{-3}$	-
JAX00067751	16	28,499,048	$1.35 \times 10^{-4}$	$4.50 \times 10^{-3}$	<i>Fgf12</i>
JAX00126081	4	150,644,666	$1.44 \times 10^{-4}$	$1.20 \times 10^{-3}$	<i>Camta1</i>
JAX00036804	12	62,664,359	$1.64 \times 10^{-4}$	$1.00 \times 10^{-4}$	<i>Lrfn5</i>
JAX00123455	4	113,903,896	$2.28 \times 10^{-4}$	$4.00 \times 10^{-4}$	<i>Skint11</i>
JAX00587308	5	82,279,118	$4.57 \times 10^{-4}$	$5.00 \times 10^{-4}$	-
JAX00309959	11	46,350,318	$4.63 \times 10^{-4}$	$9.80 \times 10^{-3}$	<i>Gm12169</i>
JAX00478394	19	44,531,281	$6.33 \times 10^{-4}$	$6.70 \times 10^{-3}$	-
JAX00595431	5	124,825,486	$6.92 \times 10^{-4}$	$5.00 \times 10^{-4}$	<i>Sbno1</i>

Table 26: Top ten loci associated with the percentage time spent on the open arm of the EPM, the first key parameter reflecting the anxiety-related behavior of tested mice. Loci are assorted according to ascending nominal p-values (Chr. = chromosome).

SNP identifier	Chr.	Mapping position [bp]	p-value nominal	p-value empiric	Locus information
JAX00050949	14	24,116,606	$4.60 \times 10^{-5}$	$1.20 \times 10^{-3}$	<i>Kcnma1</i>
JAX00103389	2	174,543,382	$6.30 \times 10^{-5}$	$5.50 \times 10^{-3}$	-
JAX00135316	5	125,382,793	$1.15 \times 10^{-4}$	$9.00 \times 10^{-4}$	<i>Zfp664</i>
JAX00440034	17	46,872,086	$1.69 \times 10^{-4}$	$6.00 \times 10^{-4}$	-
JAX00446740	17	75,872,005	$1.88 \times 10^{-4}$	$1.50 \times 10^{-3}$	<i>Rasgrp3</i>
JAX00430427	17	6,591,073	$2.17 \times 10^{-4}$	$5.20 \times 10^{-3}$	<i>Tmem181a</i>
JAX00236854	9	49,974,017	$2.35 \times 10^{-4}$	$8.50 \times 10^{-3}$	-
JAX00134644	5	116,337,492	$3.14 \times 10^{-4}$	$5.00 \times 10^{-4}$	<i>Cit</i>
JAX00481320	19	57,937,240	$3.71 \times 10^{-4}$	$2.00 \times 10^{-4}$	<i>Atrnl1</i>
JAX00113859	3	139,103,916	$6.74 \times 10^{-4}$	$2.30 \times 10^{-3}$	<i>B930007M17Rik</i>

## Results

Table 27: Top ten loci associated with the time spent in the inner zone of the OF, the second key parameter reflecting the anxiety-related behavior of tested mice. Loci are assorted according to ascending nominal p-values (Chr. = chromosome).

SNP identifier	Chr.	Mapping position [bp]	p-value nominal	p-value empiric	Locus information
JAX00031163	11	102,506,664	$1.05 \times 10^{-4}$	$9.00 \times 10^{-4}$	-
JAX00042197	13	17,761,023	$1.07 \times 10^{-4}$	$2.70 \times 10^{-3}$	<i>5033411D12Rik</i>
JAX00354790	13	36,009,260	$1.28 \times 10^{-4}$	$2.60 \times 10^{-3}$	-
JAX00089284	19	43,417,525	$1.78 \times 10^{-4}$	$1.10 \times 10^{-3}$	<i>Hpse2</i>
JAX00251722	1	56,465,746	$1.80 \times 10^{-4}$	$3.00 \times 10^{-4}$	-
JAX00565563	4	127,344,997	$1.88 \times 10^{-4}$	$3.40 \times 10^{-3}$	-
JAX00284281	10	19,179,675	$1.91 \times 10^{-4}$	$1.70 \times 10^{-3}$	-
JAX00132992	5	92,212,356	$1.95 \times 10^{-4}$	$4.90 \times 10^{-3}$	-
JAX00663942	8	28,245,239	$1.97 \times 10^{-4}$	$6.00 \times 10^{-4}$	-
JAX00129961	5	51,784,223	$2.01 \times 10^{-4}$	$1.00 \times 10^{-4}$	-

Table 28: Top ten loci associated with the time spent floating during the FST, the first key parameter reflecting the depression-like behavior of tested mice. Loci are assorted according to ascending nominal p-values (Chr. = chromosome).

SNP identifier	Chr.	Mapping position [bp]	p-value nominal	p-value empiric	Locus information
JAX00683491	8	127,957,369	$5.90 \times 10^{-5}$	$2.60 \times 10^{-3}$	<i>Sipa1l2</i>
JAX00270773	1	150,967,884	$7.70 \times 10^{-5}$	$2.80 \times 10^{-3}$	-
JAX00175893	9	114,330,617	$8.40 \times 10^{-5}$	$3.00 \times 10^{-4}$	<i>Glb1</i>
JAX00134648	5	116,381,992	$1.63 \times 10^{-4}$	$2.00 \times 10^{-4}$	<i>Cit</i>
JAX00092931	2	33,831,599	$1.69 \times 10^{-4}$	$4.00 \times 10^{-4}$	-
JAX00427027	16	87,263,808	$2.31 \times 10^{-4}$	$5.00 \times 10^{-4}$	-
JAX00113852	3	138,998,360	$2.39 \times 10^{-4}$	$6.00 \times 10^{-4}$	<i>B930007M17Rik</i>
JAX00130206	5	55,054,215	$2.46 \times 10^{-4}$	$1.00 \times 10^{-4}$	-
JAX00017391	10	44,133,271	$2.60 \times 10^{-4}$	$3.10 \times 10^{-3}$	-
JAX00075193	17	33,830,219	$2.83 \times 10^{-4}$	$6.00 \times 10^{-4}$	<i>March2</i>

Table 29: Top ten loci associated with the time spent immobile during the TST, the second key parameter reflecting the depression-like behavior of tested mice. Loci are assorted according to ascending nominal p-values (Chr. = chromosome).

SNP identifier	Chr.	Mapping position [bp]	p-value nominal	p-value empiric	Locus information
JAX00148181	6	149,122,293	$1.50 \times 10^{-5}$	$2.00 \times 10^{-4}$	<i>Amn1</i>
JAX00100376	2	134,184,125	$2.00 \times 10^{-5}$	$1.00 \times 10^{-4}$	-
JAX00041837	13	12,499,053	$2.50 \times 10^{-5}$	$4.00 \times 10^{-4}$	<i>Heatr1</i>
JAX00386775	14	92,554,883	$3.10 \times 10^{-5}$	$2.00 \times 10^{-3}$	-
JAX00032515	11	120,587,173	$5.40 \times 10^{-5}$	$5.00 \times 10^{-4}$	<i>Dcxr</i>
JAX00056672	14	102,650,784	$6.10 \times 10^{-5}$	$5.00 \times 10^{-4}$	-
JAX00418320	16	38,026,034	$8.60 \times 10^{-5}$	$2.30 \times 10^{-3}$	-
JAX00103199	2	171,879,487	$9.40 \times 10^{-5}$	$3.00 \times 10^{-4}$	-
JAX00487114	2	35,321,279	$1.04 \times 10^{-4}$	$2.00 \times 10^{-4}$	-
JAX00163546	8	77,683,474	$1.24 \times 10^{-4}$	$2.00 \times 10^{-4}$	-

Table 30: Top 10 loci associated with the corticosterone increase in the SRT, the key parameter reflecting the animal's stress reactivity. Loci are assorted according to ascending nominal p-values (Chr. = chromosome).

SNP identifier	Chr.	Mapping position [bp]	p-value nominal	p-value empiric	Locus information
JAX00439485	17	44,940,393	$1.8 \times 10^{-5}$	$8 \times 10^{-4}$	<i>Runx2, Supt3h</i>
JAX00581955	5	51,223,710	$2.2 \times 10^{-5}$	$5 \times 10^{-4}$	-
JAX00491991	2	67,591,108	$3.2 \times 10^{-5}$	$2.2 \times 10^{-4}$	-
JAX00113859	3	139,103,916	$3.4 \times 10^{-5}$	$1 \times 10^{-3}$	<i>B930007M17Rik</i>
JAX00385356	14	81,815,070	$3.5 \times 10^{-5}$	$4 \times 10^{-4}$	-
JAX00650341	7	115,395,389	$5.5 \times 10^{-5}$	$1.9 \times 10^{-3}$	-
JAX00056641	14	102,243,612	$1.4 \times 10^{-4}$	$7 \times 10^{-4}$	<i>Lmo7</i>
JAX00375069	14	24,269,502	$1.5 \times 10^{-4}$	$6 \times 10^{-4}$	<i>Kcnma1</i>
JAX00586108	5	75,115,900	$1.7 \times 10^{-4}$	$9 \times 10^{-4}$	-
JAX00166521	8	117,358,480	$2.4 \times 10^{-4}$	$1 \times 10^{-3}$	<i>Wwox</i>

#### 4.5.1.6 Confirmation of the predictive validity of an association study in 32 animals

In order to test the predictive validity of the associations calculated based on phenotypic and genotypic data of 32 CD-1 mice only, it was aimed to simulate this approach of testing 'surrogate individuals' which are representing a considerably larger population in a data set which was analyzed previously and, therefore, the result was already known. The association study revealing TMEM132D to be significantly associated with anxiety severity in humans and in HAB vs. LAB mice was chosen as control study (Erhardt *et al.*). Simulating the situation in the association study presented in this work, data of the

16 patients displaying the most severe symptoms of anxiety according to DSM-IV (SKID I and II) and of the 16 most intermediate individuals of the control group were chosen. Apart from the n number, the association was calculated with identical settings as described in the publication.

The TMEM132D locus was detected to be significantly associated also in the down-sized cohort with a nominal p-value of  $1.83 \times 10^{-4}$ . The SNP representing the locus was a different one (rs1918409; chr. 12: 129,989,303) compared to the SNP detected in the cohort as a whole (rs7309727; 12: 129,955,359). In Figure 36, markers along the human chromosome 12 were plotted against the  $-\log$  value of the respective nominal p-values, also graphically identifying the association.

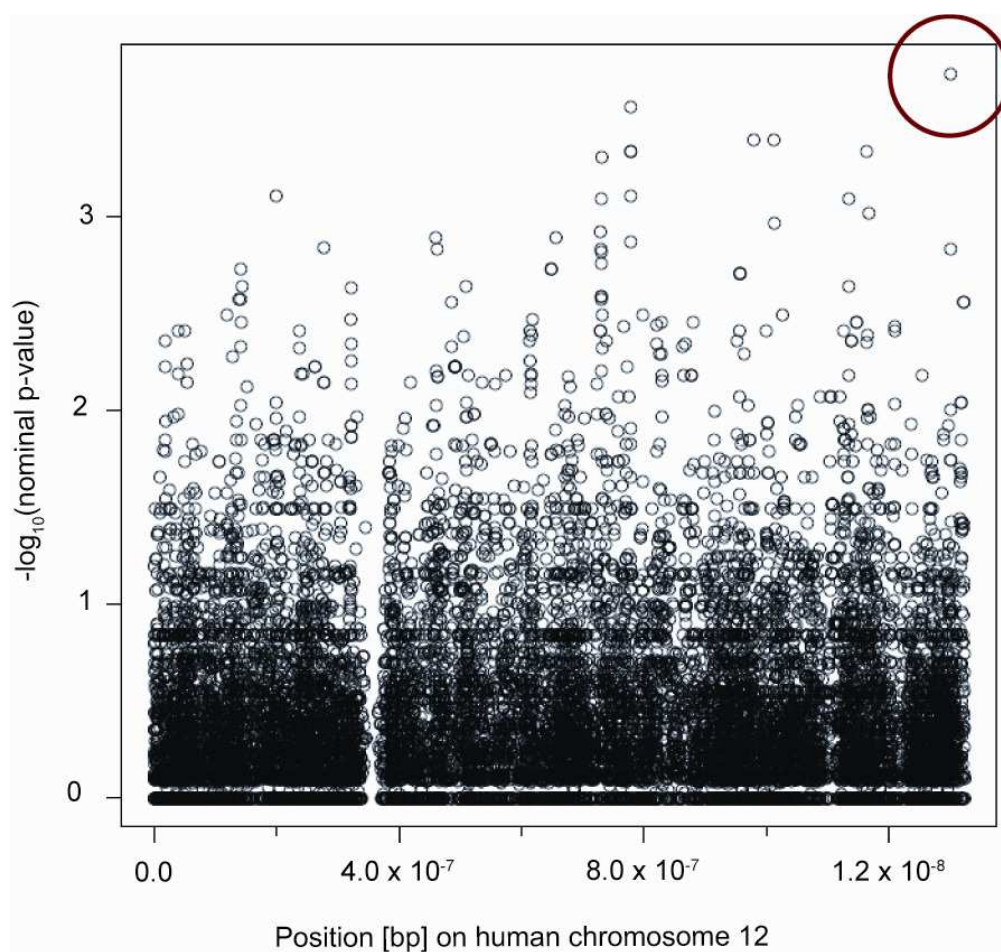


Figure 36: Markers on human chromosome 12 were plotted against the  $-\log_{10}$  value of the respective nominal p-values. The marked SNP rs1918409 at bp 129,989,303 was identified as significantly associated with the severity of anxiety. The SNP identifying the TMEM132D locus in the original publication was located 33,944 bp upstream of the SNP detecting the Tmem132d locus in the down-sized cohort.

#### 4.5.1.7 Potential expansions of the association study in 32 CD-1 mice to the total population of the 'CD-1 panel'

For the expansion of the association study conducted so far in 32 selected animals to the entire population of behaviorally characterized CD-1 mice, two potential procedural methods were prepared.

First, a chromosome-centered approach testing 384 selected SNPs on selected chromosomes was discussed and an Illumina Golden Gate Assay for 384 mice was developed accordingly. Based on former findings and on the literature of the field, six chromosomes (1, 2, 3, 5, 11, and 17) which were considered of special interest in the context of the two inbred mouse lines were defined. The selection of 384 polymorphic positions on these six chromosomes was done in a gene-centered manner. Therefore, intragenic SNPs from the overlapping SNP pool between HAB and LAB and HR and LR mice (Table S12) were selected only. In addition, genomic 'hotspots' were defined harboring genes which were known, however, to contribute to the phenotypes of the two mouse models. For example, genes detected in the microarray study to be significantly differential expressed between the lines were considered as hotspots, or loci identified as significantly associated with the anxiety-phenotype in an F2 study of the HAB/LAB model were included into the selection. As a satisfying marker density throughout the six selected chromosomes could not be achieved with 384 SNPs only, it was aimed to reach a sufficiently high marker density in the genomic hotspots, whereas genomic regions on selected chromosomes less interesting to the HAB/LAB and the HR/LR mouse models were excluded from the analysis by not covering them with SNPs. Five hotspots were allowed on chromosomes other than the ones named above as these SNPs were particularly interesting and the functional contribution of the respective gene products to the phenotype of the HAB/LAB mouse model was already shown in earlier studies (*Nps* locus on chromosome 7, *Npsr* and *Hmgn3* loci on chromosome 9, *Sci25a17* locus on chromosome 15 and *Syt4* locus on chromosome 15). In Table S17, selected 384 SNPs including chromosomal coordinates, flanking sequences and Illumina scoring results were listed. The technical feasibility for the Golden Gate assay was calculated with 0.869, the designability for the assay was 1.00, and in addition, no failure codes were detected.

Alternatively, a genome-wide SNP screening approach was considered. The Illumina iSelect assay provides the platform to genotype 6,000 SNP positions in 1,152 animals and the resulting marker density was approximately one marker per 450 kbp. The selection of the 6,000 SNPs was again done based on the overlapping SNP pool between HAB and LAB and HR and LR mice. In this case, the focus of the SNP selection

was given to a consistent distribution throughout the genome. As the overlapping SNP pool contained 17,722 SNPs, roughly every third SNP was selected, irrespective of inter- or intragenic position of the marker. In Table S18, the selection of the 6,000 SNPs is summarized including the scoring results of the Illumina assay design tool. A mean final score of 0.964 was achieved and none of the selected SNPs produced failure codes. According to these scoring results, the technical feasibility of the developed iSelect assay was considered very promising (Ingrid Du Plooy, Illumina technical support, personal communication).

### 4.6 Overview supplementary data

The external data source attached to this thesis contains the following data files:

Table S1: Differentially expressed genes microarray study

Table S2: Differentially expressed genes SAGE experiment

Table S3: Multivariate vs. univariate analyses

Table S4: Multivariate candidates only

Table S5: GO analysis cellular components

Table S6: GO analysis biological processes

Table S7: GO analysis molecular functions

Table S8: Segmental copy number variation HAB vs. LAB

Table S9: Segmental copy number variation HR vs. LR

Table S10: Heterozygous SNPs HAB vs. LAB

Table S11: Heterozygous SNPs HR vs. LR

Table S12: Overlapping SNP pool

Table S13: Phenotypic data 32 selected CD-1

Table S14: PCA 32 selected CD-1

Table S15: Polymorphic SNP recalls 32 CD-1

Table S16: Tag SNPs plus associated SNPs

Table S17: Golden Gate assay

Table S18: iSelect assay

A separate folder called 'Graphs association study' contains seven pdf-files showing plots which served for the analysis of associated loci. For the seven key phenotypes of the association study, every marker was plotted against the nominal p-value which it achieved for the respective phenotype.

## 5 Discussion

In this study, a broad spectrum of methods was used to generate genomic data and to subsequently test the functional impact of collected genomic information on the behavior of HAB vs. LAB and HR vs. LR mice, thereby making use of molecular biological, bioinformatical, and behavioral biological approaches.

### **Mitochondrial impact on endophenotypes of HR and LR mice**

First, for genetic characterization of the SR mouse model, expressional profiling experiments were conducted aiming to elucidate the functional relevance of differentially expressed genes on the endophenotypes of HR and LR mice. All attempts to genetically characterize the SR mouse model were focused on hippocampal tissue as the hippocampus is a known target region of glucocorticoids and is subjected to structural and physiological alterations upon stress exposure. It is further involved in the termination of HPA axis stress response (McEwen, 2007).

The expressional profiling of HR vs. LR mice resulted in the detection of a total of 981 genes to be differentially expressed between the lines. The initial pool of differentially expressed genes gained from the microarray study (Table S1) was extended conducting a SAGE analysis (Table S2). This probe-independent approach allowed the detection of a considerably larger fraction of genes, in particular the detection of low abundance genes known to be difficult to detect in microarray-based expression approaches (Coppee, 2008; Draghici *et al.*, 2006; Karssen *et al.*, 2006; Livesey, 2003). This fraction of low abundance genes is of special interest in an expressional profiling attempt, as respective gene products often implement crucial functions (Draghici *et al.*, 2006). The enlarged pool of differentially expressed genes resulting from the combination of two independent profiling methods increased the informative content of subsequently performed annotational cluster analyses.

In order to test the pool of differentially expressed genes for functional enrichment, annotational cluster analyses were performed using different bioinformatic tools. Analyses of the microarray-based gene pool via the DAVID Bioinformatics Database clearly pointed towards a distinct contribution of mitochondrially active genes likely to influence the endophenotypes of the SR mouse model (Table 5). Mitochondrially active genes *per se* were detected as significantly enriched in addition to a separate mitochondrial cluster containing genes assorted specifically to the mitochondrial envelope. This finding was confirmed by GO analyses using the identical gene pool. In similarity to the results gained from annotational cluster analysis using the DAVID

Bioinformatics Database, also in GO analyses mitochondrially active genes were detected as significantly enriched. This applied as well to a separate mitochondrial matrix cluster, and further clusters comprising genes of the mitochondrial large ribosomal subunit and the inner mitochondrial membrane. The gene pool resulting from the SAGE experiment strengthened the idea of a mitochondrial contribution to the endophenotypes of the mouse lines (Table 6). Eight out of 14 significantly enriched clusters (no. 1, 2, 3, 4, 6, 7, 9, and 10) suggested mitochondrially active genes as the major player in differentiating between HR and LR mice on an expressional level. Importantly, the mitochondrial envelope, which harbors the respiratory chain and therefore is crucially involved in the cells energy metabolism, was indicated in seven out of these eight clusters. A particular pathway or distinct component belonging to the mitochondrial membranes or the inner-membrane space was not detected in the annotational cluster analyses. Nevertheless, these findings strongly suggest that, on a gene expressional level, the differences in stress reactivity between HR and LR mice are primarily determined by differences in mitochondrial function and, more precisely, in energy-generating processes originating in the mitochondrial envelope.

The so-called 'respiratory chain' or electron transfer chain (Figure 37), which is located in the inner mitochondrial membrane, comprises the three classical electron transport complexes (I, III, and IV) which transfer electrons to molecular oxygen. This electron transfer is coupled to proton extrusion from the inner mitochondrial matrix and goes along with a reduction in the redox potential of electrons resulting in an electrochemical proton gradient. This gradient is used for the oxidative phosphorylation of ADP to ATP, the universal cellular energy supplier (Brand and Nicholls, 2011; Mourier and Larsson, 2011).

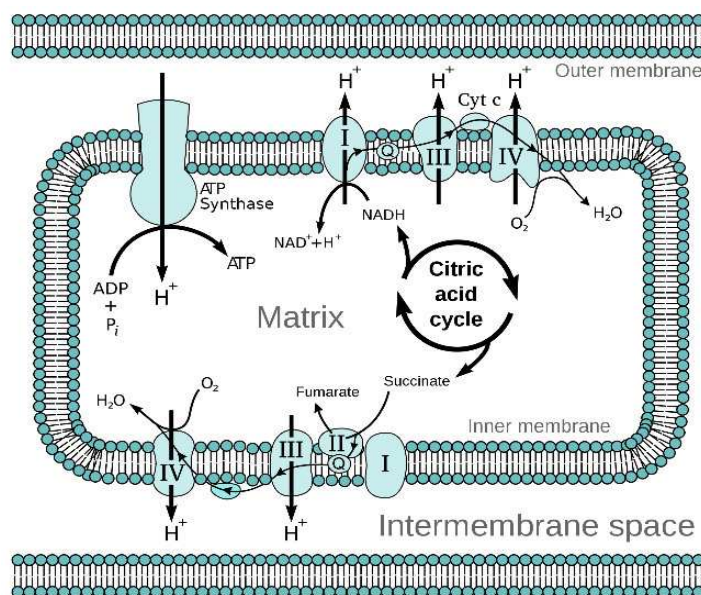


Figure 37: Schematic illustration of the electron transport chain which is integrated into the inner mitochondrial membrane. In total, five protein complexes are involved in the generation of ATP. Complexes I, III, and IV direct electrons from electron donor to electron acceptor molecules and are thereby generating a proton efflux across the inner mitochondrial membrane. The coenzyme flavin adenine dinucleotide (FAD) is involved in the electron delivery of complex II, which, in addition to complex I, delivers electrons to the acceptor molecule ubiquinone. The fifth complex is the ATP synthase, which generates ATP via oxidative phosphorylation. (Figure adopted from [www.wikipedia.org](http://www.wikipedia.org).)

For most clusters, the connection to the mitochondrion and the respiratory chain, respectively, is quite obvious, whereas in some cases the attribution as a mitochondrial cluster might require explanation. The 'iron metabolism' cluster 3 was attributed to the mitochondrion as all genes accounted into this cluster are functionally associated to the mitochondria (Kulic *et al.*, 2011; Pagliarini *et al.*, 2008; Wirtz and Schuelke, 2011) and redox processes along the respiratory chain are an iron-dependent system (Gille and Reichmann, 2011). Furthermore, six genes were annotation-based clustered to the 'FAD cluster'. FAD is the abbreviation for the coenzyme flavin adenine dinucleotide. It transfers additional electrons originating from succinate and other electron donors to the ubiquinone pool in complex II of the electron transfer chain (Hanukoglu, 2006). In cluster no. 9, genes however associated to the cytochrome P450 system were collected and also indexed as mitochondrial cluster as these hemoproteins comprise a large and rather divergent group of proteins, either membrane-associated to microsomes or to the mitochondria (Omura, 2010).

Mitochondria fulfill diverse functions, ranging from energy generation to calcium homeostasis, from the control of cellular differentiation, fission, and fusion processes to the induction of apoptosis (McBride *et al.*, 2006). They were implicated in a whole variety of neurodegenerative diseases, such as Huntington's, Parkinson's, and Alzheimer's

disease, and are known to play a pivotal role in several psychopathologies such as MDD, bipolar disorder, schizophrenia, and autism (Jou *et al.*, 2009; Rezin *et al.*, 2009). In either case, mitochondrial impairment ultimately resulting in insufficient energy supply was shown, but precise insights on a molecular level into the role of the mitochondria to psychopathologies is largely missing (de Castro *et al.*, 2010; Han *et al.*, 2011). For example, by a large-scale DNA microarray analysis, altered expression of mitochondria-related genes in post-mortem brains of bipolar disorder and schizophrenia patients was discovered. In this study, a global down-regulation of mitochondria-related genes in these patients was shown, independent of the patient's medication status and sample pH-values. Genes detected to significantly differ in their expression ranged from respiratory chain components to various mitochondrial enzymes (Clay *et al.*, 2011; Iwamoto *et al.*, 2005). A distinct pathway was, in similarity to results of annotational cluster analyses presented in this study, not distinguishable among differentially expressed genes.

In the context of pathological stress reactivity and HPA axis dysregulation, so far a mitochondrial contribution has hardly been shown (Zhang *et al.*, 2011). Considering the energy need of the brain – it accounts for roughly 2% of the total body weight, is consuming approximately 20% of total oxygen, and the mitochondria supply more than 95% of the required energy – the importance of mitochondrial homeostasis does not seem surprising (de Castro *et al.*, 2010; Rezin *et al.*, 2009). The question, if the behavioral phenotypes of HR and LR mice have their origin in mitochondrial dysfunction finally determining the differential regulation of the HPA axis, or if mitochondrial peculiarities are a result of neurophysiological conditions in these animals, could not be answered based on gene expressional profiling and subsequent annotational cluster analyses. The result of the gene expressional profiling in the mouse model for SR allows to hypothesize that the increased levels of corticosterone in the brain of HR vs. LR mice (Heinzmann *et al.*, 2010) either determine an elevated energy need in the brain of HR mice, or however destructive conditions in the brain of HR mice upon exposure to high levels of corticosterone sustainably harm mitochondrial homeostasis resulting in insufficient energy generation.

Du and colleagues proposed a dynamic influence of corticosterone on mitochondrial functions in a dose-dependent manner. According to this model, low and acute corticosterone exposure increases mitochondrial functions allowing the cell to cope with the stress impact, whereas high and chronic corticosterone concentrations disrupt mitochondrial homeostasis (Du *et al.*, 2009a; Du *et al.*, 2009b). Applying this theory to the SR mouse model would mean that LR mice profit from the substandard

corticosterone answer, whereas mitochondria in HR mice would be affected by the remarkably high corticosterone increase upon stress exposure.

### **Increased neuronal activity in dorsal hippocampus of HR vs. LR mice**

A slightly increased overall metabolic activity in the dorsal, but not intermediate or ventral, hippocampus of HR vs. LR female mice was shown in the CO staining of hippocampal brain slices (Table 9). This increased metabolic turnover indicates elevated long-term neuronal activity in the respective brain region. A certain unspecificity of the technique needs to be taken into account though as the detected signal is a cumulative signal which allows no differentiated analysis (Gonzalez-Lima and Garrosa, 1991; Harro *et al.*, 2011; Hevner and Wong-Riley, 1990). The dorsal hippocampus was functionally attributed to cognition, the ventral part to stress, emotion, and affectivity (Fanselow and Dong, 2010). Cognitive impairments regarding deficits in hippocampus-dependent memory functions in HR compared to LR mice were reported (Knapman *et al.*, 2010a) which could entail dissimilar levels of neuronal activity in the respective brain area.

Increased neuronal activity consequently entails increased energy demands. Consolidating the hypothesis of insufficient mitochondrial energy supply in HR mice (which was generated based on the annotational analyses of expressional profiling data) and the detection of increased energy demands in the dorsal hippocampus of HR mice, the latter suggests insufficient levels of energy generation. The very moderate differences detected in the CO staining, however, cannot sufficiently serve as explanation for dissimilar mitochondrial function which was indicated in the annotational-based enrichment analyses of transcriptomic data.

### **Increased energy demands – increased reactive oxygen species?**

Presuming that the respiratory chain of HR mice complies with an elevated energy demand, an increased production of reactive oxygen species (ROS), the known side product of oxidative phosphorylation, would occur in HR vs. LR mice (Mammucari and Rizzuto, 2010). In rats it was already shown, that high corticosterone plasma levels trigger ROS which caused oxidative damage and subsequent neurodegeneration in the hippocampus of test animals. These rats also showed cognitive deficits (Sato *et al.*, 2010). One consequence of increased ROS levels is the induction of apoptosis via the intrinsic mitochondrial pathway (Mehmeti *et al.*, 2011). In order to test for differences in the cytochrome c release-based apoptosis rate between the lines, a cytochrome c specific ELISA was conducted using cytosolic protein lysates of HR and LR mice. According to this assay, the apoptosis rate between the lines does not differ. This is in

line with findings that HR vs. LR mice do not exhibit major structural alterations in the brain (Knapman *et al.*, in press; Pillai *et al.*, in preparation). The animals used for the generation of the cytosolic protein lysates were about eight weeks old. Nevertheless, testing for differences in apoptosis to a later point in life would be suggested as at the age of eight weeks potential differences might not be pronounced enough to be detectable. Another known consequence of increased ROS levels is the oxidation of macromolecules, in particular the mitochondrial DNA (mtDNA) resulting in oxidative modification of purine and pyrimidine bases, the desoxyribose backbone, and DNA strand breaks. As the protein products of mtDNA are all involved in electron transfer chain and subsequent oxidative phosphorylation, damages in the respective DNA sequences are likely to interfere with mitochondrial ATP synthesis (Ott *et al.*, 2007).

A proteomic screening approach which was performed to more precisely define the character of mitochondrial dysfunction failed as only insufficient amounts of mitochondrial protein lysate were gained from hippocampal tissue.

### **qPCR confirmation of selected candidates**

Selected candidate genes, which were detected as significantly differently expressed between the lines in the microarray study, were tested for differential expression using qPCR analyses (Table 10). An algorithm or, however, unbiased strategy for the selection of candidates is not available, and the abundance of candidates did not allow to test every single candidate in the qPCR. Genes fulfilling certain criteria were therefore tested, but still, the selection of candidates was doubtlessly a biased procedure. The criteria, which were looked at, were the prior identification of the gene product and a characterization of the gene product in the literature. Furthermore, the function of the gene product needed to integrate into the neurobiological context of stress reactivity and HPA axis dysfunction. Some of the candidates, therefore, were chosen for qPCR analyses as they were shown in earlier studies to be involved in stress reactivity and/or contribute to further characteristics of HR and LR endophenotypes. Others were selected as they were detected to be differentially regulated between HAB and LAB mice. qPCR confirmation of mitochondrial candidates was largely disclaimed, as there were too many genes with known mitochondrial functions detected in the microarray-based expressional profiling to deflect further perception from confirmation or disproof of separate candidates. Mitochondrial genes as potential causative factors in the determination of extremes in stress reactivity between HR and LR mice were considered to require examination *en bloc* as a functional entity.

In general, gene expressional regulation detected in the microarray study could be confirmed in about 52% of genes selected for qPCR analyses (qPCR confirmation and neurodevelopmental study) which is a moderate level and underlines the necessity of complementary approaches to microarray-based expressional profiling attempts. The assignment of functional impact was in the focus of this study, rather than the detection of differential gene regulation between the lines. Separate genes will therefore not be discussed, with exception of two candidates, which seem particularly interesting in the context of the SR mouse model, namely *Ttbk1* and *Gabrg2*.

### **The *Ttbk1* locus**

*Ttbk1* was detected in the microarray study with the lowest adjusted p-value to be up-regulated in HR vs. LR, and this up-regulation was confirmed via qPCR. It is a serine/threonine/tyrosine kinase of the casein superfamily 1 and phosphorylates the microtubule-associated tau proteins. It is conserved among species and its expression was mapped to the cytoplasm of cortical and hippocampal neurons (Sato *et al.*, 2006; Xu *et al.*, 2010). Interestingly, TTBK1 expression was detected to be up-regulated in the brains of Alzheimer's disease patients (Sato *et al.*, 2008). A transgenic mouse encoding for the human form of TTBK1 was therefore generated. These mice showed age-dependently a significant spatial memory impairment in the radial arm water maze test which was accompanied by increased phosphorylation rates of tau and neurofilament and subsequent aggregation of these proteins (Sato *et al.*, 2008; Xu *et al.*, 2010). In addition, modification of expressional levels of several components known to be involved in memory dysfunction, such as NMDA receptor types 2B and calpain I, was found and might shed light on mechanism which are involved in the dramatic loss of memory capacity during the course of Alzheimer's disease (Sato *et al.*, 2008). Making use of a further transgenic mouse model, Xu and colleagues showed that up-regulation of *Ttbk1* expression was accompanied by locomotor dysfunction, neuroinflammation, and degeneration of motor neurons in the spinal cord (Xu *et al.*, 2010). Differences in locomotor activity were not observed in the SR mouse model, but spatial memory was shown to be impaired in HR compared to LR mice. Spatial as well as object memory impairment in HR mice so far were associated with decreased hippocampal levels of brain derived neurotrophic factor (BDNF) (Knapman *et al.*, 2010a), but detected differences in *Ttbk1* expression should likewise be considered as a determinant contributing to cognitive deficits in HR mice.

### **The *Gabrg2* locus**

*Gabrg2* was as well detected to be up-regulated in HR vs. LR mice in the microarray-study and the result was confirmed by qPCR analysis. A potential influence of *Gabrg2*, which stands for gamma 2 subunit of the gamma-aminobutyric acid (GABA) A receptor, on affective disorders was studied making use of a heterozygous *Gabrg2* knockout mouse line (*Gabrg2*<sup>+/-</sup>) which at first resulted in the detection of increased levels of harm avoidance behavior and sensitivity to negative associations in *Gabrg2*<sup>+/-</sup> vs. control mice, representing trait anxiety (Crestani et al., 1999). Based on these findings, the authors discussed GABA<sub>A</sub> receptor dysfunctions to represent a potentially causative predisposition to anxiety disorders. Taking the story further, effects of cell type-specific and developmental stage-dependent inactivation of the gamma 2 subunit were studied by a heterozygous deletion of the *Gabrg2* locus in embryonic compared to adult forebrain neurons. Independent of the inactivation time-point, adult neurogenesis was impaired and features indicating trait anxiety and depression-like behavior were observed (Earnheart et al., 2007). Finally, *Gabrg2* deficits in *Gabrg2*<sup>+/-</sup> mice were associated with hyperactivity of the HPA axis and, furthermore, with sensitivity to antidepressant agents resembling melancholic forms of depression (Shen et al., 2010). HPA axis reactivity in *Gabrg2*<sup>+/-</sup> mice is hence contradictory to the reactivity observed in HR mice. Anxiety-related and depression-like features were observed in both lines of the SR mouse model with HR mice phenotypically resembling to features associated with melancholic forms of depression and LR mice displaying symptoms indicative for atypical forms of depression (Touma et al., 2008). The features of melancholic depression in *Gabrg2*<sup>+/-</sup> mice, which were indicated by antidepressant drug sensitivity, are also in disagreement with depression-like symptoms observed in HRs. To summarize what was described so far, two different mouse models show hyper-activation of the HPA axis going along with typically associated symptoms, but with opposing levels of *Gabrg2* expression. Besides differences in experimental set-ups and strain backgrounds, the differences between the mouse models are quite obvious. In SR mice, *Gabrg2* gene expression differences are embedded in a variety of genetic factors which determine in cooperation the endophenotypes of HR and LR mice. In *Gabrg2*<sup>+/-</sup> mice, stress responsiveness and behavioral features were induced by a single targeted genetic lesion. These predominantly conflicting findings underline the importance of the respective neurotransmitter system in the context of HPA axis dysregulation, and it stresses out the genetic complexity of these disorders (Cryan and Holmes, 2005).

### **Does *Cfl-1* dose-dependently influence SR?**

In order to test the functional relevance of a gene known to be differentially expressed on animal's stress reactivity, one candidate gene was chosen to be tracked from expressional profiling data to a behavioral phenotype.

Here, *Cfl-1* was prioritized as it was shown to be significantly differently expressed in hippocampal tissue of HR vs. LR mice on mRNA and on protein level, even though with conflicting tendencies (Knapman *et al.*, in press). Furthermore, *Cfl-1* is a well characterized protein, and many of the features described in the literature supported the idea of the gene's dose-dependent functional impact on the behavior of HR and LR mice. *Cfl-1* which is ubiquitously expressed was described to be involved in the regulation of actin dynamics and actin filament branching. It features a nuclear-localization sequence, might induce the release of cytochrome c and can activate phospholipase D1 (Bernstein and Bamburg, 2010). Data gained from cell culture studies proved an inhibitory effect of *Cfl-1* on the glucocorticoid receptor, thereby causing glucocorticoid resistance. A co-precipitation of *Cfl-1* and the glucocorticoid receptor was thereby excluded; hence, one can conclude that *Cfl-1* does not bind to the glucocorticoid receptor directly. It was further shown though, that an over-expression of *Cfl-1* influences the subcellular localization of the glucocorticoid receptor (Ruegg *et al.*, 2004). Independently, it is known that *Cfl-1* in combination with the actin depolymerizing factor (ADF) is involved in the regulation of actin dynamics in a way that ADF/CFL-1 protein complexes dissociate actin filaments and hence increase the filament turnover in the neuronal cytoskeleton (Sarmiere and Bamburg, 2004). This function is particularly interesting in the context of neuronal growth cone motility and morphology (Endo *et al.*, 2003; Kuhn *et al.*, 2000; Minamide *et al.*, 2000). The activity state of *Cfl-1* is thereby depending on the phosphorylation state of the protein. Phosphorylation of *Cfl-1* via LIM or TES kinases converts it into its inactive state and dephosphorylation via slingshot phosphatases, for example, transforms *Cfl-1* to its active form (Endo *et al.*, 2003). In addition, *Cfl-1* was shown to be particularly susceptible to protein oxidation upon ROS. In its oxidized form, *Cfl-1* tends to dissociate from the actin cytoskeleton, migrates into the mitochondria and induces apoptosis via opening of the mitochondrial permeability transition pore and subsequent cytochrome c release into the cytoplasm (Chua *et al.*, 2003; Endo *et al.*, 2003; Klamt *et al.*, 2009; Zdanov *et al.*, 2010). A schematic overview over the current idea of how *Cfl-1* is being activated and deactivated and how it might be involved in mitochondria-induced apoptosis is given in Figure 38.

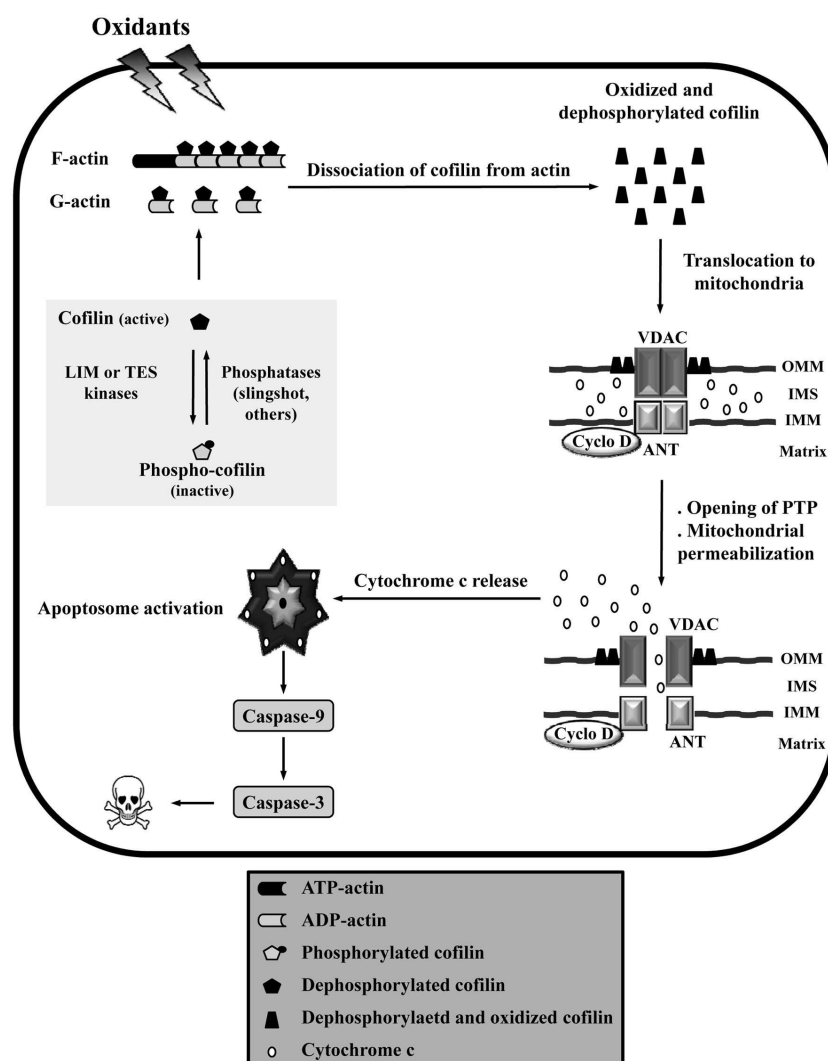


Figure 38: Schematic overview of how *Cfl-1* dissociates from the actin cytoskeleton and translocates into the mitochondria upon influence of oxidants. There, opening the permeability transition pore (PTP) finally results in the induction of cytochrome c release into the cytoplasm and cell death via apoptosis. LIM and TES kinases confer *Cfl-1* into the inactive state, whereas dephosphorylation via slingshot proteins activates *Cfl-1* and hence induces the association of phosphorylated *Cfl-1* to the actin cytoskeleton. (Figure adopted from Zdanov *et al.*, 2010.)

Another important point in describing the functionality of *Cfl-1* is its dose-dependent mode of action. The cellular function and localization of *Cfl-1* strongly depends on the ratio actin/*CFL-1* and, regardless of that, on the expression level of *Cfl-1* itself. In case of excessively high concentrations of the active form of *Cfl-1*, rod-shaped *Cfl-1*-saturated actin filament bundles, the so-called 'rods', will be formed (Bamburg *et al.*, 2010; Bernstein and Bamburg, 2010; Minamide *et al.*, 2000). This autoregulatory process of bundle formation could be considered a 'capturing' mechanism in order to neutralize non-physiologically high levels of active *Cfl-1*.

For the behavioral experiments in this study, *Cfl-1<sup>+/-</sup>* mice were used. The examination of *Cfl-1<sup>+/-</sup>* mice in an embryonic stage showed the contribution of *Cfl-1* to the migration of neural crest cells resulting in a strongly impaired development of neural crest derived tissues. Furthermore, it is an inevitable factor for proliferation and scattering of neuronal precursor cells showing as a total lack in neural tube closure (Gurniak *et al.*, 2005). Moreover, based on its regulatory impact on the actin cytoskeleton, it was associated with neuronal migration disorders and an impaired cell cycle progression in the cerebral cortex (Bellenchi *et al.*, 2007). Based on the *Cfl-1<sup>+/-</sup>* mice, additional functions in the course of the actin dynamics regulating feature of *Cfl-1* were proposed, such as shaping the characteristics of synaptic plasticity and the diffusion of extrasynaptic excitatory AMPA receptors. These findings suggest an impact of *Cfl-1* on all kinds of associative learning (Rust *et al.*, 2010). In addition, *Cfl-1* contribution to the maintenance of the mature podocyte architecture (Garg *et al.*, 2010), to platelet formation and sizing (Bender *et al.*, 2010) and, in combination with destrin, to the branching morphogenesis of the ureteric bud (Kuure *et al.*, 2010) was observed. The homozygous knockout of the *Cfl-1* gene is lethal in an early embryonic stage (Gurniak *et al.*, 2005).

The behavioral phenotyping of *Cfl-1<sup>+/-</sup>* vs. WT mice presented in this study revealed an increased anxiety-related behavior in *Cfl-1<sup>+/-</sup>* mice on the EPM (males and females; Figures 13 and 14) and in the DL box (female mice only; Figures 15 and 16). In the FST, a more active coping style of female *Cfl-1<sup>+/-</sup>* mice was detected (Figures 17 and 18), and increased stress reactivity was observed regardless of gender (Figures 19, 20, and 21). In either case, phenotypic indication was more pronounced in female compared to male mice. This could be due to the fact that also in humans women are in general more susceptible towards the respective traits than man (Cahill, 2006) and in the SR mouse model, the average corticosterone increase in HR female mice (about 400 ng/ml) is considerably higher than in males (250 ng/ml) (Touma *et al.*, 2008). However, these results show a dose-dependent effect of *Cfl-1* on the anxiety-related and depression-like behavior, as well as on the stress reactivity.

Comparing these endophenotypes observed in *Cfl-1<sup>+/-</sup>* mice to the endophenotypes of the stress reactivity mouse model, in terms of anxiety-related and depression-like behavior, *Cfl-1<sup>+/-</sup>* mice more resemble to LR mice, as this line was observed to spend less time on the open arm of the EPM and to travel a shorter distance in the OF, as well as to spent more time immobile and floating in TST and FST, respectively, in comparison to HR mice (Touma *et al.*, 2008). Regarding stress reactivity, *Cfl-1<sup>+/-</sup>* mice resemble to HR mice. Comparing the expression levels of *Cfl-1*, this gene is significantly stronger expressed in HR vs. LR mice and less expressed in the *Cfl-1<sup>+/-</sup>* mice compared to WT mice (Gurniak *et al.*, 2005). In Table 31, the comparison of behavioral traits and *Cfl-1*

expression levels are summarized. A direct comparison of, for example *Cfl-1* expression levels between *Cfl-1<sup>+/-</sup>* and LR mice was considered pointless as both mouse models were generated on dissimilar strains (C57BL/6 vs. CD-1).

Table 31: Summary of features detected in behavioral and gene expressional studies of *Cfl-1<sup>+/-</sup>* vs. WT and HR vs. LR mice. In respect to anxiety-related and depression-like traits as well as in the *Cfl-1* expression level, *Cfl-1<sup>+/-</sup>* mice resemble LRs, in respect to stress-reactivity to HRs.

Feature	<i>Cfl-1<sup>+/-</sup></i> vs. WT	HR vs. LR
Anxiety-related behavior	↑	↓
Depression-like behavior	↑	↓
Stress reactivity	↑	↑
Level of <i>Cfl-1</i> expression	↓	↑

Stress reactivity and comorbid features are, similar to depression, complex traits and determined by complex interactions of genetic, epigenetic and environmental factors. The expression level of *Cfl-1* seems to be associated with certain aspects of this complex trait, though not only *Cfl-1* expression determines behavioral effects described above. As the gene is crucially involved in neurodevelopmental processes, *Cfl-1* deficiency during this critical period presumably contributes to the phenotype displayed by *Cfl-1<sup>+/-</sup>* mice.

As mentioned above, the regulation of *Cfl-1* is clearly dose-dependent. The status quo of active *Cfl-1* after the formation of bundles could possibly be compared to the situation of insufficient levels of *Cfl-1* expression. In either case – too high or too low expression levels of *Cfl-1* – the cell is rendered with a limited and eventually deficient amount of active *Cfl-1* (Figure 39).

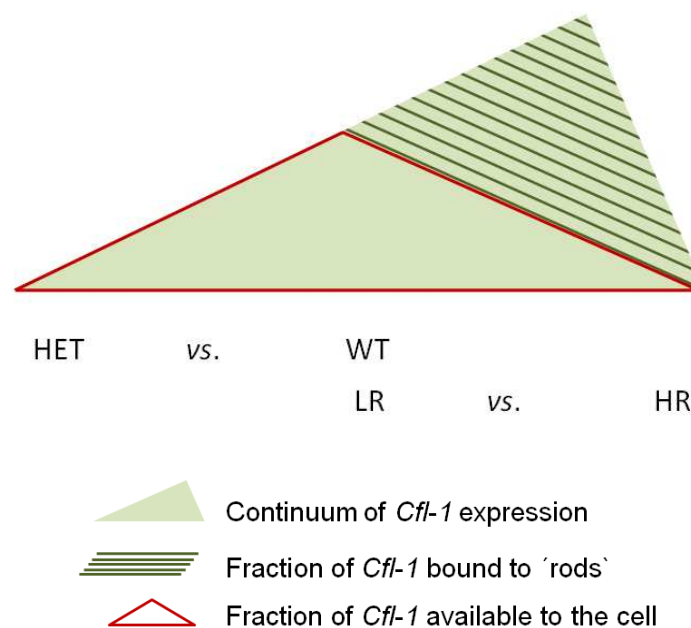


Figure 39: Unscaled illustration depicting the proposed influence of *Cfl-1* on stress reactivity in a dose-dependently, U-shaped manner. According to this model, presumable overexpression of *Cfl-1* like in HR mice in the end renders the cell with a comparable insufficient amount of *Cfl-1* which was detected in *Cfl-1*<sup>+/-</sup> mice, as after a certain *Cfl-1* concentration level the protein is bound to actin filaments and therefore no longer available for cellular processes.

As *Cfl-1*<sup>+/-</sup> mice resemble the stress reactivity to HR mice, although HRs show elevated expression levels of *Cfl-1*, a U-shaped regulation of *Cfl-1* expression in the context of stress reactivity might be proposed. In case of HR mice, the over-expression might have induced the formation of bundles, whereas in *Cfl-1*<sup>+/-</sup> mice the expressional capacity based on one allele is insufficient. The insufficiency of *Cfl-1* expression can clearly be stated based on the phenotypes observed earlier in *Cfl-1*<sup>+/-</sup> mice (Gurniak *et al.*, 2005). Furthermore, *Ssh1*, which positively regulates the actin binding capacity of *Cfl-1*, was as well significantly up-regulated in HR vs. LR mice. HR mice, therefore, do not only express more *Cfl-1*, the fraction of dephosphorylated and hence active *Cfl-1* might be increased, too.

Finally, the physiological relevance of differentially expressed *Cfl-1* was also shown in a mouse model selectively bred for extremes in aggressive behavior. An up-regulation of *Cfl-1* was detected in mice selectively bred for long attack latency (LAL) in comparison to mice displaying a short attack latency (SAL) (Feldker *et al.*, 2003). Interestingly, differences in aggressiveness were also reported from HR and LR mice, in which LR animals displayed a shorter latency to attack (Touma *et al.*, 2008). In case of both inbred

mouse models, the lines expressing *Cfl-1* at higher levels showed a longer attack latency and hence, a reduced level of aggressive behavior.

### **The neurodevelopmental study – further proof for influence of ROS on endophenotype of HR mice?**

A further approach aimed to add functional relevance to expressional profiling data was performed in the so-called 'neurodevelopmental study'. This project was based on the assumption, that a certain fraction of genes which was detected to be differentially expressed in the hippocampus of adult HR and LR mice, is causally and dose-dependently involved in mechanisms determining the extremes in SR. A further fraction, though, does not contribute to endophenotypes in a causative manner; these genes were differentially regulated during adulthood as they were brought about either by negative feedback mechanisms, or were involved in additive, cumulative or compensatory effects. All mechanisms the organism might dispose to overcome this situation of extremes in stress reactivity need to be considered as explanation for differential regulation detected in adulthood. Furthermore, regarding differential expression as a genetic marker, it also needs to be taken into account that a certain fraction of differentially expressed genes is not related to stress reactivity at all. These 'random' genetic markers were collected and conserved based on the selective breeding approach. The difficulty coming along with this is to differentiate between the fraction of genetic markers clearly contributing to the endophenotypes and the fraction of 'randomly' collected genetic markers.

The expressional levels of 13 genes in total detected to be differentially expressed in transcriptome profiling approaches using adult mice were, therefore, tested for differential expression in hippocampal tissue of ED 18, PND 7, and PND 28 mice (Tables 12 - 15). Nine out of these 13 genes were chosen as they were known from the literature to be expressed already during embryogenesis or were detected in the 'central nervous system development' cluster of GO analysis (Comai *et al.*, 2010; Diez-Roux *et al.*, 2011; Gregory *et al.*, 2007; Hard *et al.*, 2005; Kousaka *et al.*, 2008; Lamprianou *et al.*, 2011; Rybnikova *et al.*, 2002; Zhu *et al.*, 2005). The other four genes, such as for example *Cfl-1*, were selected as they seemed to be of special interest in the context of the SR mouse model.

Also the points in time were chosen for a good reason. Extremes in stress reactivity and HPA axis dysfunction are partially genetically determined (Bale, 2006; de Kloet *et al.*, 2005; Touma *et al.*, 2008). It was therefore aimed to test for expressional differences which might be detectable already at the stage of ED 18. In the mouse, the time period

ranging from postnatal day one to twelve is hallmarked by the so-called stress hyporesponsiveness (Schmidt *et al.*, 2003). PND 7 was chosen to test for gene expressional levels roughly in the middle of the HPA axis hyposensitive phase. Finally, as the trait of differential HPA axis reactivity was shown to be apparent already at postnatal day 30 (Touma *et al.*, 2008), the point in time PND 28 was selected to reflect an intermediate stage of the development between neonatal and adult animals.

The only gene confirmed to be differentially expressed in adult mice and also detected to be differentially expressed in an embryonic stage was proline dehydrogenase (*Prodh*). At both points in time *Prodh* was significantly up-regulated in HR vs. LR mice. Interestingly, during the phase of stress hyporesponsiveness (PND 7) an opposing differential expression was measured (up-regulation in LR vs. HR) and no differences were found in PND 28 mice.

Based on these findings one could argue that expressional levels of *Prodh* might be causally involved in the endophenotypes of HR and LR mice as the differential regulation is apparent already before birth and, furthermore, during the developmental phase of HPA axis hyposensitivity it is directed to the opposite (Figure 40). This allows the hypothesis that HR mice down-regulate the expression of *Prodh* when not being susceptible to stress, resulting in a lower expression in HR than in LR mice. This expressional ratio apparently disappears after the onset of stress susceptibility. During the time-period between PND 7 and PND 28, the expressional activity of *Prodh* was up-regulated HR vs. LR mice. This tendency for up-regulation seems to be continued over the time of stress exposure, as in adult HR vs. LR mice a significantly increased *Prodh* expression was measured.

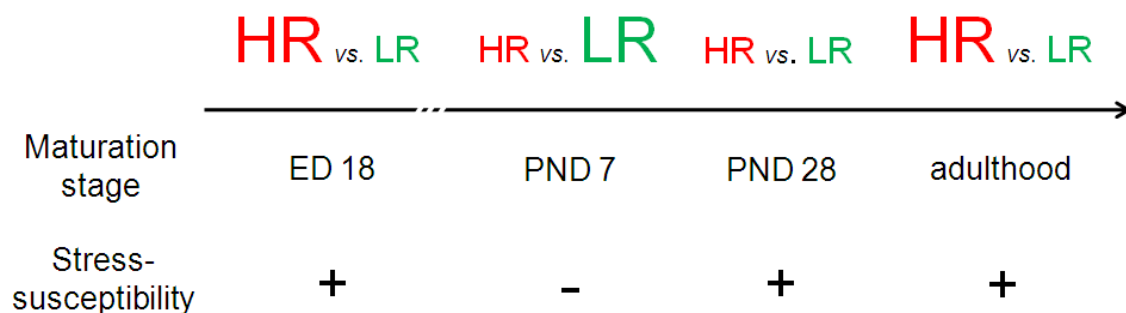


Figure 40: Graphic illustration of *Prodh* expression levels in different stages of maturation in HR and LR mice. Letter size is reflecting expression levels between the lines in a non-scale manner, whereas large letters indicate stronger and small letters weaker expression in the respective line compared to the other.

In different species, for example in humans and *Escherichia coli*, *Prodh* catalyzes the enzymatic conversion of proline into 1-pyrroline-5-carboxylate (P5C), which is the initial reaction of glutamic acid synthesis. Depending on metabolic conditions, *Prodh* activation might lead to the generation of toxic concentrations of P5C. It further might affect the cellular redox homeostasis or generate ROS. In humans it is known that an over-expression of the human form of the *Prodh* gene (Proline oxidase, POX) induces an accumulation of ROS, finally deploying mitochondria-mediated apoptosis (Cecchini *et al.*, 2011; Hu *et al.*, 2007; Maxwell and Rivera, 2003). According to this, the up-regulated expression of *Prodh* in HR mice might create elevated levels of ROS and, hence, induce apoptosis as a response to the animal's stress physiology. This finding goes along with the result of the annotational cluster analyses which might also indicate the contribution of differing levels of ROS to the endophenotypes of HR and LR mice.

Noteworthy, there is accumulating evidence in schizophrenia research that *Prodh* is among the susceptibility genes for this disease (Kempf *et al.*, 2008; O'Tuathaigh *et al.*, 2007; Roussos *et al.*, 2009).

### **CNV- and SNP-genotyping**

Analyzing genetic polymorphisms, the CNV- and SNP-genotyping of in each case one HAB and LAB as well as HR and LR 'master' animal resulted in the identification of 180 regions harboring CNVs between HAB and LAB (Table S8), and 154 such regions between HR and LR mice (Table S9). Furthermore, 60,077 polymorphic positions were detected between HAB and LAB, and 47,470 between HR and LR (Tables S10 and S11). The increased genetic heterogeneity between HAB and LAB compared to HR and LR mice is probably a result of the inbreeding strategy employed at the very beginning of the generation of the inbred mouse models. For the generation of the HAB/LAB mouse model, a selective approach combining out- and in-breeding was used, thereby incorporating a larger pool of trait relevant genetic markers than in the HR/LR mouse model, as in this case a stricter inbreeding protocol was followed right from the beginning.

CNVs were proven to impact gene expression in both mouse models (in HR/LR as presented in this study, Tables 16 and 17; also in HAB/LAB, Julia Brenndoerfer, personal communication). The influence of CNVs on the expression was controversially discussed so far. In accordance to the data presented here, some studies reported a correlation between transcripts mapping to CNV regions and differential expression. Gen-dosage effects towards both directions were detected. Positive correlations in the way of 'more copies, more transcripts', as well as inverse correlations shown by a significant down-

regulation of transcripts mapping to CNVs were found. For other genes mapping to CNVs, the copy number did not at all influence their expressional level (Dopman and Hartl, 2007; Guryev *et al.*, 2008; Henrichsen *et al.*, 2009b). The expressional effect of CNVs is apparently liable to several factors. Tissue-specific gene-dosage effects need to be considered, the regulatory and compensatory network of the gene located in a CNV (Henrichsen *et al.*, 2009b), and the epigenetic modification of the respective DNA stretch (Hogart *et al.*, 2009), to only name a few.

The clustering of CNV regions detected in both inbred mouse models was reported for the mouse before. The accumulation of rather small CNVs in proximate vicinity of both inbred mouse models could hence be regarded as a phenomenon typically observed in the species (Cutler *et al.*, 2007; Henrichsen *et al.*, 2009a), but nevertheless, a more detailed definition of CNV borders or a confirmation of CNV coordinates detected using the Jax Mouse Diversity Genotyping array, respectively, might be necessary for taking the study further, as the assessment of CNVs strongly depends on the platform applied (Henrichsen *et al.*, 2009a; Pinto *et al.*, 2011; She *et al.*, 2008).

Furthermore, the consideration of how CNVs might influence the endophenotypes of HAB/LAB and HR/LR mice needs to be taken further. To simply regard the CNVs impact on the animal's transcriptome might not be the appropriate approach in understanding CNVs functional relevance. Structural rearrangements are known to influence genomic integrity and stability over long distances, as well as chromatin architecture (Henrichsen *et al.*, 2009a; Petrov *et al.*, 2006; Sharp, 2009; Shaw and Lupski, 2004). A more integrative examination of CNV's influence on the endophenotypes should be continued. One example how to pursue testing the influence of CNVs on expression profiles and finally behavioral endophenotypes was shown in a study concerning the glyoxalase 1 (*Glo1*) locus (Hambusch *et al.*, 2010; Williams *et al.*, 2009b). Multiple genomic copies (two- to three-fold) of the *Glo1* gene were detected in LAB mice presumably determining increased gene expressional levels. HAB mice encode for a single copy of the *Glo1* gene and supposedly therefore show a lower gene expressional activity of *Glo1*. These differences in copy numbers at the *Glo1* locus were also shown in the data provided in this study. Phenotypic correlation of anxiety with *Glo1* expression levels have already been described earlier in multiple studies (Ditzen *et al.*, 2006; Kromer *et al.*, 2005; Landgraf *et al.*, 2007; Williams *et al.*, 2009b)

### **Characterization of an outbred population of CD-1 mice**

Selective breeding approaches are aimed to solidify certain genomic traits by directed mating of parental animals displaying the endophenotypic trait of interest. In parallel to

the manifestation of the endophenotypic trait, respective genetic underpinnings determining the behavioral feature can be accumulated and conserved over the generations if an inbreeding protocol is applied (Phillips *et al.*, 2002). Thereby, a certain extent of genetic characteristics found in an inbred population, such as the HAB/LAB mouse model, is closely related to the respective endophenotypes, whereas other genetic features were randomly collected as they appeared in the founder population without any contribution to the trait anxiety (El Yacoubi *et al.*, 2003). In the generation of both mouse models the risk of genetic drift was considered and efforts were made in order to reduce the risk of genetic drift (outbreeding in first eight generations for HAB/LAB vs. interfamilial mating for HR/LR), but nevertheless, a certain degree of allelic frequency shifting cannot be excluded. As it is impossible to distinguish between causal and non-causal genetic differences by exclusively analyzing the selectively bred HAB/LAB or HR/LR mice, an association study was set up in analogy to human GWAS. The classical strategy used in human GWAS is based on the incidence of a genetic variant in a group of patients suffering from the respective disease in comparison to a healthy control group. The statistical analysis of genotype frequencies being detected significantly more often in one of the groups depicts the probability of a contribution of the genetic variant to the disease pattern (Lohoff, 2010).

A population of 384 male outbred CD-1 mice, the so-called 'CD-1 panel', was therefore phenotypically characterized regarding the respective traits. The 'CD-1 panel' presented a typical outbred population in a way that a broad variety of quantitative traits was detected. As expected, the majority of mice displayed intermediate phenotypes of the behaviors tested, though extremes in both directions were observed as well (Figures 27 B, 30 B, 32 B, and 33 B). Correlated phenotypes among the 384 CD-1 mice, like for example increased levels of parameters indicating depression-like and anxiety-related behaviors, were not detected (Figure 34). The co-occurrence of these two quantitative traits is on the one hand frequently reported from animal studies (Finn *et al.*, 2003; Lifschytz *et al.*, 2011), and also the clinically relevant comorbidity of, for example GAD and MDD, is well known (Simon, 2009). On the other hand, behavioral features reflecting anxiety-related and depression-like behavior were shown to display remarkable variation in an outbred population (Jacobson and Cryan, 2007). Outbred strains, therefore, are sometimes used for scientific purposes with the presumption that they model human populations (Yalcin *et al.*, 2010).

It is therefore not surprising that in a large population of 384 mice comorbid features for depression and anxiety are not pronounced enough to show significant correlations. In the PCA, which was calculated based on phenotypic data of 32 CD-1 mice selected for

high-throughput SNP-genotyping, correlations between depression-like and anxiety-related behaviors, and the corticosterone increase were detected (Table S14). This confirmed the selection strategy for the 32 CD-1 mice as it was aimed to choose mice which resemble the endophenotypes of the inbred mouse models (so-called 'HAB-like' and 'LAB-like' features).

As commercially available chips for the genome-wide SNP-genotyping of the mouse are available from one source exclusively, the amount of resources to genotype 384 individuals is considerably limited. The development of a customized SNP chip was therefore considered. In this context, different strategies for the genotyping were discussed and two customized SNP chips, both on Illumina platforms, were designed. In either case, the overlapping pool of SNPs differing between HAB and LAB and at the same time between HR and LR mice served as SNP pool (Table S12), as the occurrence of the polymorphic position in either one of the mouse models was considered reflecting the overlapping phenotypes of the two inbred mouse models on the one hand. On the other hand, it was expected to exclude the selection of alleles with minor frequencies in the CD-1 strain, since allelic frequencies, which are too low, do not serve for the calculation of associations.

As a potential initial approach, a chromosome-centered SNP genotyping assay (Illumina Golden Gate assay, Table S17) was developed. Here, six chromosomes were chosen and genes located on these chromosomes which were considered to be of special interest in the inbred mouse lines, were covered with in total 384 markers, thereby focusing on a discrete marker density in selected areas. This initial approach could be expanded to other chromosomes, finally covering the entire genome. The clear disadvantage of this approach is that it involves diverse biased selection procedures. First, the biased selection of chromosomes and genes considered as particularly promising and second, the biased selection of SNPs based on the overlapping SNP pool. Furthermore, the identification of novel loci contributing to the behavior of the inbred mouse models was hardly possible, as all loci covered with markers were, however, already noted as potentially relevant in the context of the inbred mouse lines.

The second customized SNP genotyping assay (Illumina iSelect assay, Table S18) was developed for the genome-wide screening of 6,000 SNPs. The SNP selection was again conducted based on the overlapping SNP pool, focusing on a close to equal marker distribution throughout the genome. The identification of novel loci would be possible based on the equal marker distribution. The average marker density of about one marker per 450 kbp seemed still unsatisfying though.

The classical approach to determine the marker distribution for GWAS is usually based on haplotype blocks (Simon-Sanchez and Singleton, 2008). Marker distribution in regard of haplotype blocks allows the genotyping of a limited number of tag-SNPs as the genotypes of these tag-SNPs are representative for a varying number of other SNPs located within the same haplotype block (Cuppen, 2005). Neither in the development of the Golden Gate assay, nor in the design of the iSelect chip haplotype blocks were considered, as to date no haplotype map was available for outbred mouse lines and particularly not for the CD-1 outbred line (Yalcin *et al.*, 2010).

Along these lines, Yalcin and colleagues published a survey regarding the suitability of commercially available outbred mice for GWAS concluding that outbred CD-1 mice are a rather defective mouse strain for this purpose. This was stated based on a heterozygosity of 0.22 and an inbreeding coefficient of -1.82. Although the SNP genotyping by Yalcin and colleagues was performed on the identical platform like the one presented in this study, the heterozygosity calculated for the 32 selected CD-1 mice was 0.32 and hence reached a moderate level. This deviation could be caused by the fact that they used mice from a different source. Furthermore, the calculation of an inbreeding coefficient for CD-1 mice based on a SNP screening via a commercially available platform is *per se* considered inapplicable as the fraction of CD-1 specific SNPs and polymorphisms on commercial SNP arrays is under-represented (for details see Table S2 of supplementary data in Yalcin *et al.*) and this strain harbors a variety of polymorphic positions so far not annotated in established SNP databases (Czibere *et al.*, 2011).

The calculation of a CD-1 specific haplotype map was therefore set up to facilitate the SNP selection of a third customized SNP assay based on the haplotype map. As mentioned above, the calculation of the haplotype map required a high-density SNP genotyping of CD-1 mice. For this purpose, 32 CD-1 mice out of the population of 384 phenotypically characterized mice were genotyped using the Jax Mouse Diversity Genotyping array. Heterozygous and opposite homozygous SNPs in these mice were on the one hand used for the calculation of the CD-1 specific haplotype map, and on the other hand for the calculation of preliminary associations between phenotypic and genotypic data collected from these mice.

### **Genetic loci associated with phenotypes**

The analysis of significantly associated loci was done focusing on key phenotypes. In addition, the replication of loci detected to be significantly associated in earlier studies served as internal quality standard. For each key phenotype, the statistically considered

top ten associated loci (regarding nominal p-values) were analyzed and subsequently examined regarding a protein coding nature of the locus (Tables 24 - 30). Based on the biological function of the gene products, the most interesting loci are discussed below.

### **The *Aldh1l1* locus**

The locus encoding for *Aldh1l1* was detected to be significantly associated with the total distance animals travelled in the OF. The *Aldh1l1* gene is encoding for 10-formyltetrahydrofolate dehydrogenase, a major enzyme of the folate metabolism (Anthony and Heintz, 2007). This gene is of particular interest, as it was detected in both, the microarray and the SAGE experiment to be up-regulated in HR vs. LR mice. This regulation was confirmed via qPCR. It was described to be down-regulated in blood samples of patients suffering from high hallucination and delusion states and discussed as a potential blood biomarker for these psychotic conditions (Kurian *et al.*, 2011). Furthermore, it was reported to be up-regulated in subcortical regions of schizophrenia, MDD, and bipolar disorder patients compared to controls with no psychiatric history (Barley *et al.*, 2009). This goes along with the notion that HR mice resemble to symptoms known from melancholic depression (Touma *et al.*, 2008). In addition, in cell culture it was shown that *Aldh1l1* is able to dephosphorylate *Cfl-1*, thereby activating it and hence influencing cell motility (Oleinik *et al.*, 2010). However, the fact, that this gene was detected at the level of gene expression and on polymorphic positions associated with a disease relevant parameter, suggests its functional impact on the endophenotypes of HR and LR mice.

### **The *Kcnma1* locus**

The percentage of time animals spent on the open arm of the EPM was considered a key parameter reflecting anxiety-related behavior. Here, the *Kcnma1* locus was significantly associated. The identical locus was further identified to be associated with the corticosterone increase after the SRT. The gene product is a well characterized calcium activated potassium channel (large conductance, subfamily M, alpha member) with a regulatory effect on membrane potential (Clark *et al.*, 2011). Most importantly, it was detected in human GWAS to be associated with obesity (Jiao *et al.*, 2011), with symptoms of alcohol dependence (Kendler *et al.*, 2011) and late onset and duration of Alzheimer's disease (Burns *et al.*, 2011). Each disease pattern found in the GWAS presents a complex disorder and all of them are related to symptoms of anxiety and stress reactivity suggesting a general influence of *Kcnma1* on mental state and health. In

particular, the relationship between HPA axis dysfunction and obesity seems to be an emerging connection (Bose *et al.*, 2009; Hillman *et al.*, 2011; Stevens *et al.*, 2011).

### **The *Cit* locus**

The next locus detected as significantly associated with two behavioral parameters was the transcriptional unit encoding for Citron-N and Citron-K (*Cit-k*), the two isoforms of the *Cit* gene (Di Cunto *et al.*, 1998). For this locus, a significant association was calculated for the percentage of time animals spent on the open arm of the EPM and the time spent floating in the FST. *Cit-k* is a serine/threonine kinase and a down-stream target of activated Rho (Figure 41). In *Cit-k*<sup>-/-</sup> mice it was shown that it is involved in cytokinesis and *Cit-k* absence seems to be accompanied by apoptosis (Anastas *et al.*, 2010; Di Cunto *et al.*, 2000). Furthermore, there are reports about its contribution to dendritic morphogenesis of cortical neurons (Di Cunto *et al.*, 2003), the morphological influence on interneurons in the barrelfield cortex (Muzzi *et al.*, 2009), and a regulatory effect on axonal growth via a signaling cascade downstream of RhoGTP that converges on *Cfl-1* (Ahmed *et al.*, 2011).

In this *in vitro* study, *Cit-k* mRNA was knocked down rendering the cell with equal amounts of RhoGTP but significantly increased levels of *Cfl-1*. A structural affinity between *Cit-k* and *Rock-1* might explain the functional conjunction between *Cit-k* and *Cfl-1* (Sandvig *et al.*, 2004). However, further studies need to be conducted to enlighten this signaling cascade between *Cit-k* and *Cfl-1*, as there is evidence from the expressional profiling of HR vs. LR mice, and the phenotypic characterization of *Cfl-1*<sup>+/-</sup> mice which showed that *Cfl-1* is clearly involved in the anxiety-related and depression-like phenotypes as well as in stress reactivity.

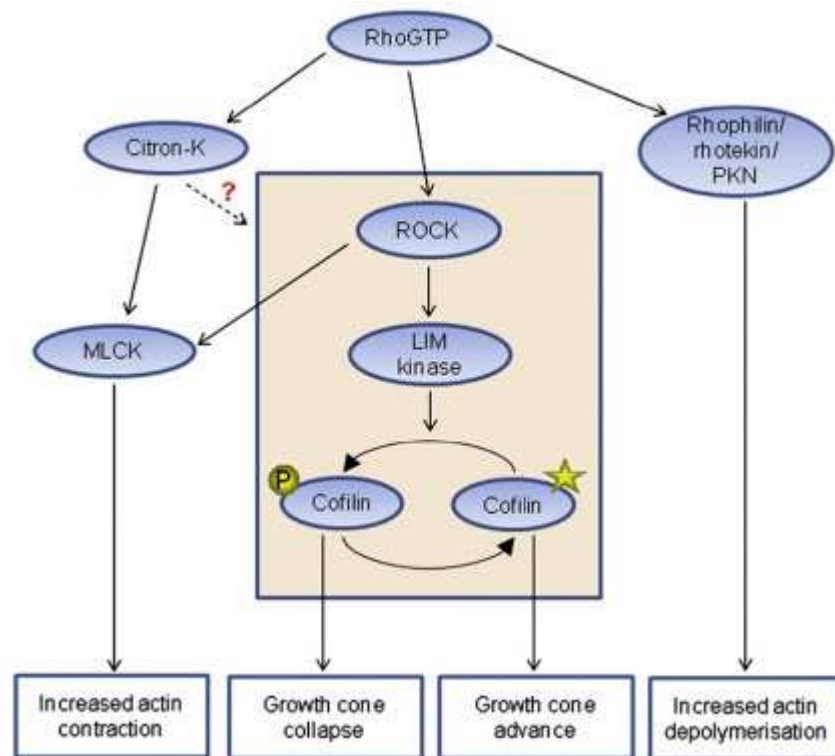


Figure 41: Schematic illustration of the model Ahmed and colleagues proposed regarding the pathway via Cit might be impacting axonal growth in the CNS. As mentioned above, *Cit* is activated by RhoGTP. A so far unknown signaling cascade consolidates on *Cfl-1* which in the phosphorylated (inactive) state depolymerizes actin resulting in growth cone collapse and in the dephosphorylated (active) state boosts growth cone development, respectively. (Figure adopted from Ahmed *et al.*, 2011.)

### The *Atrnl1* locus

Another interesting locus assessed to be significantly associated with the percentage of time animals spent on the open arm of the EPM is the locus encoding for attractin like 1 (*Atrnl1*). This gene is a known ligand of the melanocortin-4 receptor and hence involved in the regulation of energy homeostasis (Haqq *et al.*, 2003). It can furthermore compensate for loss of attractin (Walker *et al.*, 2007). Independent of that, a chromosomal microdeletion comprising the ATRNL1 locus is associated with cognitive impairments, autistic symptoms, and dysmorphic features in affected patients. Analogously, the phenotype of mice displaying homozygous mutations at the *Atrn* locus largely resembled the patient's symptoms (Bronson *et al.*, 2001; Stark *et al.*, 2010). In addition, cognitive impairments were also reported in HAB and LAB mice (Yen *et al.*, 2011).

**The *Runx2/Wox1* loci**

For the corticosterone increase, two separate loci encoding for known interaction partners at protein level were identified in the association study. The gene product of the first locus is *Runx2*, the runt related transcription factor 2; the other is *Wox1*, the WW domain-containing oxidoreductase (also known as *Wwox*). Both gene products were intensively studied and are, hence, well characterized. For example, *Runx2* is known to be a crucial factor in bone development, in particular for osteoblast differentiation and chondrocyte maturation (Baek and Kim, 2011; Komori, 2011). Mutations in the *Runx2* gene were investigated to cause cleidocranial dysplasia (Cohen, 2009). Also noteworthy, an oncogenic potential was attributed to *Runx2* (Cohen, 2009). Furthermore, an essential function of *Runx2* in the regulation of the sterol/steroid metabolism was proposed as it affects the regulation of enzymes critically involved in the respective pathways (Teplyuk *et al.*, 2009). *Wox1* was also implied in a variety of cellular functions, like cellular growth and differentiation processes, apoptosis, and tumor suppression (Del Mare *et al.*, 2009). The observation that *Wox1* is frequently de-regulated in cancer patients led to its classification as tumor suppressor (Aqeilan and Croce, 2007; O'Keefe and Richards, 2006). *Wox1*<sup>-/-</sup> mice suffered from metabolic bone disease (Aqeilan *et al.*, 2008). Furthermore, along the lines of the regulatory function of *Runx2* in the sterol/steroid metabolism, *Wox1* has also been shown to be involved in steroidogenesis (Del Mare *et al.*, 2009). A study, which involved the pharmacological manipulation of mice with a dopaminergic neurotoxin, revealed an up-regulation of *Wox1* in neurons of the striatum and the cortex ipsilaterally to the intoxication. *Wox1* was found in its phosphorylated/activated form to cluster in nuclei and mitochondria of neurodegenerative neurons inducing apoptosis and rendering animals with Parkinson's disease like symptoms. Interestingly, upon inhibition of the *Wox1* phosphorylation the neurodegenerative events were stopped (Lo *et al.*, 2008).

Its pro-apoptotic potential is mostly transmitted via its p53-binding domain, but could also be exerted via binding to other cellular components characterized to initiate cell death pathways. *Wox1/p53* complexes were shown to translocate to the mitochondria inducing apoptosis. As reaction to apoptotic events and/or stress responses, the cytosolic levels of *Wox1* were shown to rise, subsequently to its translocation into the mitochondria (Chang, 2002; Chang *et al.*, 2003).

The key point in describing the diverse functions of *Runx2* and *Wox1* is the inhibitory potential of *Wox1* on *Runx2*. Upon binding to *Runx2*, *Wox1* was shown to be able to inhibit the transactivator function of *Runx2* in certain cell types and even more, expressional profiling of *Runx2* in *Wox1*-deficient bone material disclosed its explicit up-

regulation implying a regulatory function of *Wox1* on *Runx2* (Aqeilan *et al.*, 2008). In summary, the fact, that among the top ten loci associated with the phenotypic parameter corticosterone increase two known binding partners were detected, and even more as the functional impact of these loci point towards neurodegenerative events, strongly suggests the consideration of *Runx2* and *Wox1* in further studies aimed to elucidate molecular underpinnings of extremes in stress reactivity.

### **The *B930007M17Rik* locus**

One further locus remains to be discussed. The locus which is described by the Riken clone *B930007M17Rik* was the only locus among the top ten loci of key phenotypes which was identified to be significantly associated with all three phenotypic categories; namely one parameter for anxiety-related behavior (total time spent on the open arm of the EPM), one parameter reflecting depression-like behavior (time floating in the FST), and the parameter displaying the animal's stress reactivity (corticosterone increase). This combination of phenotypes reflects the comorbidity of depression and associated diseases and the substantial traits describing the two inbred mouse lines. The locus has not been further characterized yet, but it clearly presents an interesting target in the context of comorbidity of affective disorders and pleiotropic gene functions.

### **Testing of reliability of associated loci**

Being aware, that the associations presented here were calculated based on behavioral data and SNP genotypes of 32 selected CD-1 mice only, the question of the reliability of detected loci arises. The successful identification of *Tmem132d* as a locus being associated with parameters reflecting anxiety-related behavior was considered to be an internal hallmark of the study, as this locus was shown to be associated with anxiety severity in humans as well as in mice (Erhardt *et al.*, 2010). Furthermore, the recently detected locus PPARGC1A as marker associated with anxiety disorders after the integration of diverse and complementary data sources based on human and murine screening approaches (Hettema *et al.*, 2011) was as well among significantly associated markers in this study, though not under the top ten associated loci with the key phenotypes.

In addition, the approach presented here, which simplified was the calculation of primary associations based on  $n = 32$  and the establishment of the prerequisites to subsequently extend the study to the entire 'CD-1 panel', was simulated using data of a GWAS with known outcome. The data sets underlying the identification of TMEM132D as marker for anxiety disorders by Erhardt and colleagues were used to simulate the approach

presented in this study. Therefore, 32 patients also reflecting the extremes of the cohort were selected and analysis of significantly associated loci resulted again in the identification of the TMEM132D locus among the 20 most significant markers.

It can therefore be assumed that the most promising candidate loci are among the loci identified in the smaller population, but certainly a number of false positive markers were detected as significantly associated as well. In order to confirm the associations calculated so far, it is aimed to test for associations in the entire population of 384 CD-1 mice. The basis therefore was established by the generation of the CD-1 specific haplotype map, as *lege artis*, the genome-wide distribution of SNPs is assessed based on the LD clustering of the respective species. The selection strategy for a customized haplotype map-based tag-SNP genotyping assay is currently a matter of debate. Equipping the customized assay with the 6,000 tag-SNPs would in the end cover 80% of the polymorphic positions detected genome-wide in the 32 CD-1 mice with an 80% probability. This constitutes an estimated reliability of 60% for the tag-SNPs approach. The genetic heterogeneity in the remaining genome would still render unconsidered and the question of the bias coming along with disregarding roughly one third of the heterozygous loci needs to be raised. The only alternative to the design of a tag-SNP-based customized SNP assay is a high-throughput SNP screening of the entire 'CD-1 panel' via the Jax Mouse Diversity Genotyping array.

In general, GWAS did, on the one hand, contribute to the identification of a variety of common genetic variants enhancing the susceptibility for complex diseases, such as depression and anxiety disorders. On the other hand, detected associations were often identifying loci which were difficult to interpret regarding their biological relevance in the context of the respective disease (Lohoff, 2010), and the identification of susceptibility loci seemed to strongly depend on the cohort (Patel *et al.*, 2010). In addition, the large number of SNPs usually tested in GWAS result in innumerable tests; hence, multiple comparison adjustments might frequently mask biologically relevant markers (Gershon *et al.*, 2011; Jia *et al.*, ; Jia *et al.*, 2010; Wang *et al.*, 2011). For these reasons, it seems necessary to consider data gained from GWAS as first indications for susceptibility loci which require additional confirmation. Different strategies how to potentially increase the output of GWAS were discussed recently. Gene set analysis of GWAS, which involves the testing of functionally related genes in a GWAS (Wang *et al.*, 2011), or pathway-based GWAS were also applied in psychiatric research (Jia *et al.*, 2010). Another promising idea, how to condense and filter the enormous amount of data gained from GWAS, was demonstrated in the aforementioned publication by Hetteema and

colleagues, which involved the integration of murine and human GWAS plus a multitude of *in silico* analyses to finally prioritize one locus. The extension of the association study to the entire 'CD-1 panel' will likely confirm certain loci detected to be associated so far. The investigation of these loci's functional impact on the endophenotypes of the HAB/LAB and the HR/LR mouse models offers a promising approach to verify the contribution of the respective loci to the mosaic of factors which in a complex interplay determine the quantitative traits.



## 6 Perspectives

The findings presented in this study provide the basis for various consecutive projects which, in part, were already initiated.

First, the results of the transcriptome analysis from HR and LR mice, and the projects which resulted from these gene expression profiling attempts so far, clearly suggest the characterization of the mitochondria in a comparative approach in HR vs. LR mice. To precise the kind of potential mitochondrial dysfunction, the repetition of the proteomic screening with mitochondrial protein lysates, which failed in individuals upon insufficient protein yield, should be conducted using pooled mitochondrial protein lysates from at least three animals to reach sufficient protein loads. In general, the more defined the kind of dysfunction is, the more precise techniques can be applied in order to investigate the modes of mitochondrial functions in HR and LR mice. In any case, as the primary mitochondrial task is the generation of ATP adapted to energy demands, potential differences in the ATP turnover between the lines should be determined.

Along these lines, the assessment of ROS levels in HR and LR seems an obvious future step. The mutation rate in mtDNA could therefore be determined, as dissimilar mutation frequencies between HR and LR might serve as a primary indicator for differing levels of ROS. Furthermore, the activity state of antioxidant enzymes catalyzing the detoxification of ROS, such as superoxide dismutase (SOD) and glutathion peroxidase (GPx), would shed light on potential differences in oxidative stress between the lines.

In addition, a time-dependent accumulation of pro-apoptotic signals might enable the detection of differing apoptosis rates in animals older than the ones used for the cytochrome c ELISA.

Ultimately, the gene expression profiling attempts should be extended to further tissues relevant in the context of stress reactivity and HPA axis dysfunction. Gene regulatory differences in, for example the pituitary or the adrenal glands, would supply a more comprehensive idea about endophenotype relevant transcriptional activity.

Second, to further characterize the role of *Cfl-1* in the context of stress reactivity, quantitative real-time analyses in order to determine the gene expression levels of known *Cfl-1* interaction partners will be conducted in *Cfl-1* vs. WT mice. In addition, using perfused brains of these animals, the subcellular localization of the glucocorticoid receptor will be investigated considering temporal aspects. As *Cfl-1* was shown to dose-dependent influence the nuclear translocation of the glucocorticoid receptor, potential differences in glucocorticoid receptor migration will be looked at via immunohistochemical staining.

Third, the extension of the preliminary association study based on 32 mice only to the entire population of the 'CD-1 panel' should be further pursued. Whether a tag-SNP genotyping approach in a third customized assay, which is detecting 6,000 markers genome-wide, or a high-throughput SNP assay, which allows the simultaneous genotyping for more than 623,000 SNPs and even more invariant probe sequences, should be used, is currently a matter of debate. Regarding the results of the haplotype map and tag-SNP approach calculations, the Jax Mouse Diversity Genotyping array is the most promising and, therefore, favorable approach to accomplish this project.

## 7 Abbreviations

2D	2-dimensional
5-HT	5-hydroxytryptamin
ADF	actin depolymerizing factor
ADP	adenosin diphosphat
APS	ammonium persulfate
ATP	adenosin triphosphat
bp	basepairs
BSA	bovine serum albumine
WT	C57BL/6 mice
chr.	chromosome
CNV	copy number variant
CO	cytochrome c oxidase
conc.	concentration
CP	crossing points
cRNA	copy RNA
DAB	3,3-diaminobenzadine
DL box	dark-light box
DTT	Dithiothreitol
ED	embryonic day
EDTA	ethylenediaminetetraacetic acid
EGTA	ethyleneglycoltetraacetic acid
ELISA	enzyme-linked immunosorbent assay
EPM	elevated plus-maze
F2	filial generation 2
FAD	flavin adenine dinucleotide
FC	fold change
FST	forced swim test
g	rcf; relative centrifugal force
GO	gene ontology
GWAS	genome-wide association study
HAB	high anxiety-related behavior
HEPES	4-(2-hydroxyethyl)-1-piperazineethanesulfonic acid
HR	high stress reactivity
IAA	iodoacetamide
IST	Independent student's t-test
K <sub>2</sub> HPO <sub>4</sub>	Dipotassium phosphate
Kbp	kilobasepair
KCl	kalium chloride
LAB	low anxiety-related behavior
LD	linkage disequilibrium
LR	low stress reactivity
lx	lux
mbp	megabasepairs

## Abbreviations

---

MgCl <sub>2</sub>	magnesium chloride
mRNA	messenger ribonucleic acid
MWU	Mann -Whitney U test
n. a.	not applicable
n. s.	not significant
Na <sub>2</sub> HPO <sub>4</sub>	Disodium phosphate
NGS	next generation sequencing
Ni(NH <sub>4</sub> ) <sub>2</sub> (SO <sub>4</sub> ) <sub>2</sub>	Nickel ammonium sulfate
OD	optical density
OF	open field test
PBS	phosphate buffered saline
PCA	principle component analysis
PCR	polymerase chain reaction
PFA	paraformaldehyde
PMSF	phenylmethylsulfonylfluoride
PND	post-natal day
PVC	polyvinyl chloride
qPCR	quantitative real-time PCR
R <sup>2</sup>	correlation coefficient
RF	Random Forest
ROS	reactive oxygen species
RT	room temperature
SAGE	serial analysis of gene expression
SDS	sodium dodecyl sulfate
SEM	standard error of the mean
SNP	single nucleotide polymorphism
SR	stress reactivity
SRT	stress reactivity test
SVM-RFE	support vector machines with recursive feature elimination
TGS	Tris/glycine/SDS
T <sub>m</sub>	melting temperature
Tris	trisaminomethane
TST	tail suspension test
u	unit
V	Volt

## 8 Bibliography

Ahmed, Z., Douglas, M. R., Read, M. L., Berry, M. and Logan, A. (2011): Citron kinase regulates axon growth through a pathway that converges on cofilin downstream of RhoA. *Neurobiol Dis* 41(2): 421-429.

Akiskal, H. S. (1998): Toward a definition of generalized anxiety disorder as an anxious temperament type. *Acta Psychiatr Scand Suppl* 393: 66-73.

Anastas, S. B., Mueller, D., Semple-Rowland, S. L., Breunig, J. J. and Sarkisian, M. R. (2010): Failed cytokinesis of neural progenitors in citron kinase-deficient rats leads to multiciliated neurons. *Cereb Cortex* 21(2): 338-344.

Anisman, H., Merali, Z. and Hayley, S. (2008): Neurotransmitter, peptide and cytokine processes in relation to depressive disorder: comorbidity between depression and neurodegenerative disorders. *Prog Neurobiol* 85(1): 1-74.

Anthony, T. E. and Heintz, N. (2007): The folate metabolic enzyme ALDH1L1 is restricted to the midline of the early CNS, suggesting a role in human neural tube defects. *J Comp Neurol* 500(2): 368-383.

Aqeilan, R. I. and Croce, C. M. (2007): WWOX in biological control and tumorigenesis. *J Cell Physiol* 212(2): 307-310.

Aqeilan, R. I., Hassan, M. Q., de Bruin, A., Hagan, J. P., Volinia, S., Palumbo, T., Hussain, S., Lee, S. H., Gaur, T., Stein, G. S., Lian, J. B. and Croce, C. M. (2008): The WWOX tumor suppressor is essential for postnatal survival and normal bone metabolism. *J Biol Chem* 283(31): 21629-21639.

Augustin, R., Lichtenthaler, S. F., Greeff, M., Hansen, J., Wurst, W. and Trumbach, D. (2011): Bioinformatics identification of modules of transcription factor binding sites in Alzheimer's disease-related genes by in silico promoter analysis and microarrays. *Int J Alzheimers Dis* 2011: 154325.

Baek, W. Y. and Kim, J. E. (2011): Transcriptional regulation of bone formation. *Front Biosci (Schol Ed)* 3: 126-135.

Bailey, K. R. and Crawley, J. N. (2009). Methods of Behavior Analysis in Neuroscience. Boca Raton, Taylor & Francis Group, LLC.

Bale, T. L. (2006): Stress sensitivity and the development of affective disorders. *Horm Behav* 50(4): 529-533.

Bamburg, J. R., Bernstein, B. W., Davis, R. C., Flynn, K. C., Goldsbury, C., Jensen, J. R., Maloney, M. T., Marsden, I. T., Minamide, L. S., Pak, C. W., Shaw, A. E., Whiteman, I. and Wiggan, O. (2010): ADF/Cofilin-actin rods in neurodegenerative diseases. *Curr Alzheimer Res* 7(3): 241-250.

Barley, K., Dracheva, S. and Byne, W. (2009): Subcortical oligodendrocyte- and astrocyte-associated gene expression in subjects with schizophrenia, major depression and bipolar disorder. *Schizophr Res* 112(1-3): 54-64.

- Becker, J., Schmidt, P., Musshoff, F., Fitzenreiter, M. and Madea, B. (2004): MOR1 receptor mRNA expression in human brains of drug-related fatalities—a real-time PCR quantification. *Forensic Sci Int* 140(1): 13-20.
- Bellenchi, G. C., Gurniak, C. B., Perlas, E., Middei, S., Ammassari-Teule, M. and Witke, W. (2007): N-cofilin is associated with neuronal migration disorders and cell cycle control in the cerebral cortex. *Genes Dev* 21(18): 2347-2357.
- Bender, M., Eckly, A., Hartwig, J. H., Elvers, M., Pleines, I., Gupta, S., Krohne, G., Jeanclos, E., Gohla, A., Gurniak, C., Gachet, C., Witke, W. and Nieswandt, B. (2010): ADF/n-cofilin-dependent actin turnover determines platelet formation and sizing. *Blood* 116(10): 1767-1775.
- Benjamini, Y., Drai, D., Elmer, G., Kafkafi, N. and Golani, I. (2001): Controlling the false discovery rate in behavior genetics research. *Behav Brain Res* 125(1-2): 279-284.
- Bernstein, B. W. and Bamburg, J. R. (2010): ADF/cofilin: a functional node in cell biology. *Trends Cell Biol* 20(4): 187-195.
- Binder, E. B., Owens, M. J., Liu, W., Deveau, T. C., Rush, A. J., Trivedi, M. H., Fava, M., Bradley, B., Ressler, K. J. and Nemeroff, C. B. (2010): Association of polymorphisms in genes regulating the corticotropin-releasing factor system with antidepressant treatment response. *Arch Gen Psychiatry* 67(4): 369-379.
- Bondy, B. (2011): Genetics in psychiatry: are the promises met? *World J Biol Psychiatry* 12(2): 81-88.
- Bose, M., Olivan, B. and Laferrere, B. (2009): Stress and obesity: the role of the hypothalamic-pituitary-adrenal axis in metabolic disease. *Curr Opin Endocrinol Diabetes Obes* 16(5): 340-346.
- Bourin, M. and Hascoet, M. (2003): The mouse light/dark box test. *Eur J Pharmacol* 463(1-3): 55-65.
- Brand, M. D. and Nicholls, D. G. (2011): Assessing mitochondrial dysfunction in cells. *Biochem J* 435(2): 297-312.
- Bronson, R. T., Donahue, L. R., Samples, R., Kim, J. H. and Naggert, J. K. (2001): Mice with mutations in the mahogany gene *Atrn* have cerebral spongiform changes. *J Neuropathol Exp Neurol* 60(7): 724-730.
- Burns, L. C., Minster, R. L., Demirci, F. Y., Barmada, M. M., Ganguli, M., Lopez, O. L., DeKosky, S. T. and Kamboh, M. I. (2011): Replication study of genome-wide associated SNPs with late-onset Alzheimer's disease. *Am J Med Genet B Neuropsychiatr Genet* 156B(4): 507-512.
- Cahill, L. (2006): Why sex matters for neuroscience. *Nat Rev Neurosci* 7(6): 477-484.
- Carboni, S., Antonsson, B., Gaillard, P., Gotteland, J. P., Gillon, J. Y. and Vitte, P. A. (2005): Control of death receptor and mitochondrial-dependent apoptosis by c-Jun N-terminal kinase in hippocampal CA1 neurones following global transient ischaemia. *J Neurochem* 92(5): 1054-1060.
- Cassano, P. and Fava, M. (2002): Depression and public health: an overview. *J Psychosom Res* 53(4): 849-857.

- Cecchini, N. M., Monteoliva, M. I. and Alvarez, M. E. (2011): Proline dehydrogenase is a positive regulator of cell death in different kingdoms. *Plant Signal Behav* 6(8): 1195-1197.
- Cerda, M., Sagdeo, A., Johnson, J. and Galea, S. (2010): Genetic and environmental influences on psychiatric comorbidity: a systematic review. *J Affect Disord* 126(1-2): 14-38.
- Chang, N. S. (2002): A potential role of p53 and WOX1 in mitochondrial apoptosis (review). *Int J Mol Med* 9(1): 19-24.
- Chang, N. S., Doherty, J., Ensign, A., Lewis, J., Heath, J., Schultz, L., Chen, S. T. and Oppermann, U. (2003): Molecular mechanisms underlying WOX1 activation during apoptotic and stress responses. *Biochem Pharmacol* 66(8): 1347-1354.
- Charmandari, E., Tsigos, C. and Chrousos, G. (2005): Endocrinology of the stress response. *Annu Rev Physiol* 67: 259-284.
- Chinopoulos, C. (2011): Mitochondrial consumption of cytosolic ATP: not so fast. *FEBS Lett* 585(9): 1255-1259.
- Chomczynski, P. and Sacchi, N. (1987): Single-step method of RNA isolation by acid guanidinium thiocyanate-phenol-chloroform extraction. *Anal Biochem* 162(1): 156-159.
- Chua, B. T., Volbracht, C., Tan, K. O., Li, R., Yu, V. C. and Li, P. (2003): Mitochondrial translocation of cofilin is an early step in apoptosis induction. *Nat Cell Biol* 5(12): 1083-1089.
- Cichon, S., Craddock, N., Daly, M., Faraone, S. V., Gejman, P. V., Kelsoe, J., Lehner, T., Levinson, D. F., Moran, A., Sklar, P. and Sullivan, P. F. (2009): Genomewide association studies: history, rationale, and prospects for psychiatric disorders. *Am J Psychiatry* 166(5): 540-556.
- Clark, R. B., Kondo, C., Belke, D. D. and Giles, W. R. (2011): Two-pore domain K<sup>+</sup> channels regulate membrane potential of isolated human articular chondrocytes. *J Physiol* 589(Pt 21): 5071-5089.
- Clay, H. B., Sullivan, S. and Konradi, C. (2011): Mitochondrial dysfunction and pathology in bipolar disorder and schizophrenia. *Int J Dev Neurosci* 29(3): 311-324.
- Cohen, M. M., Jr. (2009): Perspectives on RUNX genes: an update. *Am J Med Genet A* 149A(12): 2629-2646.
- Colman, I. and Ataullahjan, A. (2010): Life course perspectives on the epidemiology of depression. *Can J Psychiatry* 55(10): 622-632.
- Comai, G., Boutet, A., Neirijnck, Y. and Schedl, A. (2010): Expression patterns of the Wtx/Amer gene family during mouse embryonic development. *Dev Dyn* 239(6): 1867-1878.
- Connolly, K. R. and Thase, M. E. (2011): If at first you don't succeed: a review of the evidence for antidepressant augmentation, combination and switching strategies. *Drugs* 71(1): 43-64.

- Coppee, J. Y. (2008): Do DNA microarrays have their future behind them? *Microbes Infect* 10(9): 1067-1071.
- Corder, E. H., Saunders, A. M., Strittmatter, W. J., Schmechel, D. E., Gaskell, P. C., Small, G. W., Roses, A. D., Haines, J. L. and Pericak-Vance, M. A. (1993): Gene dose of apolipoprotein E type 4 allele and the risk of Alzheimer's disease in late onset families. *Science* 261(5123): 921-923.
- Costall, B., Jones, B. J., Kelly, M. E., Naylor, R. J. and Tomkins, D. M. (1989): Exploration of mice in a black and white test box: validation as a model of anxiety. *Pharmacol Biochem Behav* 32(3): 777-785.
- Cox, B. and Emili, A. (2006): Tissue subcellular fractionation and protein extraction for use in mass-spectrometry-based proteomics. *Nat Protoc* 1(4): 1872-1878.
- Craddock, N., O'Donovan, M. C. and Owen, M. J. (2008): Genome-wide association studies in psychiatry: lessons from early studies of non-psychiatric and psychiatric phenotypes. *Mol Psychiatry* 13(7): 649-653.
- Crawford, M. and Masterson, F. A. (1982): Species-specific defense reactions and avoidance learning. An evaluative review. *Pavlov J Biol Sci* 17(4): 204-214.
- Crawley, J. and Goodwin, F. K. (1980): Preliminary report of a simple animal behavior model for the anxiolytic effects of benzodiazepines. *Pharmacol Biochem Behav* 13(2): 167-170.
- Crawley, J. N. (1999): Behavioral phenotyping of transgenic and knockout mice: experimental design and evaluation of general health, sensory functions, motor abilities, and specific behavioral tests. *Brain Res* 835(1): 18-26.
- Crestani, F., Lorez, M., Baer, K., Essrich, C., Benke, D., Laurent, J. P., Belzung, C., Fritschy, J. M., Luscher, B. and Mohler, H. (1999): Decreased GABAA-receptor clustering results in enhanced anxiety and a bias for threat cues. *Nat Neurosci* 2(9): 833-839.
- Cryan, J. F. and Holmes, A. (2005): The ascent of mouse: advances in modelling human depression and anxiety. *Nat Rev Drug Discov* 4(9): 775-790.
- Cryan, J. F., Mombereau, C. and Vassout, A. (2005): The tail suspension test as a model for assessing antidepressant activity: review of pharmacological and genetic studies in mice. *Neurosci Biobehav Rev* 29(4-5): 571-625.
- Cuppen, E. (2005): Haplotype-based genetics in mice and rats. *Trends Genet* 21(6): 318-322.
- Cutler, G., Marshall, L. A., Chin, N., Baribault, H. and Kassner, P. D. (2007): Significant gene content variation characterizes the genomes of inbred mouse strains. *Genome Res* 17(12): 1743-1754.

- Czibere, L., Baur, L. A., Wittmann, A., Gemmeke, K., Steiner, A., Weber, P., Putz, B., Ahmad, N., Bunck, M., Graf, C., Widner, R., Kuhne, C., Panhuysen, M., Hamsch, B., Rieder, G., Reinheckel, T., Peters, C., Holsboer, F., Landgraf, R. and Deussing, J. M. (2011): Profiling trait anxiety: transcriptome analysis reveals cathepsin B (*Ctsb*) as a novel candidate gene for emotionality in mice. *PLoS One* 6(8): e23604.
- de Castro, I. P., Martins, L. M. and Tufi, R. (2010): Mitochondrial quality control and neurological disease: an emerging connection. *Expert Rev Mol Med* 12: e12.
- de Kloet, E. R., Joels, M. and Holsboer, F. (2005): Stress and the brain: from adaptation to disease. *Nat Rev Neurosci* 6(6): 463-475.
- Del Mare, S., Salah, Z. and Aqeilan, R. I. (2009): WWOX: its genomics, partners, and functions. *J Cell Biochem* 108(4): 737-745.
- Di Cunto, F., Calautti, E., Hsiao, J., Ong, L., Topley, G., Turco, E. and Dotto, G. P. (1998): Citron rho-interacting kinase, a novel tissue-specific ser/thr kinase encompassing the Rho-Rac-binding protein Citron. *J Biol Chem* 273(45): 29706-29711.
- Di Cunto, F., Ferrara, L., Curtetti, R., Imarisio, S., Guazzone, S., Broccoli, V., Bulfone, A., Altruda, F., Vercelli, A. and Silengo, L. (2003): Role of citron kinase in dendritic morphogenesis of cortical neurons. *Brain Res Bull* 60(4): 319-327.
- Di Cunto, F., Imarisio, S., Hirsch, E., Broccoli, V., Bulfone, A., Migheli, A., Atzori, C., Turco, E., Triolo, R., Dotto, G. P., Silengo, L. and Altruda, F. (2000): Defective neurogenesis in citron kinase knockout mice by altered cytokinesis and massive apoptosis. *Neuron* 28(1): 115-127.
- Diez-Roux, G., Banfi, S., Sultan, M., Geffers, L., Anand, S., Rozado, D., Magen, A., Canidio, E., Pagani, M., Peluso, I., Lin-Marq, N., Koch, M., Bilio, M., Cantiello, I., Verde, R., De Masi, C., Bianchi, S. A., Cicchini, J., Perroud, E., Mehmeti, S., Dagand, E., Schrunner, S., Nurnberger, A., Schmidt, K., Metz, K., Zwingmann, C., Brieske, N., Springer, C., Hernandez, A. M., Herzog, S., Grabbe, F., Sieverding, C., Fischer, B., Schrader, K., Brockmeyer, M., Dettmer, S., Helbig, C., Alunni, V., Battaini, M. A., Mura, C., Henrichsen, C. N., Garcia-Lopez, R., Echevarria, D., Puelles, E., Garcia-Calero, E., Kruse, S., Uhr, M., Kauck, C., Feng, G., Milyaev, N., Ong, C. K., Kumar, L., Lam, M., Semple, C. A., Gyenesei, A., Mundlos, S., Radelof, U., Lehrach, H., Sarmientos, P., Raymond, A., Davidson, D. R., Dolle, P., Antonarakis, S. E., Yaspo, M. L., Martinez, S., Baldock, R. A., Eichele, G. and Ballabio, A. (2011): A high-resolution anatomical atlas of the transcriptome in the mouse embryo. *PLoS Biol* 9(1): e1000582.
- Ditzen, C., Jastorff, A. M., Kessler, M. S., Bunck, M., Teplytska, L., Erhardt, A., Kromer, S. A., Varadarajulu, J., Targosz, B. S., Sayan-Ayata, E. F., Holsboer, F., Landgraf, R. and Turck, C. W. (2006): Protein biomarkers in a mouse model of extremes in trait anxiety. *Mol Cell Proteomics* 5(10): 1914-1920.
- Dopman, E. B. and Hartl, D. L. (2007): A portrait of copy-number polymorphism in *Drosophila melanogaster*. *Proc Natl Acad Sci U S A* 104(50): 19920-19925.
- Draghici, S., Khatri, P., Eklund, A. C. and Szallasi, Z. (2006): Reliability and reproducibility issues in DNA microarray measurements. *Trends Genet* 22(2): 101-109.
- Du, J., McEwen, B. and Manji, H. K. (2009a): Glucocorticoid receptors modulate mitochondrial function: A novel mechanism for neuroprotection. *Commun Integr Biol* 2(4): 350-352.

Du, J., Wang, Y., Hunter, R., Wei, Y., Blumenthal, R., Falke, C., Khairova, R., Zhou, R., Yuan, P., Machado-Vieira, R., McEwen, B. S. and Manji, H. K. (2009b): Dynamic regulation of mitochondrial function by glucocorticoids. *Proc Natl Acad Sci U S A* 106(9): 3543-3548.

Earnheart, J. C., Schweizer, C., Crestani, F., Iwasato, T., Itohara, S., Mohler, H. and Luscher, B. (2007): GABAergic control of adult hippocampal neurogenesis in relation to behavior indicative of trait anxiety and depression states. *J Neurosci* 27(14): 3845-3854.

El Yacoubi, M., Bouali, S., Popa, D., Naudon, L., Leroux-Nicollet, I., Hamon, M., Costentin, J., Adrien, J. and Vaugeois, J. M. (2003): Behavioral, neurochemical, and electrophysiological characterization of a genetic mouse model of depression. *Proc Natl Acad Sci U S A* 100(10): 6227-6232.

El Yacoubi, M. and Vaugeois, J. M. (2007): Genetic rodent models of depression. *Curr Opin Pharmacol* 7(1): 3-7.

Endo, M., Ohashi, K., Sasaki, Y., Goshima, Y., Niwa, R., Uemura, T. and Mizuno, K. (2003): Control of growth cone motility and morphology by LIM kinase and Slingshot via phosphorylation and dephosphorylation of cofilin. *J Neurosci* 23(7): 2527-2537.

Erhardt, A., Czibere, L., Roeske, D., Lucae, S., Unschuld, P. G., Ripke, S., Specht, M., Kohli, M. A., Kloiber, S., Ising, M., Heck, A., Pfister, H., Zimmermann, P., Lieb, R., Putz, B., Uhr, M., Weber, P., Deussing, J. M., Gonik, M., Bunck, M., Kebler, M. S., Frank, E., Hohoff, C., Domschke, K., Krakowitzky, P., Maier, W., Bandelow, B., Jacob, C., Deckert, J., Schreiber, S., Strohmaier, J., Nothen, M., Cichon, S., Rietschel, M., Bettecken, T., Keck, M. E., Landgraf, R., Muller-Myhsok, B., Holsboer, F. and Binder, E. B. (2010): TMEM132D, a new candidate for anxiety phenotypes: evidence from human and mouse studies. *Mol Psychiatry* 16(6): 647-663.

Fanselow, M. S. and Dong, H. W. (2010): Are the dorsal and ventral hippocampus functionally distinct structures? *Neuron* 65(1): 7-19.

Feldker, D. E., Datson, N. A., Veenema, A. H., Meulmeester, E., de Kloet, E. R. and Vreugdenhil, E. (2003): Serial analysis of gene expression predicts structural differences in hippocampus of long attack latency and short attack latency mice. *Eur J Neurosci* 17(2): 379-387.

Filiou, M. D., Zhang, Y., Teplytska, L., Reckow, S., Gormanns, P., Maccarrone, G., Frank, E., Kessler, M. S., Hamsch, B., Nussbaumer, M., Bunck, M., Ludwig, T., Yassouridis, A., Holsboer, F., Landgraf, R. and Turck, C. W. (2011): Proteomics and metabolomics analysis of a trait anxiety mouse model reveals divergent mitochondrial pathways. *Biol Psychiatry* 70(11): 1074-1082.

Finn, D. A., Rutledge-Gorman, M. T. and Crabbe, J. C. (2003): Genetic animal models of anxiety. *Neurogenetics* 4(3): 109-135.

Franz, C. E., York, T. P., Eaves, L. J., Mendoza, S. P., Hauger, R. L., Hellhammer, D. H., Jacobson, K. C., Levine, S., Lupien, S. J., Lyons, M. J., Prom-Wormley, E., Xian, H. and Kremen, W. S. (2010): Genetic and environmental influences on cortisol regulation across days and contexts in middle-aged men. *Behav Genet* 40(4): 467-479.

Freeborough, A. and Kimpton, J. (2011): Discovering new genetic and psychosocial pathways in Major Depressive Disorder: the NewMood project. *Psychiatr Danub* 23 Suppl 1: S138-141.

- Garg, P., Verma, R., Cook, L., Soofi, A., Venkatareddy, M., George, B., Mizuno, K., Gurniak, C., Witke, W. and Holzman, L. B. (2010): Actin-depolymerizing factor cofilin-1 is necessary in maintaining mature podocyte architecture. *J Biol Chem* 285(29): 22676-22688.
- Gelenberg, A. J. (2010): The prevalence and impact of depression. *J Clin Psychiatry* 71(3): e06.
- Gershon, E. S., Alliey-Rodriguez, N. and Liu, C. (2011): After GWAS: searching for genetic risk for schizophrenia and bipolar disorder. *Am J Psychiatry* 168(3): 253-256.
- Gille, G. and Reichmann, H. (2011): Iron-dependent functions of mitochondria--relation to neurodegeneration. *J Neural Transm* 118(3): 349-359.
- Goate, A., Chartier-Harlin, M. C., Mullan, M., Brown, J., Crawford, F., Fidani, L., Giuffra, L., Haynes, A., Irving, N., James, L. and et al. (1991): Segregation of a missense mutation in the amyloid precursor protein gene with familial Alzheimer's disease. *Nature* 349(6311): 704-706.
- Gold, P. W. and Chrousos, G. P. (1999): The endocrinology of melancholic and atypical depression: relation to neurocircuitry and somatic consequences. *Proc Assoc Am Physicians* 111(1): 22-34.
- Gold, P. W. and Chrousos, G. P. (2002): Organization of the stress system and its dysregulation in melancholic and atypical depression: high vs low CRH/NE states. *Mol Psychiatry* 7(3): 254-275.
- Gold, P. W., Goodwin, F. K. and Chrousos, G. P. (1988): Clinical and biochemical manifestations of depression. Relation to the neurobiology of stress (1). *N Engl J Med* 319(6): 348-353.
- Gonzalez-Lima, F. and Garrosa, M. (1991): Quantitative histochemistry of cytochrome oxidase in rat brain. *Neurosci Lett* 123(2): 251-253.
- Gregory, G. D., Vakoc, C. R., Rozovskaia, T., Zheng, X., Patel, S., Nakamura, T., Canaani, E. and Blobel, G. A. (2007): Mammalian ASH1L is a histone methyltransferase that occupies the transcribed region of active genes. *Mol Cell Biol* 27(24): 8466-8479.
- Grippe, A. J. and Johnson, A. K. (2009): Stress, depression and cardiovascular dysregulation: a review of neurobiological mechanisms and the integration of research from preclinical disease models. *Stress* 12(1): 1-21.
- Groeneweg, F. L., Karst, H., de Kloet, E. R. and Joels, M. (2011a): Mineralocorticoid and glucocorticoid receptors at the neuronal membrane, regulators of nongenomic corticosteroid signalling. *Mol Cell Endocrinol*.
- Groeneweg, F. L., Karst, H., de Kloet, E. R. and Joels, M. (2011b): Rapid non-genomic effects of corticosteroids and their role in the central stress response. *J Endocrinol* 209(2): 153-167.
- Gross, C., Santarelli, L., Brunner, D., Zhuang, X. and Hen, R. (2000): Altered fear circuits in 5-HT(1A) receptor KO mice. *Biol Psychiatry* 48(12): 1157-1163.
- Gurniak, C. B., Perlas, E. and Witke, W. (2005): The actin depolymerizing factor n-cofilin is essential for neural tube morphogenesis and neural crest cell migration. *Dev Biol* 278(1): 231-241.

- Guryev, V., Saar, K., Adamovic, T., Verheul, M., van Heesch, S. A., Cook, S., Pravenec, M., Aitman, T., Jacob, H., Shull, J. D., Hubner, N. and Cuppen, E. (2008): Distribution and functional impact of DNA copy number variation in the rat. *Nat Genet* 40(5): 538-545.
- Hamsch, B., Chen, B. G., Brenndorfer, J., Meyer, M., Avrabos, C., Maccarrone, G., Liu, R. H., Eder, M., Turck, C. W. and Landgraf, R. (2010): Methylglyoxal-mediated anxiety involves increased protein modification and elevated expression of glyoxalase 1 in the brain. *J Neurochem* 113(5): 1240-1251.
- Hamet, P. and Tremblay, J. (2005): Genetics and genomics of depression. *Metabolism* 54(5 Suppl 1): 10-15.
- Han, X. J., Tomizawa, K., Fujimura, A., Ohmori, I., Nishiki, T., Matsushita, M. and Matsui, H. (2011): Regulation of mitochondrial dynamics and neurodegenerative diseases. *Acta Med Okayama* 65(1): 1-10.
- Hanukoglu, I. (2006): Antioxidant protective mechanisms against reactive oxygen species (ROS) generated by mitochondrial P450 systems in steroidogenic cells. *Drug Metab Rev* 38(1-2): 171-196.
- Haqq, A. M., Rene, P., Kishi, T., Khong, K., Lee, C. E., Liu, H., Friedman, J. M., Elmquist, J. K. and Cone, R. D. (2003): Characterization of a novel binding partner of the melanocortin-4 receptor: attractin-like protein. *Biochem J* 376(Pt 3): 595-605.
- Hard, M. L., Abdoell, M., Robinson, B. H. and Koren, G. (2005): Gene-expression analysis after alcohol exposure in the developing mouse. *J Lab Clin Med* 145(1): 47-54.
- Harro, J., Kanarik, M., Matrov, D. and Panksepp, J. (2011): Mapping patterns of depression-related brain regions with cytochrome oxidase histochemistry: Relevance of animal affective systems to human disorders, with a focus on resilience to adverse events. *Neurosci Biobehav Rev* 35(9): 1876-1889.
- Heinzmann, J. M., Thoeringer, C. K., Knapman, A., Palme, R., Holsboer, F., Uhr, M., Landgraf, R. and Touma, C. (2010): Intrahippocampal corticosterone response in mice selectively bred for extremes in stress reactivity: a microdialysis study. *J Neuroendocrinol* 22(11): 1187-1197.
- Heitzer, M. D., Wolf, I. M., Sanchez, E. R., Witchel, S. F. and DeFranco, D. B. (2007): Glucocorticoid receptor physiology. *Rev Endocr Metab Disord* 8(4): 321-330.
- Henderson, N. D., Turri, M. G., DeFries, J. C. and Flint, J. (2004): QTL analysis of multiple behavioral measures of anxiety in mice. *Behav Genet* 34(3): 267-293.
- Henrichsen, C. N., Chaignat, E. and Reymond, A. (2009a): Copy number variants, diseases and gene expression. *Hum Mol Genet* 18(R1): R1-8.
- Henrichsen, C. N., Vinckenbosch, N., Zollner, S., Chaignat, E., Pradervand, S., Schutz, F., Ruedi, M., Kaessmann, H. and Reymond, A. (2009b): Segmental copy number variation shapes tissue transcriptomes. *Nat Genet* 41(4): 424-429.
- Hettema, J. M., Neale, M. C., Myers, J. M., Prescott, C. A. and Kendler, K. S. (2006): A population-based twin study of the relationship between neuroticism and internalizing disorders. *Am J Psychiatry* 163(5): 857-864.

- Hettema, J. M., Webb, B. T., Guo, A. Y., Zhao, Z., Maher, B. S., Chen, X., An, S. S., Sun, C., Aggen, S. H., Kendler, K. S., Kuo, P. H., Otowa, T., Flint, J. and van den Oord, E. J. (2011): Prioritization and association analysis of murine-derived candidate genes in anxiety-spectrum disorders. *Biol Psychiatry* 70(9): 888-896.
- Hevner, R. F. and Wong-Riley, M. T. (1990): Regulation of cytochrome oxidase protein levels by functional activity in the macaque monkey visual system. *J Neurosci* 10(4): 1331-1340.
- Higuchi, R., Fockler, C., Dollinger, G. and Watson, R. (1993): Kinetic PCR analysis: real-time monitoring of DNA amplification reactions. *Biotechnology (N Y)* 11(9): 1026-1030.
- Hillman, J. B., Dorn, L. D., Loucks, T. L. and Berga, S. L. (2011): Obesity and the hypothalamic-pituitary-adrenal axis in adolescent girls. *Metabolism*.
- Hogart, A., Leung, K. N., Wang, N. J., Wu, D. J., Driscoll, J., Vallero, R. O., Schanen, N. C. and LaSalle, J. M. (2009): Chromosome 15q11-13 duplication syndrome brain reveals epigenetic alterations in gene expression not predicted from copy number. *J Med Genet* 46(2): 86-93.
- Hogg, S. (1996): A review of the validity and variability of the elevated plus-maze as an animal model of anxiety. *Pharmacol Biochem Behav* 54(1): 21-30.
- Holsboer, F. (2001): Stress, hypercortisolism and corticosteroid receptors in depression: implications for therapy. *J Affect Disord* 62(1-2): 77-91.
- Hu, C. A., Donald, S. P., Yu, J., Lin, W. W., Liu, Z., Steel, G., Obie, C., Valle, D. and Phang, J. M. (2007): Overexpression of proline oxidase induces proline-dependent and mitochondria-mediated apoptosis. *Mol Cell Biochem* 295(1-2): 85-92.
- Hu, D., Xu, X. and Gonzalez-Lima, F. (2005): Hippocampal cytochrome oxidase activity of rats in easy and difficult visual discrimination learning. *Int J Neurosci* 115(5): 595-611.
- Huang da, W., Sherman, B. T. and Lempicki, R. A. (2009): Systematic and integrative analysis of large gene lists using DAVID bioinformatics resources. *Nat Protoc* 4(1): 44-57.
- Huttemann, M., Pecina, P., Rainbolt, M., Sanderson, T. H., Kagan, V. E., Samavati, L., Doan, J. W. and Lee, I. (2011): The multiple functions of cytochrome c and their regulation in life and death decisions of the mammalian cell: From respiration to apoptosis. *Mitochondrion* 11(3): 369-381.
- Insel, T. R. and Charney, D. S. (2003): Research on major depression: strategies and priorities. *Jama* 289(23): 3167-3168.
- Iwamoto, K., Bundo, M. and Kato, T. (2005): Altered expression of mitochondria-related genes in postmortem brains of patients with bipolar disorder or schizophrenia, as revealed by large-scale DNA microarray analysis. *Hum Mol Genet* 14(2): 241-253.
- Jacobson, L. H. and Cryan, J. F. (2007): Feeling strained? Influence of genetic background on depression-related behavior in mice: a review. *Behav Genet* 37(1): 171-213.
- Jia, P., Wang, L., Meltzer, H. Y. and Zhao, Z. Pathway-based analysis of GWAS datasets: effective but caution required. *Int J Neuropsychopharmacol* 14(4): 567-572.

Jia, P., Wang, L., Meltzer, H. Y. and Zhao, Z. (2010): Pathway-based analysis of GWAS datasets: effective but caution required. *Int J Neuropsychopharmacol* 14(4): 567-572.

Jiao, H., Arner, P., Hoffstedt, J., Brodin, D., Dubern, B., Czernichow, S., van't Hooft, F., Axelsson, T., Pedersen, O., Hansen, T., Sorensen, T. I., Hebebrand, J., Kere, J., Dahlman-Wright, K., Hamsten, A., Clement, K. and Dahlman, I. (2011): Genome wide association study identifies KCNMA1 contributing to human obesity. *BMC Med Genomics* 4: 51.

Joachim, H. (1890). Papyrus Ebers: Das älteste Buch über Heilkunde. Berlin, Reimer.

Jou, S. H., Chiu, N. Y. and Liu, C. S. (2009): Mitochondrial dysfunction and psychiatric disorders. *Chang Gung Med J* 32(4): 370-379.

Karssen, A. M., Li, J. Z., Her, S., Patel, P. D., Meng, F., Evans, S. J., Vawter, M. P., Tomita, H., Choudary, P. V., Bunney, W. E., Jr., Jones, E. G., Watson, S. J., Akil, H., Myers, R. M., Schatzberg, A. F. and Lyons, D. M. (2006): Application of microarray technology in primate behavioral neuroscience research. *Methods* 38(3): 227-234.

Kempf, L., Nicodemus, K. K., Kolachana, B., Vakkalanka, R., Verchinski, B. A., Egan, M. F., Straub, R. E., Mattay, V. A., Callicott, J. H., Weinberger, D. R. and Meyer-Lindenberg, A. (2008): Functional polymorphisms in PRODH are associated with risk and protection for schizophrenia and fronto-striatal structure and function. *PLoS Genet* 4(11): e1000252.

Kendler, K. S., Kalsi, G., Holmans, P. A., Sanders, A. R., Aggen, S. H., Dick, D. M., Aliev, F., Shi, J., Levinson, D. F. and Gejman, P. V. (2011): Genomewide association analysis of symptoms of alcohol dependence in the molecular genetics of schizophrenia (MGS2) control sample. *Alcohol Clin Exp Res* 35(5): 963-975.

Kessler, R. C., Berglund, P., Demler, O., Jin, R., Koretz, D., Merikangas, K. R., Rush, A. J., Walters, E. E. and Wang, P. S. (2003): The epidemiology of major depressive disorder: results from the National Comorbidity Survey Replication (NCS-R). *Jama* 289(23): 3095-3105.

Kessler, R. C., Nelson, C. B., McGonagle, K. A., Liu, J., Swartz, M. and Blazer, D. G. (1996): Comorbidity of DSM-III-R major depressive disorder in the general population: results from the US National Comorbidity Survey. *Br J Psychiatry Suppl*(30): 17-30.

Kiewe, P., Gueller, S., Komor, M., Stroux, A., Thiel, E. and Hofmann, W. K. (2009): Prediction of qualitative outcome of oligonucleotide microarray hybridization by measurement of RNA integrity using the 2100 Bioanalyzer capillary electrophoresis system. *Ann Hematol* 88(12): 1177-1183.

Klamt, F., Zdanov, S., Levine, R. L., Pariser, A., Zhang, Y., Zhang, B., Yu, L. R., Veenstra, T. D. and Shacter, E. (2009): Oxidant-induced apoptosis is mediated by oxidation of the actin-regulatory protein cofilin. *Nat Cell Biol* 11(10): 1241-1246.

Knapman, A., Heinzmann, J. M., Hellweg, R., Holsboer, F., Landgraf, R. and Touma, C. (2010a): Increased stress reactivity is associated with cognitive deficits and decreased hippocampal brain-derived neurotrophic factor in a mouse model of affective disorders. *J Psychiatr Res* 44(9): 566-575.

- Knapman, A., Heinzmann, J. M., Holsboer, F., Landgraf, R. and Touma, C. (2010b): Modeling psychotic and cognitive symptoms of affective disorders: Disrupted latent inhibition and reversal learning deficits in highly stress reactive mice. *Neurobiol Learn Mem* 94(2): 145-152.
- Knapman, A., Kaltwasser, S. F., Martins-de-Souza, D., Holsboer, F., Landgraf, R., Turck, C. W., Czisch, M. and Touma, C. (in press): Increased stress reactivity is associated with reduced hippocampal activity and neuronal integrity along with changes in energy metabolism. *European Journal of Neuroscience*.
- Komori, T. (2011): Signaling networks in RUNX2-dependent bone development. *J Cell Biochem* 112(3): 750-755.
- Kousaka, K., Kiyonari, H., Oshima, N., Nagafuchi, A., Shima, Y., Chisaka, O. and Uemura, T. (2008): Slingshot-3 dephosphorylates ADF/cofilin but is dispensable for mouse development. *Genesis* 46(5): 246-255.
- Kromer, S. A., Kessler, M. S., Milfay, D., Birg, I. N., Bunck, M., Czibere, L., Panhuysen, M., Putz, B., Deussing, J. M., Holsboer, F., Landgraf, R. and Turck, C. W. (2005): Identification of glyoxalase-I as a protein marker in a mouse model of extremes in trait anxiety. *J Neurosci* 25(17): 4375-4384.
- Kuhn, T. B., Meberg, P. J., Brown, M. D., Bernstein, B. W., Minamide, L. S., Jensen, J. R., Okada, K., Soda, E. A. and Bamburg, J. R. (2000): Regulating actin dynamics in neuronal growth cones by ADF/cofilin and rho family GTPases. *J Neurobiol* 44(2): 126-144.
- Kulic, L., Wollmer, M. A., Rhein, V., Pagani, L., Kuehnle, K., Cattepoel, S., Tracy, J., Eckert, A. and Nitsch, R. M. (2011): Combined expression of tau and the Harlequin mouse mutation leads to increased mitochondrial dysfunction, tau pathology and neurodegeneration. *Neurobiol Aging* 32(10): 1827-1838.
- Kurian, S. M., Le-Niculescu, H., Patel, S. D., Bertram, D., Davis, J., Dike, C., Yehyaw, N., Lysaker, P., Dustin, J., Caligiuri, M., Lohr, J., Lahiri, D. K., Nurnberger, J. I., Jr., Faraone, S. V., Geyer, M. A., Tsuang, M. T., Schork, N. J., Salomon, D. R. and Niculescu, A. B. (2011): Identification of blood biomarkers for psychosis using convergent functional genomics. *Mol Psychiatry* 16(1): 37-58.
- Kuure, S., Cebrian, C., Machingo, Q., Lu, B. C., Chi, X., Hyink, D., D'Agati, V., Gurniak, C., Witke, W. and Costantini, F. (2010): Actin depolymerizing factors cofilin1 and destrin are required for ureteric bud branching morphogenesis. *PLoS Genet* 6(10): e1001176.
- Lamprianou, S., Chatzopoulou, E., Thomas, J. L., Bouyain, S. and Harroch, S. (2011): A complex between contactin-1 and the protein tyrosine phosphatase PTPRZ controls the development of oligodendrocyte precursor cells. *Proc Natl Acad Sci U S A* 108(42): 17498-17503.
- Landgraf, R., Kessler, M. S., Bunck, M., Murgatroyd, C., Spengler, D., Zimbelmann, M., Nussbaumer, M., Czibere, L., Turck, C. W., Singewald, N., Rujescu, D. and Frank, E. (2007): Candidate genes of anxiety-related behavior in HAB/LAB rats and mice: focus on vasopressin and glyoxalase-I. *Neurosci Biobehav Rev* 31(1): 89-102.
- Levinson, D. F. (2005): Meta-analysis in psychiatric genetics. *Curr Psychiatry Rep* 7(2): 143-151.

- Li, H. and Durbin, R. (2009): Fast and accurate short read alignment with Burrows-Wheeler transform. *Bioinformatics* 25(14): 1754-1760.
- Lifschytz, T., Broner, E. C., Zozulinsky, P., Slonimsky, A., Eitan, R., Greenbaum, L. and Lerer, B. (2011): Relationship between Rgs2 gene expression level and anxiety and depression-like behaviour in a mutant mouse model: serotonergic involvement. *Int J Neuropsychopharmacol*: 1-12.
- Lightman, S. L. and Conway-Campbell, B. L. (2010): The crucial role of pulsatile activity of the HPA axis for continuous dynamic equilibration. *Nat Rev Neurosci* 11(10): 710-718.
- Lister, R. G. (1987): The use of a plus-maze to measure anxiety in the mouse. *Psychopharmacology (Berl)* 92(2): 180-185.
- Livak, K. J. and Schmittgen, T. D. (2001): Analysis of relative gene expression data using real-time quantitative PCR and the 2(-Delta Delta C(T)) Method. *Methods* 25(4): 402-408.
- Livesey, F. J. (2003): Strategies for microarray analysis of limiting amounts of RNA. *Brief Funct Genomic Proteomic* 2(1): 31-36.
- Lo, C. P., Hsu, L. J., Li, M. Y., Hsu, S. Y., Chuang, J. I., Tsai, M. S., Lin, S. R., Chang, N. S. and Chen, S. T. (2008): MPP+-induced neuronal death in rats involves tyrosine 33 phosphorylation of WW domain-containing oxidoreductase WOX1. *Eur J Neurosci* 27(7): 1634-1646.
- Lohoff, F. W. (2010): Overview of the genetics of major depressive disorder. *Curr Psychiatry Rep* 12(6): 539-546.
- Lydall, G. J., Bass, N. J., McQuillin, A., Lawrence, J., Anjorin, A., Kandaswamy, R., Pereira, A., Guerrini, I., Curtis, D., Vine, A. E., Sklar, P., Purcell, S. M. and Gurling, H. M. (2011): Confirmation of prior evidence of genetic susceptibility to alcoholism in a genome-wide association study of comorbid alcoholism and bipolar disorder. *Psychiatr Genet* 21(6): 294-306.
- Mammucari, C. and Rizzuto, R. (2010): Signaling pathways in mitochondrial dysfunction and aging. *Mech Ageing Dev* 131(7-8): 536-543.
- Maoz, H. (2007): Failure of first SSRI for depression--what is the next step? *Isr J Psychiatry Relat Sci* 44(4): 327-329.
- Matthews, K., Christmas, D., Swan, J. and Sorrell, E. (2005): Animal models of depression: navigating through the clinical fog. *Neurosci Biobehav Rev* 29(4-5): 503-513.
- Maxwell, S. A. and Rivera, A. (2003): Proline oxidase induces apoptosis in tumor cells, and its expression is frequently absent or reduced in renal carcinomas. *J Biol Chem* 278(11): 9784-9789.
- McBride, H. M., Neuspiel, M. and Wasiak, S. (2006): Mitochondria: more than just a powerhouse. *Curr Biol* 16(14): R551-560.
- McCormick, C. M. and Mathews, I. Z. (2010): Adolescent development, hypothalamic-pituitary-adrenal function, and programming of adult learning and memory. *Prog Neuropsychopharmacol Biol Psychiatry* 34(5): 756-765.

- McEwen, B. S. (2007): Physiology and neurobiology of stress and adaptation: central role of the brain. *Physiol Rev* 87(3): 873-904.
- Mehmeti, I., Gurgul-Convey, E., Lenzen, S. and Lortz, S. (2011): Induction of the intrinsic apoptosis pathway in insulin-secreting cells is dependent on oxidative damage of mitochondria but independent of caspase-12 activation. *Biochim Biophys Acta* 1813(10): 1827-1835.
- Melmed, S., Polonsky, K. S., Larsen, P. R. and Kronenberg, H. M. (2011). Williams Textbook of Endocrinology, Saunders Elsevier.
- Minamide, L. S., Striegl, A. M., Boyle, J. A., Meberg, P. J. and Bamburg, J. R. (2000): Neurodegenerative stimuli induce persistent ADF/cofilin-actin rods that disrupt distal neurite function. *Nat Cell Biol* 2(9): 628-636.
- Moffitt, T. E., Caspi, A., Harrington, H., Milne, B. J., Melchior, M., Goldberg, D. and Poulton, R. (2007): Generalized anxiety disorder and depression: childhood risk factors in a birth cohort followed to age 32. *Psychol Med* 37(3): 441-452.
- Mormede, P., Foury, A., Barat, P., Corcuff, J. B., Terenina, E., Marissal-Arvy, N. and Moisan, M. P. (2011): Molecular genetics of hypothalamic-pituitary-adrenal axis activity and function. *Ann N Y Acad Sci* 1220: 127-136.
- Mourier, A. and Larsson, N. G. (2011): Tracing the trail of protons through complex I of the mitochondrial respiratory chain. *PLoS Biol* 9(8): e1001129.
- Muller, M. B. and Holsboer, F. (2006): Mice with mutations in the HPA-system as models for symptoms of depression. *Biol Psychiatry* 59(12): 1104-1115.
- Murphy, K. C., Jones, L. A. and Owen, M. J. (1999): High rates of schizophrenia in adults with velo-cardio-facial syndrome. *Arch Gen Psychiatry* 56(10): 940-945.
- Murray, F., Smith, D. W. and Hutson, P. H. (2008): Chronic low dose corticosterone exposure decreased hippocampal cell proliferation, volume and induced anxiety and depression like behaviours in mice. *Eur J Pharmacol* 583(1): 115-127.
- Muzzi, P., Camera, P., Di Cunto, F. and Vercelli, A. (2009): Deletion of the citron kinase gene selectively affects the number and distribution of interneurons in barrel cortex. *J Comp Neurol* 513(3): 249-264.
- Neumann, I. D., Wegener, G., Homberg, J. R., Cohen, H., Slattery, D. A., Zohar, J., Olivier, J. D. and Mathe, A. A. (2011): Animal models of depression and anxiety: What do they tell us about human condition? *Prog Neuropsychopharmacol Biol Psychiatry* 35(6): 1357-1375.
- Nosjean, A., Franc, B. and Laguzzi, R. (1995): Increased sympathetic nerve discharge without alteration in the sympathetic baroreflex response by serotonin<sub>3</sub> receptor stimulation in the nucleus tractus solitarius of the rat. *Neurosci Lett* 186(1): 41-44.
- O'Keefe, L. V. and Richards, R. I. (2006): Common chromosomal fragile sites and cancer: focus on FRA16D. *Cancer Lett* 232(1): 37-47.
- Oleinik, N. V., Krupenko, N. I. and Krupenko, S. A. (2010): ALDH1L1 inhibits cell motility via dephosphorylation of cofilin by PP1 and PP2A. *Oncogene* 29(47): 6233-6244.

- Omura, T. (2010): Structural diversity of cytochrome P450 enzyme system. *J Biochem* 147(3): 297-306.
- Ott, M., Gogvadze, V., Orrenius, S. and Zhivotovsky, B. (2007): Mitochondria, oxidative stress and cell death. *Apoptosis* 12(5): 913-922.
- O'Tuathaigh, C. M., Babovic, D., O'Meara, G., Clifford, J. J., Croke, D. T. and Waddington, J. L. (2007): Susceptibility genes for schizophrenia: characterisation of mutant mouse models at the level of phenotypic behaviour. *Neurosci Biobehav Rev* 31(1): 60-78.
- Pacher, P. and Kecskemeti, V. (2004): Trends in the development of new antidepressants. Is there a light at the end of the tunnel? *Curr Med Chem* 11(7): 925-943.
- Pagliarini, D. J., Calvo, S. E., Chang, B., Sheth, S. A., Vafai, S. B., Ong, S. E., Walford, G. A., Sugiana, C., Boneh, A., Chen, W. K., Hill, D. E., Vidal, M., Evans, J. G., Thorburn, D. R., Carr, S. A. and Mootha, V. K. (2008): A mitochondrial protein compendium elucidates complex I disease biology. *Cell* 134(1): 112-123.
- Parker, G., Graham, R., Hadzi-Pavlovic, D., Friend, P., Synnott, H. and Barrett, M. (2011): Does testing for bimodality clarify whether the bipolar disorders are categorically or dimensionally different to unipolar depressive disorders? *J Affect Disord*.
- Patel, S. D., Le-Niculescu, H., Koller, D. L., Green, S. D., Lahiri, D. K., McMahon, F. J., Nurnberger, J. I., Jr. and Niculescu, A. B., 3rd (2010): Coming to grips with complex disorders: genetic risk prediction in bipolar disorder using panels of genes identified through convergent functional genomics. *Am J Med Genet B Neuropsychiatr Genet* 153B(4): 850-877.
- Pego, J. M., Morgado, P., Pinto, L. G., Cerqueira, J. J., Almeida, O. F. and Sousa, N. (2008): Dissociation of the morphological correlates of stress-induced anxiety and fear. *Eur J Neurosci* 27(6): 1503-1516.
- Pellow, S., Chopin, P., File, S. E. and Briley, M. (1985): Validation of open:closed arm entries in an elevated plus-maze as a measure of anxiety in the rat. *J Neurosci Methods* 14(3): 149-167.
- Petit-Demouliere, B., Chenu, F. and Bourin, M. (2005): Forced swimming test in mice: a review of antidepressant activity. *Psychopharmacology (Berl)* 177(3): 245-255.
- Petrov, A., Pirozhkova, I., Carnac, G., Laoudj, D., Lipinski, M. and Vassetzky, Y. S. (2006): Chromatin loop domain organization within the 4q35 locus in facioscapulohumeral dystrophy patients versus normal human myoblasts. *Proc Natl Acad Sci U S A* 103(18): 6982-6987.
- Phillips, T. J., Belknap, J. K., Hitzemann, R. J., Buck, K. J., Cunningham, C. L. and Crabbe, J. C. (2002): Harnessing the mouse to unravel the genetics of human disease. *Genes Brain Behav* 1(1): 14-26.
- Pillai, A., de Jong, D., Krugers, H., Knapman, A., Heinzmann, J. M., Holsboer, F., Landgraf, R., Joels, M. and Touma, C. (in preparation): Morphology of hippocampal and amygdalar neurons in young-adult mice is resilient to genetic differences in stress reactivity. *PLoS One*.

- Pinto, D., Darvishi, K., Shi, X., Rajan, D., Rigler, D., Fitzgerald, T., Lionel, A. C., Thiruvahindrapuram, B., Macdonald, J. R., Mills, R., Prasad, A., Noonan, K., Gribble, S., Prigmore, E., Donahoe, P. K., Smith, R. S., Park, J. H., Hurles, M. E., Carter, N. P., Lee, C., Scherer, S. W. and Feuk, L. (2011): Comprehensive assessment of array-based platforms and calling algorithms for detection of copy number variants. *Nat Biotechnol* 29(6): 512-520.
- Porsolt, R. D., Bertin, A. and Jalfre, M. (1977): Behavioral despair in mice: a primary screening test for antidepressants. *Arch Int Pharmacodyn Ther* 229(2): 327-336.
- Porsolt, R. D., Bertin, A. and Jalfre, M. (1978): "Behavioural despair" in rats and mice: strain differences and the effects of imipramine. *Eur J Pharmacol* 51(3): 291-294.
- Prut, L. and Belzung, C. (2003): The open field as a paradigm to measure the effects of drugs on anxiety-like behaviors: a review. *Eur J Pharmacol* 463(1-3): 3-33.
- Rezin, G. T., Amboni, G., Zugno, A. I., Quevedo, J. and Streck, E. L. (2009): Mitochondrial dysfunction and psychiatric disorders. *Neurochem Res* 34(6): 1021-1029.
- Riddle, D. R. and Forbes, M. E. (2005): Regulation of cytochrome oxidase activity in the rat forebrain throughout adulthood. *Neurobiol Aging* 26(7): 1035-1050.
- Roussos, P., Giakoumaki, S. G. and Bitsios, P. (2009): A risk PRODH haplotype affects sensorimotor gating, memory, schizotypy, and anxiety in healthy male subjects. *Biol Psychiatry* 65(12): 1063-1070.
- Ruegg, J., Holsboer, F., Turck, C. and Rein, T. (2004): Cofilin 1 is revealed as an inhibitor of glucocorticoid receptor by analysis of hormone-resistant cells. *Mol Cell Biol* 24(21): 9371-9382.
- Rust, M. B., Gurniak, C. B., Renner, M., Vara, H., Morando, L., Gorlich, A., Sassoe-Pognetto, M., Banhaabouchi, M. A., Giustetto, M., Triller, A., Choquet, D. and Witke, W. (2010): Learning, AMPA receptor mobility and synaptic plasticity depend on n-cofilin-mediated actin dynamics. *Embo J* 29(11): 1889-1902.
- Rybnikova, E., Karkkainen, I., Peltto-Huikko, M. and Huovila, A. P. (2002): Developmental regulation and neuronal expression of the cellular disintegrin ADAM11 gene in mouse nervous system. *Neuroscience* 112(4): 921-934.
- Sandvig, A., Berry, M., Barrett, L. B., Butt, A. and Logan, A. (2004): Myelin-, reactive glia-, and scar-derived CNS axon growth inhibitors: expression, receptor signaling, and correlation with axon regeneration. *Glia* 46(3): 225-251.
- Sarmiere, P. D. and Bamberg, J. R. (2004): Regulation of the neuronal actin cytoskeleton by ADF/cofilin. *J Neurobiol* 58(1): 103-117.
- Sato, H., Takahashi, T., Sumitani, K., Takatsu, H. and Urano, S. (2010): Glucocorticoid Generates ROS to Induce Oxidative Injury in the Hippocampus, Leading to Impairment of Cognitive Function of Rats. *J Clin Biochem Nutr* 47(3): 224-232.
- Sato, S., Cerny, R. L., Buescher, J. L. and Ikezu, T. (2006): Tau-tubulin kinase 1 (TTBK1), a neuron-specific tau kinase candidate, is involved in tau phosphorylation and aggregation. *J Neurochem* 98(5): 1573-1584.

- Sato, S., Xu, J., Okuyama, S., Martinez, L. B., Walsh, S. M., Jacobsen, M. T., Swan, R. J., Schlautman, J. D., Ciborowski, P. and Ikezu, T. (2008): Spatial learning impairment, enhanced CDK5/p35 activity, and downregulation of NMDA receptor expression in transgenic mice expressing tau-tubulin kinase 1. *J Neurosci* 28(53): 14511-14521.
- Schmidt, M. V., Enthoven, L., van der Mark, M., Levine, S., de Kloet, E. R. and Oitzl, M. S. (2003): The postnatal development of the hypothalamic-pituitary-adrenal axis in the mouse. *Int J Dev Neurosci* 21(3): 125-132.
- Schulze, T. G. (2010): Genetic research into bipolar disorder: the need for a research framework that integrates sophisticated molecular biology and clinically informed phenotype characterization. *Psychiatr Clin North Am* 33(1): 67-82.
- Sharp, A. J. (2009): Emerging themes and new challenges in defining the role of structural variation in human disease. *Hum Mutat* 30(2): 135-144.
- Shaw, C. J. and Lupski, J. R. (2004): Implications of human genome architecture for rearrangement-based disorders: the genomic basis of disease. *Hum Mol Genet* 13 Spec No 1: R57-64.
- She, X., Cheng, Z., Zollner, S., Church, D. M. and Eichler, E. E. (2008): Mouse segmental duplication and copy number variation. *Nat Genet* 40(7): 909-914.
- Shen, Q., Lal, R., Luellen, B. A., Earnheart, J. C., Andrews, A. M. and Luscher, B. (2010): gamma-Aminobutyric acid-type A receptor deficits cause hypothalamic-pituitary-adrenal axis hyperactivity and antidepressant drug sensitivity reminiscent of melancholic forms of depression. *Biol Psychiatry* 68(6): 512-520.
- Shyn, S. I., Shi, J., Kraft, J. B., Potash, J. B., Knowles, J. A., Weissman, M. M., Garriock, H. A., Yokoyama, J. S., McGrath, P. J., Peters, E. J., Scheftner, W. A., Coryell, W., Lawson, W. B., Jancic, D., Gejman, P. V., Sanders, A. R., Holmans, P., Slager, S. L., Levinson, D. F. and Hamilton, S. P. (2011): Novel loci for major depression identified by genome-wide association study of Sequenced Treatment Alternatives to Relieve Depression and meta-analysis of three studies. *Mol Psychiatry* 16(2): 202-215.
- Silberstein, S., Vogl, A. M., Bonfiglio, J. J., Wurst, W., Holsboer, F., Arzt, E., Deussing, J. M. and Refojo, D. (2009): Immunology, signal transduction, and behavior in hypothalamic-pituitary-adrenal axis-related genetic mouse models. *Ann N Y Acad Sci* 1153: 120-130.
- Simon, N. M. (2009): Generalized anxiety disorder and psychiatric comorbidities such as depression, bipolar disorder, and substance abuse. *J Clin Psychiatry* 70 Suppl 2: 10-14.
- Simon-Sanchez, J. and Singleton, A. (2008): Genome-wide association studies in neurological disorders. *Lancet Neurol* 7(11): 1067-1072.
- Siu, H., Zhu, Y., Jin, L. and Xiong, M. (2011): Implication of next-generation sequencing on association studies. *BMC Genomics* 12: 322.
- Stark, Z., Bruno, D. L., Mountford, H., Lockhart, P. J. and Amor, D. J. (2010): De novo 325 kb microdeletion in chromosome band 10q25.3 including ATRNL1 in a boy with cognitive impairment, autism and dysmorphic features. *Eur J Med Genet* 53(5): 337-339.

- Steiner, M. A., Marsicano, G., Nestler, E. J., Holsboer, F., Lutz, B. and Wotjak, C. T. (2008): Antidepressant-like behavioral effects of impaired cannabinoid receptor type 1 signaling coincide with exaggerated corticosterone secretion in mice. *Psychoneuroendocrinology* 33(1): 54-67.
- Sterner, E. Y. and Kalynchuk, L. E. (2010): Behavioral and neurobiological consequences of prolonged glucocorticoid exposure in rats: relevance to depression. *Prog Neuropsychopharmacol Biol Psychiatry* 34(5): 777-790.
- Steru, L., Chermat, R., Thierry, B. and Simon, P. (1985): The tail suspension test: a new method for screening antidepressants in mice. *Psychopharmacology (Berl)* 85(3): 367-370.
- Stevens, A., Begum, G. and White, A. (2011): Epigenetic changes in the hypothalamic pro-opiomelanocortin gene: a mechanism linking maternal undernutrition to obesity in the offspring? *Eur J Pharmacol* 660(1): 194-201.
- Sullivan, P. F. (2010): The psychiatric GWAS consortium: big science comes to psychiatry. *Neuron* 68(2): 182-186.
- Tarantino, L. M., Sullivan, P. F. and Meltzer-Brody, S. (2011): Using animal models to disentangle the role of genetic, epigenetic, and environmental influences on behavioral outcomes associated with maternal anxiety and depression. *Front Psychiatry* 2: 44.
- Tecott, L. H. (2003): The genes and brains of mice and men. *Am J Psychiatry* 160(4): 646-656.
- Teplyuk, N. M., Zhang, Y., Lou, Y., Hawse, J. R., Hassan, M. Q., Teplyuk, V. I., Pratap, J., Galindo, M., Stein, J. L., Stein, G. S., Lian, J. B. and van Wijnen, A. J. (2009): The osteogenic transcription factor runx2 controls genes involved in sterol/steroid metabolism, including CYP11A1 in osteoblasts. *Mol Endocrinol* 23(6): 849-861.
- Touma, C., Bunck, M., Glasl, L., Nussbaumer, M., Palme, R., Stein, H., Wolfenstatter, M., Zeh, R., Zimbelmann, M., Holsboer, F. and Landgraf, R. (2008): Mice selected for high versus low stress reactivity: a new animal model for affective disorders. *Psychoneuroendocrinology* 33(6): 839-862.
- Trivedi, M. H., Rush, A. J., Wisniewski, S. R., Nierenberg, A. A., Warden, D., Ritz, L., Norquist, G., Howland, R. H., Lebowitz, B., McGrath, P. J., Shores-Wilson, K., Biggs, M. M., Balasubramani, G. K. and Fava, M. (2006): Evaluation of outcomes with citalopram for depression using measurement-based care in STAR\*D: implications for clinical practice. *Am J Psychiatry* 163(1): 28-40.
- Trumbach, D., Graf, C., Putz, B., Kuhne, C., Panhuysen, M., Weber, P., Holsboer, F., Wurst, W., Welzl, G. and Deussing, J. M. (2010): Deducing corticotropin-releasing hormone receptor type 1 signaling networks from gene expression data by usage of genetic algorithms and graphical Gaussian models. *BMC Syst Biol* 4: 159.
- Varadarajulu, J., Lebar, M., Krishnamoorthy, G., Habelt, S., Lu, J., Bernard Weinstein, I., Li, H., Holsboer, F., Turck, C. W. and Touma, C. (2011): Increased anxiety-related behaviour in Hint1 knockout mice. *Behav Brain Res* 220(2): 305-311.
- Vaswani, M., Linda, F. K. and Ramesh, S. (2003): Role of selective serotonin reuptake inhibitors in psychiatric disorders: a comprehensive review. *Prog Neuropsychopharmacol Biol Psychiatry* 27(1): 85-102.

- Vreeburg, S. A., Hoogendijk, W. J., van Pelt, J., Derijk, R. H., Verhagen, J. C., van Dyck, R., Smit, J. H., Zitman, F. G. and Penninx, B. W. (2009): Major depressive disorder and hypothalamic-pituitary-adrenal axis activity: results from a large cohort study. *Arch Gen Psychiatry* 66(6): 617-626.
- Walker, W. P., Aradhya, S., Hu, C. L., Shen, S., Zhang, W., Azarani, A., Lu, X., Barsh, G. S. and Gunn, T. M. (2007): Genetic analysis of attractin homologs. *Genesis* 45(12): 744-756.
- Walsh, R. N. and Cummins, R. A. (1976): The Open-Field Test: a critical review. *Psychol Bull* 83(3): 482-504.
- Wang, L., Jia, P., Wolfinger, R. D., Chen, X. and Zhao, Z. (2011): Gene set analysis of genome-wide association studies: methodological issues and perspectives. *Genomics* 98(1): 1-8.
- Williams, J. W., Jr., Slubicki, M. N., Tweedy, D. S., Bradford, D. W., Trivedi, R. B. and Baker, D. (2009a): Evidence Synthesis for Determining the Responsiveness of Depression Questionnaires and Optimal Treatment Duration for Antidepressant Medications.
- Williams, R. t., Lim, J. E., Harr, B., Wing, C., Walters, R., Distler, M. G., Teschke, M., Wu, C., Wiltshire, T., Su, A. I., Sokoloff, G., Tarantino, L. M., Borevitz, J. O. and Palmer, A. A. (2009b): A common and unstable copy number variant is associated with differences in *Glo1* expression and anxiety-like behavior. *PLoS One* 4(3): e4649.
- Wirtz, S. and Schuelke, M. (2011): Region-specific expression of mitochondrial complex I genes during murine brain development. *PLoS One* 6(4): e18897.
- Wust, S., Federenko, I. S., van Rossum, E. F., Koper, J. W., Kumsta, R., Entringer, S. and Hellhammer, D. H. (2004): A psychobiological perspective on genetic determinants of hypothalamus-pituitary-adrenal axis activity. *Ann N Y Acad Sci* 1032: 52-62.
- Xu, J., Sato, S., Okuyama, S., Swan, R. J., Jacobsen, M. T., Strunk, E. and Ikezu, T. (2010): Tau-tubulin kinase 1 enhances prefibrillar tau aggregation and motor neuron degeneration in P301L FTDP-17 tau-mutant mice. *Faseb J* 24(8): 2904-2915.
- Yalcin, B., Nicod, J., Bhomra, A., Davidson, S., Cleak, J., Farinelli, L., Osteras, M., Whitley, A., Yuan, W., Gan, X., Goodson, M., Klenerman, P., Satpathy, A., Mathis, D., Benoist, C., Adams, D. J., Mott, R. and Flint, J. (2010): Commercially available outbred mice for genome-wide association studies. *PLoS Genet* 6(9).
- Yang, H., Ding, Y., Hutchins, L. N., Szatkiewicz, J., Bell, T. A., Paigen, B. J., Graber, J. H., de Villena, F. P. and Churchill, G. A. (2009): A customized and versatile high-density genotyping array for the mouse. *Nat Methods* 6(9): 663-666.
- Yen, Y., Anderzhanova, E., Kleinknecht, K., Bunck, M., Micale, V., Landgraf, R. and Wotjak, C. (2011): Inbred low anxiety-related behavior (LAB) mice - a mouse model of attention-deficit hyperactivity disorder (ADHD)? *Pharmacopsychiatry* 44: 312.
- Zdanov, S., Klamt, F. and Shacter, E. (2010): Importance of cofilin oxidation for oxidant-induced apoptosis. *Cell Cycle* 9(9): 1675-1677.

Zhang, L. F., Shi, L., Liu, H., Meng, F. T., Liu, Y. J., Wu, H. M., Du, X. and Zhou, J. N. (2011): Increased hippocampal tau phosphorylation and axonal mitochondrial transport in a mouse model of chronic stress. *Int J Neuropsychopharmacol*: 1-12.

Zhou, X. and Tuck, D. P. (2007): MSVM-RFE: extensions of SVM-RFE for multiclass gene selection on DNA microarray data. *Bioinformatics* 23(9): 1106-1114.

Zhu, P., Sang, Y., Xu, H., Zhao, J., Xu, R., Sun, Y., Xu, T., Wang, X., Chen, L., Feng, H., Li, C. and Zhao, S. (2005): ADAM22 plays an important role in cell adhesion and spreading with the assistance of 14-3-3. *Biochem Biophys Res Commun* 331(4): 938-946.



## 9 Acknowledgements

First of all, I'd like to thank Prof. Rainer Landgraf for giving me the opportunity to conduct this thesis in his research group. He allowed the freedom to take my own decisions and to make my own mistakes and at the same time kept his door open and patiently listened to all the problems I discovered when testing this freedom. At this point, I am not going to praise his scientific achievements. Whoever is interested in that can search for his name in Pubmed. Throughout my time as a Ph.D. student in his group, I was impressed by his personal integrity and his political incorrectness, which I mean as positive as can be. This allows him an analytical and unvarnished view to the world. I think he doesn't know, but these characters made him a 'doctoral father' in the purest sense of the word.

I cordially thank Prof. Grupe and all the members of the committee for their willingness to act as referees for this thesis.

I'd further like to thank Dr. Chadi Touma for the opportunity to work with animals of the SR mouse model and for his kind introduction into the topic of stress reactivity and HPA axis dysfunction.

In addition to a 'doctoral father' I was so lucky to have a 'doctoral family'. In particular my supervisor Dr. Ludwig Czibere ('doctoral brother') who supported my work with practical hints, encouraging words, creative chaos and great ideas. As the Landgraf department is a huge one, I can't name everyone. But I'd like to thank all the members – present and former ones – for their support and for creating an atmosphere, which made going to the Institute something to look forward to every day.

Furthermore, I'd like to stress out the friendly and collaborative atmosphere within the Institute which allowed working in several collaborative projects. Without these collaborations, the methodological diversity presented in this study would never have been possible. I very much thank Dr. Alana Knapman, who was my collaboration partner in the neurodevelopmental study and the Cofilin-1 project; Kathrin Henes for showing to me how to do CO staining; Dr. Peter Weber, Dr. Benno Pütz, Dr. André Altmann, and Monika Rex-Haffner who contributed to microarray and SAGE experiments; the department of Prof. Turck who showed me how to do mitochondrial proteomics; the department of Prof. Müller-Myhsok which helped with the association study, the PCAs, and the analysis of CNV data; Dr. Dietrich Trümbach and Regina Augustin from the

Helmholtz Zentrum who were kindly supporting me with GO term and multivariate analyses of microarray data; Dr. Angelika Erhardt-Lehmann and Darina Czamara who supported my work with the down-sized analysis of the TMEM132D study. I also want to thank the friendly people from RGs Touma, Deussing, Refojo, Eder, Rein, and Almeida for their support in coping with every day lab problems.

Last, but not at all least, I'd like to thank the IMPRS program for having me as a member. The IMPRS curriculum was a more than stimulating add on program. I'd also like to thank the members of my thesis advisory committee - Prof. Chris Turck, Dr. Ilona Kadow, and Dr. Ulrike Schmidt - for their valuable input to my thesis. Many thanks go to the program coordinator Hans-Jörg Schäffer and to his colleagues from the IMPRS coordination office, who always have an open ears for Ph.D. student's issues.

## 10 Curriculum vitae

Name	Regina Andrea Widner-Andrä
Date of birth	March 22 <sup>nd</sup> 1976
Place of birth	Benediktbeuern
Since October 2008	Ph.D. student at the Ludwig Maximilian University in Munich, Faculty of Biology Research group of Prof. Dr. Rainer Landgraf, Max Planck Institute of Psychiatry ‘Assignment of functional impact on genetic data in two mouse models of affective disorders’
October 2003 - July 2008	Studies of Molecular Medicine, University in Erlangen
September 2001 - July 2003	Second-change education, Berufsoberschule in Miesbach
April 1994 - September 2001	Employments as PTA (‘Pharmazeutisch-technische Assistentin’)
September 1992 - March 1994	Apprenticeship as PTA
July 1992	Graduation from ‘Realschule’



## **11 Declaration/Erklärung**

Hiermit versichere ich, die vorliegende Arbeit selbstständig und nur mit den angegebenen Hilfsmitteln und Quellen angefertigt zu haben. Ausführungen, die wörtlich oder sinngemäß übernommen wurden, sind als solche gekennzeichnet. Ich versichere ebenfalls, nicht anderweitig versucht zu haben, eine Dissertation einzureichen oder mich einer Doktorprüfung zu unterziehen.

München, 25. Mai 2012

Regina Widner-Andrä